The effect of vegetation on the bank erosion pattern and the lateral migration rate of the Groenlose Slinge, the Netherlands

MSc Thesis Physical Geography

Final version

S.H.A.M. De Keijzer (3221598)
Supervisor: Dr. M.G. Kleinhans
Second corrector: F. Schuurman
27 January 2012

Utrecht University
Department of Physical Geography
Faculty of Geosciences

Abstract

The Groenlose Slinge is a stream in the east of the Netherlands that was re-meandered between spring 2007 and summer 2008. Re-meandering is frequently done in the Netherlands because it has a positive effect on the ecology. However, the effect of vegetation on the bank erosion pattern of (re-) meandering streams is not clear. The main aim of this research is to analyse the effect of vegetation on the bank erosion pattern and the lateral migration rate of the Groenlose Slinge. Secondly, the morphological evolution of the Groenlose Slinge is studied.

Fieldwork was carried out and also the two dimensional Bank Stability and Toe Erosion Model (BSTEM) was used. Moreover, the results of former studies to the Groenlose Slinge were used.

Bank erosion only takes place in outer bends and never in inner bends, indicating that the channel was dug wide enough. No effect of most grasses, herbs and young trees on the erosion pattern is found; the added strength of these types is too small to overcome the unstable bank. Only reed, bulrush and mature forest can prevent erosion in outer bends. As a result, only these vegetation types can influence the pattern of erosion in outer bends. No different effect of different vegetation on the migration rate of the Groenlose Slinge was found. The most obvious morphological evolution is that between 2008 and 2011 on average 1.5 m^2 net deposition per metre length took place. The deposition leads to higher banks and to narrower channels in 2011 than in 2008. Also most bends of the Groenlose Slinge became sharper which led to higher water depths.

Thus, concerning the main aim of this research, it can be concluded that the bank erosion pattern of the Groenlose Slinge is globally reflected by the pattern of outer bends and that vegetation has no effect on the lateral migration rate. Concerning the second aim of this research, it can be concluded that net deposition took place between 2008 and 2011.

Key words: Groenlose Slinge, bank erosion pattern, lateral migration rate, added strength by vegetation, Bank Stability and Toe Erosion Model

Preface

This master thesis is part of the Master of Science degree program in Physical Geography at Utrecht University. The thesis consists of an analysis, synthesis and evaluation of results and is supported by an extensive literature review. The results were obtained from fieldwork in the Groenlose Slinge and the application of a two dimensional model. The Groenlose Slinge is a recently re-meandered stream in the east of the Netherlands. The fieldwork took place in June and August 2011. Also results obtained by Hans Wytema, Mariëlle Jansen and Anja van de Kruijs were used. They did their fieldwork for their master thesis in the Groenlose Slinge in 2008.

I would like to thank my supervisor Maarten Kleinhans, who was always willing to help and to listen. A second word of thanks goes to Domien de Winter, Ellen Bollen Weide, Hannie ter Maat and Gert van den Houten from Waterschap Rijn en IJssel (the local waterboard) for their good support. Domien, you told me interesting things about the Groenlose Slinge and the vegetation around it. Finally, I would like to thank Henk Markies for taking the good quality air- and land photos and Maarten Zeylmans for installing ArcGIS on my laptop.

Steffie de Keijzer, January 2012

Table of contents

List of Figures

List of Tables

Chapter 1. Introduction

1.1. Reasons for re-meandering

Over the last hundred years, natural streams have been canalised on a large scale to improve the drainage for better agriculture (Brooker, 1988). As a result, the natural variety in environments and conditions has destroyed and the natural value of most ecosystems has seriously declined (Wolfert, 2001). However, since the seventies/eighties, the ecological value of nature and the negative effects of canalisation have increased (Wolfert, 2001). This led to re-naturalization of streams in the Netherlands and in the rest of Europe. Re-meandering is one of the measures to re-naturalize streams.

Re-meandering of formerly canalised streams takes place in connection with the European Water Framework Directive (European WFD) (Dutch: Europese Kader Richtlijn Water (Europese KRW)). This directive ensures that organizations, like waterboards and municipalities, improve the water quality. The aim of the European WFD is to establish healthy ecological and chemical conditions in all European waters in the year 2015.

Re-meandering has a positive effect on the ecology because the flow characteristics, bedforms and bed material of a meandering stream are very heterogeneous (Wolfert, 2001). There are deep pools, steep banks, variations in stream velocity and areas for pioneer vegetation like point bars. In consequence, there is a large heterogeneity in habitats which leads to a positive impulse in the biodiversity. A meandering stream also causes dynamics which also have a positive effect on the ecology. Finally, a meandering stream has a positive effect on the ecology because a meandering stream has a relatively long retention time of water in the fluvial system (Wolfert, 2001). Due to the relatively long retention time, the groundwater level increases within the surrounding parts of the drainage basin and also the flooding frequency increases. An increased groundwater level in stream valleys may support riparian wetland vegetation, which increases nutrient retention. An increased nutrient retention reduces the nutrient concentration in the streams, which is positive for the ecology downstream (Wolfert, 2001).

Besides the positive effect on the ecology, re-meandering of streams also has other advantages. In an aesthetic point of view a meandering stream is appreciated (Wolfert, 2001). It can lead to an increase of recreation in the re-meandering area. A last advantage is that a free meandering stream requires little maintenance (Van der Vossen and Verhagen, 2009). However, when the space is limited and the stream is not free to meander anymore, it might even need more maintenance than before the re-meandering project.

The streams are re-naturalized by *human being* so one cannot not speak of a *natural* stream, although the stream shows natural characteristics. However, human help is always needed as autogenic meander initiation is not possible because time and triggers are necessary (Lanzoni et al., 2006). Such a trigger has to be upstream of the location where meandering characteristics are desired.

1.2. Problems related to re-meandering streams

When plans are made for re-meandering a stream, other functions and interests in the stream and the surrounding area have to be taken into account (Wolfert, 2001). Re-meandered streams need

one specific management strategy, but other functions and interests can require another management strategy. This can lead to conflicts between different needs. The use of the (limited) space is often the point of discussion. An effect of meandering is the lateral migration of bends which can be in conflict with land ownership. This suggests that there are constraints to re-meander streams. The less constraints there are, the higher the degree of re-naturalization can be. But in a densely populated area such as the Netherlands, human constraints are inevitable.
In the past, there have been re-meandering projects in which as much erosion occurred that the economic damage in the neighbouring areas was significant. These incidents happen because the problem is that one cannot exactly predict how the stream is going to meander. Especially vegetation makes prediction of meandering very complicated. According to Ellen Bollen Weide (2011) (Waterschap Rijn en IJssel) also the Groenlose Slinge meandered in a different way than predicted. In any case, meandering cannot be predicted precisely. If one had more knowledge about re-meandering of streams and the effect of vegetation on re-meandering, agencies would tend to re-meander streams earlier because problems like unwanted meander bend migrations can be better prevented.
Thus, as shown in this section, because of the different interests and the difficulty in predicting meandering, there is a clearly need for further research on this topic.

1.3. Research

During this research, fieldwork was carried out at the stream the 'Groenlose Slinge' in the east of the Netherlands. For this research area was chosen because meandering and the effect of vegetation could be studied from its infancy. This was an unique opportunity and it was expected that this type of research gives the best results. In fact, it was an experiment on real scale.
In 2008, 2009 and 2010, three Physical Geography Master of Science students from Utrecht University carried out extensive research to the Groenlose Slinge, supervised by Dr. M.G. Kleinhans and in partnership with Waterschap Rijn en IJssel (A 'Waterschap' is a kind of district water board in the Netherlands). Mariëlle Jansen studied the long term meandering trends in the Groenlose Slinge in response to discharge regime and the presence of vegetation. Mariëlle Jansen only gives a global view of vegetation around the Groenlose Slinge. She tried to predict the effect of vegetation by use of a meander migration model. In this meander migration model the stream is schematized by a centreline of different nodes. Mariëlle Jansen (2009) showed that the computer meander simulation models do not give reliable results. The possibility to introduce physical characteristics of the environment like vegetation is limited. Moreover, the migration rate is underpredicted with default settings. Hans Wytema carried out research on the influence of vegetation on streambank instability and Anja van de Kruijs specialized in sharp bends. Hans Wytema studied the effect of vegetation on a small scale, on the scale of bends. However, the spatial reach was quite small as he just studied six bends of the Groenlose Slinge. Wytema offers some suggestions about types of vegetation that could have much influence on erosion, but this suggestion was only based on Bank Stability and Toe Erosion Model and he indicates that this has to be tested by monitoring.
In order to obtain better migration results than Jansen obtained and test BSTEM more extensively than Wytema did, in this research the Bank Stability and Toe Erosion Model, version 5.2. (BSTEM-5.2) is used in addition to the field results. In contrast to the model that Jansen used, BSTEM-5.2. describes vegetation variety more precisely which should result in a more accurate prediction of erosion and lateral migration. Data obtained from the field are used as input for BSTEM-5.2. to

predict bank stability and bank erosion. Finally, the model results are compared with the field observations. In this way the quality of the Bank Stability and Toe Erosion Model can be discussed.
Thus, although already some research on the effect of vegetation on meandering in the Groenlose Slinge has been done, these studies need extension to really determine the effect of vegetation. In this extension, it is desirable to use a spatial scale and a time scale which is smaller than the scale in the research of Mariëlle Jansen, but larger than the scale in the research of Hans Wytema.

1.4. Aim and research questions

The main aim of this research is:

'Determining the effect of vegetation on the bank erosion pattern and the lateral migration rate of the Groenlose Slinge'

Insights gained by the three students and Waterschap Rijn en IJssel have been used. In contrast to studies of the three previous students, there is a strong focus on the role of vegetation. The intention is that this proper research gives a more complete view than the former researches on the role of vegetation on meandering of the Groenlose Slinge. Besides the effect of vegetation on the bank erosion pattern, also more general aspects like the morphological evolution have been researched.

In 2007, 2008, 2009, 2010 and 2011 waterlines, bank lines and twenty profiles at fixed locations were measured. Also many land photos and airphotos from the Unmanned Airborne Vehicle of University Utrecht were available. These data provide a general view of the Groenlose Slinge and also give a good opportunity to get insight in the morphological and hydrological evolution of the Groenlose Slinge. These data lead to the first research question:

> *1) What are the morphological and hydrological characteristics of the Groenlose Slinge? How did these characteristics change between 2008 and 2011?*

Besides the morphological and hydrological characteristics of the Groenlose Slinge also the vegetation around the Groenlose Slinge contributes to the general view of the Groenlose Slinge. When general characteristics of the vegetation are obtained, more specific knowledge about the vegetation is desired to know:

> *2) What vegetation and what vegetation patterns do occur around the Groenlose Slinge?*

> *3) What are the characteristics of this vegetation? What is known about vegetation roots and added vegetation strength?*

Another key question is:

> *4) Where does erosion take place and what is the lateral migration rate? Does a relation exist between erosion and vegetation and does a relation exist between the lateral migration rate and vegetation?*

The sharp bend in the Groenlose Slinge has already been researched before. Therefore, also in this research it is interesting to look to this sharp bend again:

> *5) What are hydrological and morphological characteristics in the sharp bend of the Groenlose Slinge and what is the role of vegetation in this sharp bend?*

To understand and to discuss the answers of above questions the next two questions are raised:

> *6) How does stream bank erosion work? What processes and what factors do play a role?*

> *7) What are the differences between the prediction of the 2011 profile by the Bank Stability and Toe Erosion Model based on the profile of 2008 and the measured profile of 2011? What are the sensitive parameters of BSTEM and how sensitive are they? And what is the prediction of the profiles of 2012?*

1.5. Guide to the reader

This thesis consists of four parts. Part I consists of a literature review. In this literature review characteristics of meandering streams (*Chapter 2*), streambank erosion (*Chapter 3*) and the study area (*Chapter 4*) are discussed. Also hypotheses on the research questions (*Chapter 5*) are given. Part II contains the methods and is about the justification of the methodology (*Chapter 6*), the field methods (*Chapter 7*), the methods of analysing (*Chapter 8*) and about the application of the Bank Stability and Toe Erosion Model (BSTEM) (*Chapter 9*). In part III the results can be found. It contains chapters about morphological evolution (*Chapter 10*), about deposition and bank erosion (*Chapter 11*), vegetation characteristics (*Chapter 12*) and the Bank Stability and Toe Erosion Model (BSTEM) (*Chapter 13*). Part IV consists of a discussion (*Chapter 14*) and a conclusion (*Chapter 15*). After part IV a Dutch summary of the most important results concerning management of re-meandered streams for Waterschap Rijn en IJssel (*Chapter 16*) and an overview of the used literature (*Chapter 17*) can be found. After these two chapters 11 appendices can be found.

Part I: Literature review

This literature review consist of four chapters. *Chapter 2* is about the characteristics of meandering streams, *Chapter 3* is about streambank erosion and *Chapter 4* is about the study area. In *Chapter 5* the hypotheses on the research questions are given.

Chapter 2. Characteristics of meandering streams

In *Section 2.1.* the definition and classification of meandering streams is discussed. *Section 2.2.* is about the morphology of meandering streams and *Section 2.3.* is about stream characteristics in meandering streams. Finally, *Section 2.4.* is about the characteristics of sharp meander bends.

2.1. Definition and classification

Several definitions of a meandering stream exist. One definition is that a meandering stream is a sinuous, immobile stream. Another definition is that a meandering stream is a sinuous stream that moves by bank erosion, called meander migration. In this study, the second definition of a meandering stream is used. Besides meandering streams or rivers, also immobile rivers and braided rivers can exist. Which river or stream type exists, depends on the strength of the potential specific stream power (ω) and the grain size. The potential specific stream power (ω) represents the amount of energy to remove sediment; it is the rate of potential energy expenditure per unit length of the channel (Kleinhans and Van den Berg, 2010).

2.2. Morphology

Meandering streams are here defined as single-thread sinuous rivers with a sinuosity larger than 1.5 (Knighton, 1998). The sinuosity can be determined by dividing the channel length by the straight line valley length. To describe the meandering pattern of a stream, besides sinuosity, also terms like mean radius of curvature, angle of curvature, axis of bend (apex), point of inflection, convex bank, concave bank, length and amplitude are used. In *Figure 1,* this terminology is represented. According to Leopold et al. (1964) and Struiksma et al. (1985), the meander wave length is commonly about ten times the channel width and about five times the mean radius of curvature.

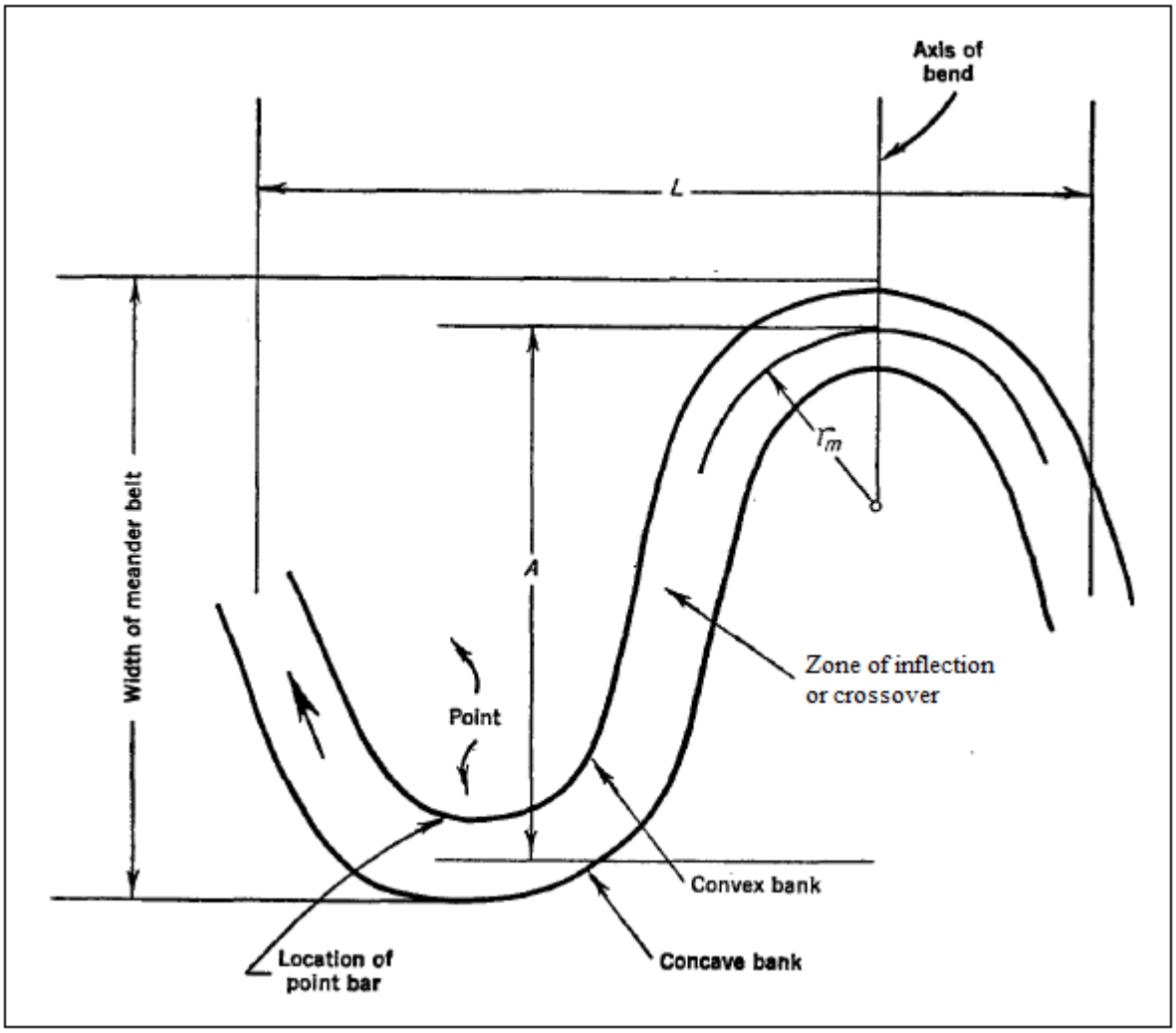

Figure 1: Terminology of a meander bend, L=meander length (wave length), A=amplitude, r_m=mean radius of curvature (Leopold and Wolman, 1960).

The convex bank is the inner bank and the concave bank is the outer bank, also called cut bank. In a meandering stream sediment is eroded from the outer bank and deposited in the inner bank causing typical cross sections. In bends, the cross sections of meandering streams usually show a triangular shape; deep in the outer bend and shallow in the inner bend. Between two bends, the straight section in *Figure 1*, the cross sections have a more rectangular shape (Crosato, 1990). The deepest parts of a meandering steam are called pools. They are located at the outer bends. Upstream and downstream of these pools, shallow parts are present which are called riffles. These riffles are on the transition of two meander bends. They link successive point bars with each other. Riffles are characteristically spaced at about five to seven times the channel width. Also the distance between the pools is often constant (De Kramer et al., 2000).

A meandering stream consists of several morphological units. Wolfert (2001) designed a classification for morphological units of streams which can be seen in *Table 1*. In this classification, he distinguished macroforms, mesoforms and microforms. It can be seen that the larger the bedform group, the larger the formative discharge and the larger the time span to form these bedforms.

Bedform group	Bedform	Formative event	Time-span
macroforms	pool, major channel, point bar (scroll bars), riffles, levees	bankfull discharge	years-decades
mesoforms	chute channel, obstacle bar, chute bar	medium to low discharges	weeks-months
microforms	sand ripples and sand dunes	all discharges	hours-days

Table 1: Classification of bedforms in a meandering stream (Wolfert, 2001).

Figure 2 gives a schematic view of a meandering river. Notice that this figure represents the morphology of a river and not of a stream. The difference between a river and stream is that a stream is shallower, narrower and has smaller stream velocities, but no exact values to distinguish between them exist. The morphology of a stream and a river are globally the same, but the morphology of a stream is less obvious than the morphology of a river. This is because of the smaller dimensions and smaller stream velocities in case of streams. A point bar, which is noted in *Table 1* and in *Figure 2*, is a bedform that consists of scroll bars (De Kramer et al., 2000). *Figure 3* also represents a scroll bar. Scroll bars are crescent-forming bars that are mostly located at the inner bend of the channel, more or less parallel to the stream. They form at peak discharge as a compensation for the released space due to bank erosion. Scroll bars often form a pattern of ridges in the inner bend (Kleinhans and Van den Berg, 2010 and De Kramer et al., 2000). This pattern is the typical ridge and swale topography which is the result of lateral accretion. *Figure 4* shows the typical ridge and swale topography consisting of scroll bars.

Also levees are a typical feature for meandering rivers. Natural levees are elongate ridges on either side of the river channel, which are formed when overbank flow occurs (Wolfert, 2001). In case of overbank flow, sediment is deposited because flow enters the shallower floodplain and loses much of its velocity and consequently transport capacity. Natural levee deposits are coarser in texture compared to the overbank sediments in distal parts of the floodplain, which are mainly deposited by settling of fine material in tranquil water. Natural levee overbank deposition is a characteristic of many meandering rivers occurring in rural landscapes. For that reason it is an important process in the management of semi-natural rivers in rural landscapes (Wolfert, 2001).

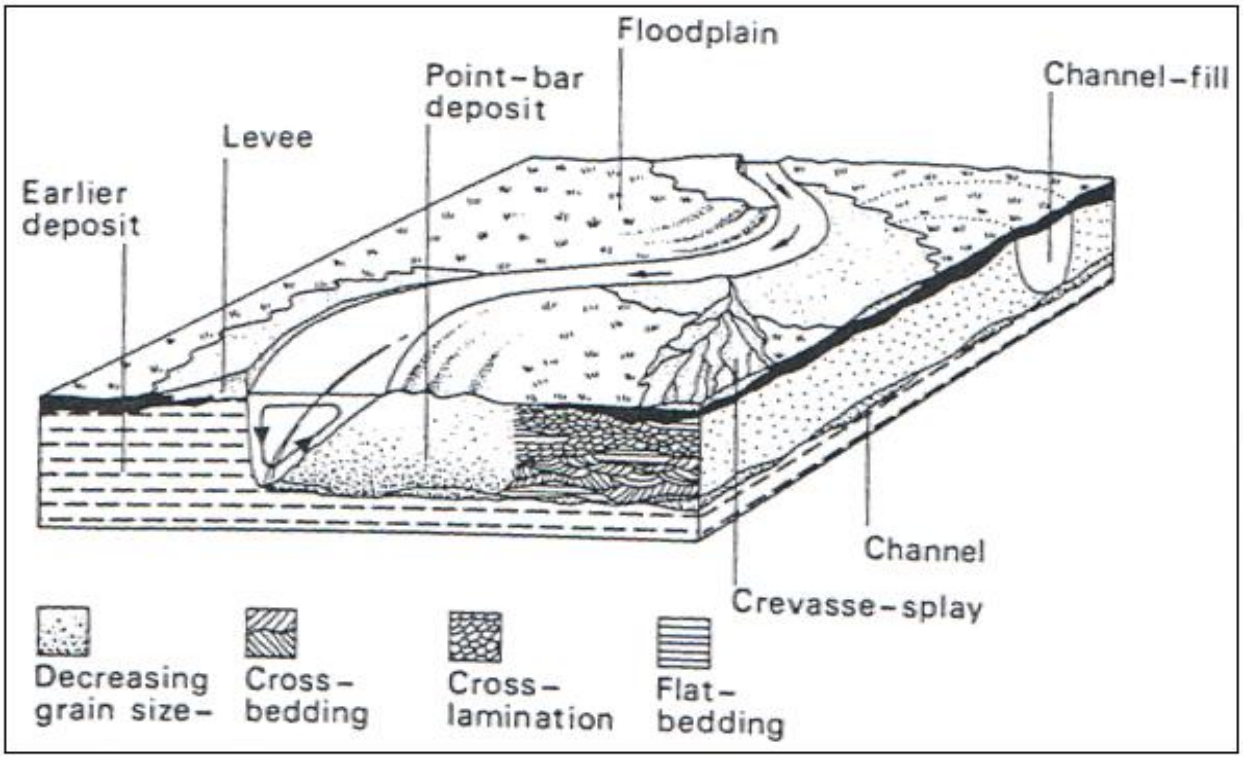

Figure 2: Schematic view of morphological characteristics of a meandering river (Allen, 1964).

Figure 3: Point bar in the inner bend of a meandering stream (Moorhead, 2011).

Figure 4: Typical ridge and swale topography consisting of scroll bars, meandering river in Alaska (U.S. Fish & Wildlife Service Digital Library System, 2011).

Other types of bars that can be formed are chute bars. Chute bars are horse-hoe shaped lobes formed at the downstream end of a chute or chute channel that crosses a braid bar at peak discharge (Kleinhans and Van den Berg, 2010). Chute bars are related to a higher stream power than scroll bars. It is expected that chute bars are increasingly present when the river shows more braiding characteristics.

2.3. Flow patterns

In a characteristic meandering stream, a three-dimensional spiral-like current exists (*Figure 5*). This three-dimensional flow consists of primary and secondary flows which together form the helical flow. This helical motion cell is also called the centre-region cell. The primary flow is the current parallel to the stream (indicated by v_s in *Figure 5*) and the secondary flow is the current normal to the stream (indicated by v_n in *Figure 5*). The velocity of the primary flow is largest in the thalweg, where the flow depth is largest. The primary velocity increases with increasing water depth for which the bottom friction decreases. This primary current is influenced by secondary currents (Thorne et al., 1985). The existence of this secondary flow pattern in channel bends has been known for a long time (Van Bendegom, 1947 and Allen and Van Bendegom, 1978). The basic reason is that flow is faster near the water surface, so that conserved momentum of flow through a bend leads to a developing helical motion (De Vriend, 1977; Blanckaert and De Vriend, 2003). In other words, secondary currents arise when the fast running surface water, that approaches a bend, impinges on the outer bend. This results in a super elevation of water in that outer bend. This local increase of the water level causes an increase in water pressure. As a consequence of this extra pressure, an inward near-bed flow exists, also called downwelling. Due to this downwelling, the fast flowing surface water flows in the direction of the outer bend. The velocity of this motion depends on the water depth, the bank radius and the friction. By advecting flow momentum, the cross-stream secondary flow determines the

spatial distribution of the velocities and the boundary shear stresses (Blackaert and Graf, 2001). Thereby it shapes the topography in case of a mobile bottom. Although some knowledge about the helical flow exists, the exact mechanisms are still poorly understood.
The secondary velocities are typically one order of magnitude smaller than the primary velocities (Bathurst et al., 1979). Field observations show that the secondary currents are weakest during low and during high discharges and that secondary currents are strongest in case of an average discharge (Bathurst et al., 1979). It is the consequence of changes in centrifugal forces and channel perimeter shapes with varying water levels. In summary, the three dimensional helical flow is a result of the interaction of curvature and the vertical gradient of flow velocity.

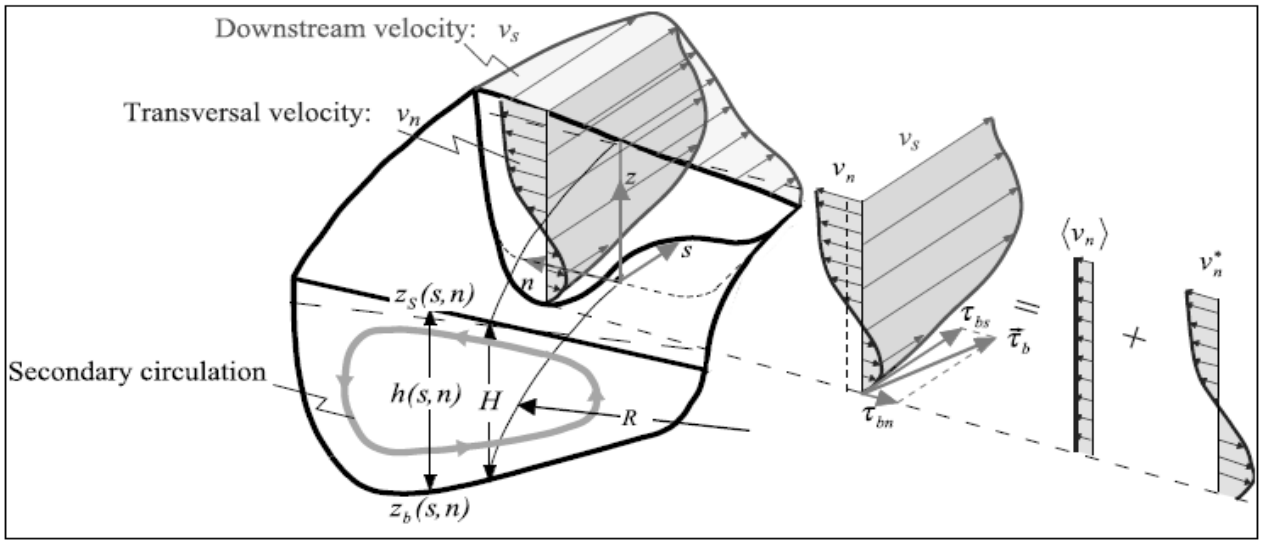

Figure 5: Helical flow in a meandering river bend (Blanckaert and Vriend, 2003). V_s=current parallell to the stream and v_n=current normal to the stream.

Besides the described secondary flow above (v_n), there is also another typical secondary flow, which is called the outer bank cell. The outer bank cell is shown in *Figure 6.* This is a weaker and smaller counter-rotating circulation cell than the centre-region cell. This current is often observed near the outer bank. Although this cell is relatively small and weak, this outer-bank cell is important because it leads to a reduction of flow strength and turbulence at the bank and possibly to a reduction in bank erosion (Thorne et al, 1985; Blanckaert and Graf, 2001). The mechanisms underlying this outer-bank cell are still poorly understood. Their numerical simulation still poses problems, not least due to lack of detailed experimental data. There are several hypotheses for the occurrence of this type of secondary flow: it might be a relic from the secondary circulation of the bend upstream, it might be arise because at a steep bank the water cannot follow the exact boundary of the channel (Bathurst et al., 1979) and it might be caused by a stagnation point were the water would pull up.

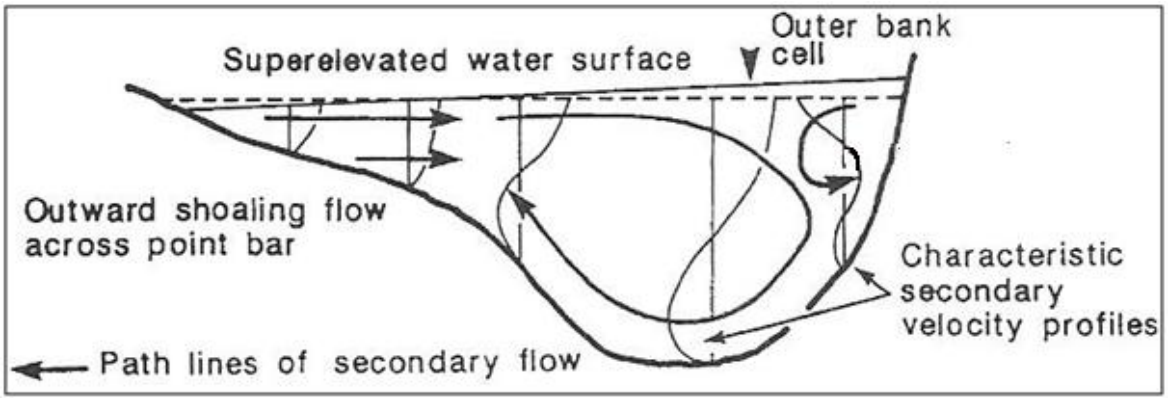

Figure 6: Secondary stream in a meandering river bend, notice the outer bank cell on the right side and the centre region cell (v_n) in the middle (Thorne et al, 1997).

The described stream pattern in a meandering river is different than the stream pattern in a straight, immobile river. In general, the stream velocity in straight rivers is larger than in meandering rivers. This is mainly the result of the lower slope in case of a meandering river than in case of a straight river. Velocity depends on the friction (Chézy coefficient), the water depth and the slope:

(Eq. 1) $u = C(RS)^{0.5}$

In which:
u = stream velocity (m/s)
C = Chézy coefficient ($m^{0.5}/s$)
R = hydraulic radius (=wet area / wet perimeter ≈ water depth)(m)
S = bottom slope (-)

As can be seen, a lower slope leads to a smaller stream velocity. Accordingly, meandering streams have lower stream velocities for a certain discharge in comparison to straight rivers.

2.4. Sharp bends

In sharp bends the flow pattern as well as the erosion and deposition pattern is different than in gentle bends. In nature, sharp bends are associated with channels with strong banks and limited to no dynamical meandering (Ferguson, 1987). Natural sharp bends can be found in rivers of all dimensions. Because only in case of strong banks, sharp bends can exist, the existence of sharp bends depends on the bank strength (Friedkin, 1945 and Ferguson, 1987.) There is no dependence of Froude number as found by Leeder and Bridges in 1975 (Blanckaert et al., 2010). An example of a sharp bend can be seen in *Figure 7*. Notice that this bend is constructed by human and is not existed by nature. *Section 2.4.1.* is about when a bend can be classified as a sharp bend and *Section 2.4.2.* is about the stream pattern in sharp bends and about the erosion and deposition pattern in sharp bends.

Figure 7: Sharp bend in the Groenlose Slinge. In this picture the flow direction is from right (south) to left (north) (Photo taken by Henk Markies, May 2011).

2.4.1. Definition of sharp bends

Hodskinson and Ferguson (1998) and Kleinhans et al. (2009) suggested defining a sharp bend as a bend with a tightness of $R_m/w \leq 2$, where R_m is the mean radius of curvature of a meander bend and w the channel width. But according to Leeder and Bridges (1975) a certain water stage must be reached at which the flow along the inner boundary becomes unstable and breaks away from the boundary resulting in a recirculation eddy. So, there is no clear, fixed definition that describes what sharp bends are. However, it is assumed that when flow separation is present, it is certainly a sharp bend. Flow separation occurs when the stream does not follow the sharp bend anymore.

2.4.2. Flow pattern and erosion and deposition pattern in sharp bends

In sharp channel bends the flow separates from the bank which leads to a bank erosion and deposition pattern that differs from gentler meander bends (Bridges and Leeder, 1976; Leeder and Bridges, 1975; Andrle, 1994; Hodskinson and Ferguson, 1998 and Ferguson et al., 2003). In case of flow separation, the main flow separates from the inner-bend channel boundary and directly impinges on the outer bank at a high angle just downstream of the apex (Leeder and Bridges, 1975 and Ferguson et al, 2003) (*Figure 8*). Upwelling and erosion occurs at that location, which focuses the water to flow to both left (*Figure 8*) (upstream) and right (*Figure 8*) (downstream) of the stagnation point. The flow to the left results in the slow flowing outer-bank vortex where deposition takes place. The flow to the right of the stagnation point has still a high velocity and stays at the outer bank. Because of this stream pattern in the outer bend, just downstream of the apex at the inner bank, a so called 'dead flow zone' (an extreme slow flow zone) occurs with a recirculation cell. This is the second horizontal vortex (Kleinhans et al., 2009) in which deposition takes place. These complicated three-dimensional vortices upstream of the outer bend and downstream of the inner bend are also called recirculation cells or recirculation eddies. As a result of this deposition and erosion pattern the bend sharpens and may develop a peculiar angular shape (Kleinhans, 2009) (*Figure 9*).

Figure 8: Flow separation in sharp bends: there are slow flowing vortices upstream of the outer bend apex and downstream of the inner bend apex (Kleinhans et al., 2009).

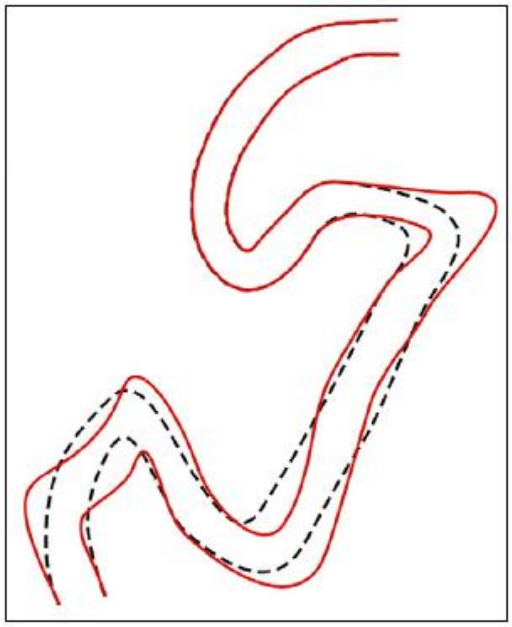

Figure 9: Bend migration in sharp bends; the red line indicates the position of the river a few years after the river was at the location of the dotted line (Kleinhans et al., 2009).

Summary of Chapter 2

A meandering stream is a sinuous stream that migrates due to bank erosion and has a sinuosity larger than 1.5.. A characteristic morphological unit of a meandering stream is a point bar consisting of scroll bars. The flow pattern consists of the typical helical flow. However, also another typical secondary flow exists, called the outer bank cell. In sharp bends the stream pattern is different because of flow separation and is determined by slow flowing vortices upstream of the outer bend apex and downstream of the inner bend apex.

Chapter 3. Streambank erosion

Streambank erosion is the detachment and removal of particles or aggregates from the streambank by hydraulic forces occurring during flood events (Lawler et al., 1997). It is important to study bank erosion because bank erosion is necessary for dynamic meandering. The higher the rate of bank erosion is, the higher the rate of meandering. The rate of bank erosion is determined by the strength of the banks and the flow strength. In *Section 3.1.* the process of streambank erosion is discussed. Streambank erosion consists of two steps: bank undercutting or toe erosion by fluvial erosion and bank failure by mass wasting. *Section 3.1.1.* is about bank undercutting by fluvial erosion and *Section 3.1.2.* is about bank failure by mass wasting. In *Section 3.2.* the factors that determine bank erosion are discussed. These factors are split up into factors that determine the flow strength, discussed *Section 3.2.1.* and factors that determine the bank strength which are discussed in *Section 3.2.2.*. In *Section 3.3.* the effect of vegetation on streambank erosion is highlighted. *Section 3.3.1.* is about the stabilizing effect of vegetation and *Section 3.3.2.* is about the destabilizing effect of vegetation. The effects of different types of vegetation are discussed in *Section 3.3.3.*. Finally, *Section 3.4.* is about modelling streambank erosion.

3.1. The process of streambank erosion

Bank erosion occurs in two steps: bank undercutting or toe erosion by fluvial erosion and bank failure by mass wasting. In *Figure 10* this process is shown. First, subaqueous processes or bank scour cause toe erosion during high water events, leaving an unstable, undercut bank (Thorne and Tovey, 1981; Osman and Thorne, 1988; Thorne and Osman, 1988; Darby et al., 2000; Simon et al., 2000; Simon and Collinson, 2002 and Darby et al, 2007). The bank toe is the lower, sloping part of the bank. After a drop in water level, the streambank can be unstable and can collapse and deposit additional material at the bank toe. In the Bank Stability and Toe Erosion Model (BSTEM), the model that is used in this research, these two steps can also be recognized: the model consists of a toe erosion and a bank stability part. More specific information about this model can be found in *Appendix 1*. The content of this section is mainly obtained from Lawler, 1992; Lawler, 1993, Lawler et al., 1997; Lawler, 2004; Lawler, 2005; Simon et al., 2000, Simon and Collision, 2002 and Kleinhans, 2011.

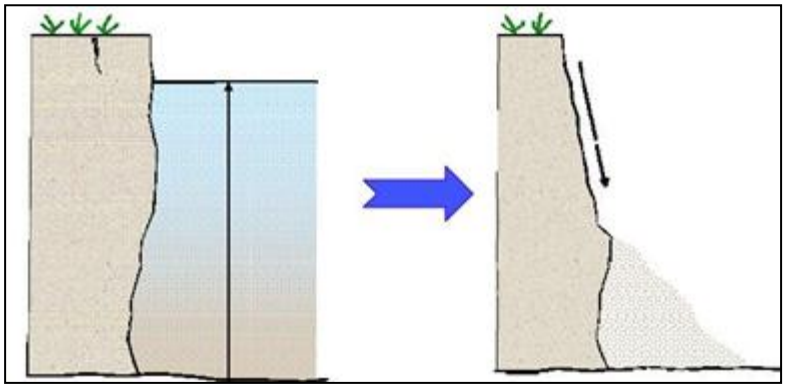

Figure 10: Process of bank erosion: toe erosion during high water followed by bank instability leading to mass failure during low water (after VT-BSE-TMDL Centre, 2006).

3.1.1. Bank undercutting by toe erosion

The rate of bank undercutting by toe erosion due to fluvial erosion depends on the flow shear stress and the strength of the sediment at the base of the banks. Although shear stress can be argued to increase with depth, the flow pattern in bends, particularly in sharp bends, has not been clarified to such extent that it is clear how exactly banks are eroded.

There are two processes that can cause bank undercutting: bank scour and subaqueous processes. Bank scour means erosion due to flow and is also called fluvial entrainment. The water that streams along the bank scours the sediment away. The process of scour is closely related to near-bank flow energy conditions. This means that with increasing flow velocity, the shear stress and the erosive power also increase. At a high flow velocity the entrainment is larger than at a low flow velocity. The shear stress is the force per unit area. There is often a spatial delay between the maximum velocity and the maximum shear stress. This is partly because the secondary circulation leads the high velocity surface flow across the channel, but limits the movement of the high velocity flow near the wall. The latter is responsible for the region with the peak of boundary shear stress. Also the deepening of the bed near the outer bend decreases the near wall velocity, which slows down the crossover of the region of high boundary shear stress (Bathurst et al., 1979). Due to the delay, the location with the maximum velocity is not necessary the location with the highest shear stress. Bank scour is often dominant in small streams with non cohesive bank material and in the upper reaches of large streams and rivers. Second processes that can cause bank undercutting are subaqueous processes. Subaqueous processes are processes under the ground and refer to weathering processes through the action of local climatic variation. Examples are freeze-thaw activity, drought and groundwater movement (Thorne, 1982).

To determine the force on a bank, the excess of shear stress (τ_{ex}) is used instead of discharge because discharge is not a direct measure of force (Julian and Torres, 2006). The excess shear stress is determined by the bank shear stress (τ_{bank}) minus the critical shear stress (τ_{cr}). According to Julian and Torres (2006), the maximum peak of excess shear stress best predicts the amount of bank erosion for moderately cohesive banks, while the variability of all peaks of excess shear stress best predicts the erosion for minimally cohesive banks. According to Gautier et al. (2007) and Julian and Torres (2006) the duration of the discharge event is only important in case of high discharge peaks.

3.1.2. Mass failure of the bank

The second step in bank erosion is the mass failure of the bank (Thorne and Tovey, 1981; Osman and Thorne, 1988; Thorne and Osman, 1988; Darby et al., 2000; Simon et al, 2000 and Simon and Collinson, 2002). This process is more akin to mass wasting in mountainous areas than to other fluvial processes. Bank failures denote the physical collapse of all or part of the streambanks as a consequence of geotechnical instability. Large volumes of bank material become unstable and topple or slide into the stream. Bank failure is in fact the consequence of bank scour or subaqueous processes. Mass failure is often dominant in the lower reaches of large streams. They are grouped into different types: rotational slumping (*Figure 11a),* wedge failures (*Figure 11b*), cantilever failure of undercut banks (*Figure 11c*) and toppling of vertical arranged slabs (*Figure 11d*) (Thorne et al, 1981). The type of failure reflects the degree of undercutting (if any) by toe erosion as a result of fluvial scour or subaqueous processes and the nature of the bank materials (Simon and Collison, 2002). The cantilever failure comes into existence when the upper part of the bank is stronger than

the under part of the bank. The upper part of the bank is often stronger because it consists generally of more cohesive materials, like clay and silt and dense vegetation roots are present that add extra strength. As a consequence, the upper part of the bank is undermined and so a kind of lever exists. When the undermined block (the 'cantilever') becomes unstable, it rolls or slides over the bank wall downwards.

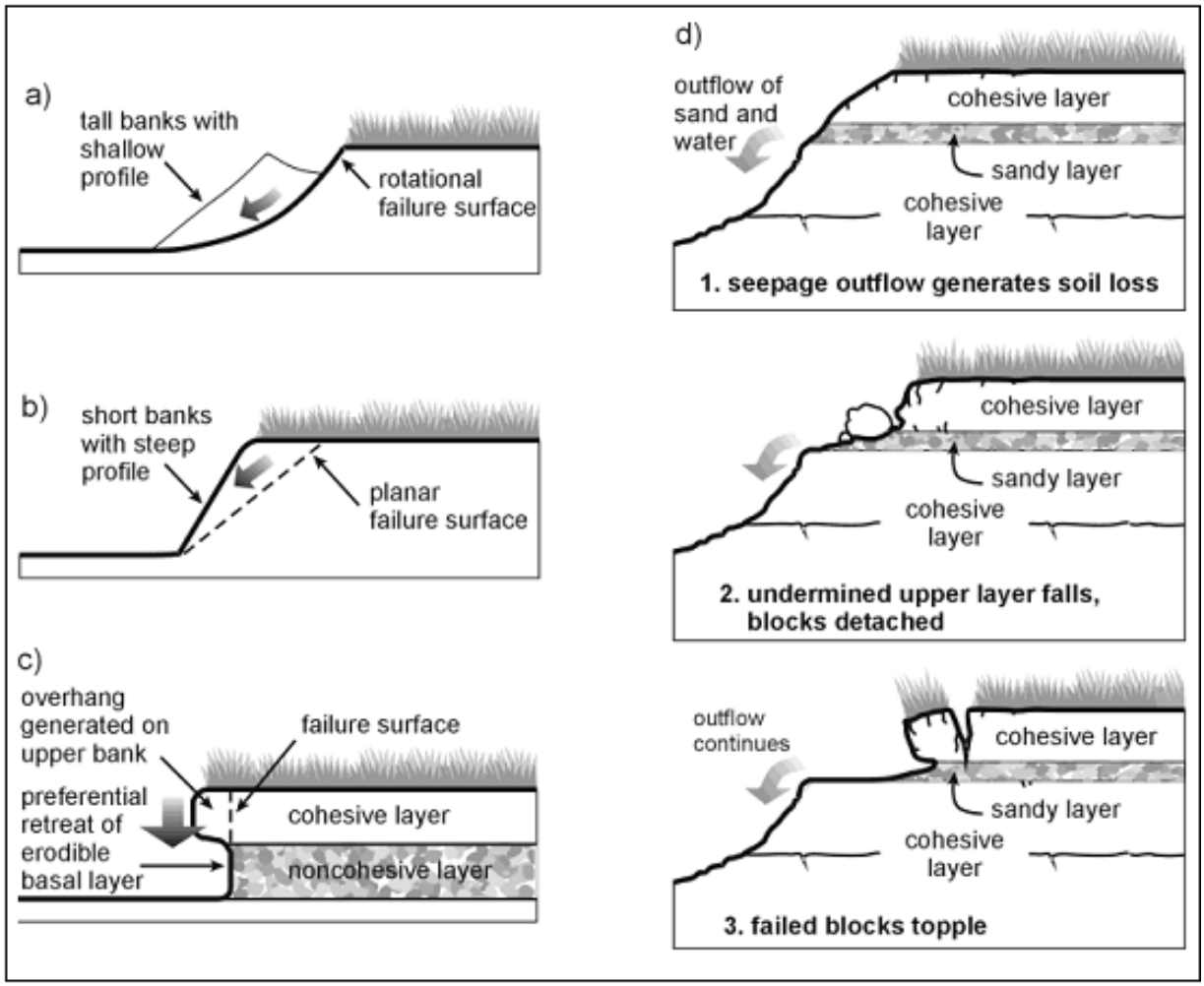

Figure 11: Different types of mass failure: a=rotational slumping, b=wedge failure, c=cantilever failure of undercut banks and d=toppling of vertical arranged slabs (Thorne et al., 1981).

There are various failure mechanisms that can occur because these mechanisms depend on bank height, bank oversteeping due to fluvial undercutting, composition and layering of the bank material, presence, nature and age of vegetation (Pollen, 2007), and history of water levels and groundwater level. In the next sections a more detailed view on these factors is given. Once a failed block deposits on the river bed, it modifies the morphology and the flow locally. Eventually, it will be eroded by the flow. The composition and possible vegetation on the block determine how long the block remains in place and to what extent it protects the bed (Fagherazzi et al., 2004).

The stability of a bank is often represented by the 'factor of safety (Fs)'. This is determined by the interaction of stabilizing and destabilizing forces: Fs = resisting forces (shear strength) / driving forces (shear stress) (Simon and Collison, 2002). Streambank collapse happens when the driving forces are

larger than the resisting forces. Thus, factors of safety larger than one indicate bank stability and values smaller than one indicate instability.

3.2. Factors determining the rate of bank erosion

The factors that determine the rate of bank erosion can be grouped into factors that determine the flow shear strength and factors that determine the bank strength.

3.2.1. Factors determining the flow strength

One of the factors that influences the flow strength is the valley slope. A steeper slope leads to a higher stream power leading to more bank erosion.

A second factor that influences the flow strength is the discharge. A larger discharge correlates to higher velocities and higher depths, leading to a higher flow strength. As a result, most erosion occurs during flood peaks and most deposition occurs during tranquil circumstances. Besides a higher flow strength, a higher depth also causes a larger flow adaptation length and shifts the area of maximum erosion in downstream direction. Also, the deeper the water, the larger the meander length and the larger the meander amplitude.

The last factors that influence the rate of erosion via the flow shear strength are the properties and the form of bends including the curvature of bends. According to Knighton (1998), the rate of migration is empirically largest when $2 < r_c / w < 3$ with r_c being the mean radius of curvature and w being the channel width. The sharper the bend is, the smaller the radius of curvature is. The rate of migration decreases with bends sharper than $r_c / w < 2$, probably because erosion is not concentrated on the outer bank anymore. In *Section 2.4.1.* it was noticed that bends are classified as sharp when $r_c /w < 2$. Hence, it can be concluded that sharp bends have a small migration rate. When bends are gentler than $r_c / w > 3$, the rate of migration also decreases. This is because bank erosion is spread out over a larger part of the outer bank (Hooke, 2006).

According to Friedkin (1945) during low water the highest flow strength is often concentrated at upstream parts of the bends. During intermediate water levels the highest flow strength is concentrated at the apex and during high water the highest flow strength is downstream of the apex.

3.2.2. Factors determining the bank strength

The shear strength of a streambank with a saturated soil can be described by the law of Mohr-Coulomb (*Equation 2*) (Simon and Collison, 2002).

(Eq. 2) $\tau_f = c' + (\sigma - \mu_w) \tan (\phi')$

In which:
- τ_f = soil shear strength stress (kPa)
- c' = effective cohesion (kPa)
- σ = normal stress (kPa)
- μ_w = pore-water pressure (kPa)
- ϕ' = effective angle of internal friction (degrees)

According to Pollen-Bankhead and Simon (2010) streambank stability is particularly sensitive to changes in groundwater table and therefore in soil matrix suction. The matrix suction is the same as

the negative pore-water pressure. An increase of pore water in the bank material leads to an increase of pore water pressure (μ_w in *Equation 2*). Due to an increased pore pressure the cohesion decreases and the bank strength decreases (Simon and Collision, 2002) (*Equation 2*). An increased matrix suction leads to a higher cohesion and to a higher bank strength. It was shown that a small increase in positive pore pressures can already trigger mass failures and thus bank erosion. The strength of streambanks also depends largely on the lithology of bank material and the lithology of bed substrate, which determine the degree of cohesion *(Wolfert, 2001).* Clay loams and densely rooted peat soils provide stability to banks because of their large cohesion, while gravels, sand and some silts are associated with higher rates of bank erosion as they have a much smaller cohesion. The cohesion is expressed as a stress. It can be interpreted as the total of attractive forces between particles per representative bulk area. The larger the cohesion is, the larger the bank strength is (*Equation 2*). According to the Bank Stability and Toe Erosion model (BSTEM) also the bank elevation and bank slope influence the streambank strength. Due to a different distribution of forces on the bank, a high, steep bank is more sensitive to erosion than a gentle, low bank (Simon and Collision, 2002). Finally, it is expected that the type and density of vegetation is very important for the bank strength. The effect of vegetation on bank strength is discussed in *Section 3.3.*.

3.3. Effects of vegetation on streambank erosion

The influence of vegetation on the rate of bank erosion is relatively high in small rivers and streams, especially because of added strength due to roots (Wolfert, 2001). The shallow water depth of streams in combination with the low potential specific stream power makes streams highly suitable for submerged and floating plants (Wolfert, 2001). Pioneer vegetation settles on the higher and better drained grounds (or perhaps on the wetter near-channel grounds in semi-arid regions) and successes into riparian forest (Johnson, 1994; Tal and Paola, 2007; Perucca et al., 2007). Vegetated channels erode more slowly than non-vegetated ones and are in general they are deeper and narrower than non-vegetated channels (Gran and Paola, 2001). Plant growth also has additional effects on the formation and distribution of bed forms. Stems and leaves obstruct the flow, which disturbs the regular interaction between the water and the bare channel bed. In general, solitary plants induce scour around stems and exposed roots, followed by local downstream deposition, whereas dense vegetation results in reduced flow velocities, enhancing deposition of bed load (Wolfert, 2001) and decreasing erosion. In this section and also in this research in general, there is concentrated on the effect of vegetation on banks and not on the effect of vegetation on the floodplain and the bed.

3.3.1. Stabilizing effect of vegetation

Several effects of vegetation on streambank erosion that have a stabilizing effect can be mentioned. The first effect is root binding. Due to root binding, the bank stability increases and consequently the threshold shear stress needed to initiate sediment transport increases (Perucca et al., 2007 and Tal and Paola, 2007). Plant roots provide mechanical reinforcement to a soil matrix due to the different responses of soils and roots to stresses (Greenway, 1987). Soil is strong in compression but weak in tension. Conversely, roots are weak in compressing, but strong in tension. The presence of roots in the soil thus produces a reinforced matrix in which stress is transferred to the roots during loading of the soil (Thorne, 1990). The ability of roots to resist pullout is a function of root length, branching patterns, root tortuosity and soil type (Abernethy and Rutherfurd, 1998). A second effect of

vegetation is that vegetation increases the matric suction which leads to more stable streambanks (Section 3.2.2.) (Pollen-Bankhead and Simon, 2010). A third effect of vegetation is that vegetation causes an increase of hydraulic resistance. Consequently, the local velocity decreases and the drag velocity increases. This results in a reduction of the fluid stress available for erosion and transport (Perucca et al., 2007 and Tal and Paola, 2007) and thus leads to a decrease of streambank erosion. The vegetation cover and the corresponding litter have also influence on bank erosion because it protects the soil surface from erosion. The last noticed stabilizing effect of vegetation is that it protects the bank from extreme temperature fluctuations. This minimizes the subaqueous processes like freeze-thaw activity (Abernethy and Rutherfurd, 1998). Due to these effects, vegetation on inner-bend bars promotes the transition from bar to levee so that the channel maintains its width.

3.3.2. Destabilizing effect of vegetation

The above mentioned effects of vegetation all have a stabilizing effect on bank erosion. However, there are some theories that vegetation can also have a destabilizing effect (Simon and Collison, 2002). A hypothesis is that vegetation improves the soil structure by rooting and litter production and promotes the soil biological activity. This results in meso- and macropores that increase the infiltration capacity which has, according to Mamo and Bubenzer (2001a and 2001b), a destabilizing effect. Another theory about the destabilizing effect of vegetation is that, due to interception and stem flow, rainfall concentrates locally around the stem of plants. This results in a deep concentrated flow into the banks (Simon and Collision, 2002). This hydrologic effect is largest in arid or semi-arid channels, because these channels are normally unsaturated. Another effect of vegetation that can also have a destabilizing effect is that large trees and other objects can add significant load to a riverbank. This additional load is also called surcharge. It has both a stabilizing and a destabilizing effect (Thorne, 1990). The net effect of surcharge is determined by the slope of the shear stress and the effective friction angle of the soil. In most cases the net effect is destabilizing as a consequence of the steep shear-surface slopes of streambank failures. The bank material is most stable when it is not too dry and also not too wet. In case of a dry ground, vegetation can have a destabilizing effect because the ground becomes even dryer as the canopy reduces the amount and intensity of rainfall reaching the soil by interception (Coppin and Richards, 1990). Also, vegetation depletes the soil moisture storage by transpiration.

3.3.3. Effect of different vegetation types

The effect of each type of vegetation on the rate of bank erosion is different for several reasons. One reason for this different effect is the different rooting depth of different species. The larger the rooting depth is, the larger the stabilizing effect is. Also the rooting density has influence on the rate of erosion. A high root density leads to a low lateral mobility and to a deep and narrow channel. Root density at the bank toe is more important for bank stability than root density on the bank top, since hydraulic shear stress increases with stream depth (Davies-Colley, 1997). Root densities vary in time and space and with species. Another effect which is different for each type of vegetation is the length of roots. Long roots (>15-20 cm) do little to increase shear strength, but instead act as soil anchors (Simon and Darby, 1999). Also the root tensile strength values and the root diameters vary by species and vary in time and space (Greenway, 1987; Pollen et al., 2004; Simon and Collision, 2002.) The last reason why each type of vegetation has a different effect on bank erosion is that the mass of the above ground biomass differs for each type of vegetation.

Thus, there are several reasons why each vegetation type has a different effect on bank stability. For example grasses grow very quickly and have a dense protective ground cover which reduces surface erosion (Gray and Sotir, 1996). Herbaceous plants have leaves and stems that die down at the end of the growing season to soil level. They have no persistent woody stem above the ground, but they often form a low and dense ground cover with a shallow root system. Herbaceous plants have a greater density of fine roots as compared with woody vegetation (Tufekcioglu et al., 1999). It must be noticed that in many cases herbaceous plants are concentrated in the upper soil profile and on top of the riverbank instead of at the toe of the riverbank where hydraulic stresses are highest. Therefore, undercutting of bank is often observed (Davies-Colley, 1997). The root system of woody and herbaceous plants physically binds bank soils in place, increasing the soil critical shear stress, τ_c (Gray and Leiser, 1982). Enlarged areas vegetated by natural shrubs and forests will increase the flow resistance of the floodplain and may raise the water stages during high discharge events to unacceptably high levels (Wolfert, 2001).

3.4. Modelling streambank erosion

Streambank erosion can be modelled by use of computer models. The basic principle of most meander migration models is that the rate of erosion is modelled with a linear relationship between an erodibility coefficient and the excess longitudinal velocity (Micheli and Kirchner, 2002; Camporeatle et al., 2005 and Perucca et al., 2007) (*Equation 3)*.

(Eq. 3) $M = E * U$

In which: M = bank erosion velocity (or the lateral migration rate (Perucca et al., 2007) (m/s)
E = coefficient of erodibility (-)
U = local excess bank longitudinal velocity at the outer bank (m/s)

Also, *Equation 4* can be used to model streambank erosion. When the near-bank flow velocity is smaller than the cross-sectional averaged velocity and when the near-bank water depth is smaller than the cross-sectional averaged water depth, then no bank erosion but only deposition takes place. Consequently, the excess flow velocity and the excess water depth are used in *Equation 4* and U and H are a kind of threshold parameters (Crosato, 2007).

(Eq. 4) $M = E_u U + E_h H$

In which: M = lateral channel shift in time (m)
E_u =the flow induced erodibility coefficient (-)
U = the near-bank excess flow velocity (m/s)
E_h = the water depth induced erodibility coefficient (-)
H = the near-bank excess water depth (m)

It should be noticed that *Equation 3* as well as *Equation 4* are very simplistic ways of formulating erosion. Although there is a relation between water depth, velocity and erosion rate, these equations neglect all factors that influence bank stability, such as vegetation and bank material, i.e. it does not

depend on physical characteristics of the environment (Darby et al., 2002). As a consequence, the erodibility coefficient must be calibrated with historical data, airphotos and remote-sensing images in order to reproduce accurate channel changes (Crosato, 2007). Another problem associated with these equations is that the migration rate of the bends is often over predicted. These over predictions can be reduced by using a curvature smoothing filter. Unfortunately, besides reducing the bank erosion rate, these filters can also affect the shape of meander bends.

There are also meander migration models that include the detailed effects of bank stability, mass failure, the subsequent removal of the debris from the bed and vegetation (Darby et al., 2002). This gives a more physically based model for which no bank erodibility coefficient is necessary (Darby et al, 2002). An example of such a meander migration model is the Bank Stability and Toe Erosion model (BSTEM) (Simon et al., 2009). In the last versions of this model also vegetation can be included. In the Bank Stability and Toe Erosion Model (BSTEM) (*Appendix 1*), the RipRoot model is included. This model can calculate the added strength due to roots. In former versions of the BSTEM the added strength by vegetation was calculated by Wu et al. (1979). Wu et al. assume a simultaneous breakage of all roots. In consequence, they often overestimate the added strength due to roots. In most recent versions of BSTEM, including the RipRoot model, the added strength due to roots according to Wu et al. (1979) is still also given. RipRoot (Pollen and Simon, 2005) is a global load-sharing fibre-bundle model. It explicitly simulates both the snapping and slipping of roots through the soil matrix, by determining the minimum applied load required to either break each root or pull each root out of the soil matrix. An initial (external) load is distributed evenly between n roots. Every root has a certain strength. The initial load is increased until it exceeds the strength of one of the roots and consequently breaks. The load that was carried by the broken roots is redistributed equally to the remaining (n-1) intact roots. This is because the load does not 'disappear'. If more roots break by load distribution, the load is again distributed equally to the remaining roots. If no more roots break anymore, the model adds more load to the bundle until a certain root breaks. The model loop stops as soon as all roots have been broken or when the total load on roots is larger than the driving force on the bank. More information about BSTEM is present in *Appendix 1*.

Summary of Chapter 3

In summary, bank erosion consists of two steps. First, bank undercutting by toe erosion due to fluvial erosion takes place during high water, followed by bank failure due to mass wasting during low water. The flow strength and the bank strength determine the amount of erosion. The factors that determine the flow strength are: valley slope, discharge and the properties and the form of bends including the curvature of bends. Factors determining the bank strength are: groundwater level, lithology, bank elevation, bank slope and vegetation. Vegetation can have a stabilizing effect on banks because of root binding. Moreover, vegetation increases the hydraulic resistance and protects the soil from surface erosion due to the vegetation cover and the corresponding litter. Secondly, vegetation can stabilize banks because it protects the bank from extreme temperature fluctuations, minimizing subaqueous processes. However, vegetation can also have a destabilizing effect as a consequence of hydrological effects and surcharge. The effect of each type of vegetation on streambank erosion is different because of differences in rooting depth, root density, root diameter, root length, above ground mass and root strength. Streambank erosion can be modelled by a linear relationship between an erodibility coefficient and the excess longitudinal velocity. There are also

meander migration models in which factors, like vegetation or other detailed physical effects, can be included, for example the Bank Stability and Toe Erosion Model (BSTEM). In BSTEM the RipRoot model is included that calculates the added strength of roots.

Chapter 4. Study area

In 2008, 2009 and 2010 research was carried out by three master students. Also Waterschap Rijn en IJssel, the local waterboard, did research. Below, some general information and obtained information from researches are shown. *Section 4.1.* shows the exact location of the research area, *Section 4.2.* is about the history of the Groenlose Slinge and *Section 4.3.* is about the vision on the Groenlose Slinge. *Section 4.4.* gives an overview of the morphological and hydrological characteristics of the Groenlose Slinge and *Section 4.5.* highlights vegetation in the Groenlose Slinge.

4.1. Location

The Groenlose Slinge is part of the Slinge. The Slinge is a stream in the Achterhoek (region of the province Gelderland) in the east of the Netherlands, close to the Dutch-German border (*Figure 12*). The Slinge arises eastward of Winterswijk, flows to the north over a sandy ground and pours into the stream the Berkel (*Figure 13).* Near Winterswijk the Slinge is fed by the Ratumse beek, the Willinkbeek and the Beurzerbeek ('beek' is Dutch for stream) (Waterschap Rijn en IJssel, 2008). These streams arise in Germany close to the Dutch-German border on a high plateau. Because of their limited size, they are not represented in *Figure 13.* The research area is to the west of Beltrum, between Groenlo and Ruurlo (*Figure 13 and Figure 14*). This part of the Slinge is called the Groenlose Slinge. Notice that in *Figure 13* as well as in *Figure 14* the Groenlose Slinge is still a straight stream.

Figure 12: Location of research area (BRIDGIS Bv, Tiel, 2008 by Jansen, 2009).

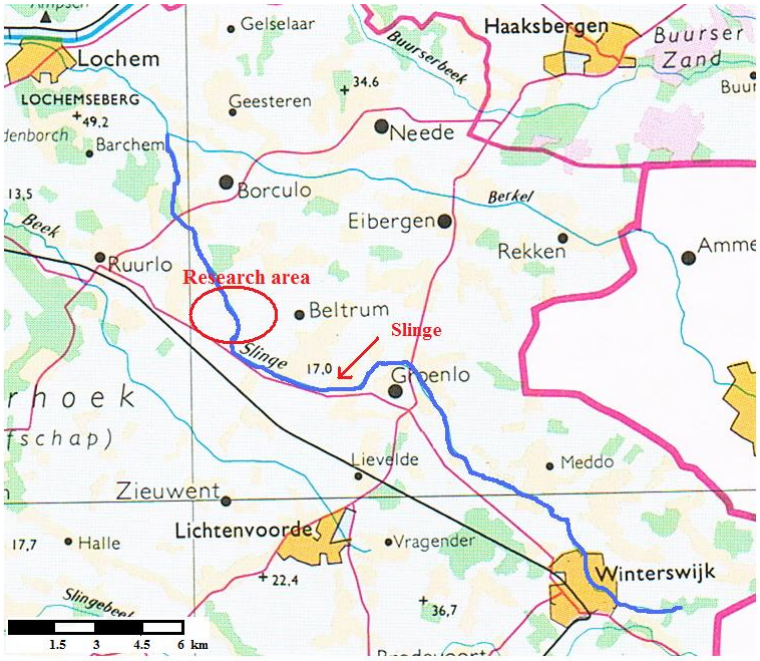

Figure 13: Location of the Groenlose Slinge and research area (After De Grote Bostatlas 2001/2002). Notice that the Groenlose Slinge is still a straight stream.

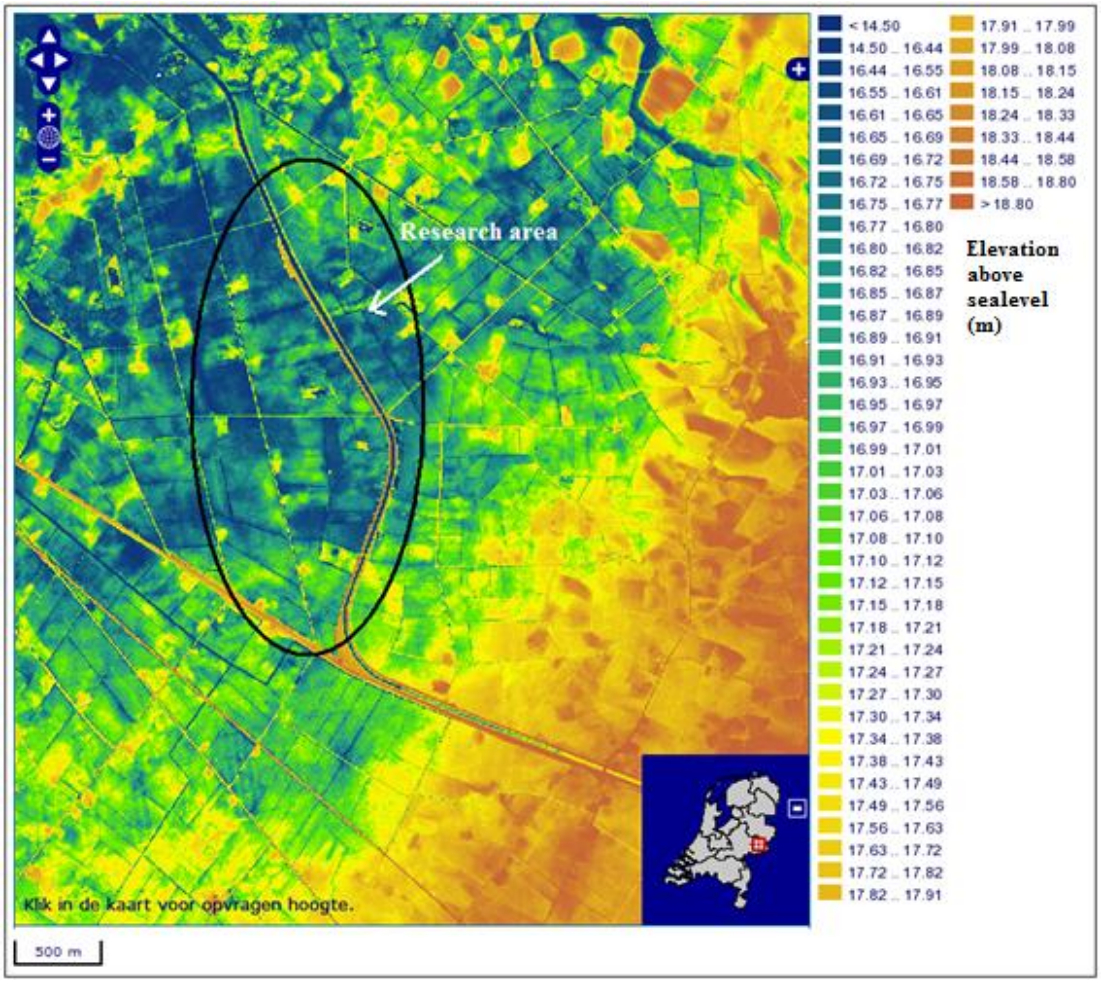

Figure 14: AHN (Algemeen Hoogtebestand Nederland) around the Groenlose Slinge and research area (www.ahn.nl/viewer, 2011). Notice that the Groenlose Slinge is still a straight stream on the figure.

4.2. History

By nature the Groenlose Slinge is a meandering stream. However, in the 1960s the stream was canalised within the framework of drainage of the Roerlose broek ('broek' is Dutch for marsh), so more agriculture could take place (Bollen Weide, 2011). As a result of canalisation, the Groenlose Slinge became a straight stream with high banks and had the function of a large drainage channel. From summer 2007 to spring 2008 this stream was partly transformed back to a shallow, meandering stream by digging bends. These plans already arose in 1992, but when in 2004 the Grolsch factory in Groenlo closed, more space became available and detailed plans could be made (Bollen Weide, 2011). The available space has the largest influence on the locations of the bends. Before re-meandering took place, the upper layer of (former) farmland was removed. Accordingly, the vegetation was scarce after re-meandering. This situation introduced an unique opportunity to study re-meandering of a stream and the effect of vegetation in its infancy.

4.3. Vision

The vision of re-naturalization of the Groenlose Slinge arose in 1992. The target image of a dynamic meandering stream was pursued. This is the highest possible category and has the best match with a natural stream. Recently, the target image of the Groenlose Slinge was refined to a stream with structure rich banks. These structure rich banks consist of an alternation and gradual transition of trees and shrubs, high rough vegetation, low vegetation consisting of grasses and herbs and sandy, bare parts. This target image can only be achieved by grazing of horses during the growing season. It is estimated that about two horses per five ha are necessary (Hanny ter Maat, Waterschap Rijn en IJssel, 2011). Cows and sheep are not suitable because these animals do not eat woody vegetation. For that reason cows and sheep are not able to prevent closing by trees and shrubs.

4.4. Overview of several hydrological and morphological characteristics

In *Table 2* some hydrological and morphological characteristics of the Groenlose Slinge are summarized. These values are based on fieldwork carried out by Waterschap Rijn en IJssel or by one of the three Utrecht University students.

The recurrence interval of bankfull discharge is 74 days which means five days of bankfull discharge per year (Jansen, 2009). It is determined that only 182.5 days a year the discharge is above the threshold for sediment motion (2008). This means that over half of the year there will not be any sediment transport and consequently not any channel migration. Discharges larger than the maximum bankfull discharge occur approximately 0.25 days a year (Jansen, 2009). Although bankfull discharge occurs just a few days a year, it still causes the largest sediment transport.

In 2008 and also in 2011 some scroll bars were observed in the Groenlose Slinge, but the typical ridge and swale topography was still absent. In *Figure 15,* a scroll bar in the Groenlose Slinge is shown. Besides bars, also bank collapse in the outer bends could be detected (*Figure 16*).

The D_{50} of the sediment is equal to $1.7*10^{-4}$ m and is classified as very fine sand. The D_{90} of the sediment and the D_{10} of the sediment do not differ significantly. Thus, it can be concluded that the sediment is very well sorted and is very uniform.

Characteristic:	Unit:	Value:	According to:	Year:
Catchment area / drainage area	ha	19,000	WRIJ	2011
Length of stream	m	35 km	WRIJ	2011
Type of stream according to WFD		R5	WRIJ	2011
Recovery length	m	14 km	WRIJ	2011
Average low water depth to bottom	m	0.4	Jansen	2008
Average low water depth to non-compacted sediment	m	0.34	Jansen	2008
Depth	m	1	WRIJ	2011
Maximum average low water depth	m	0.8	Jansen	2008
Minimum average low water depth	m	0.1	Jansen	2008
Bottom width	m	7	WRIJ	2011
Maximum width	m	17.04	Jansen	2008
Average low width	m	9.27	Jansen	2008
Average high water velocity	m/s	0.4	Jansen	2008
Bankfull discharge	m^3/s	4.97 – 9.12 (average 7)	Jansen	2008
Discharge during fieldwork summer 2008	m^3/s	0.5	Van de Kruijs	2008
Discharge 1 to 2 days a year	m^3/s	15.5	WRIJ	2011
Low discharge	m^3/s	0.11 – 0.12	Jansen	2008
Average bend angle	deg	14.4		
Average radius of curvature	m	88	Jansen	2008
r_c/w	-	5.17	Jansen	2008
r_c/w	-	4.24	Jansen	2008
Sinuosity	-	1.3	Jansen	2008
Average transverse bed slope	-	0.103 (most profiles) / 0.088	Jansen	2008
Average water surface slope	-	0.00001052 (10.5 cm/km)	Jansen	2008
Slope valley	-	0.0002	Jansen	2008
Taluds	-	1:3 to 1:4	WRIJ	2011
Particle diameter	m	$1.1*10^{-4}$	Wytema	2008
D_{50}	m	$1.7*10^{-4}$	Jansen	2008
D_{90}	m	$3.4*10^{-4}$	Jansen	2008
D_{35}	m	$1.4*10^{-4}$	Jansen	2008
D_{10}	m	$9*10^{-5}$	Jansen	2008
Cohesion	kPa	5.8	Wytema	2008
Critical shear stress	Pa	0.08	Wytema	2008
Mean soil friction angle	deg	31.8	Wytema	2008
Shear surface angle	deg	60.9	Wytema	2008
Average migration rate of the bends	m/yr	3.55	Jansen	2008
Erodibility coefficient	cm^3/Ns	0.345	Wytema	2008

Table 2: Hydrological and morphological characteristic values of the Groenlose Slinge.

Figure 15: Scroll bar in the Groenlose Slinge, 2011.

Figure 16: Bank collapse in outer bend of Groenlose Slinge, 2011.

4.5. Vegetation around the Groenlose Slinge

In 2008, the observed vegetation in the area surrounding the Groenlose Slinge varied considerably. Establishments of plants were inhibited in pools because of attenuation of light. Establishments of plants were also inhibited in erosion sensitive channels because of permanently high flow velocities. The vegetation varied from some mosses to quickly growing poplars and mature oaks in the surroundings. In 2008, Jansen globally mapped the vegetation: agriculture land, large trees on dikes (which are mainly oaks and poplars), small young willows and poplars and cane and grassland containing herbs, grasses and clovers were present. In some cross sections of the Groenlose Slinge, fossil roots and organic structures could be found at about one metre below the surface. These roots belong to older root systems of trees that have been removed. Investigation of the roots revealed that almost all strength was disappeared.

Chapter 5. Hypotheses

Supported by background knowledge on key topics of this research, hypothetical answers can be provided on the research questions. Subsequently, these answers will be tested in part III and part IV, where the field results and the model results will be described, analyzed and evaluated.

1) What are the morphological and hydrological characteristics of the Groenlose Slinge? How did these characteristics change between 2008 and 2011?

The Groenlose Slinge is a re-meandered stream. Consequently, it is assumed that the Groenlose Slinge has the morphological and hydrological characteristics of a meandering stream: This means a sinuosity larger than 1.5, one major channel, pools, point bars (scroll bars), riffles, levees, obstacle bars, potentially chute bars and chute channels, sand ripples and sand dunes. It is assumed that a helical flow is present and in case of sharp bends flow separation takes place. Also the hypothesis is that erosion takes mainly place in outer bends and deposition mainly in inner bends. Due to meander migration the bends can become sharper, leading to a smaller radius of curvature. As a consequence of damming up water, the sharper bends can lead to a lower velocity which can cause higher water levels in case of the same discharge. It is thought that the scroll bars that were present in 2008 are still visible in 2011. The significant erosion that was present in 2008 could be less in 2011 because of the vegetation that is older in 2011 than in 2008 has strengthened the banks. However, also levees, that were not present in 2008, can be present in 2011 because of discharge peaks. For the same reason, also overbank deposition could be more obvious in 2011 than in 2008.

2) What vegetation and what vegetation patterns do occur around the Groenlose Slinge?

It is assumed that in 2011 globally the same vegetation is present than in 2008, but it is expected that the density of the vegetation assemblage is larger and the vegetation length is higher. Because of succession, in 2011 also other species can be present that were not present in 2008. Because of a lateral gradient in groundwater level it is hypothesised that a lateral vegetation pattern is found. It is assumed that the vegetation in inner bends in different than the vegetation in outer bends as the vegetation in outer bends has to be more erosion resistant than the vegetation in inner bends. It is assumed that trees are more erosion resistant than grasses and herbs and for that reason it is thought that in outer bends more often trees are present than in inner bends.

3) What are the characteristics of this vegetation? What is known about their roots and their added strength?

It is hypothesized that the density of grass roots is larger than the density of tree roots and that herb roots have an intermediate density. However, it is also hypothesized that the strength of one single root is larger in case of trees than in case of grasses because of the larger diameter of tree roots. Grasses grow very quickly and have already reached their maximum added strength in an early stage. Because trees grow more slowly and have just a few roots in their young years, it is likely that grasses add more strength than young trees. However, mature trees could add more strength than grasses.

4) Where does erosion take place and what is the lateral migration rate? Does a relation between erosion and vegetation and a relation between the lateral migration rate and vegetation exist?

It is hypothesized that erosion takes place in outer bends and deposition in inner bends. According to theory the migration rate is maximal when $2 < r_c/w < 3$. Because the radius of curvature could be decreased in 2011, also the migration rate can be changed. The migration rate can also be influenced by vegetation. Especially as a consequence of root binding the vegetation can decrease the migration rate. It is assumed that this decrease is largest in case of mature forest. Whether the effect on restricting erosion is larger in case of grasses or young trees depends on the root development and thus the age of the young trees. It is assumed that herbs have an intermediate effect on decreasing the migration rate. The vegetation matured, so the added strength will have increased too. Consequently it is thought that the migration rate in 2011 is smaller than in 2008. Besides the effect on the migration rate, vegetation could have an erosion restrictive effect in the outer bends where erosion is common to take place.

5) What are hydrological and morphological characteristics in the sharp bend of the Groenlose Slinge and what is the role of vegetation in this sharp bend?

In case of sharp bends, r_c/w is smaller than two and as a result flow separation takes place. Due to this flow separation, the erosion and deposition pattern is expected to be different than in gentle bends and the migration rate is expected to be lower than in gentle bends. It is hypothesized that vegetation on the banks of sharp bends does not play any important role because the geometry of the bend has a dominant role on the morphological and hydrological characteristics.

6) How does stream bank erosion work? What processes and what factors do play a role?

Steam bank erosion consists of two steps: first, bank undercutting takes place by toe erosion due to fluvial erosion during high water and secondly, bank failure takes place due to mass wasting during low water. The flow strength and the bank strength together determine the amount of erosion. The factors that determine the flow strength are: valley slope, discharge and the properties and the form of bends including the curvature of bends. Factors determining the bank strength are: groundwater depth, lithology, bank elevation, bank slope and vegetation.

7) What are the differences between the prediction of the 2011 profile by the Bank Stability and Toe Erosion Model based on the profile of 2008 and the measured profile of 2011? What are the sensitive parameters of BSTEM and how sensitive are they? And what is the prediction of the bank erosion of 2012?

In BSTEM the radius of curvature cannot be inserted in the model. For that reason the principle that the migration rate has a peak value around a certain r_c/w value is not included. Accordingly, the possible change in migration rate of 2011 due to a possible changed radius of curvature cannot be included. Moreover, BSTEM is only able to model erosion and no deposition. Hence, it is assumed that the erosion in BSTEM is overestimated. Due to the more mature vegetation and the

corresponding increased effect of root binding, it is assumed that the predicted erosion per year in 2012 is smaller than the erosion per year in the period between 2008 and 2011. It is hypothesized that the sensitive parameters in BSTEM are reach slope, the duration of flow, the reach length, the water level, the groundwater depth, the vegetation, the lithology and the geometry.

Part II: Methods

In this part about the methods *Chapter 6* discusses the justification of the methodology. *Chapter 7* is about the field methods and *Chapter 8* is about the methods of analysing. Finally, the application of the Bank Stability and Toe Erosion Model (BSTEM) is highlighted in *Chapter 9*.

Chapter 6. Justification of the methodology

The three most straightforward ways to determine the effect of vegetation on the bank erosion pattern at the lateral migration rate are doing fieldwork, carrying out a model experiment for example in a stream tube and using computer models. In this research the methodology is fieldwork in combination with a computer model. The fieldwork took place at the stream the 'Groenlose Slinge' in the east of the Netherlands. This research area is selected because meandering and the effect of vegetation can be studied from its infancy. This is a unique opportunity and it is expected that this type of research will give promising results. In fact, it is an experiment on real scale. Jansen (2009) showed that computer meander simulation models do not give good results because these do hardly depend on physical characteristics of the environment like vegetation. In these meander simulation models also the shape of meander bends is influenced. In this research the Bank Stability and Toe Erosion Model, version 5.2. (BSTEM-5.2) is used in addition to the field results. In contrast to the model that Jansen used, vegetation can be added in this model. Wytema did already use BSTEM, but he just applied it to a few bends and it this research BSTEM will be tested more extensively than Wytema did. Data obtained from the field are used as input for BSTEM-5.2. to predict bank stability and bank erosion. Finally, the model results are compared with the field observations and measurements and in this way the quality of the Bank Stability and Toe Erosion Model can be discussed.

Chapter 7. Field methods

In this chapter different field methods are discussed. *Section 7.1.* is about the method to determine the profiles, *Section 7.2.* is about measuring bank lines and *Section 7.3.* is about measuring waterlines. Then, *Section 7.4.* is about creating the erosion and deposition map based on observations, *Section 7.5.* is about the vegetation map, *Section 7.6.* is about the airphoto map and finally, *Section 7.7.* is about the method to determine root characteristics.

7.1. Profiles

In the fieldwork area twenty cross sections were measured in November 2008, September 2009, April 2010 and June 2011. In *Figure 17 the* locations of the cross sections are shown. The length that the crow flies between cross section 1 and cross section 20 is 1530 metres. Between profile 10 and profile 11 the Zeggelinks-Hagbrug is located. In the field, the locations of these cross sections are marked with blue poles, although at some locations the poles have disappeared. In 2011 the twenty profiles were measured by geodetic instance RPS (*Figure 18*), using a surveying agency called a DGPS. In 2008, 2009 and 2010 at the same locations cross sections were measured by Waterschap Rijn en IJssel. In 2008 also three physical geography master students assisted measuring. Also the construction profiles of 2007 are known. The maximal allowed deviation for all measurements is five centimetres in the z-direction and the maximal deviation in the x and y direction is then automatically 3.3 centimetres (a factor of 1.5 smaller). In all years at least all striking nod points were measured. However, the average distance between the measurement points decreases: in 2008 the average distance was equal to 1.4 m and in 2011 the average distance was equal to 1.0 m. This means that the accuracy of the profiles has increased.

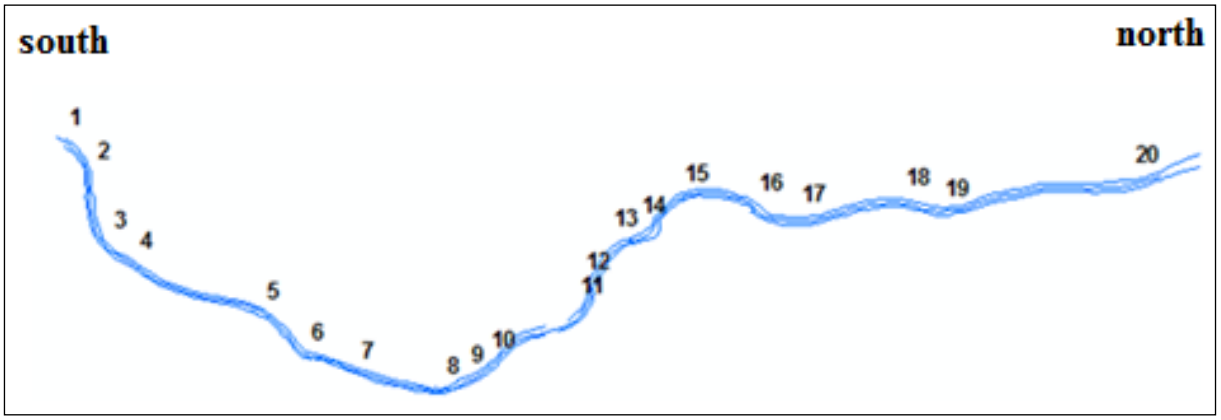

Figure 17: Locations of the twenty studied profiles in the Groenlose Slinge measured in 2008, 2009, 2010 and 2011. Length that the crow flies between profile 1 and 20 is 1530 metres. The middle of profile 1 is located at the coordinates x=233132.062 and y=453859.174 from the Dutch Rijksdriehoekstelsel and the middle of profile 20 is located at the coordinates x=232791.369 and y=454349.653 from the Dutch Rijksdriehoekstelsel. Between profile 10 and profile 11 the Zeggelink-Hagbrug is located. The profiles 5, 6, 15, 18 and 19 are located at the apices of bends.

Figure 18: Measuring of profiles by RPS using a DGPS, a measuring rod and a boat (June, 2011).

7.2. Bank lines

In order to study the migration of the Groenlose Slinge over the years, the locations of the bank lines were measured in 2007, 2008, 2009, 2010 and 2011. A bank line is obtained by connecting bank points. The location of a bank point represents an increase in bank slope (*Figure 19*). A trick to detect this bank point is that in many cases the vegetation changes at the bank line. Determining the bank point is very sensitive to different interpretations. In many cases the slope decreases twice in lateral direction; once close to the stream and once further away from the stream *(Figure 19*). When both decreases in steepness are visible the one closest to the stream is interpreted as the bank point. In June 2011 the bank line was determined by De Winter and De Keijzer as well as by RPS. RPS indicated, during measuring the 20 profiles, where they found the bank point of that profile. In the profiles (*Appendix 3*) the differences in determining the location of the bank point can be seen. De Winter and De Keijzer measured the bank points by a DGPS (Differential Global Positioning System) at a maximal interval of 20 metres, depending on the variation of the location of the bank line and on the possibility to measure. In case of forest it was difficult to find the bank point and also the satellite connection was not always good enough to measure. The maximal inaccuracy of the DGPS is 16.6 cm in the x- and y direction. After measuring, the points were plotted and were linked by lines.

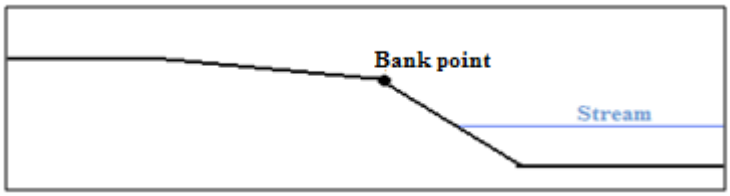

Figure 19: Position of bank point. Connecting the bank points gives the bank line.

7.3. Waterlines

Another way to study the migration of the Groenlose Slinge is determining the waterline. Like the bank lines the waterlines are also obtained by connecting points. The waterline represents simply the start of the water. In June 2011 the waterlines were determined by De Winter and De Keijzer at a maximal interval of 20 metres using a DGPS (*Figure 20*). The measuring took place in a period of four days. During this period the water level was low, varying between 15.18 m +NAP and 15.27 m +NAP

at the Zeggelinks-Hagbrug (NAP = Normaal Amsterdams Peil = normal Amsterdam Level ≈ elevation above sea level). Like the bank lines, the waterlines were also determined in 2007, 2008, 2009 and 2010 by De Winter. In contrast to the bank lines, determining the waterlines is not sensitive to different interpretations. However, the disadvantage of using waterlines for studying changes of position is that the water level is not every year the same. Also during the period of measuring the water level of the whole course can change. Although the exact water level during measuring in 2008 is not known, according to hydrographs (*Appendix 9*) and personal communication also then the water level was low.

Figure 20: Measuring the waterline points by a DGPS. Notice that it is not easy to measure the waterline at the other side of the stream because of the dense vegetation.

7.4. Erosion / deposition map based on observations

In the field, observations of erosion and deposition were done. The coordinates of the locations of these observations were written down resulting in a map with bank observation points and a corresponding list with notes. Using this list and map, a map with locations of erosion and deposition was created. Also photos with known locations were used to create the erosion / deposition map.

7.5. Vegetation map

The vegetation map is based on the airphoto map as well as on observation points. The observation points are often located on borders or transitions of different vegetation. Also photos with a known location were used to create the vegetation map.

7.6. Airphoto map

The airphoto map was used to create the vegetation map. The airphotos taken by the Unmanned Airborne Vehicle of University Utrecht, controlled by Henk Markies, were put together in ArcGIS using the georeferencing option. The topographical map was used as background. In first instance, known points on the photos were referred to the same recognized points on the topographical map.

However, because the topographical map is from before the re-naturalisation and not everything on the photos can be recognized on the topographical map also a second way was used to georeference photos. This second way was looking for corresponding points on two pictures and then link these points. In the field also some ground control points were measured, for example at the edge of a corn field or at the edge of a picknick seat. However, this method was not accurate enough to use for georeferencing. At some locations it was very difficult to stick the airphotos together because of no recognized points. In those cases the vegetation map was used as background. Also in 2008 an airphoto map was created by Jansen. Unfortunately, the accuracy of the positions in the photo maps of 2008 and 2011 was too low to determine the amount of lateral migration by comparing the air photos. Also, the imageresolution was too low to distinguish the small morphological characteristics.

7.7. Root characteristics

In the field observations of roots were done. Characteristics like density of roots, root diameter and root length were written down. It was difficult to do good root observations because the roots are in general below the surface. However, they could be studied because sometimes roots were exposed due to erosion or small vegetation was dug out. In other, most cases, the sand above the roots was dug away. In case of measuring the root diameters, the thickest part of the root was measured and the branches of roots were not included.

Chapter 8. Methods of analysing

This chapter discusses how the field data was analysed to deliver other results and to reduce the data. *Section 8.1.* is about determining averaged morphologic parameter values, *Section 8.2.* is about determining the significance of relations and differences, *Section 8.3.* is about determining water levels and *Section 8.4.* is about determining lateral migration. *Section 8.5.* discusses determining the centre of gravity and *Section 8.6.* discusses determining the radius of curvature and the sinuosity. Next, *Section 8.7.* is about determining the net amount of erosion or deposition, *Section 8.8* is about determining and analyzing other morphologic and hydrologic characteristics and *Section 8.9* is about interviewing a hydrologist, an ecologist and a technical employee.

8.1. Averaged morphologic parameter values

For many results it is important that the average value of the concerning parameter over the whole course, between profile 1 and 20, is given. When calculating the average value of a specific parameter over the whole course, it is assumed that the value measured at a profile is representative for the part downstream and upstream of the profile up to the middle between two profiles. The average value can be calculated by *Equation 5*:

(Eq. 5.)

$$\text{averaged over the whole course value (y)} = \frac{\sum_{i=0}^{N-1}((x_i - x_{i-1})/2 + (x_{i+1} - x_i)/2) * Y_i)}{\sum_{i=0}^{N-1}((x_i - x_{i-1})/2) + (x_{i+1} - x_i)/2))}$$

In which: Y_i = calculated value at x_i
i = certain point in the linear regression series (numerical mathematics)
+1 or -1 = one step forward or one step back in the linear regression series (numerical mathematics)

8.2. Significance of relations and differences

In this research relations between several parameters are discussed, for example the relation between different lateral migration methods or between the width and the elevation of the profiles. The significance of the relations can be shown at a 5%-error level (95% confidence level) (Wonnacott and Wonnacott, 1990). To check this significance, the values of one parameter have to be plotted on the y-axis and the values of the other parameter on the x-axis. Then a linear trend line with a known equation has to be fitted through the points. Next, several values have to be calculated: the y^ (the y-value according to the equation), y-y^, $(y-y^)^2$, sum($(y-y^)^2$), $x_{average}$, $x-x_{average}$, $(x-x_{average})^2$, sum($(x-x_{average})^2$). Also the degrees of freedom have to be known and are equal to the amount of combinations (n, observations) minus two. In the next step the residual variance (s^2) can be determined by *Equation 6* and the estimated standard error can be calculated by *Equation 7*. b is equal to the slope value of the equation of the fitted trend line and $t_{.025}$ is equal to the t-value at a 5%-error level which can be looked up in a table. The t-value depends on the degrees of freedom and the error level. Finally, the 95% confidence interval for the slope can be calculated (*Equation 8*).

When this interval includes zero, the relation is not significant at a 5%-error level and when this interval does not include zero the relation is significant at a 5%-error level.

(Eq. 6) $s^2=(1/(n-2))\sum(Y-Y\hat{})^2$

In which: s^2 = residual variance
n = degrees of freedom
Y = y-value
Y^=estimated y-value

(Eq. 7) $SE = s/(\sqrt{(\sum(x-x_{average})^2)})$

In which: SE = estimated standard error
s = standard deviation
x = x-value
$x_{average}$ = average x-value

(Eq. 8) $\beta = b \pm t.025(s/\sqrt{(\sum(x-x_{average})^2)})$

In which: β = confidence interval for the slope
s = standard elevation
x = x-value
$x_{average}$ = average x-value

Apart from the significance of relations, in this research also the significance of differences between 2008 and 2011 is given. For example, it is studied whether the change in bank elevation is significant or not. For each difference a 95%-significance interval can be calculated by *Equation 9*. Again, when this interval includes zero the difference is not significant at a 95%-significance interval and when the interval does not include zero the difference is significant at a 95%-significance interval.

(Eq. 9) Upper difference: $d + Z_{.025} * SE$
Lower difference: $d - Z_{.025} * SE$

In which: x = mean difference between 2011 and 2008 (value 2011 – value 2008)
$Z_{.025} = 1.96 \approx 2$
SE = standard error (Eq. 10)

(Eq. 10) $SE = s/\sqrt{n}$

In which: SE = standard error
s = standard deviation (Eq. 11)
n = amount of observations

(Eq. 11) $s = (\sqrt{\sum((x-d)^2)})/ (n-1)$

In which: s = standard deviation
d= mean difference between 2011 and 2008 (value 2011 – value 2008)
$x = \sum(d-d_{gem})^2$

8.3. Water levels

In the twenty profiles of 2008 and 2011 a high waterline and a low waterline have been drawn. The low waterline is based on the waterlines of the waterlines map. Thus, the measured waterlines are considered to be low water. At the locations of the cross sections the distance between the west-beginning of the profile (a blue pole in the field) and the west- and east waterline were measured using ArcGIS. Then this distance was put in the corresponding cross sections and a corresponding elevation could be found. It was expected that the elevation at the west side and the east side of the profile are about the same. However, after applying this method of determining the elevation by inserting the distance, it was shown that this is not always the case. The difference between the east and west water elevation can vary up to 40 centimetres. Three reasons can be noticed for this difference. The first reason is measurement inaccuracy. A second reason is that the waterline is not exactly measured at the location of the profile but at random points that were linked together. A third reason is that the east- and west waterline were not measured at exactly the same moment which could result into a different water level. When a difference between the west and east part exists, an average value of the water level is taken.
The high water level is based on the bankfull water level. In theory there are two ways to determine the bankfull water level. The first method is applying the 'Top of the bank' definition. According to this method the bankfull elevation is at the beginning of the floodplain, i.e. a relatively horizontal area (Jansen, 2009). The second method to determine bankfull waterlevel is the 'Bank inflection' method. This method takes the bankfull elevation at the break in the bank slope, i.e. the end of the abrupt part of the bank. In practice these two methods cannot always easily be distinguished. In this research a combination of both methods was used. In one profile the first method was used, in another profile the second method was used and in other cases a combination was used. The high water level determined at one bank is also representative for the bank top level. Both sides of the stream have often a different bankfull elevation. Because the water level is more or less horizontal, the bank side with the lowest bankfull elevation was chosen as the high water level.

8.4. Lateral migration

Lateral migration can be represented in different ways: the lateral migration of the centres of gravity of profiles can be determined and the lateral migration of the deepest points of profiles can be determined. Also the migration of the low waterlines and the migration of the top of banks can be representative for the lateral migration of the Groenlose Slinge *(Figure 21)*. Besides, also observations in the field can show characteristics of lateral migration (erosion or deposition). The migration of the centre of gravity is a very robust way to qualify the lateral migration. The migration of the lowest point represents the migration of the thalweg, while the low waterline represents the lateral migration of about the middle of the profile. The observations and the migration of the tops of the banks are most representative for the migration of the top of the bank.

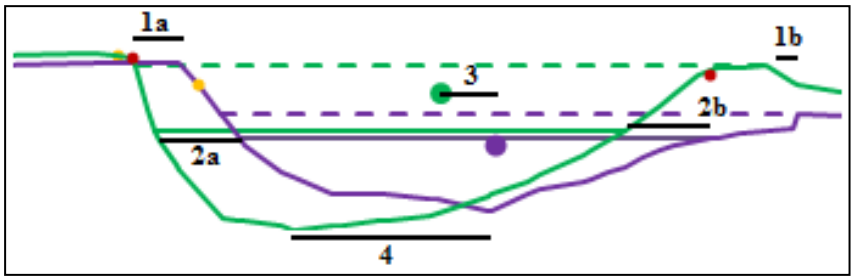

Figure 21: Different ways to determine lateral migration (1a=lateral migration top bank west, 1b=lateral migration top bank east, 2a=lateral migration low waterline west, 2b=lateral migration low waterline east, 3=lateral migration centre of gravity and 4=lateral migration lowest point).

The average lateral migration of the different methods was calculated. This average value could be relatively low, because positive as well as negative values are included when the different methods show different directions of migration. Because the different methods represent different parts of the profile, the mean value of these different methods, including postive and negative values, is most representative to show lateral migration of the whole east or west part of the profiles. For the west parts the average of the migration of the west waterline, the west bank top line, the lowest point and the centre of gravity was taken. For the east parts the average of the migration of the east waterline, the east bank top line, the lowest point and the centre of gravity was taken. In the next step the average migration over the west part of all profiles as well as over the east part of all profiles was calculated. In these calculations the absolute values of migration were used. Next, also the migration averaged over the mean east and the mean west bank migration was determined.

8.5. Centre of gravity

The centre of gravity in case of a two dimensional figure is the point in the figure which is the average location of its entire surface. When the figure should hang on a string going through this point, the two dimensional figure is exactly in balance. For the profiles the centre of gravity was determined for the surface up to the high water level. In *Figure 22 the* centres of gravity are shown for profile 18.

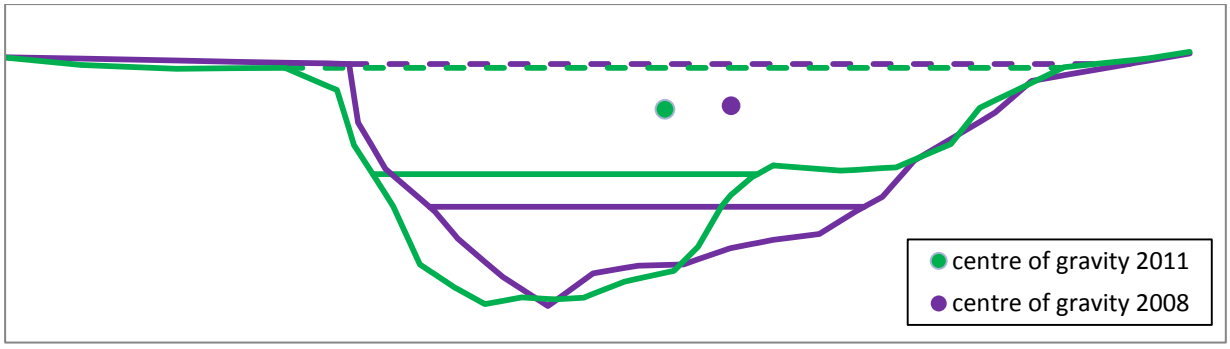

Figure 22: Centres of gravity (2008 and 2011) for profile 18 of the Groenlose Slinge.

The x-coordinate of the centre of gravity can be calculated by *Equation 12* and the y-coordinate can be determined by *Equation 13*.

(Eq. 12) $$x(\text{centre of gravity}) = \frac{\sum_{i=0}^{N-1}(x_i * y_1 * (x_{i+1} - x_i))}{\sum_{i=0}^{N-1}(y_i * (x_{i+1} - x_i))}$$

In which: x= x-coordinate centre of gravity (m)
y = y-coordinate centre of gravity (m)
y_i = y-value at x_i (m)
i = certain point in the linear regression series (numerical mathematics)
+1 = one step forward in the linear regression series (numerical mathematics)

(Eq. 13) $$y(\text{centre of gravity}) = \text{highest y} - \frac{\sum_{i=0}^{N-1}((h_i + h_{i+1})/2) * (x_{i+1} - x_i))}{\sum_{i=0}^{N-1}(h_i - y_i)}$$

In which: h = highest y - y_i (m)
x = x-coordinate profile (m)
y = y-coordinate centre of gravity (m)
y_i = y-value at x_i
i = certain point in the linear regression series (numerical mathematics)
+1 = one step forward in the linear regression series (numerical mathematics)

8.6. Radius of curvature and sinuosity

The radius of curvature indicates the sharpness of a bend (*Figure 1, Section 2.2*). It can be determined by choosing three points on the centreline. The centreline is located in the middle of the west and east waterline and this line was drawn in ArcGIS. By applying some equations the radius of curvature can be calculated when the coordinates of the three points are known. The points are called P_1, P_2 and P_3 and the coordinates can easily be known using ArcGIS. Because the sharpness of a bend varies along the stream, the distances between the points are always between 20 and 21 metres. The central point, P_2, is located at the concerning cross section. The radius of curvature can be calculated using the principle shown in *Figure 23.* Two lines can be formed through two pairs of the three points, the first line (line a) passes through the first two points P_1 and P_2. Line b passes through the next two points P_2 and P_3.

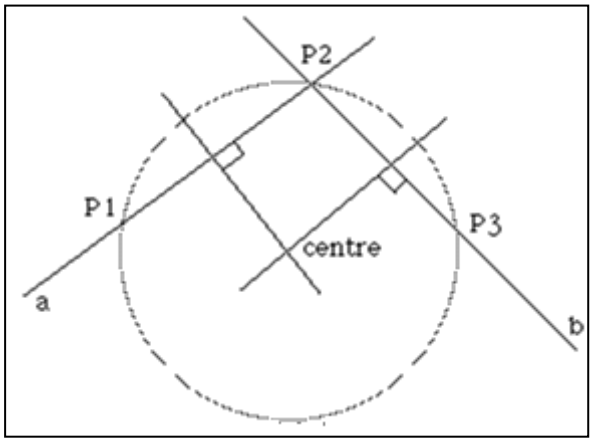

Figure 23: Principle to determine the centre of a circle (Bourke, 1990).

The equations of line a and b are given by *Equation 14* and *Equation 15* respectively. In those equations m_a and m_b are equal to the slope of the line which can be calculated by *Equation 16* and *Equation 17* respectively.

(Eq. 14) $y_a = m_a (x - x_1) + y_1$

(Eq. 15) $y_b = m_b (x - x_2) + y_2$

(Eq. 16) $m_a = (y_2-y_1)/(x_2-x_1)$

(Eq. 17) $m_b = (y_3-y_2)/(x_3-x_2)$

The centre of the circle is the intersection of the two lines perpendicular to and passing through the midpoints of the lines p_1p_2 and p_2p_3. The perpendicular of a line with slope m has slope -1/m. *Equation 18* shows the equation of the line perpendicular to line a and passing through the midpoint p_1p_2 and *Equation 19* shows the equation of line perpendicular to line b and passing through midpoint p_2p_3. Then the x-coordinate of the centre of radius of curvature is represented by the intersection of those two lines (*Equation 20*). The y-coordinate can be calculated by substituting the calculated x-value (*Equation 20)* in *Equation 18* or *Equation 19*. As now the coordinates of the centre are known and also the coordinates of the points on the circle are known, the radius can easily be calculated by *Equation 21*. Because applying all those equations for each bend, for each profile and for 2008 as well as for 2011 is quite time consuming, the equations were implemented in Python.

(Eq. 18) $y'_a = -1 / m_a (x - (x_1 + x_2) / 2) + (y_1+y_2) / 2$

(Eq. 19) $y'_b = -1 / m_b (x - (x_2 + x_3) / 2) + (y_2+y_3) / 2$

(Eq. 20) $x = (m_am_b(y_1 - y_3) + (m_b(x_1 + x_2) - m_a(x_2 + x_3)) / (2(m_b - m_a))$

(Eq. 21) $r_c = \sqrt{((P_x - x)^2 + P_y - y)^2)}$

The sinuosity of the whole course was determined by dividing the centre line length from profile 1 to 20 by the length that the crow flies between profile 1 and profile 20.

8.7. Net amount of erosion or deposition

The amount of net erosion or deposition for the period between 2008 and 2011 was determined by the profiles of 2008 and 2011. The surface under the profile of 2011 minus the surface under the profile of 2008 determines whether net erosion or deposition took place. A positive value represents deposition and a negative value represents erosion. Using *Equation 22* the net erosion or deposition at a profile can be calculated. Because the x-coordinates of the profiles from 2008 are not the same as the x-coordinates from the 2011 profiles, interpolation had to take place. In case of interpolating it was assumed that the profile between two points linearly increases or decreases.

(Eq. 22) net erosion or deposition =

$$\sum_{i=0}^{N-1}\left(\left(\frac{y_{i+1(2011)}-y_{i(2011)}}{2}-\frac{y_{i+1(2008)}-y_{1\ (2008)}}{2}\right)*(x_{i+1}-x_i)\right)$$

In which: x= x-coordinate profile (m)
y = y-coordinate profile (m)
y_i = y-value at x_i (m)
i = certain point in the linear regression series (numerical mathematics)
+1 = one step forward in the linear regression series (numerical mathematics)

8.8. Remaining morphological characteristics

Concerning the width, the low water level widths as well as the high water level widths were determined for 2008 and 2011. The low water width as well as the high water width was simply determined by subtracting the distances (x-coordinates) of the waterlines as displayed in the profiles. Because of the trapezium form of the cross sections, in all cases the high water width is larger than the low water width.

Several measurements of elevations of the profile were plot against the lateral distance: the lowest point of the profile, the elevation of the centre of gravity, the top of the bank elevation and the mean elevation. The mean elevation is the mean elevation between the top of the bank and the lowest point. To calculate the mean elevation, each 0.1 m of the distance the elevation (y-value) is determined assuming a linear relation. Then the average of those values is determined representing the mean elevation. To check whether relations between widths and elevations measurements exist also scatter plots were created.

Because the water levels as well as the deepest points are known, also the maximum water depths could be calculated. The high water level depth is equal to the high water level minus the lowest point of the profile. The low water level depth is equal to the low water level minus the lowest point.

A relation exists between the Chézy coefficient, the mean velocity, the hydraulic radius and the bottom slope given in *Equation 1 (Section 2.3).* The Chézy coefficient in this equation represents the roughness of the stream. The larger the Chézy coefficient, the smoother the roughness. In case of high water, the velocity is also high and also the hydraulic radius increases. The bottom slope remains the same. According to Kleinhans (2011, personal communication) and Jansen (2009) a logical C-value is about 25 $m/s^{0.5}$ in case of the Groenlose Slinge. Comparing this value of the Chézy coefficient with the Chézy coefficient determined by *Equation 1*, it can be checked whether the found values for v (velocity), R (hydraulic radius) and S (bottom slope) are logical values. The hydraulic radius, also used in this equation, is equal to the wet area divided by the wet perimeter and is exactly equal to the water depth in case of a rectangular cross section. The wet area is the surface of the profile below the waterline and the wet perimeter is equal to the perimeter of the cross sectional area that is 'wet'. The wet area can be calculated by *Equation 23* and the wet perimeter can be calculated by *Equation 24.*

(Eq. 23)

$$\text{wet area} = \sum_{i=0}^{N-1} ((x_{i+1} - x_i) * (\frac{h_i + h_{i+1}}{2}))$$

In which:

h = highest y - y_i (m)
x = x-coordinate profile (m)
y = y-coordinate centre of gravity (m)
y_i = y-value at x_i
i = certain point in the linear regression series (numerical mathematics)
+1 = one step forward in the linear regression series (numerical mathematics)

(Eq. 24)

$$\text{wet perimeter} = \sum_{i=0}^{N-1} \sqrt{x_{i+1} - x_i + y_{i+1} - y_i}$$

In which:

h = highest y - y_i (m)
x = x-coordinate profile (m)
y = y-coordinate centre of gravity (m
y_i = y-value at x_i
i = certain point in the linear regression series (numerical mathematics)
+1 = one step forward in the linear regression series (numerical mathematics)

8.9. Interviewing a hydrologist, ecologist and a technical employee of Waterschap Rijn en IJssel

Questions were asked to Ellen Bollen Weide (hydrologist), Hannie ter Maat (ecologist) and Domien de Winter (technical employee), all from Waterschap Rijn en IJssel. They have specific knowledge about the history, hydrology and ecology of the Groenlose Slinge which cannot be found in literature. Examples of questions are 'which species is that tree?', 'what would you do different when the Groenlose Slinge could be re-meandered again?', 'which kind of stream do you want?', 'what did you expect about the effect of vegetation?' and 'what about the WFD-score (Dutch: KRW-score)?'.

Chapter 9. Application of the Bank Stability and Toe Erosion Model (BSTEM)

This chapter is about the methods applied in the Bank Stability and Toe Erosion Model. *Section 9.1.* is about selecting profiles for BSTEM and *Section 9.2.* is about the input values.

9.1. Selecting profiles for the Bank Stability and Toe Erosion Model (BSTEM)

In order to do a good prediction for the erosion between 2011 and 2012, the modelled erosion between 2008 and 2011 and the measured erosion between 2008 and 2011 were compared to each other. The Bank Stability and Toe Erosion Model can only model erosion and no deposition. So, for the comparison between the measured and modelled erosion, only banks are suitable that suffer erosion at their whole elevation, from its lowest point to its bank top. That means that all methods to determine lateral migration must show the same direction of lateral migration. It is also whished that over the whole period between 2008 and 2011 erosion took place. This can be checked by *Appendix 2* in which the profiles of each year are shown. The profile that is inserted in BSTEM must be half of a cross section, from the most east or most west point to the deepest point. Notice that in case of a east bank, values have to be 'exchanged' from east to west because in the model only a bank can be inserted with on the east side the water. Also the top of the toe has to be inserted. The top of the toe is there where the bank slope decreases and is mostly located below the water.

9.2. Input values

This section consists of three sections: in *Section 9.2.1.* the general inputs are highlighted, *Section 9.2.2.* is about the duration of flow and the water level and in *Section 9.2.3.* the input of vegetation in BSTEM is discussed.

9.2.1. General inputs

The Bank Stability and Toe Erosion Model needs several input values which are shown in *Table 3*.

input reach length (m)	5
input reach slope (m/m)	0.0002
input duration of flow (hrs)	120
Input elevation of flow (m)	depends on profile
bank material	fine rounded sand
water table below bank top (m)	= bank top - water level in channel

Table 3: General input values in BSTEM.

The input reach length is the length over which the concerning profile is representative and is set equal to 5 m. This value was used to calculate the sediment inputs in the stream. The input reach slope and the bank material are based on former research and the input elevation of flow is different for each profile. Based on the slope, the elevation of flow and the bank material the model can determine the flow velocity. Concerning the water table below bank top, it is assumed that the

groundwater level is equal to the water level in the channel. The input duration of flow is the duration that toe erosion takes place and this will be discussed in *Section 9.2.2*..
To check the sensitivity of the model, it was checked first which parameters are sensitive to the bank stability model and which parameters were sensitive to the toe erosion model. When it was known which parameters have influence on which part of the model, the degree of sensitivity could be checked by changing the value of that parameter.

9.2.2. Duration of flow and water level

In the model also the duration of flow and the water level must be inserted. These parameters need some discussion: in BSTEM, the new failed profile due to bank erosion and the new profile due to toe erosion can be inserted and can be run again. Therefore, to model erosion in a specific period, more runs can be done. As noticed from the theory, during high water mainly toe erosion takes place and during low water mainly bank failure takes place. In this research, the erosion of a period of three years must be modelled, from 2008 to 2011. But when just one run for the whole period is done, it is assumed that only at the end of the period bank failure can take place. In reality there could be more periods of low water during which bank failure can take place. Another issue is which elevation of flow has to be inserted. One single value for the water level should not be representative because in reality the water level often changes. So, what are the most realistic durations of flow to model the erosion of a period of three years? What must the duration of flow be, how many time steps are needed and what is the water level elevation? In the text below a solution for these issues is formulated.
According to Jansen (2009) five days (120 hours) a year average bankfull discharge occurs in the Groenlose Slinge. The measurements on which this statement is based are from before re-naturalisation. For that reason the situation could be different nowadays. But because no other measurements are available, it is a good indication to start with.
According to the analysed profiles, the average bankfull water level for the Groenlose Slinge is equal to 16.27 m averaged over the years 2008 and 2011. A mean daily water level hydrograph of 2010 of stream the Meibeek is available (*Appendix 9*). The Meibeek is a stream close to the Groenlose Slinge and according to hydrologist Gert van den Houten (Waterschap Rijn en IJssel) the water level pattern is the same as in the Groenlose Slinge. By comparing some known water levels of the Groenlose Slinge with water levels of the Meibeek, it can be concluded that the water level in the Meibeek is about 1.4 m lower than in the Groenlose Slinge. Thus, the average bankfull water level in the Meibeek should be equal to 14.87 m. When looking to the hydrograph of the Meibeek 2010, it can be seen that six days a year the water level is above 14.87 m. Thus, this amount of six days is close to the five days according to Jansen (2009). However, studying the hydrographs from 2009 and 2011 these five to six days are a high indication. For only about half of the year 2009 and for about half of the year 2011 a hydrograph of the Meibeek is available. In these two times a half year hydrographs, just one day the water level is higher than average bankfull water level. As a result, the five days of bankfull water level could be a high estimation and the toe erosion that happens during high water can be over estimated. But because the lack of data, in this research it is assumed that five days a year bankfull water level takes place.
Another assumption that has to be made is that only during bankfull water level toe erosion takes place. In reality also during less high water levels toe erosion can take place. But because it is assumed that erosion is by far largest during bankfull water, only the five days with bankfull water

levels are modelled. The periods with less high water levels are neglected. This could lead to an underprediction of the total toe erosion. However, as discussed earlier, the estimation of the duration of bankfull discharge could lead to an overestimation and consequently, the underestimation due to only taking the bankfull water levels could balance the total toe erosion.
A third assumption is that these five days with bankfull water level are five successive days. According to the hydrograph of the Meibeek (*Appendix 9*) also the five days with bankfull water level in 2010 were successive.

9.2.3. Inserting vegetation

Also the assemblage and age of vegetation has to be inserted in the RipRoot model of BSTEM. The added strength of vegetion is added to the top one metre of the bank strength. Because in the model not all vegetation can be selected that is found in the field, a 'translation' between the vegetation found in the field and in the model has to be made. This translation must be based on the same contribution of strength to the bank. The assemblage of vegetation can be determined by photos and by the vegetation map. The age of all young vegetation is estimated as 1.5 years in 2008, 2.5 years in 2009 and 3.5 years in 2010. This estimation is based on the fact that the start of re-meanding took place in 2007. All mature, old vegetation is estimated to be 50 years old as many trees were planted during the sixties.

Part III: Results

In this part the results of the research are shown. In *Chapter 10* the results of the morphological evolution are shown and in *Chapter 11* the results of observations and measurements of erosion and deposition are given. *Chapter 12* is about the results of vegetation characteristics and *Chapter 13* shows the results of the Bank Stability and Toe Erosion Model. All excel data can be found on CD1 and all ArcGIS data can be found on CD2.

Chapter 10. Morphological evolution

In *Section 10.1.* the results of the profiles, banklines map and waterlines map are given. *Section 10.2.* is about the results of the channel width, *Section 10.3.* is about the results of the channel elevations and *Section 10.4.* is about results of the relations between channel widths and channel elevations. *Section 10.5.* shows the results of the water level and water depth and *Section 10.6.* shows the results of the lateral migration. In *Section 10.7.* the results of the radius of curvature and sinuosity are represented, in *Section 10.8.* the relation between the radius of curvature and the migration rate is shown. In *Section 10.9.* the calculated Chézy value is given, *Section 10.9.* is about the calculated discharge and *Section 10.10.* represents an overview of morphological and hydrological characteristics.

10.1. Profiles, bank lines map and waterlines map

Section 10.1.1. highlights the evolution of profiles, *Section 10.1.2.* is about the theoretical profiles and *Section 10.1.3.* is about the bank lines and water lines map.

10.1.1. Evolution of profiles

In *Appendix 2* the twenty cross sections from the year 2007, 2008, 2009, 2010 and 2011 are given. In *Appendix 3* only the profiles for 2008 and 2011 are given, but now also the low and high waterlines are included. In case of profile 2 one has to take care to interpret the changes in this profile because the location of this profile was changed. The location of this profile was changed because when the fish ladder was constructed, the profile was located between stone banks. Also profile 1 is located near the fish ladder.

It can be seen that each profile shows significant erosion between 2007 and 2008, varying between 0.5 and 1.5 metres in vertical direction. A reason for this significant erosion is that just after constructing the profile in 2007 much loose sand with less cohesion that can easily be eroded was present. This sand has not yet 'settled'. According to Ellen Bollen Weide (2011) and according to the profiles of *Appendix 2* the erosion in this period to the south of the Zeggelink-Hagbrug (upstream) is larger than the erosion to the north of this bridge (downstream) leading to a gentler valley slope than before.

In the period between 2008 and 2011 in some channels of profiles as well a period of net deposition as a period of net erosion took place, for example in the channel of profile 8 and in the channel of profile 14. In these channels, between 2008 and 2010 net deposition took place and between 2010 and 2011 net erosion took place. At many profiles the changes in morphology between 2009 and 2010 are smaller than the changes between 2008 and 2009 and between 2010 and 2011. This is clearly visible at profile 1, profile 4, profile 5, profile 10, profile 14, profile 15, profile 17 and profile 18 (*Appendix 2*). A reason for these least differences can be that the time span between measuring those profiles (2009 and 2010) is the shortest: seven months. The period between the other profiles is ten months for 2008 and 2009 and 13 months for 2010 and 2011. Apart from the longer time span between the profile measurements, a reason for the relatively large differences between 2010 and 2011 is that in August 2010 a period of high water took place which led to significant overbank deposition and significant erosion (*Appendix 9*).

10.1.2. Theoretical profiles

Interesting are the theoretical profiles. These are the constructed profiles in 2007 and they represent the juridical profile (*Appendix 2*). When the profiles are shallower than the theoretical profiles one is allowed to require dredging. All theoretical profiles have a width of eight metres. The banks have a slope of 1:2. Although between 2008 and 2011 net deposition took place, the 2011 profile is still below the theoretical profile. This is because between 2007 and 2008 significant erosion took place due to the loose sand. However, in some profiles a bar is higher than the theoretical profile. Because in this situation just a part of the profile is higher than the theoretical profile and other parts of the profile are below the theoretical profile of 2007, it is debatable whether the bar legally speaking has to be dug away. When dredging has to take place, the morphodynamics can stop. This is probably not whished for the ecology because these morphodynamics are assumed to be very important for the ecology. A solution in case of dredging could be to put back the sediment upstream of the Groenlose Slinge.

10.1.3. Bank lines map and waterlines map

In *Appendix 4* the bank lines map is shown and in *Appendix 5* the waterlines map can be found. Like the profiles also the bank lines and waterlines are in many cases not exactly sequential by year, indicating that periods of erosion and periods of deposition took place. The waterlines and the bank lines show generally the same pattern as the profiles of *Appendix 2*. The profiles and maps were analysed leading to the other results of this chapter. When in the next chapters the average values are discussed, the average values over the whole course (from profile 1 to profile 20) are meant and not the values averaged over the profiles.

10.2. Channel width

In *Figure 24* the widths of the profiles of the Groenlose Slinge are represented. The bankfull water level width as well as the low water level width for 2008 and for 2011 and average widths over these two years are shown. Also the average widths over all profiles are shown. The averaged over both years high water level width varies between 11 m at profile 16 and profile 19 to 27 m at profile 20 with an average width of 16.06 m. The average low water level width is equal to 8.64 metres, varying from 3 m at profile 5 to 16 m at profile 14. In 2008 the average high water level width is equal to 15.91 m and in 2011 the average high water level width is equal to 16.20 m. This means an increase of 0.29 m. In 2008 the average low water level width was equal to 9.12 m and in 2011 the low water level width was equal to 8.16 m, which means a decrease of 0.96 m. Thus, the high water level with increased between 2008 and 2011 and the low water width decreased between 2008 and 2011. A reason for the increase in high water level width can be the occurrence of floods. Especially the high water level period with a high discharge Q in August 2010 can cause an increase in bankfull width. The increase in high water level width is also related to the increase in the mean water level of 0.2 m. Because the channel has a trapezium-like form, the corresponding width automatically increases when the water level increases. The decrease of 0.96 m in low water with is the consequence of deposition.

At profile 14 a sharp bend is located causing another flow pattern and another erosion- and deposition pattern than in more gentle bends. For that reason the morphologly characterisitics of

profile 14 are different from the other profiles. More results of profile 14 can be found in *Section 10.4* and *Section 11.1.*.

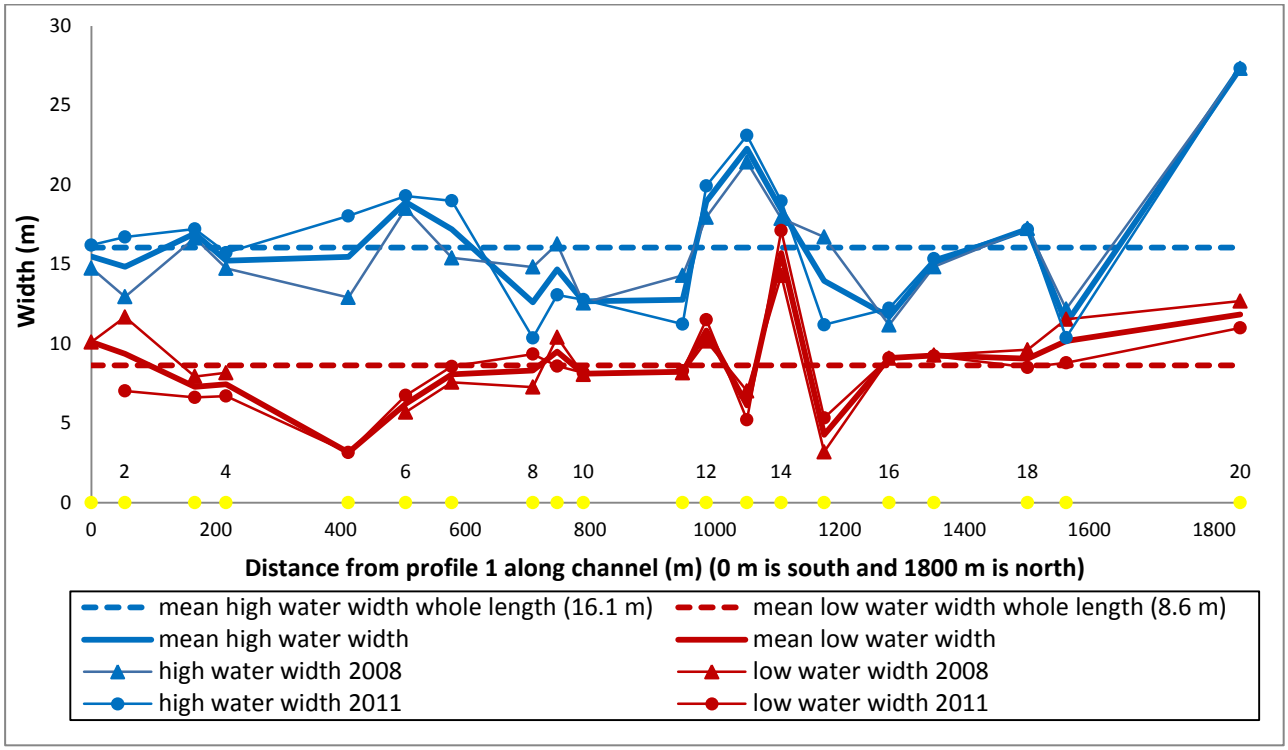

Figure 24: High water width and low water width at each profile of the Groenlose Slinge, 2008 and 2011. At 14 a sharp bend is located. (See Figure 17 in Section 7.1. for overall locations of profiles.)

10.3. Channel elevations

In *Figure 25* to *Figure 27* graphs of various channel elevation measurements against the lateral distance are given: *Figure 25* represents the deepest point elevations of the profiles and the elevations of the centres of gravity, *Figure 26* represents the bank top elevations and *Figure 27* shows the mean elevations of the profiles. All different elevation measurements, except the deepest point elevations, show an increase of average elevation between 2008 and 2011. The elevation of the centre of gravity increased by 0.04 m, the elevation of the top of the bank increased by 0.17 m and the mean elevation increased by 0.11 m. The dashed curves of mean elevations have a slope of 0.0002. This slope is the average of all different elevation measurements of 2011 and is equal to the slope in 2008.

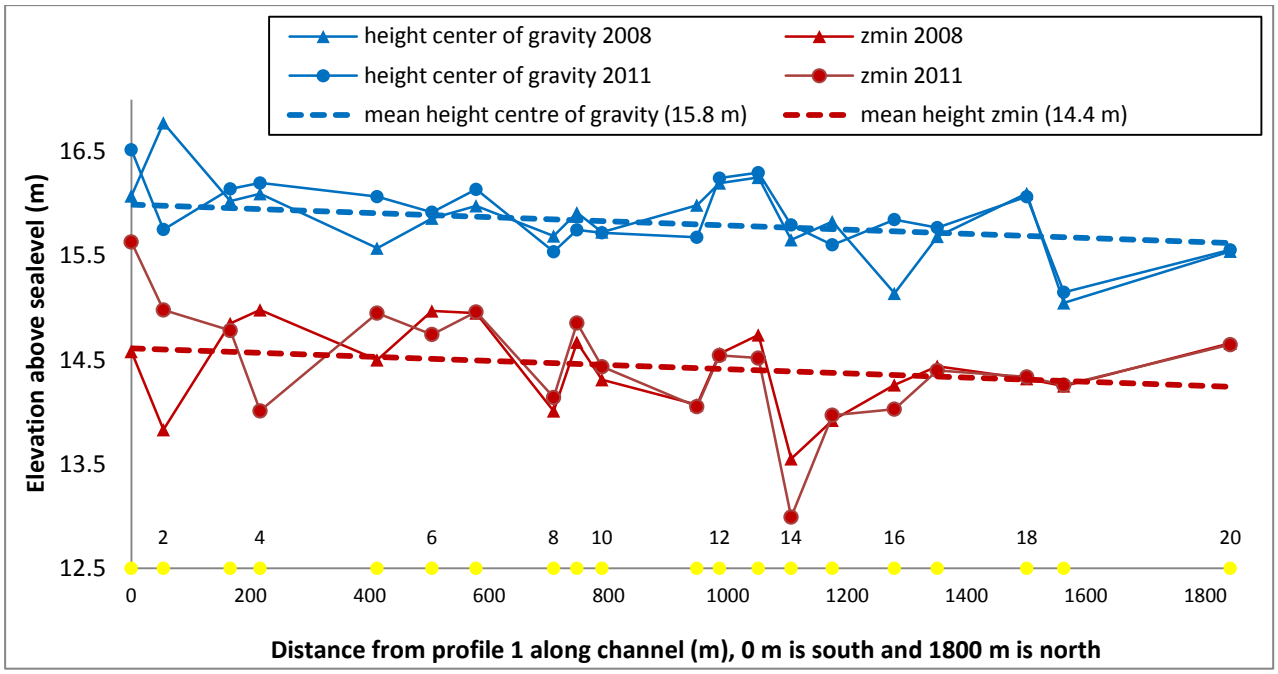

Figure 25: Elevation of lowest point and elevation centre of gravity at each profile of the Groenlose Slinge, 2008 and 2011. The dashed curves of mean elevations have a slope of 0.0002. This slope is an average of all different elevation measurements and is equal to the slope in 2008. At 14 a sharp bend is located. (See Figure 17 in Section 7.1. for overall locations of profiles.)

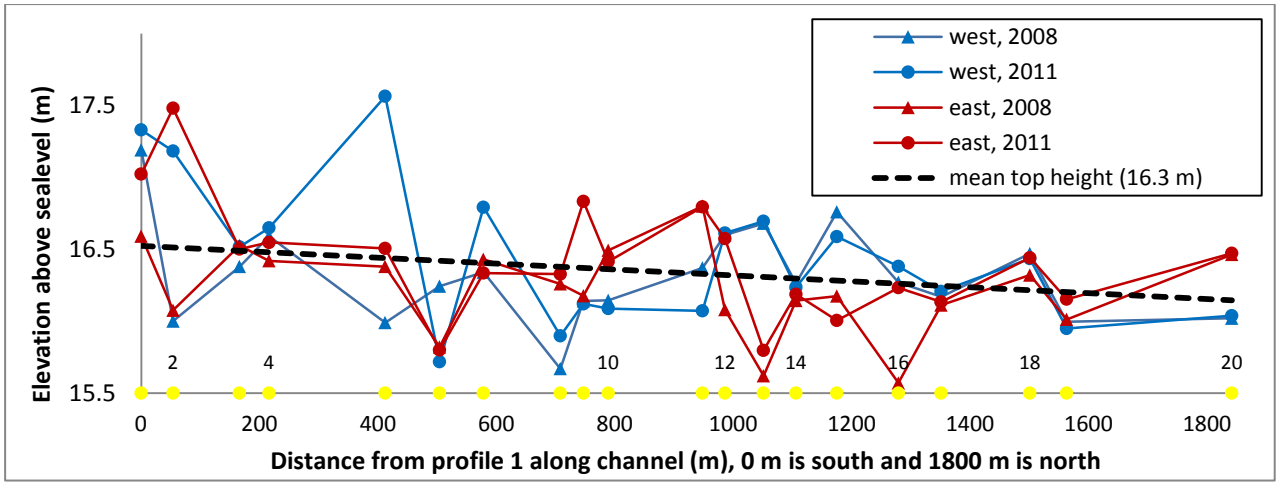

Figure 26: West bank top elevation and east bank top elevation at each profile of the Groenlose Slinge, 2008 and 2011. The dashed mean top bank elevation curve has a slope of 0.0002. This slope is an average of all different elevation measurements and is equal to the slope in 2008. At 14 a sharp bend is located. (See Figure 17 in Section 7.1. for overall locations of profiles.)

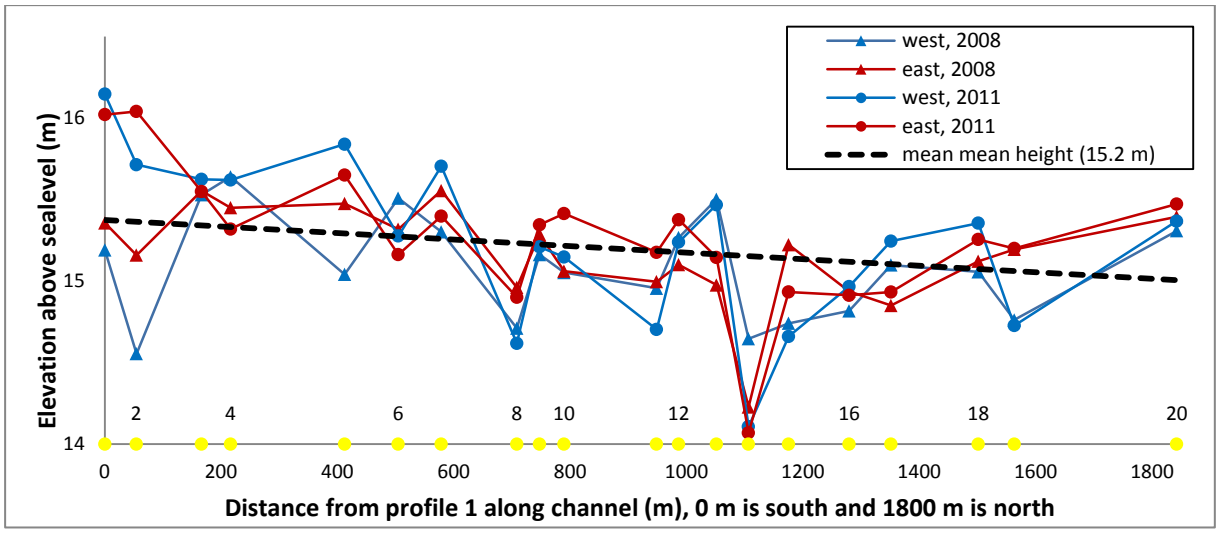

Figure 27: West mean bank elevation and east mean bank elevation at each profile of the Groenlose Slinge, 2008 and 2011. The dashed mean mean elevation curve has a slope of 0.0002. This slope is an average of all different elevation measurements and is equal to the slope in 2008. At 14 a sharp bend is located. (See Figure 17 in Section 7.1. for overall locations of profiles.)

10.4. Relations between channel widths and channel elevations

In *Figures 28, 29, 30* and *31* scatter plots of the elevations and corresponding widths are shown for the year 2011. In the *Figures 32, 33, 34* and *35* scatter plots of the elevations and corresponding widths are shown for the year 2008.

As well in this section as in *section 10.2.* and *Section 10.3.* some outliers in widths and elevations can be observed. The most obvious profile that is different than the other ones is profile 14. The channel of this profile has become deeper between 2008 and 2011, leading to a very small deepest point elevation in comparison to other profiles. Profile 14 also has a relatively high low water width and relatively low banks. Profile 5, 13 and 15 have a relatively small low water width. Profile 19 has a relatively low high water width and profile 13 and profile 20 have a relativelty high high water width. Besides profile 14, also profile 8, profile 6, profile 15 and profile 16 show relatively low banks. The different geometry of profile 14 is caused by a different stream pattern as will be discussed in *Section 11.1*.

In each scatter plot a trend line is fitted. Because of the different characteristics of profile 14, profile 14 was not included when fitting this trend line. Also the equations of the trend lines are given. For each scatter plot it is checked whether the relations are significance at a 5%-error level. When the relation is significance, the trend line is green coloured and when the relation is not significant, the trend line is red coloured. It can be seen that from these relations only the relation between the mean bank elevation and the high water width 2011 and the relation between the lowest point elevation and the high water width 2008 are significant at a 5%-error level. Although most relations are not significant at a 5%-error level, all fitted trend lines show that an increase in elevation correlates to an increase in high water width and to a decrease in low water width.

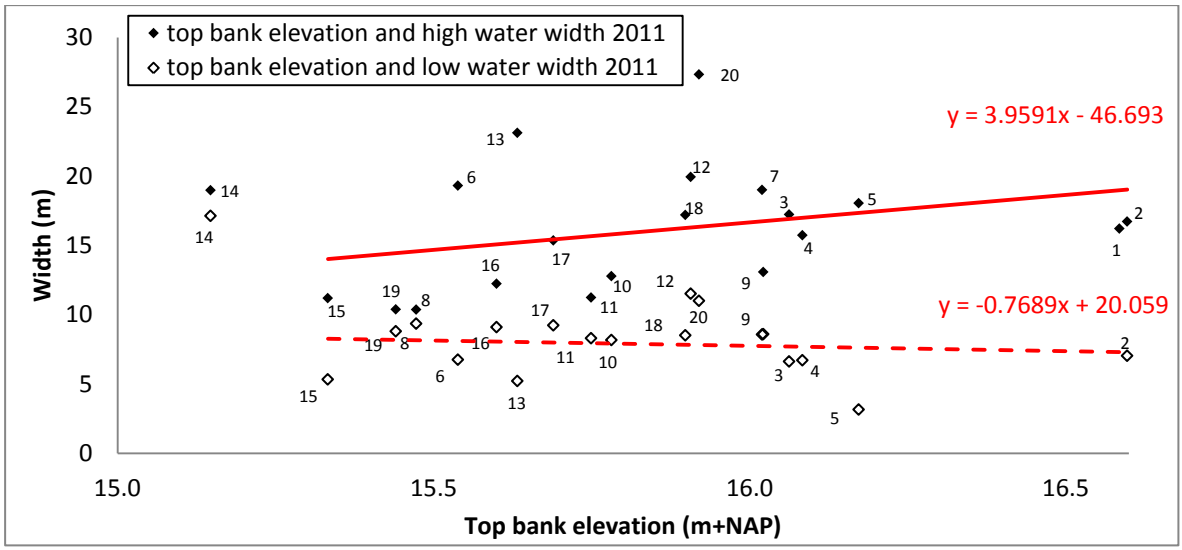

Figure 28: Relation between low and high water width and mean top bank elevation, 2011. Both relations are not significant at a 5%-error level. At 14 a sharp bend is located. (See Figure 16 in Section 7.1. for a global view of the profiles.)

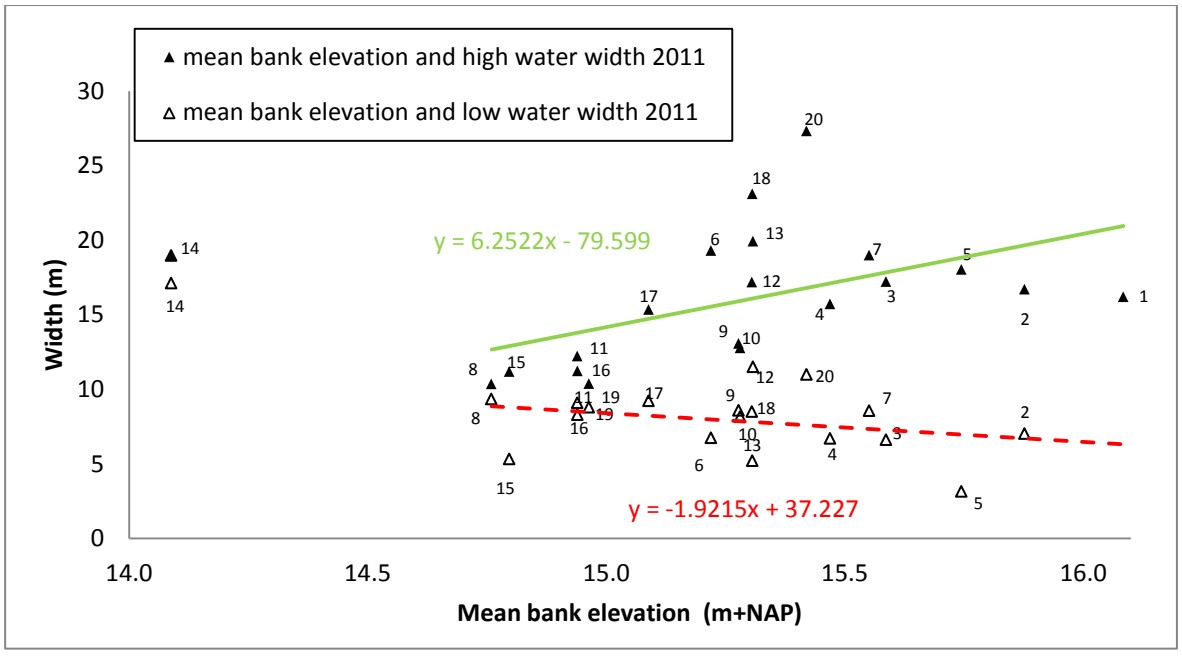

Figure 29: Relation between low and high water width and mean bank elevation, 2011. The relation with high water with is significant at a 5%-error level and the relation with low water width is not significant at a 5%-error level. At 14 a sharp bend is located. (See Figure 17 in Section 7.1. for overall locations of profiles.)

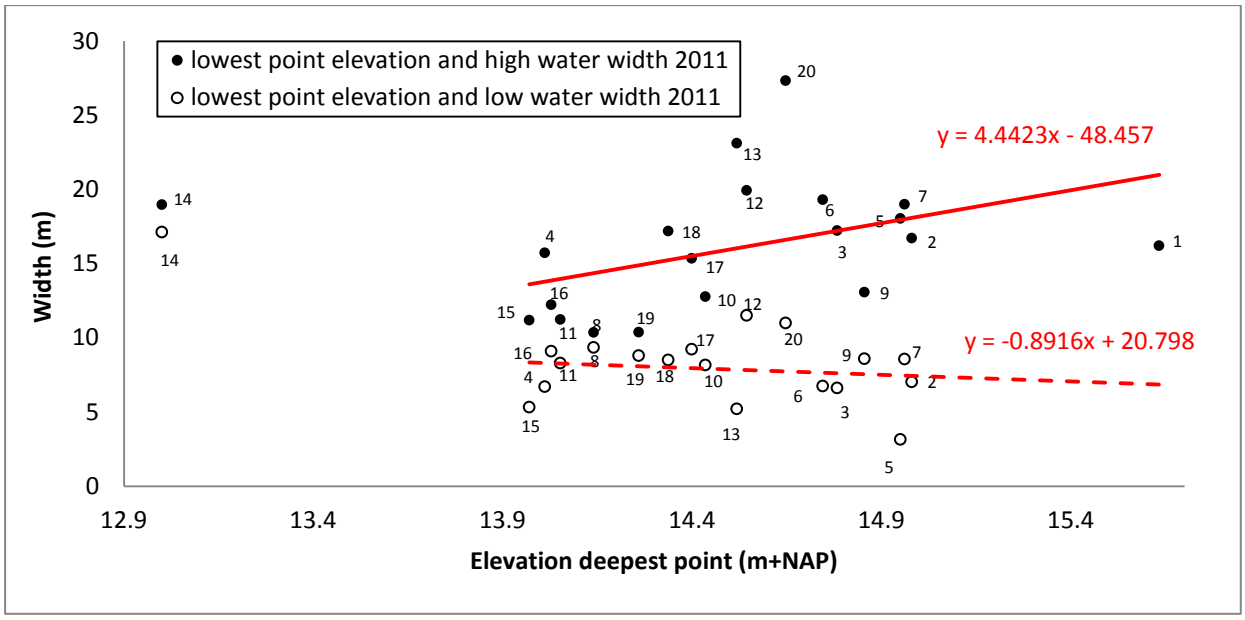

Figure 30: Relation between low and high water width and elevation lowest point, 2011. Both relations are not significant at a 5%-error level. At 14 a sharp bend is located. (See Figure 17 in Section 7.1. for overall locations of profiles.)

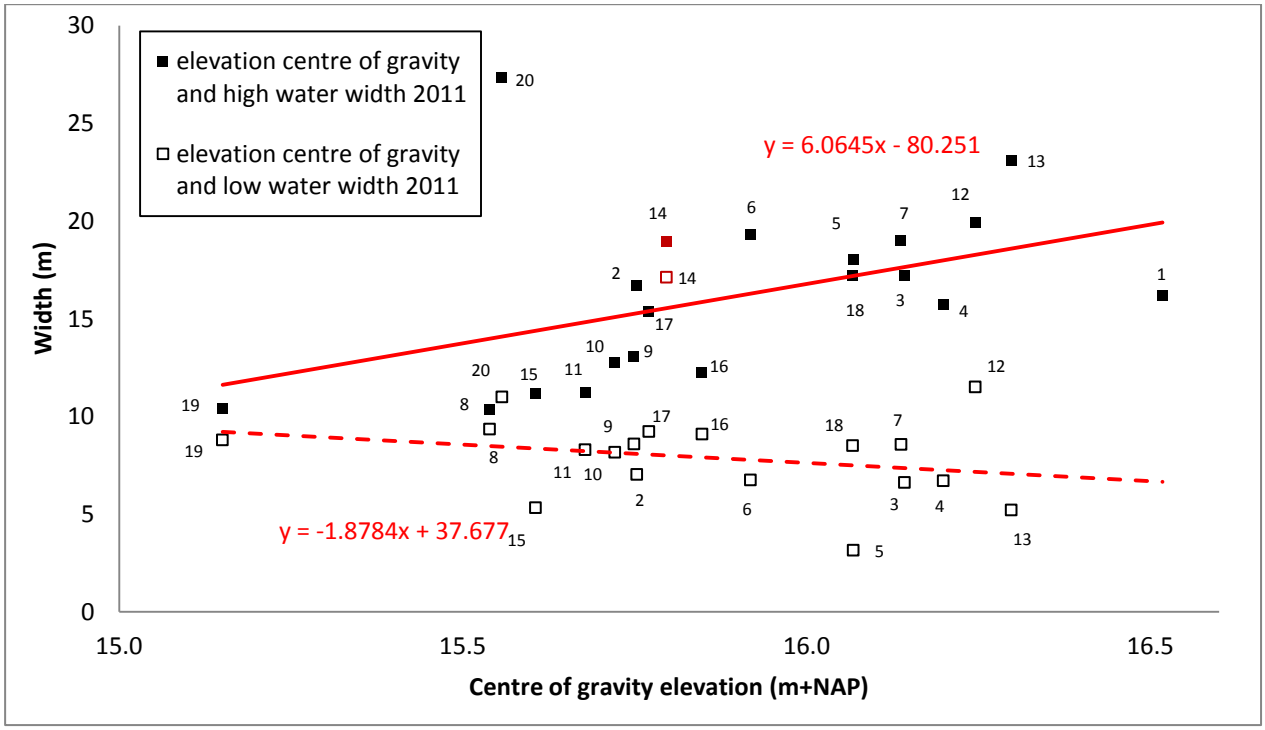

Figure 31: Relation between low and high water width and elevation centre of gravity, 2011. Both relations are not significant at a 5%-error level. At 14 a sharp bend is located. (See Figure 17 in Section 7.1. for overall locations of profiles.)

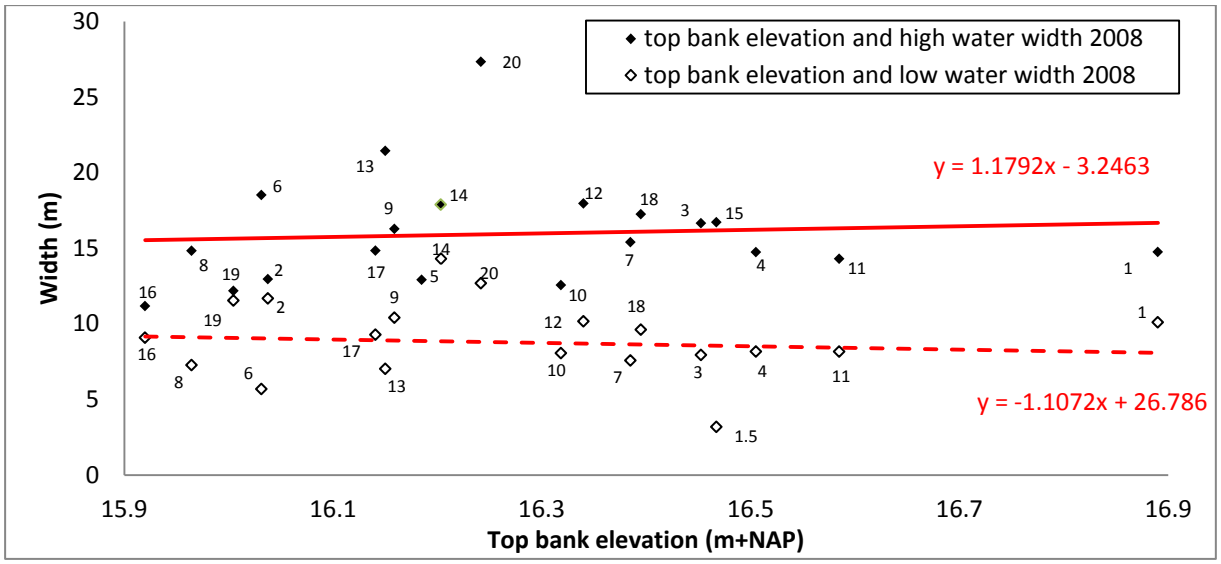

Figure 32: Relation between low and high water width and mean top bank elevation, 2008. Both relations are not significant at a 5%-error level. At 14 a sharp bend is located. (See Figure 17 in Section 7.1. for overall locations of profiles.)

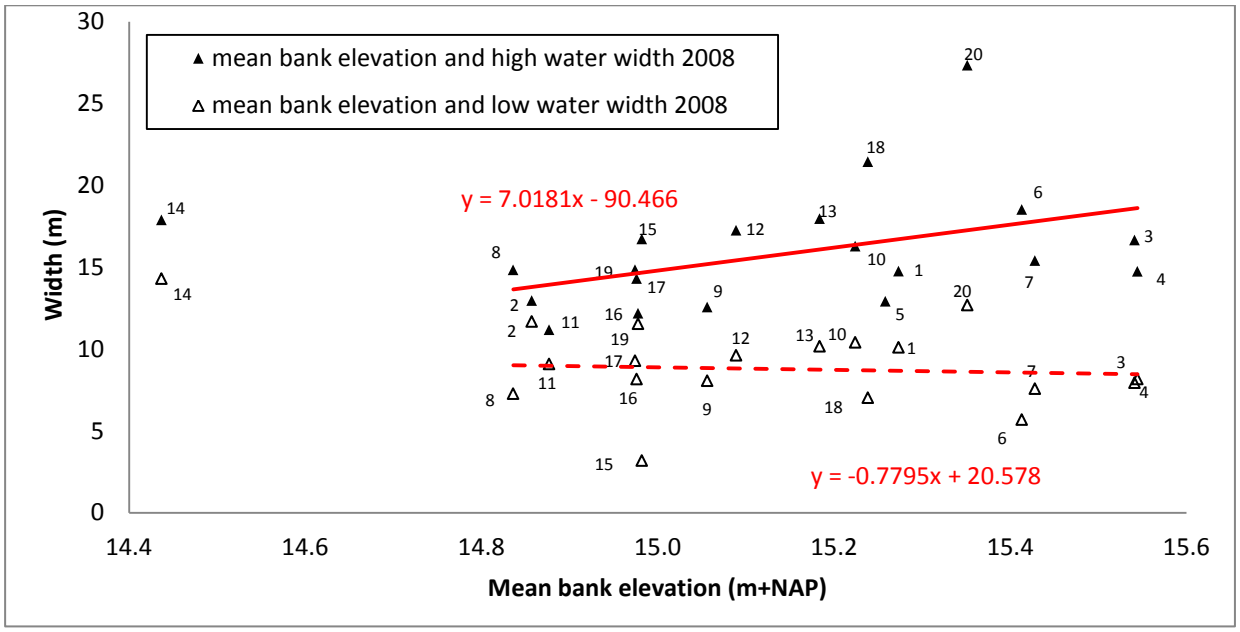

Figure 33: Relation between low and high water width and mean bank elevation, 2008. Both relations are not significant at a 5%-error level. At 14 a sharp bend is located. (See Figure 17 in Section 7.1. for overall locations of profiles.)

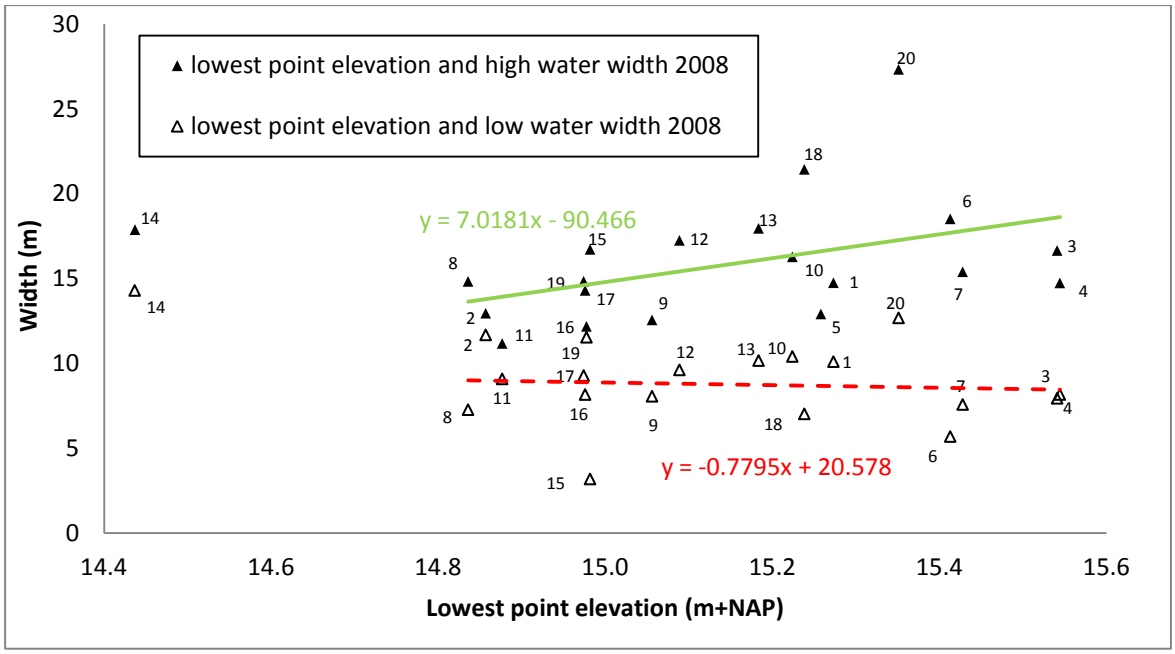

Figure 34: Relation between low and high water width and elevation lowest point, 2008. The relation with high water with is significant at a 5%-error level and the relation with low water width is not significant at a 5%-error level. At 14 a sharp bend is located. (See Figure 17 in Section 7.1. for overall locations of profiles.)

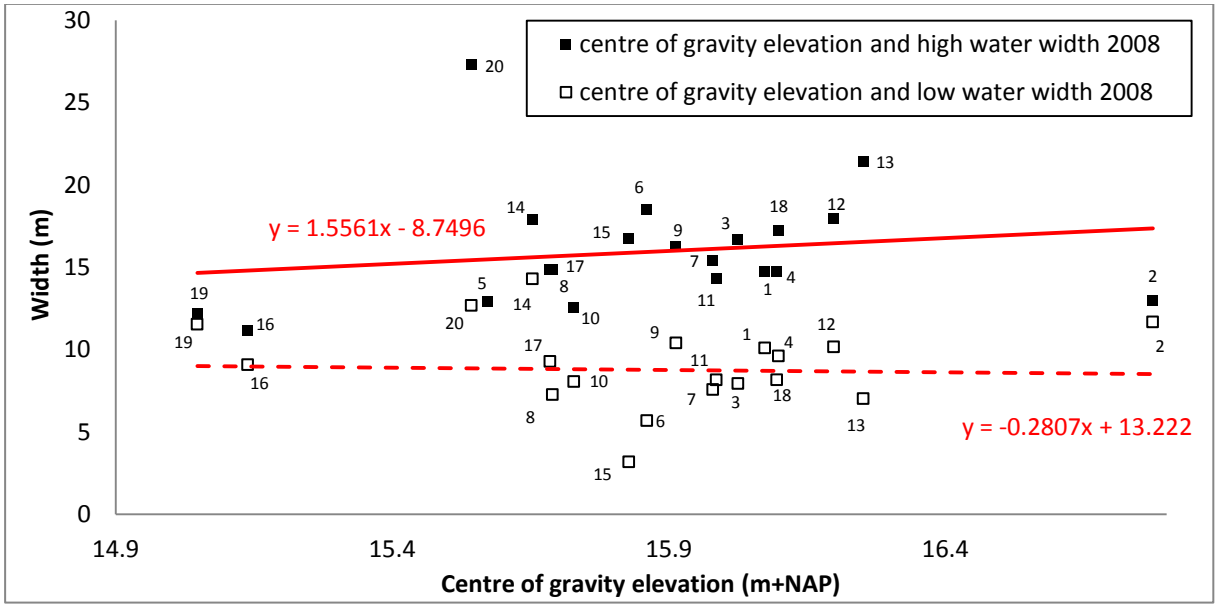

Figure 35: Relation between low and high water width and elevation centre of gravity, 2008. Both relations are not significant at a 5%-error level. At 14 a sharp bend is located. (See Figure 16 in Section 7.1. for a global view of the location of the profiles.)

Thus, an increase in all elevation measurements weakly correlates to an increase in high water width and to a decrease in low water width. To understand this relation, first the relation of bank top elevation and deepest point elevatoin to water depth is studied.
Concerning *Figure 36* it can be concluded that a lower (high and low) water depth correlates to a larger mean top elevation and to a larger deepest point elevation. Thus, a larger water depth correlates to a lower mean top bank elevation and to a lower deepest point elevation. All four relations in *Figure 36*, except the relation between high water depth and top bank elevation, are significant at a 5%-error level.

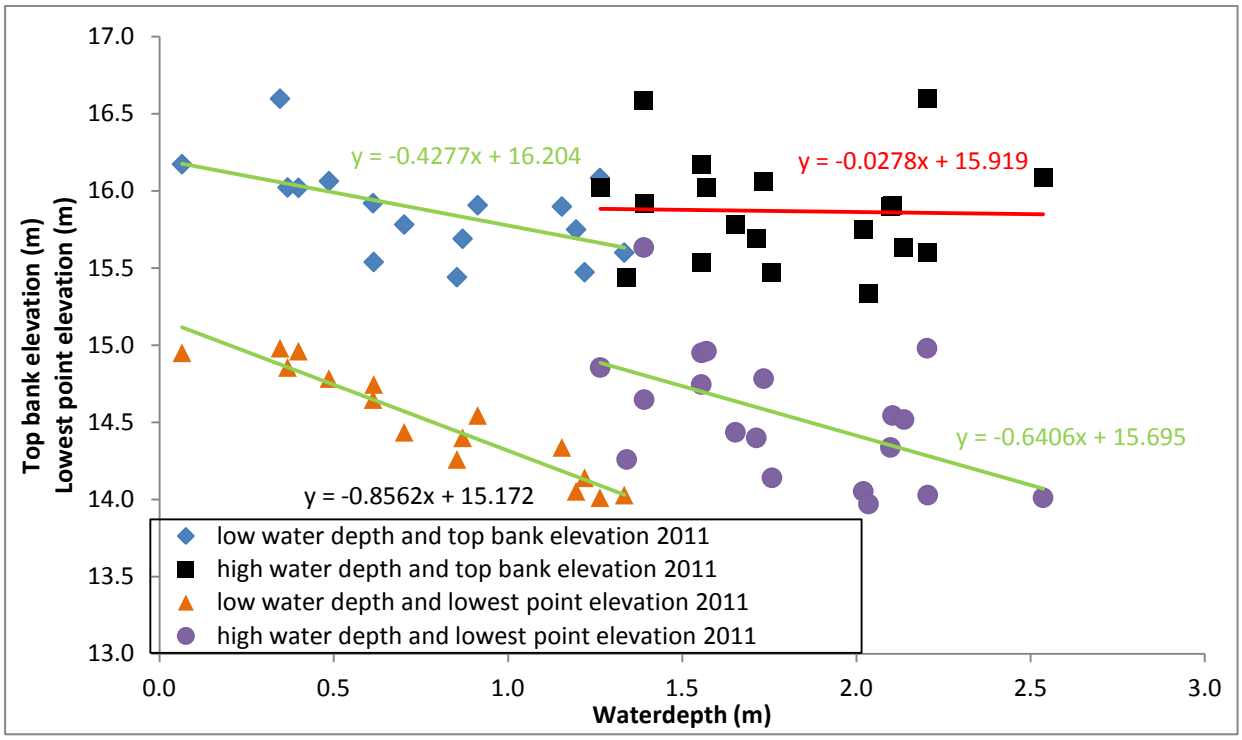

Figure 36: Relation between elevation and water depth. A larger water low- and high depth correlates to lower elevations. A green coloured trend line indicates a significant relation at a 5%-error level and a red coloured trend line indicates a non-significant relation at a 5%-error level.

As noticed, an increase in all elevation measurements correlates to a increase in high water width and to a decrease in low water width. A situation that meets this relation and also the relation found in *Figure 36* is drawn in *Figure 37.* In this figure it can be seen that the profile with higher elevations is more v-shaped than the profile with lower elevations. However, this idea of more v-shaped profiles in case of higher elevations cannot be observed in the measured profiles. Neither an explanation for the idea of more v-shaped profiles in case of higher elevations can be found.

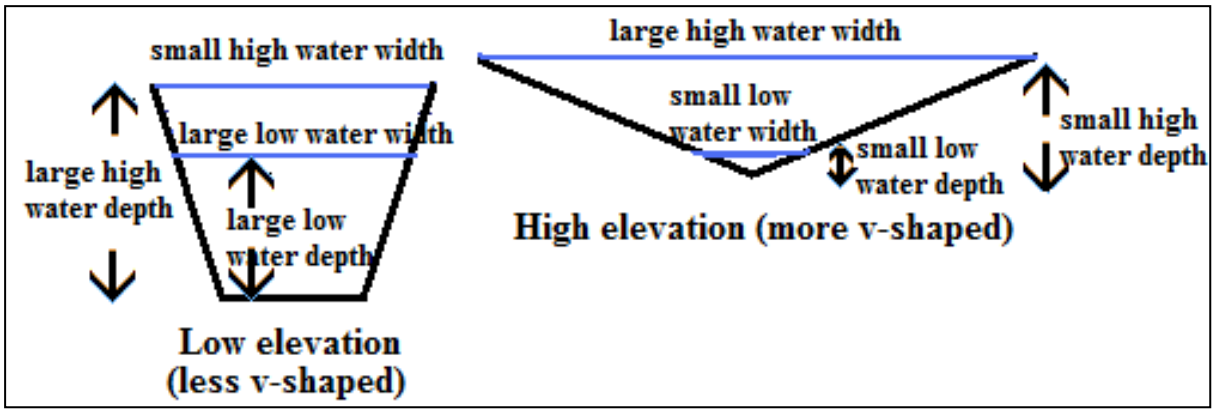

Figure 37: Situation of relation between profile with large elevations above sea level and profile with low elevation above sea level.

10.5. Water level and water depth

In *Figure 38* the measured water level is plotted against the lateral distance. The low water levels of profile 13 and profile 15 are not plotted because of very extreme values that cannot exist in reality because water is not able to stream very steeply upward. The low water levels of profile 4 and profile 5 cannot be plotted because they were not measured. Because of inaccuracies and assumptions one has to take care to conclude things. The average high water level in 2008 was equal to 16.14 m +NAP, in 2011 the high water level was equal to 16.27 m +NAP, the average low water level of 2008 was equal to 15.20 m +NAP and the average low water level of 2011 was equal to 15.27 m +NAP. According to the results this means an increase of 0.07 m for the low water level and an increase of 0.13 m for the high water level. Because the top bank elevation also increased by 0.17 metres the chance on flooding does not change due to the higher water levels. The increase in water level can cause higher groundwater levels in the surrounding land. In times of drought the land owners probably like the increase in groundwater level and in times of wetness the land owners probably dislike the increased groundwater level. Notice that an essential difference between the high water curves and the low water curves exists. The high water curves show the bankfull level, but this level is not reached at all profiles at the same discharge. In contrast, the low water curves do represent more or less equal discharges.

Because apart from the water levels also the lowest point elevations of the profiles are known (*Section 10.3.*), also the maximum water depths can be calculated. Averaged over the length, the low water depth in 2008 is equal to 0.79 m and in 2011 equal to 0.88 m. The averaged high water depth in 2008 is equal to 1.71 m and in 2011 equal to 1.84 m. According to the results this means an increase of the low water depth of 0.09 m and an increase of the high water depth of 0.13 m between 2008 and 2011. According to the results, in 15 of the 20 bends a bend that has becomes sharper between 2008 and 2011 corresponds to an increase in water depths or a bend that has become less sharp corresponds to a decrease in water depth. On average, in 2011 the bends were sharper than in 2008 (*Section 10.7*). Thus, an explanation for the on average higher water depth in 2011 is that the bends in 2011 are sharper than in 2008, causing damming up of the water.

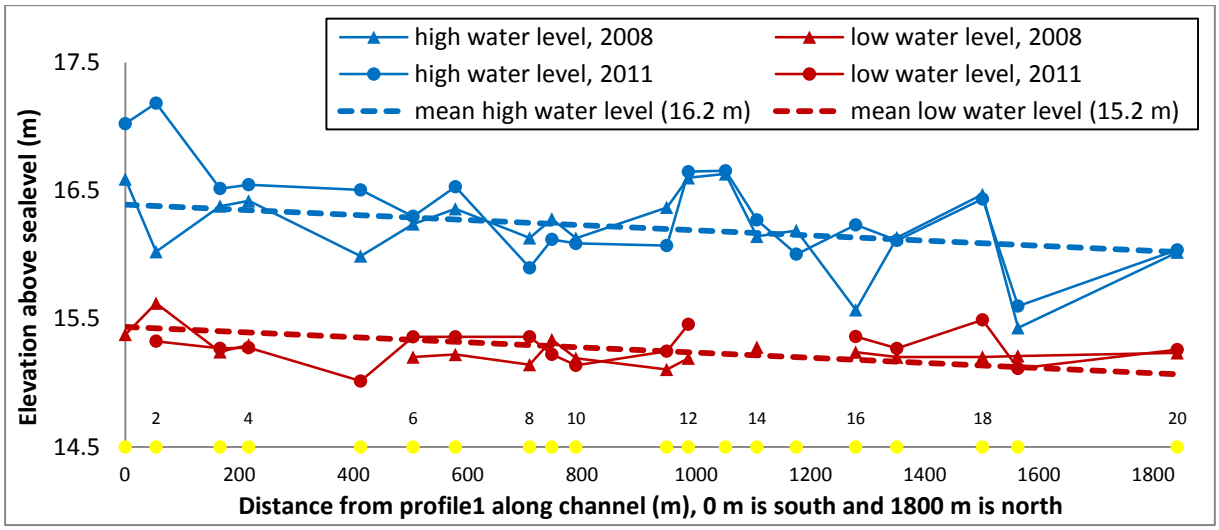

Figure 38: Water level at each profile of the Groenlose Slinge, 2008 and 2011. The dashed mean water level curves have a slope of 0.0002. This slope is an average of all different elevation measurements and is equal to the slope in 2008. (See Figure 17 in Section 7.1. for overall locations of profiles.)

10.6. Lateral migration

In *Figure 39* the lateral migration of the profiles of the Groenlose Slinge according to different methods is shown for the period between 2008 and 2011. Also the lateral migration averaged over these methods is shown. A positive value means lateral migration to the east and a negative value means lateral migration to the west. As can be seen in *Figure 39*, the different methods can show different directions of migration. This is because each method represents another part of the profile (see *Section 8.4.*). In this research the modelled erosion has to be compared to the measured erosion. For that reason only profiles where erosion takes place over the whole height can be used for comparison to the modelled erosion. After comparing the directions according to different methods, including the observations, only the west part of profile 16, the west part of profile 18 and the east part of profile 8 were left and available for comparison. Only those banks show erosion over its whole height. In profile 8E the whole period between 2008 and 2011 erosion took place, in profile 16W also during this whole period erosion took place, except between 2008 and 2009 a little bit net deposition took place (*Appendix 2*). Profile 18W shows especially between 2010 and 2011 erosion. Between 2008 and 2010 the profile hardly changes (*Appendix 2*). Also the observations of profile 18W show just a little bit erosion. For profile 16W the average measured lateral migration between 2008 and 2011 is equal to 2.04 metres, for profile 18W the average measured lateral migration is equal to 1.74 metres and for profile 8E the average measured lateral migration between 2008 and 2011 is equal to 2.06 metres.

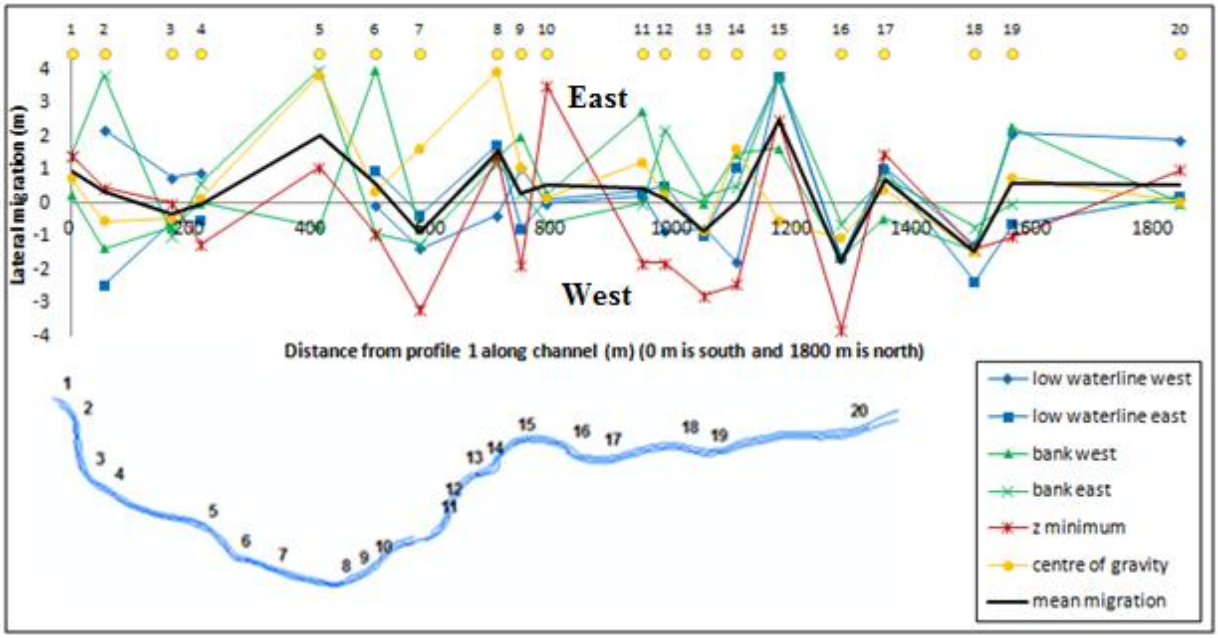

Figure 39: Lateral migration between 2008 and 2011 according to different methods at each profile of the Groenlose Slinge. A positive value means migration to the east and a negative value means migration to the west. (See Figure 17 in Section 7.1. for overall locations of profiles.)

For all combinations of methods to determine lateral migration it is determined whether the relation is significant. Whether a relation is significant or not is determined by the calculating the confidence intervals for the slope of the fitted linear trendline of the relation between two methods. When this interval contains zero, the relation is not significance for the chosen error level. *Table 4* shows that many combinations of methods to determine lateral migration do not give a significant relation based on a 5%- or 10%-error level. However, based on a statistical F-test, it can concluded the large differences in methods occurred because each method is erratic, not because a difference in methods to determine lateral migration. Thus, the migration rates and migration directions of different parts of a profile are not necessarily the same. For example it could be possible that the thalweg migrates to the west and the top of the west bank to the east or that the thalweg does not migrate while the top of the bank migrates one metre per year. Because of the differences in migration at the different heights of the profile, the form of the profile can change. Although there are differences in significance of relations between methods, this does not definitely mean than one method is more representative for the lateral migration than another method. Hence, it is assumed that the lateral migration averaged over the different methods is the most representative way to show the rate of lateral migration.

In *Table 5* the values for the mean west and mean east migration are given. Profile 16W, profile 18W and profile 8E, the banks of the profiles that show the same direction of migration in each method, are marked. The lateral migration averaged over the twenty profiles and then averaged over east and west is equal to 0.89 m per three years which corresponds to 0.30 m/year. This seems low, but note that all profiles are included, also straight parts of the stream where hardly any migration takes place. When only bends are included, the average migration will be higher. Only taking into account the profiles that are located at the apex of bends, the mean lateral migration is 0.46 m/yr in the period 2008-2011. Averaged over the whole length of this part of the Groenlose Slinge the mean

lateral migration is equal to 0.92 m per three years which corresponds to 0.31 m/year. As the averaged value over the whole length is more representative than averaged over all profiles it can be assumed that the average migration of the Groenlose Slinge between 2008 and 2011 is equal to 0.92 m.

	Waterline west		Waterline east		Bank line west		Bank line east		Deepest point		Centre of gravity	
Waterline west			**95%**	**90%**	**95%**	**90%**	**95%**	**90%**	**95%**	**90%**	**95%**	**90%**
Waterline east					**95%**	**90%**	**95%**	**90%**	**95%**	**90%**	**95%**	**90%**
Bank line west							**95%**	**90%**	**95%**	**90%**	**95%**	**90%**
Bank line east									**95%**	**90%**	**95%**	**90%**
Deepest point											**95%**	**90%**
Centre of gravity												

Table 4: 95% means a 5%-error level and 90% means a 10%-error level. A green marked 95% and a green marked 90% means that the chance is 95% and 90% respectively that a significance relation exists between the two methods to determine lateral migration. A red marked percentage means that no significant relation exists concerning that percentage of chance on a significant relation.
The F-value is equal to 1.389. This means that the p-value is then just less than 0.25 and that the large differences in methods thus occurred because each method is erratic, not because a difference in methods to determine lateral migration.

Profile	mean migration west (m) (2008-2011)	Profile	mean migration east (m) (2008-2011)
1W	0.81	1E	1.21
2W	0.19	2E	0.33
3W	0.11	3E	0.50
4W	0.04	4E	0.25
5W	*1.40*	*5E*	*2.96*
6W	*0.84*	*6E*	*0.12*
7W	0.94	7E	0.80
8W	1.60	8E	2.06
9W	0.56	9E	0.32
10W	0.98	10E	0.78
11W	0.60	11E	0.04
12W	0.47	12E	0.29
13W	1.09	13E	1.10
14W	0.27	14E	0.19
15W	*1.86*	*15E*	*2.39*
16W	2.04	16E	1.78
17W	0.62	17E	0.93
18W	*1.38*	*18E*	*1.48*
19W	*1.04*	*19E*	*0.22*
20W	0.74	20E	0.32
Average:	0.88	Average:	0.90
Average east and west, averaged over profiles: 0.89 m / 3 years = 0.30 m / year **Average east and west, averaged over length: 0.92 m / 3 years = 0.31 m / year**			

Table 5: Average lateral migration for each profile. The profiles 5, 6, 15, 18 and 19 are located at the apexes of bends (slanted in table).

10.7. Radius of curvature and sinuosity

In *Figure 40* the reciprocal of the radius of curvature averaged over 2008 and 2011 is plotted for the twenty profiles. The average reciprocal of radius of curvature between 2008 and 2011 and not a single curve for each year is given because the differences in radius of curvature between 2008 and 2011 are very small at the profiles. The larger the radius of curvature, the smoother the bend. This means that a high reciprocal of the radius of curvature represents a relatively sharp bend. The sharpest bend is found at profile 14 which has a radius of curvature of 33 metres. Although the differences *at the profiles* are very small, differences in radius of curvature at the *bends* between 2008 and 2011 exist. Averaged over all *bends* the radius of curvature is equal to 76 m in 2011 and equal to 88 m in 2008. Also Jansen (2009) calculated an average radius of curvature of 88 m for the Groenlose Slinge in 2008. Thus, the mean radius of curvature of all bends shows a decrease of 12

metres. This means that the bends have become sharper between 2008 and 2011. The reason for increase in bend sharpness is that deposition in the inner bends takes place and erosion in the outer bends. Because the profiles are in general not located at the apexes of bends and there less erosion and deposition takes place, the difference in radius of curvature measured at the profiles is much less obvious.

This research shows that no significance difference between the sinuosity in 2008 and 2011 exists. In both years the measured sinuosity is equal to 1.2. Because the sinuosity is less than 1.5, strictly seen the Groenlose Slinge is not a meandering stream but a straight stream.

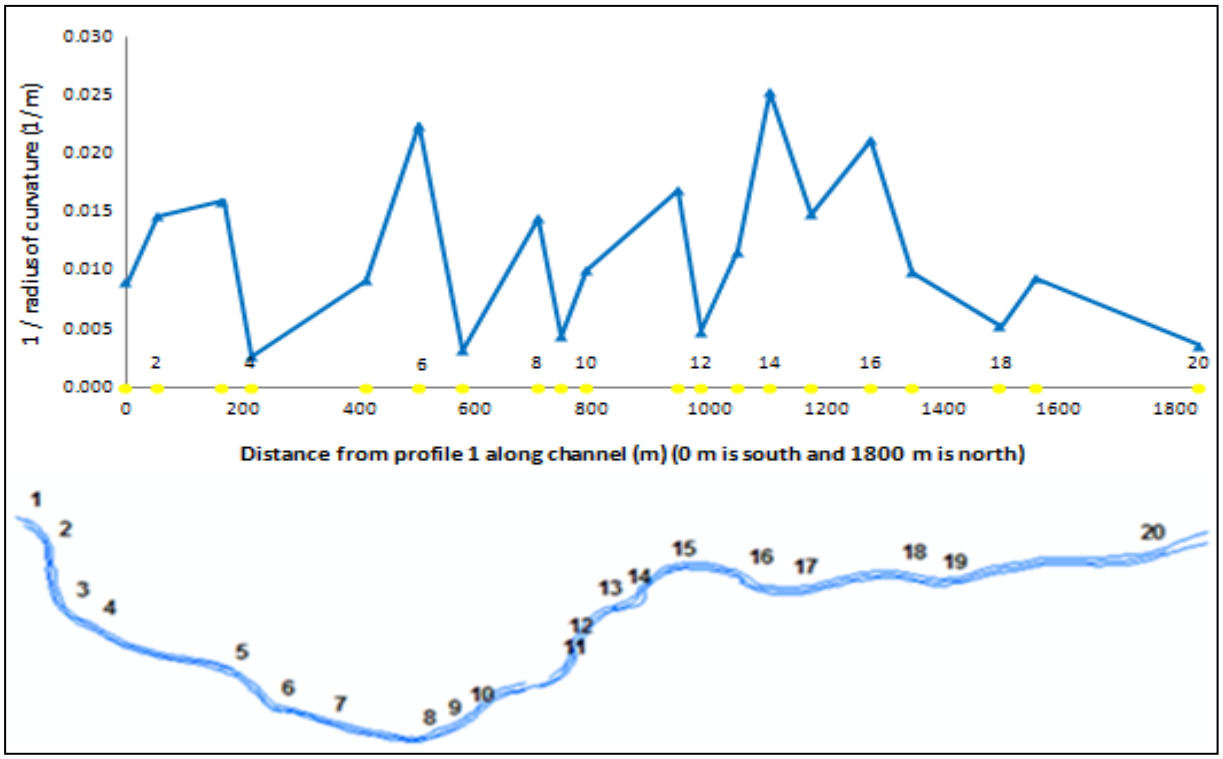

Figure 40: Reciprocal of radius of curvature at each profile of the Groenlose Slinge, average of 2008 and 2011. The larger one divided by the radius of curvature (reciprocal of radius of curvature), the sharper the bend at the concerning profile.

10.8. Relation between radius of curvature and lateral migration rate

As discussed in the literature review (*Section 3.2.1.*) the migration of a bend is optimal when $2 < r_c / w < 3$. In *Figure 41* it can be seen that in this case also an optimum of r_c/w where migration is highest exists, but the optimum r_c/w is a bit higher than between two and three, about four. In *Figure 41* also the type of vegetation is shown. However, it can be seen that no relation exists between the type of vegetation and the migration rate. The lateral migration is totally determined by the ration between the radius of curvature and the width. It can be seen that the migration of profile 14 is very low and that r_c/w is low. This is because profile 14 is a sharp bend in which flow separation takes place and as a result the erosion is not concentrated on the outer bank any more. Also at profile 4 the migration is low, but r_c/w is high. The reason that also this high r_c/w leads to a low migration rate is that the bank erosion spreads out over a large part of the outer bend.

In this *Figure 41* the average migration on the y-axis is divided by the corresponding bankfull width. The reason for dividing by the width is that also a weak relation between migration and width exists: a higher width correlates to a lower migration rate and thus a narrower stream correlates to a higher migration rate (*Figure 42*). The reason for this relation can be that a higher migration rate can lead to more widening of the channel and consequently the narrower the stream the higher the rate of widening. So, the width over the whole section becomes more equal and therefore the relation in *Figure 42* can be a readjustment of the initial profile.
In *Figure 43* it can be seen that also a weak relation between the bankfull width and the radius of curvature exists: a larger bankfull width correlates with a larger radius of curvature. Because larger elevations correlate with larger widths (*Figure 28* to *Figures 35* in *Section 10.4.*), larger elevations also correlate to higher radii of curvature (*Figure 43*).

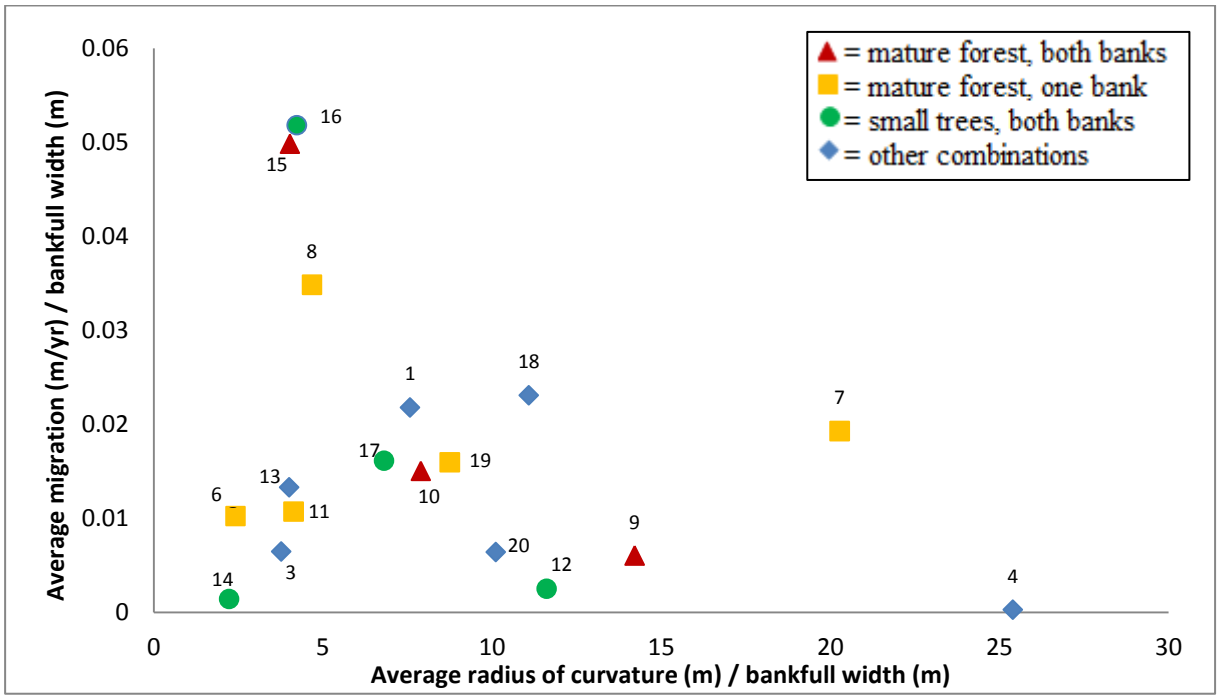

Figure 41: Relation between migration, radius of curvature and bankfull width for 2008-2011. Notice that the migration divided by the bankfull width is largest when the radius of curvature divided by the bankfull width is equal to about four. No influence of vegetation on the migration rate can be detected. (See Figure 17 in Section 7.1. for overall locations of profiles.)

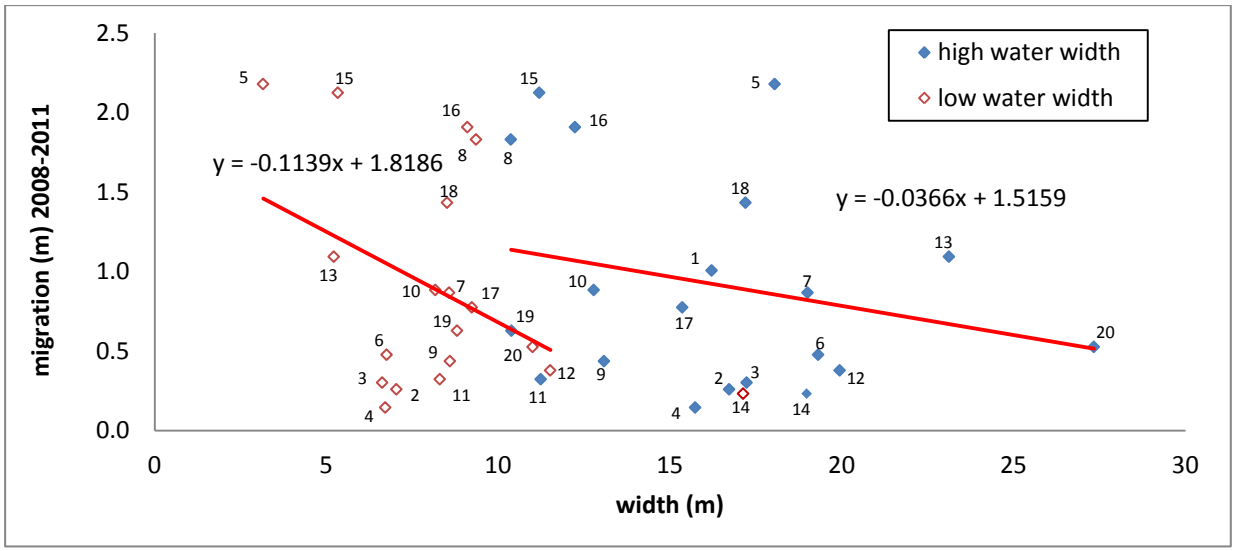

Figure 42: Relation between migration and width: a larger width correlates to a lower migration rate, 2008-2011. Profile 14 is excluded when fitting the trend line. The relations are not significant at a 5%-error level. (See Figure 17 in Section 7.1. for overall locations of profiles.)

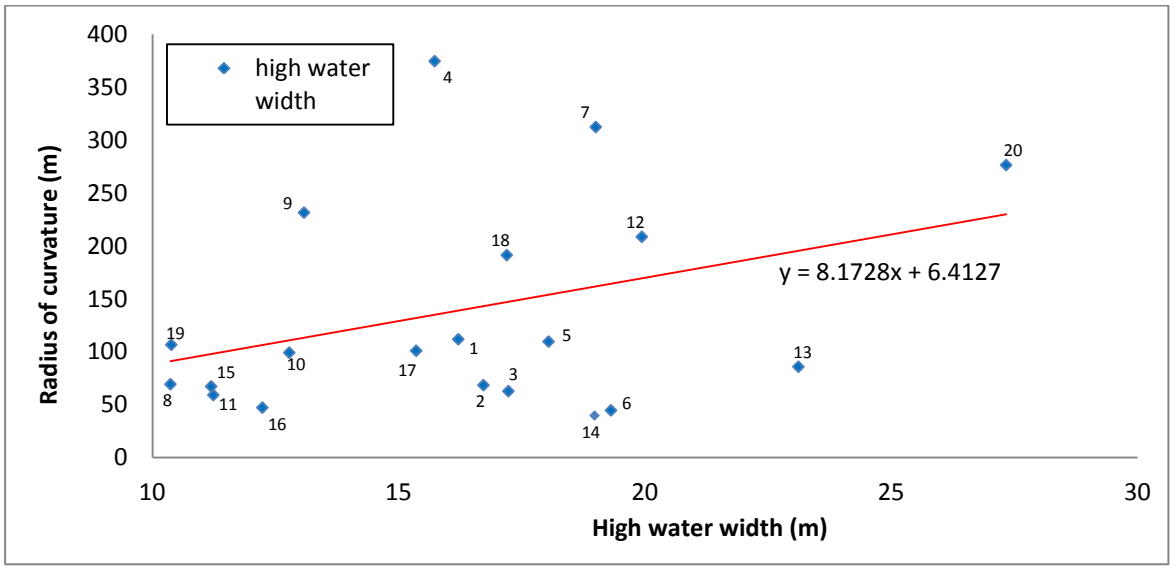

Figure 43: Relation between radius of curvature and high water width: a larger high water width correlates to a higher radius of curvature, 2008. Profile 14 is excluded from the trend line. The relation is not significant at a 5%-error level. (See Figure 17 in Section 7.1. for overall locations of profiles.)

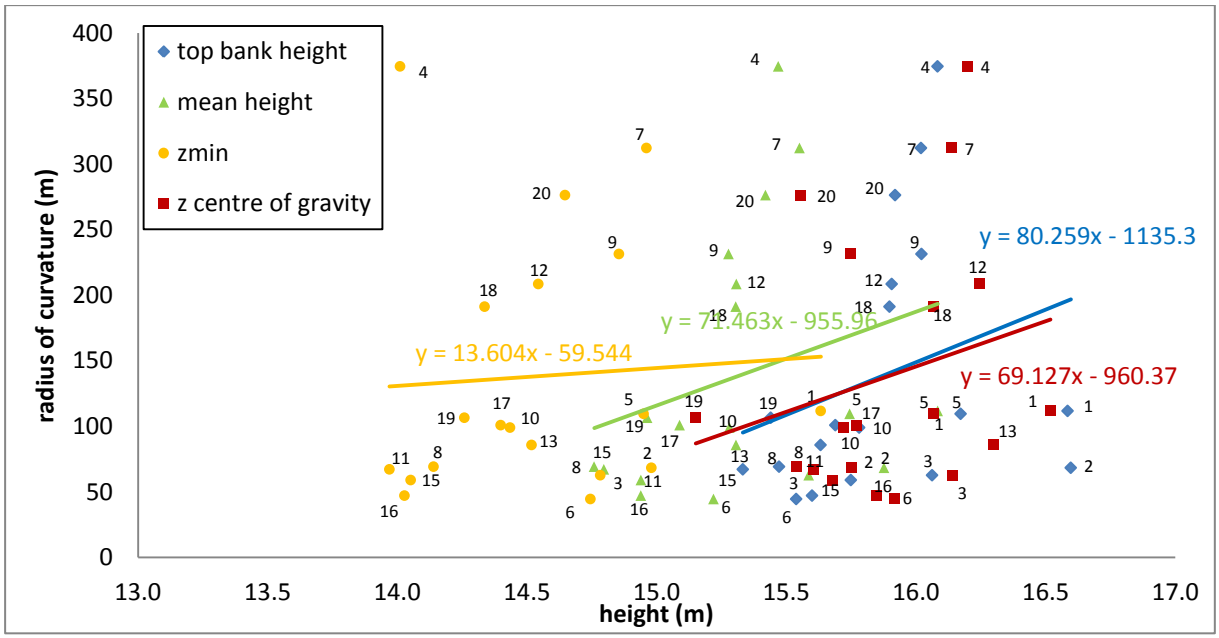

Figure 44: Relation between radius of curvature and elevations: a higher elevation correlates to a higher radius of curvature, 2008. None of the four relations is significant at a 5%-error level. (See Figure 17 in Section 7.1. for overall locations of profiles.)

10.9. Wet area and wet perimeter

According to *Equation 1* in *Section 2.3.* a relation between the velocity, radius of curvature, valley slope and Chézy coefficient exists. In *Figure 45* the wet area of each profile and the wet perimeter of each profile for 2008 and 2011 are shown. Notice the large wet areas and wet perimeters at and around profile 14. Profile 14 is excluded for calculating the mean wet area as part of the profile is taken by vortices that are not flowing. The average wet area in 2008 is equal to 15.7 m^2 and the average wet perimeter is equal to 17.0 m. The hydraulic radius is equal to the wet area (m^2) divided by the wet perimeter (m), leading to a hydraulic radius of 0.92 m. In 2011 the average wet area is equal to 16.2 m^2 and the average wet perimeter is equal to 16.8 m; the average hydraulic radius (R) is then equal to 0.96 m.

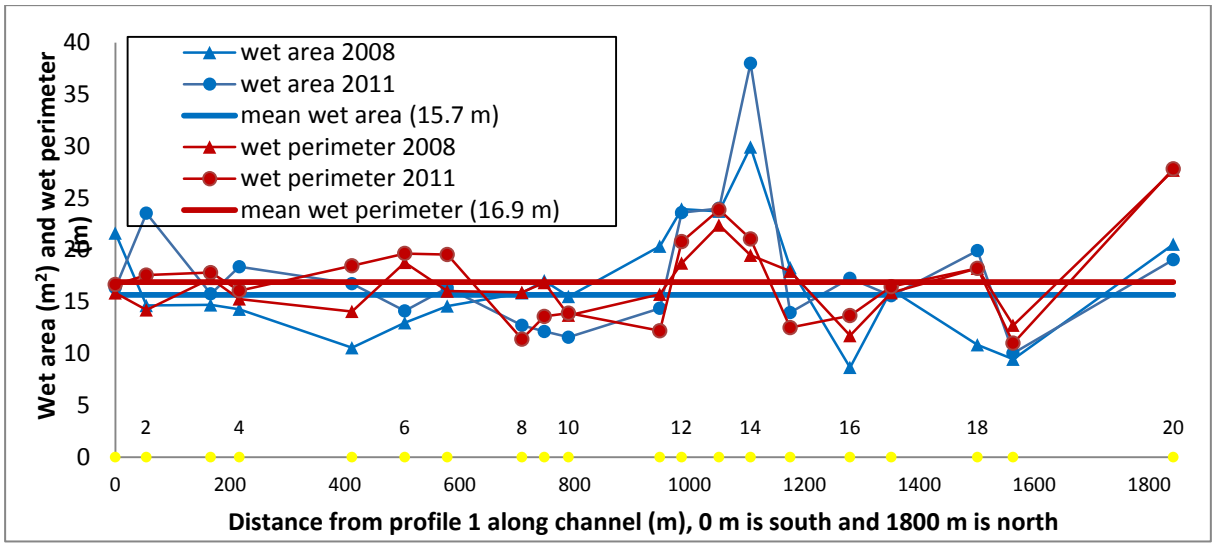

Figure 45: Wet area and wet perimeter at each profile of the Groenlose Slinge, 2008 and 2011. Profile 14 is excluded for calculating the mean wet area as part of the profile is taken by vortices that are not flowing. (See Figure 17 in Section 7.1. for overall locations of profiles.)

10.10. Calculated Chézy value and calculated bankfull discharge

As noticed in *Section 10.9.* in 2008 the hydraulic radius was equal to 0.92 m and in 2011 the hydraulic radius was equal to 0.96 m. According to Jansen (2009) the high water velocity is approximately 0.4 m/s and the slope is equal to 0.0002. Assuming this velocity during bankfull water level, the Chézy coefficients can be calculated and are equal to 29 $m^{1/2}/s$ for both years. This value seem to be logical values for the roughness of the Groenlose Slinge because according to Kleinhans (2011, personal communication) and Jansen (2009) a logical C-value is about 25 $m/s^{0.5}$. Accordingly, the other values for the parameters velocity and slope are likely to be in the right order of magnitude.

Because it is assumed that the bankfull discharge velocity is equal to 0.4 m/s and the average wet area in 2011 is equal to 16.24 m^2, the average bankfull discharge can be assumed to be equal to 6.5 m^3/s (= 16.24 m^2 * 0.4 m/s).

10.11. Overview of morphological and hydrological characteristics

In *Table 6* an overview is given of the morphological and hydrological characteristics of the Groenlose Slinge in 2008 and 2011 as determined in this research. In *Table 2* (*Section 4.4*) an overview of morphological and hydrological characteristics determined by earlier research is shown. In the table also the 95% confidence level is shown. When this interval includes zero the difference is not significant at a 95% confidence level and when this interval does not include zero the difference is significant at a 95% confidence level. According to the table, only the decrease in low water width, the increase in bank top and the increase in wet area are significant differences between 2008 and 2011.

	2008	2011	Difference (2011 minus 2008)	95% confidence interval
Bankfull width (m)	15.91	16.20	0.29	-0.91 – 1.48
Low water width (m)	9.12	8.16	-0.96	-1.82 - -0.11
Bankfull water depth (m)	1.71	1.84	0.13	-0.04 – 0.31
Low water depth (m)	0.79	0.88	0.09	-0.16 – 0.34
Bankfull water level (m+NAP)	16.14	16.27	0.14	-0.01 – 0.28
Low water level (m+NAP	15.20	15.27	0.07	-0.04 – 0.18
Deepest point (m+NAP)	14.43	14.42	-0.01	-0.19 – 0.17
Mean elevation centre of gravity (m+NAP)	15.79	15.83	0.04	-0.11 – 0.19
Bank top (mean east and west) (m+NAP)	16.25	16.41	0.17	0.01 – 0.33
Mean elevation (mean east and west) (m+NAP)	15.13	15.25	0.11	-0.02 – 0.33
Mean longitudinal gradients (all elevation measurements)	0.0002	0.0002	0	
Wet perimeter (m)	16.75	17.0	0.25	0.13 – 0.37
Wet area (m^2)	15.07*	16.24*	1.17*	-0.94 – 3.28
Radius of curvature (m)	87.6	76.4	-11.3 (sharper)	-25.0 – 2.4
Sinuosity (-)	1.2	1.2	0	
Low water velocity (m/s)	0	0	0	
Bankfull discharge (m^3/s)		6.5		
Chézy coefficient ($m^{1/2}/s$)	29	29	0	
Deposition (m^2/m)**	1.5			
Mean lateral migration (m/year)	0.31			

Table 6: Hydrological and morphological characteristic values of the Groenlose Slinge determined in this research. In Table 2 (Section 4.4.) the overview of hydrological and morphological characteristic values determined by earlier research can be found. A 95%- significance interval including zero is not a significant difference (red coloured), a 95%-significance interval not including zero is a significant difference.

**** Profile 14 is not included***

***** For the period between 2008 and 2011, the unit m^2/m means squared metre erosion vertical height times lateral width) per metre longitudinal length of the stream.***

Chapter 11. Deposition and bank erosion

This chapter consists of two sections: *Section 11.1.* is about observations of erosion and deposition and *Section 11.2.* is about measurements of erosion and deposition.

11.1. Observations of erosion and deposition

In *Appendix 6* a map with observations of erosion and deposition can be found. In *Figure 46* it can be seen whether according to the observations erosion, deposition at the bank top or erosion at the toe and deposition at the bank top takes place at the profiles. Both, erosion and deposition takes place at the west part of profile 12, at the west part of profile 13 and at the east part of profile 14. Erosion can be seen at the west part of profile 2, the west part of profile 14, the west part of profile 14, the west part of profile 18 and the east part of profile 8 and profile 11. The observed activity of erosion is not equally at these parts of profiles. At some profiles tension cracks are visible and active erosion takes place. At other profiles the erosion is not such active any more. Also deposition can take place. In the other cases, the yellow colour in the figure, no erosion and no deposition is found. Between profile 10 and profile 11 the Zegglink-Hagbrug is located. It is noticed that to the north of this bridge (downstream) more 'happens' than to the south of this bridge (upstream): more erosion and deposition takes place at the north part of the bridge. In the research area different forms of bank failure are found; as well rotational slumping as failure of undercut banks as toppling of vertical arranged slabs are found.

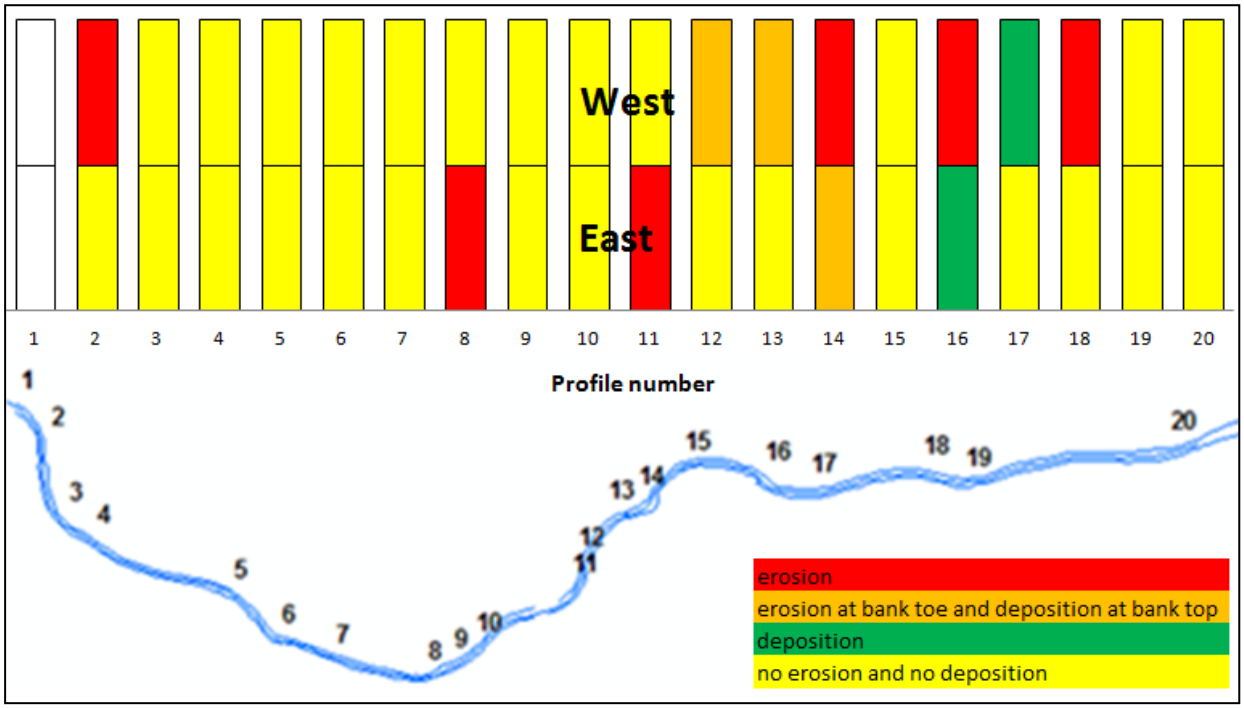

Figure 46: Observations of erosion and/or deposition at the profiles of the Groenlose Slinge (2011). The upper row represents the west banks and the lower row the east banks.

In *Figure 47* to *Figure 83* photos of the locations of the profiles where erosion, deposition or both takes place. Also the corresponding measured cross sections are shown. To see the differences and similarities of the morphology in time, as well photos of May 2009 as photos of May 2011 are shown. All photos were taken in northern (downstream) direction.

Profile 2

Notice that the location of profile 2 was moved a few metres between 2008 and 2011. When this exactly happened is not clear. As can be seen in the photo of 2009 (*Figure 48*) as well as in the photo of 2011 (*Figure 49*) erosion takes place at the west bank of the profile. Also a fish ladder is close by that seems to cause this erosion. However, in the profile (*Figure 47*) no erosion can be detected at the west part, but net deposition is visible. Thus, because of net deposition according to the cross section, between 2008 and 2011 the total the amount of deposition is larger than the total amount of erosion. Looking to the period between 2008 and 2011 into more detail (*Appendix 2*), it can be seen that between 2008 and 2010 net deposition took place and between 2010 and 2011 net erosion took place. Comparing the photos of 2009 and 2011, the net deposition is also visible because the west bank in 2011 is significantly higher than in 2009, similar to the cross section. According to the cross section of the profile also at the east bank and in the channel deposition took place.

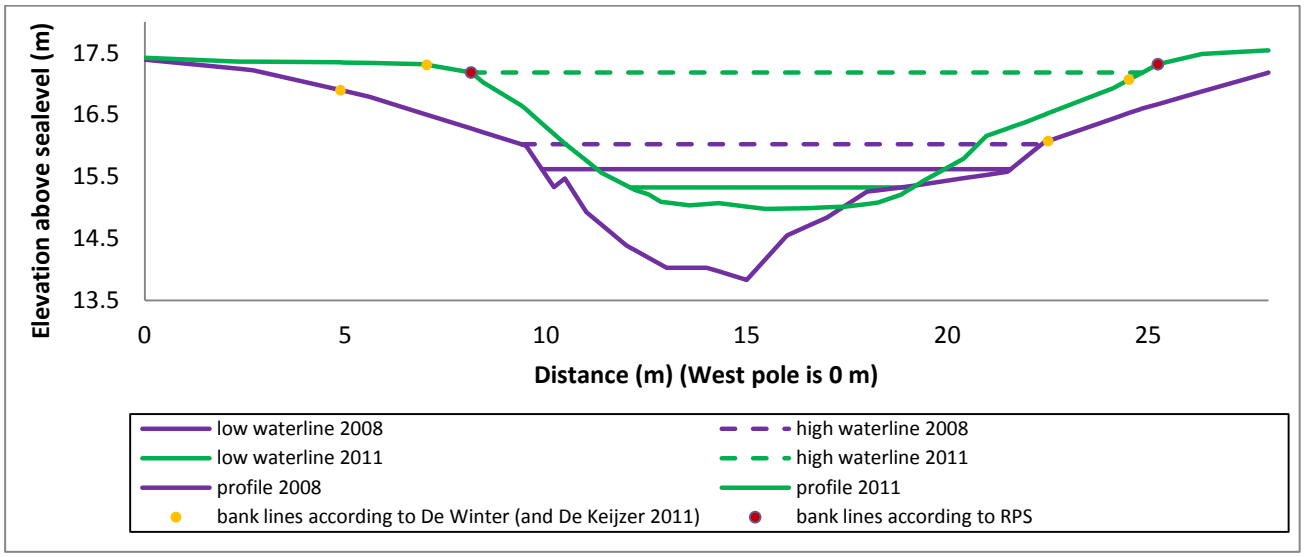

Figure 47: Cross section profile 2. This profile is considerably influenced by human action.

Figure 48: Profile 2 (May 2009).

Figure 49: Profile 2 (May 2011).

Profile 8

According to the photos (*Figure 51* and *Figure 52*) at the east bank of profile 8 erosion takes place as well in 2009 as in 2011. This is also confirmed by the profile (*Figure 50*). At and around the east bank of this profile active erosion takes place: slides including vegetation and tension cracks are visible (*Figure 53* and *Figure 54)*. A measured slide block is about 1.2 m * 0.3 m * 0.3 m. The vegetation at the slide block has a maximal height of 50 cm, consisting of Salix alba (while willow), *Alnus* (alder) and grasses. The block is partly under water. The vegetation around the slide block consists of Tanacetum vulgare (tancy) and other herbs and grasses. The tension cracks are about ten cm deep and one cm wide. About ten metres to the north of this profile, old, mature forest is present at the east bank. The start of this forest is also at the photos visible. It is striking that there where the forest begins, the erosion stops and the stream becomes narrower. The profile shows that on the west bank a scroll bar is present.

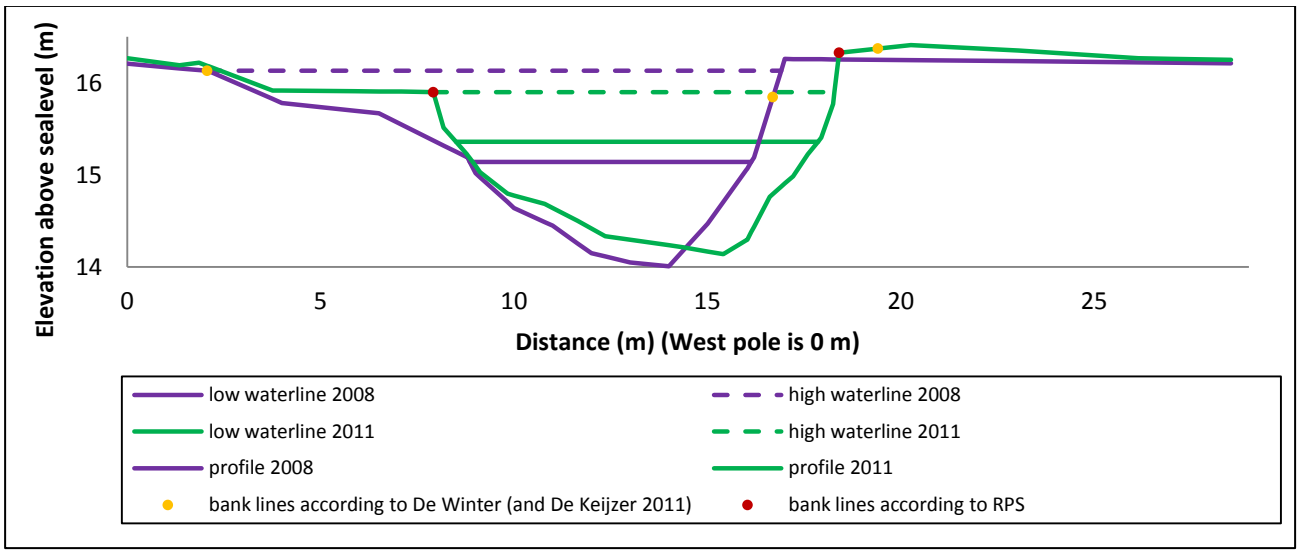

Figure 50: Cross section profile 8. Note the scroll bar on the west (left) bank.

Figure 51: Profile 8 (May 2009).

Figure 52: Profile 8 (May 2011).

Figure 53: Active erosion at the east bank of profile 8, slides and tension cracks are visible.

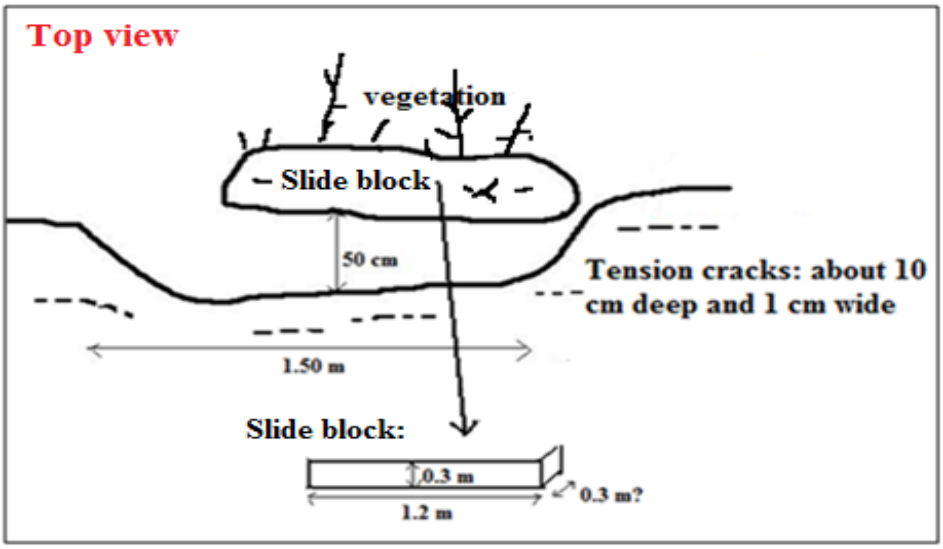

Figure 54:Schematic top view of active erosion at the east bank of profile 8. The vegetation at the slid block has a maximal height of 50 cm and consists of Salix alba (white willow), Alnus (alder) and grasses. The vegetation around the slide block consists of Tanacetum vulgare (tancy) and other herbs and grasses.

Profile 11

According to the observations erosion is visible at the east side of profile 11 (*Figure 57*). According to *Figure 56* also in 2009 erosion was present. This erosion is not very active, because no tension cracks and slide blocks are found. In the cross section of *Figure 55* nearly no erosion is visible at the east bank and the net erosion/deposition is equal to zero. In the profile of *Figure 55* it can be seen that on the west bank a scroll bar was formed between 2008 and 2011. On the banks herbs and grasses are present. However, about ten metres to the north of profile 11 more active erosion is observed (*Figure 58*). Here, the vegetation on the high bank consists of mature forest and hanging roots are visible. It is clearly visible that the upper layers of the bank profile are less eroded than the lower layers.

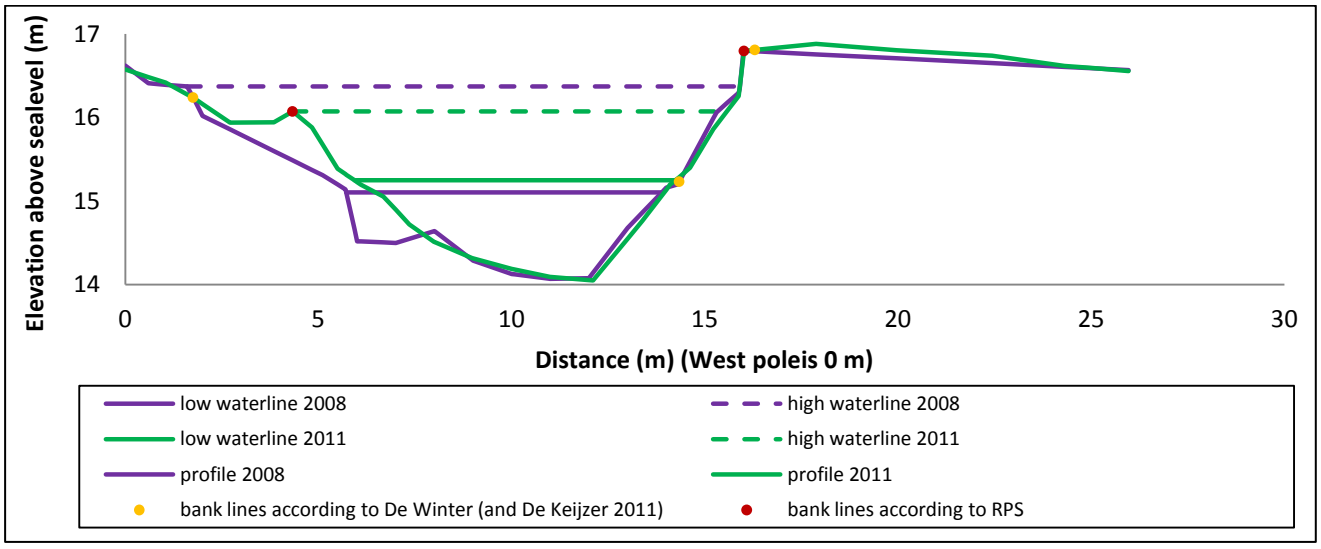

Figure 55: Cross section of profile 11. Note the scroll bar on the west (left) bank.

Figure 56: Profile 11 (May 2011).

Figure 57: Profile 11 (May 2009).

Figure 58: Erosion to the north of profile 11, east bank.

Profile 12

At the west bank of profile 12 deposition is visible at the upper part of the bank and a little bit erosion is visible at the lower part of the bank (*Figure 60* and *Figure 61*). In the cross sections of profile 12 (*Figure 59*) it can also be seen that at the upper part of the west bank deposition took place and at the lower part of the west bank erosion took place. In *Figure 62* the deposition at the west bank is clearly visible. Also significant overbank deposition is found. The deposited sand is grown by herbs called Conyza canadensis (Canadian Horseweed), a pioneering species. Directly at the waterline Salix alba (white willow) and *Alnus* (alder) are growing. In the deposited overbank sand

small hills of sand can be found behind small vegetation. These hills are called lee bars (*Figure 63*). Lee bars can be formed by overbank flow during high water.

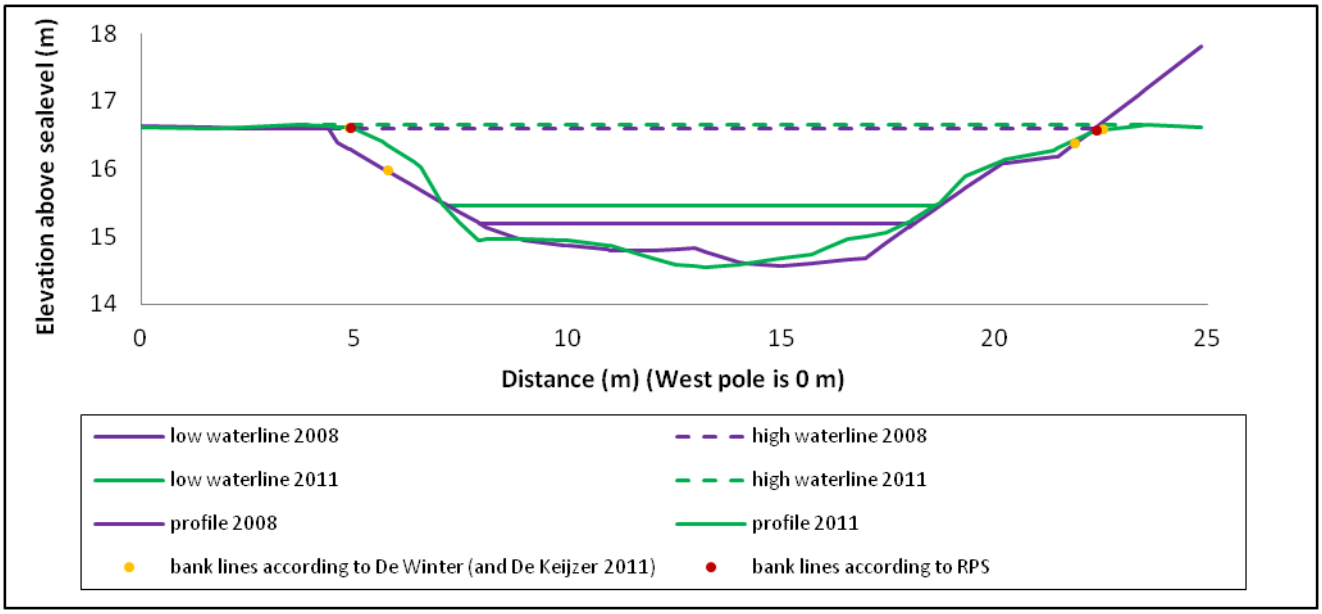

Figure 59: Cross section profile 12.

Figure 60: Profile 12 (May 2009).

Figure 61: Profile 12 (May 2011).

Figure 62: Deposition at the west bank of profile 12, covered by Conyza Canadensis (Canadian horseweed). Some small trees are present at the waterline.

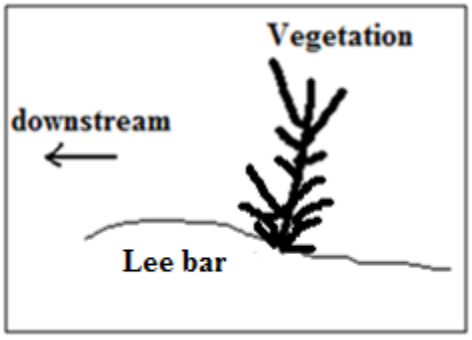

Figure 63: Lee bar behind vegetation.

Profile 13

At profile13 still the same situation as at profile 12 exists (*Figure 65* and *Figure 66*), but more erosion and less deposition is visible. This observation is reflected in the cross sections of *Figure 64* because now over the whole west part of the profile net erosion is visible instead of only at the lower part like in case of profile 12. On the east bank a scroll bar was formed between 2008 and 2011.

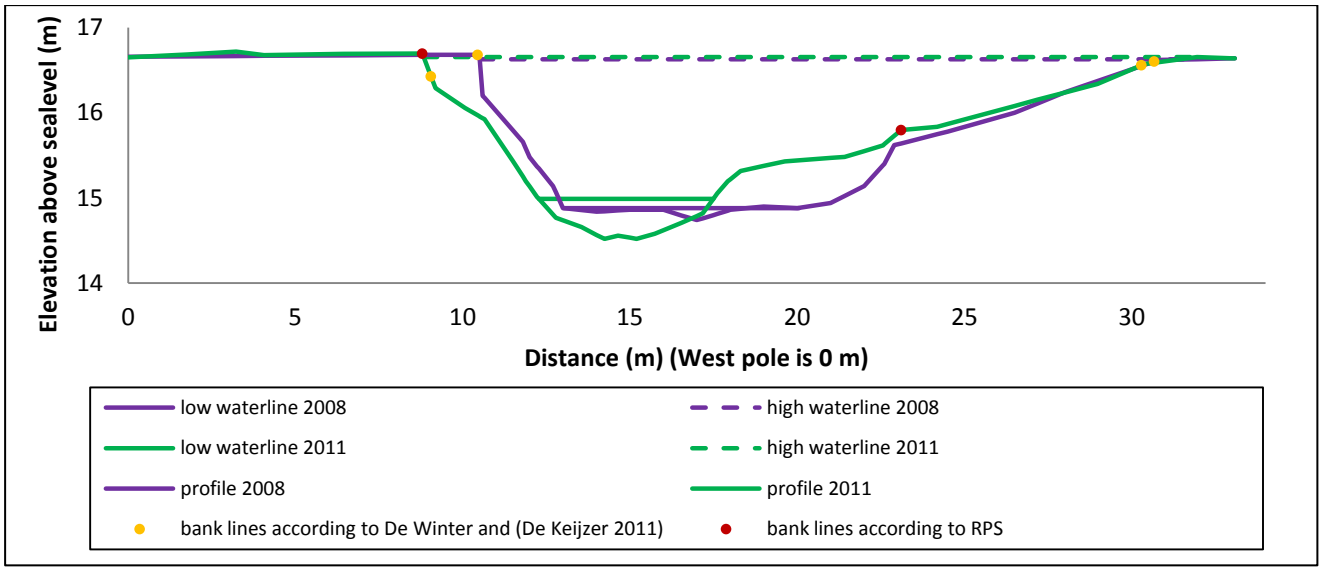

Figure 64: Cross section profile 13. Notice the scroll bar on the east (right) bank.

Figure 65: Profile 13 (May 2009).

Figure 66: Profile 13 (May 2011).

Profile 14

According to observations (*Figure 68* and *Figure 69*), at the west part of profile 14 a bit erosion takes place and at the east part erosion and deposition takes place. To the south of the west bank of profile 14 (upstream) more erosion takes place and to the north of the west bank the erosion disappears. Also the profiles (*Figure 67*) show erosion at the west bank and erosion and deposition at the east bank. However, the profile shows also deposition at the west bank. Profile 14 is located in a wide, sharp bend. A few metres to the south (upstream) of profile 14, the apex of this bend is located. Most deposition of sand is found at the banks where the bend is widest. Profile 14 is very striking in comparison to other profiles of the stream. The bend of profile 14 is very wide in comparison to other bends and at both sides erosion takes place. In contrast to other profiles this profile is deeper than in 2008. According to the (air)photos (*Figure 68, Figure 69*, *Figure 70* and *Figure 71*), also in 2009 this bend was already striking and different than the other ones. The lateral

migration of this bend is small: 0.27 m between 2008 and 2011 at the west bank and 0.19 m in this period at the east bank. Also the stream pattern in this bend of profile 14 is striking. In the middle of the channel a stream goes in downstream direction, but at the east and west sides a stream goes in upward direction (*Figure 72*).

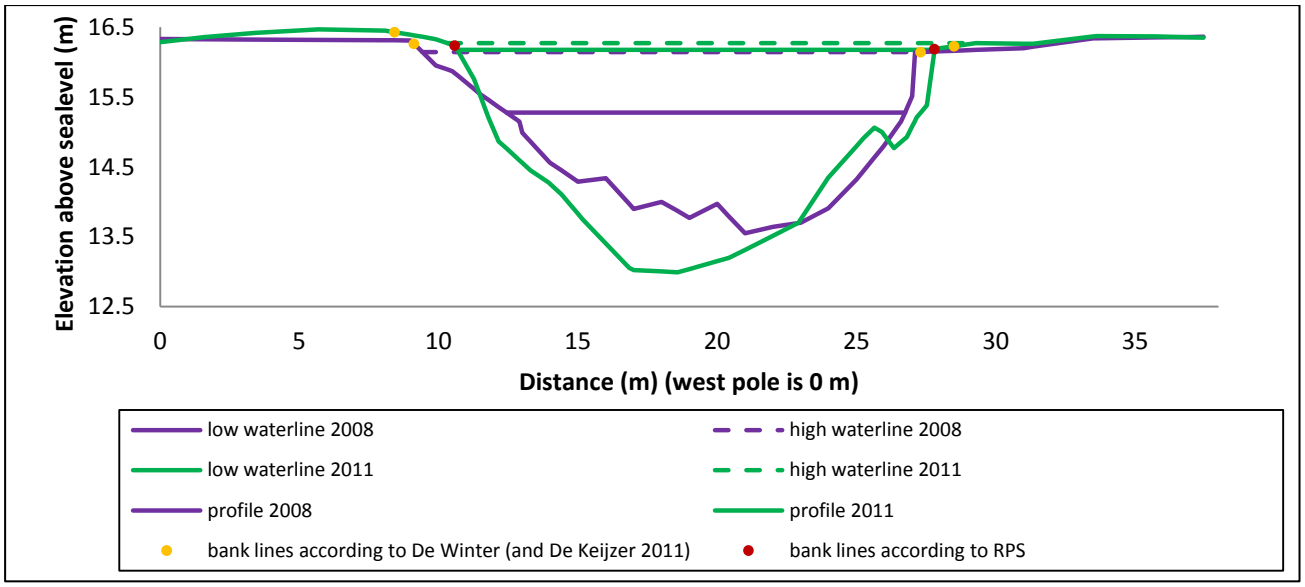

Figure 67: Cross section profile 14.

Figure 68:Profile 14 (May 2009).

Figure 69: Profile 14 (May 2011).

Figure 70: Airphoto of profile 14 (Markies, May 2009).

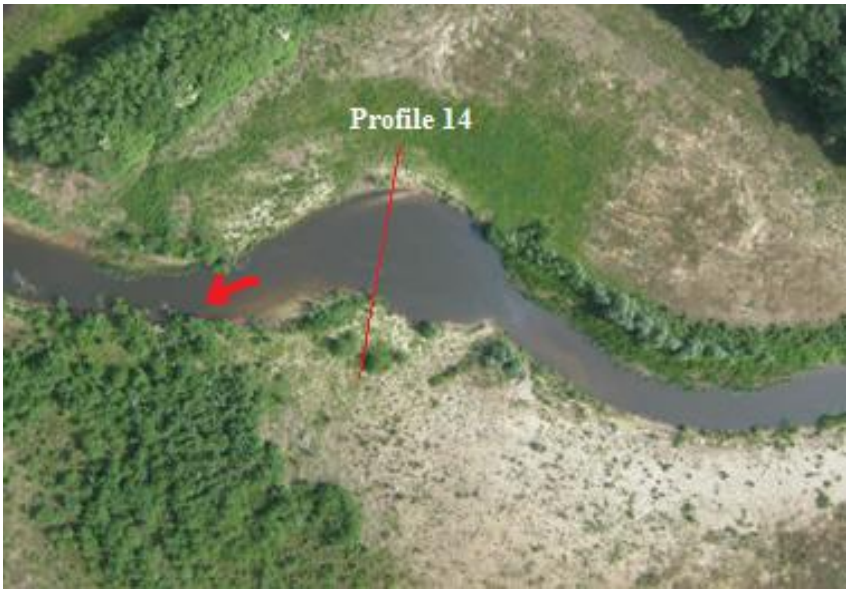

Figure 71: Airphoto of profile 14 (Markies, May 2011).

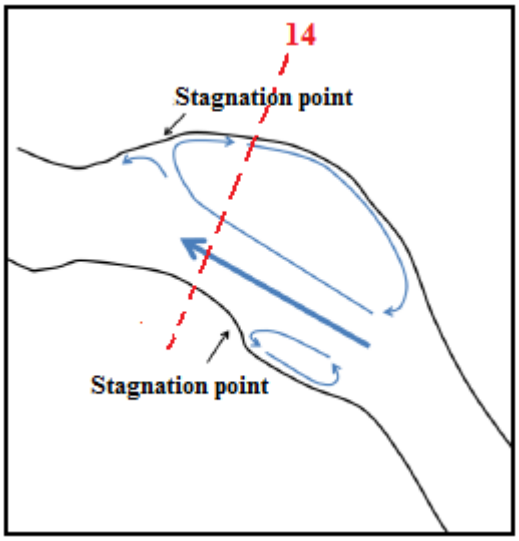

Figure 72: Flow lines of sharp bend at profile 14 (Van der Kruijs, 2010).

Profile 16

According to observations, at the west part of profile 16 erosion takes place and at the east part deposition. This is clearly confirmed by the profiles in *Figure 73*. Comparing the two photos (*Figure 74* and *Figure 75*), the deposition was also clearly visible in 2009. This deposition is part of a scroll bar which is visible in *Figure 76* and *Figure 77*, a few metres north of profile 16. The scroll bars have a spit like appearance. As can be seen, also in 2009 this scroll bar was already visible, but the scroll bar in 2011 is higher than the scroll bar in 2009.

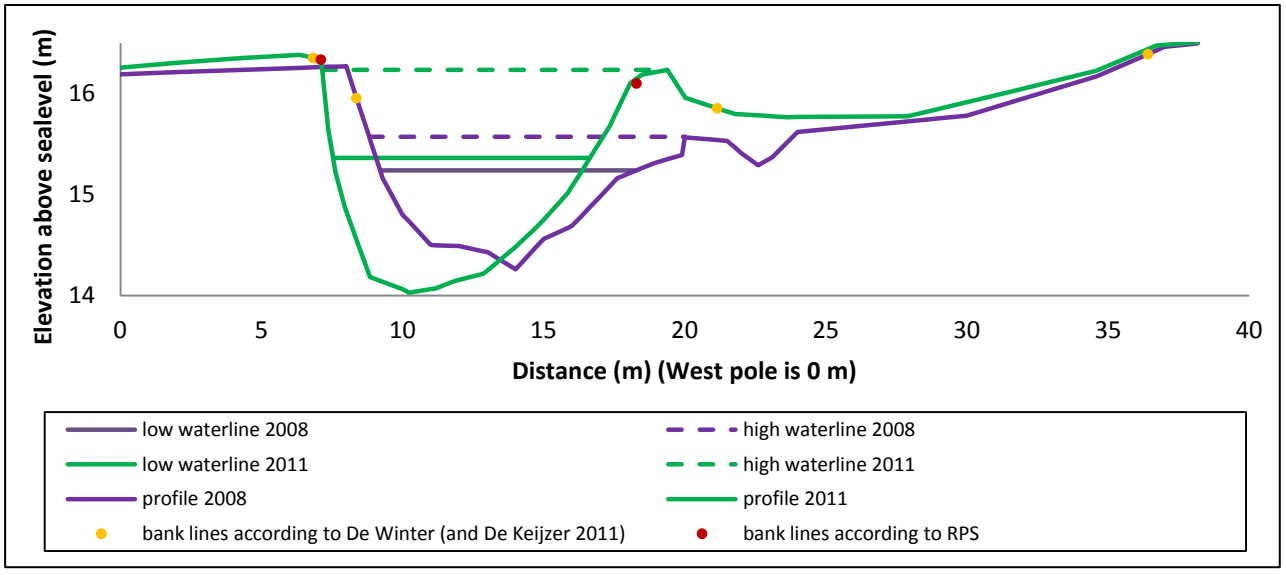

Figure 73: Cross section profile 16. Notice the scroll bar on the east (right) bank.

Figure 74: Profile 16 (May 2009).

Figure 75: Profile 16 (May 2011).

Figure 76: Few metres north of profile 16 (May 2011), scroll bar.

Figure 77: Few metres north of profile 16 (May 2009), scroll bar.

Profile 17

At the west part of profile 17 deposition is visible. As can be seen on the photos (*Figure 79* and *Figure 80*), this deposition was not yet present in May 2009. The deposition at the west bank is also visibile in the cross sections of *Figure 77*. About 0.5 m deposition in vertical direction took place and the deposition has the form of a ridge with a length of about 100 metres. On the one hand, this feature can be called a levee because of its length, but on the other hand it cannot be called a levee because the feature is located in the channel which indicates a sroll bar. However, it is debatable whether this long deposition form can still be called a scroll bar.

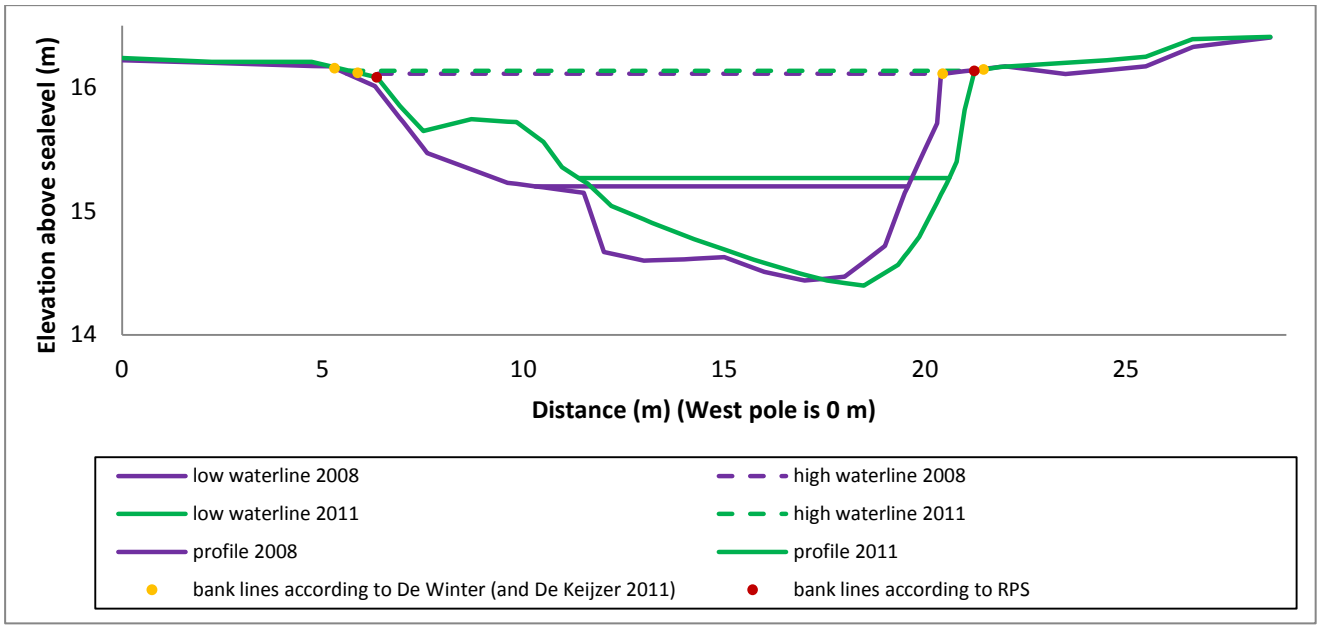

Figure 78: Cross section profile 17. Note the deposition at the west (left) bank.

Figure 79: Profile 17 (May 2009).

Figure 80: Profile 17 (May 2011).

Profile 18

In case of profile 18, deposition at the east bank is observed (*Figure 82* and *Figure 83*). This is also confirmed by the profile in *Figure 81* which also show deposition at the east part.

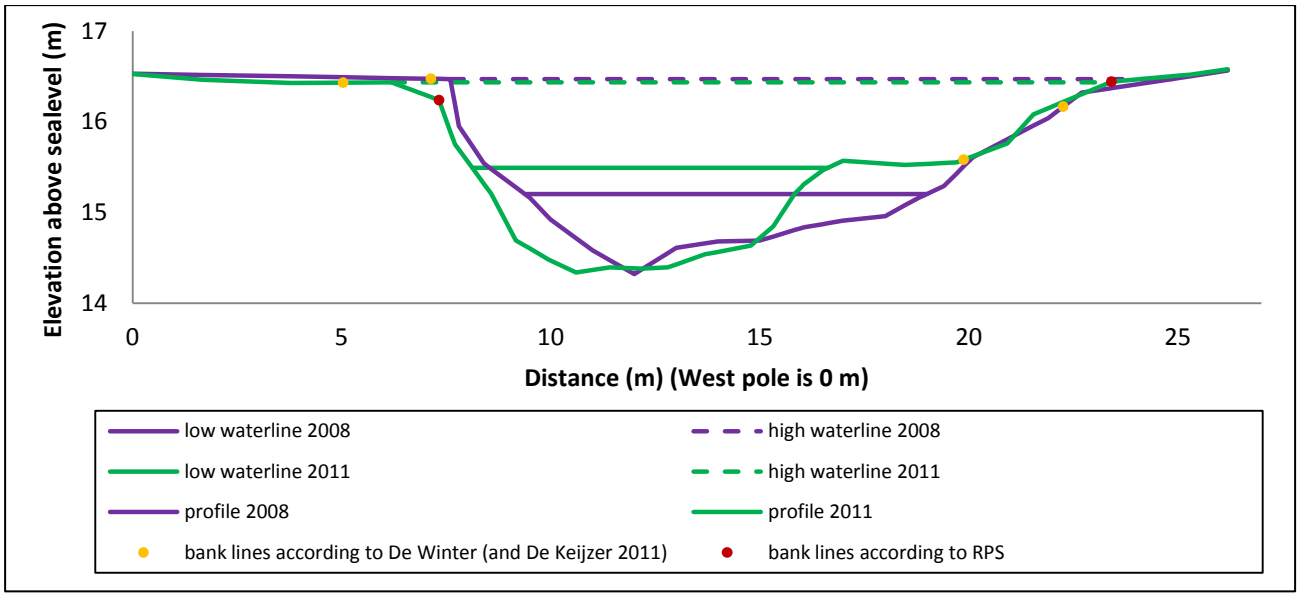

Figure 81: Cross section profile 18. Note the scroll bar on the east (right) bank.

Figure 82: Profile 18 (May 2009).

Figure 83: Profile 18 (May 2011).

11.2. Measurements of erosion and deposition

In *Figure 84* the net amount of erosion or deposition in m^2 is shown for each profile, except for profile 1 and 2. Especially profile 2 shows a very high amount of net deposition (14.4 m^2), but because of the construction of a fish ladder and the displacement of the profile, the net deposition of this profiles is not reliable and thus not included. Also at profile 1 the net deposition is relatively high (13.8 m^2). Again, the fish ladder is constructed around this profile and in consequence also this profile is not included. In *Figure 84* a positive value means net deposition and a negative value means net erosion between 2008 and 2011. Looking to the figure, nearly at all profiles net deposition took place, except at profile 4 and at profile 14 where net erosion took place. Also at profile 6, profile 8 and profile 18 a bit net erosion took place. Studying the figures that represent the width (*Figure 24* and *Figure 28* to *Figure 35*), it can be seen that at the profiles downstream of the profiles where net erosion takes place the width is relatively small: at profile 4 net erosion takes place and profile 5 has a relatively small width, at profile 14 net erosion takes place and profile 15 has a relatively small width and also a profile 18 a relatively a bit net erosion takes place and profile 19 has a relatively small width. That could mean that the erosion in the profiles 4, 14 and 18 stimulates deposition in the profile downstream. The net deposition averaged over the length of this part of the Groenlose Slinge is equal to 1.5 m^2 per metre length and thus 2700 m^3 net deposition for the section between profile 3 and profile 20 for the period 2008-2011. This means an average net deposition of 0.5 m^2 per metre per year and 900 m^3 per year for this whole section. This deposition is reflected by the increases in different elevation measurements of the profiles. The deposited sand must come from upstream. Upstream from the fieldwork area also dig activities in the Groenlose Slinge took place. These activities took place recently, after the activities in the research area (Bollen Weide, 2011). The activities can cause much erosion as also in the research part of the Groenlose Slinge between 2007 and 2008 happened. The eroded sand from upstream could deposit in the researched part of the Groenlose Slinge. In the course upstream of the fieldwork area no measurements were done and neither clear observations of erosion are visible. However, this course upstream where activities took place has a much longer length than the fieldwork course. Accordingly, just a few centimetres of erosion per metre length can already lead to significant deposition in the shorter course between profile 3 and profile 20. However, measurements should take place to confirm this hypothesis that the dug activities upstream deliver the sand for deposition downstream. Although it is not exactly known where the sand comes from, it can be assumed that the sediment is not coming from upstream of Winterswijk because near Winterswijk yearly 800 m^3 sediment is caught.

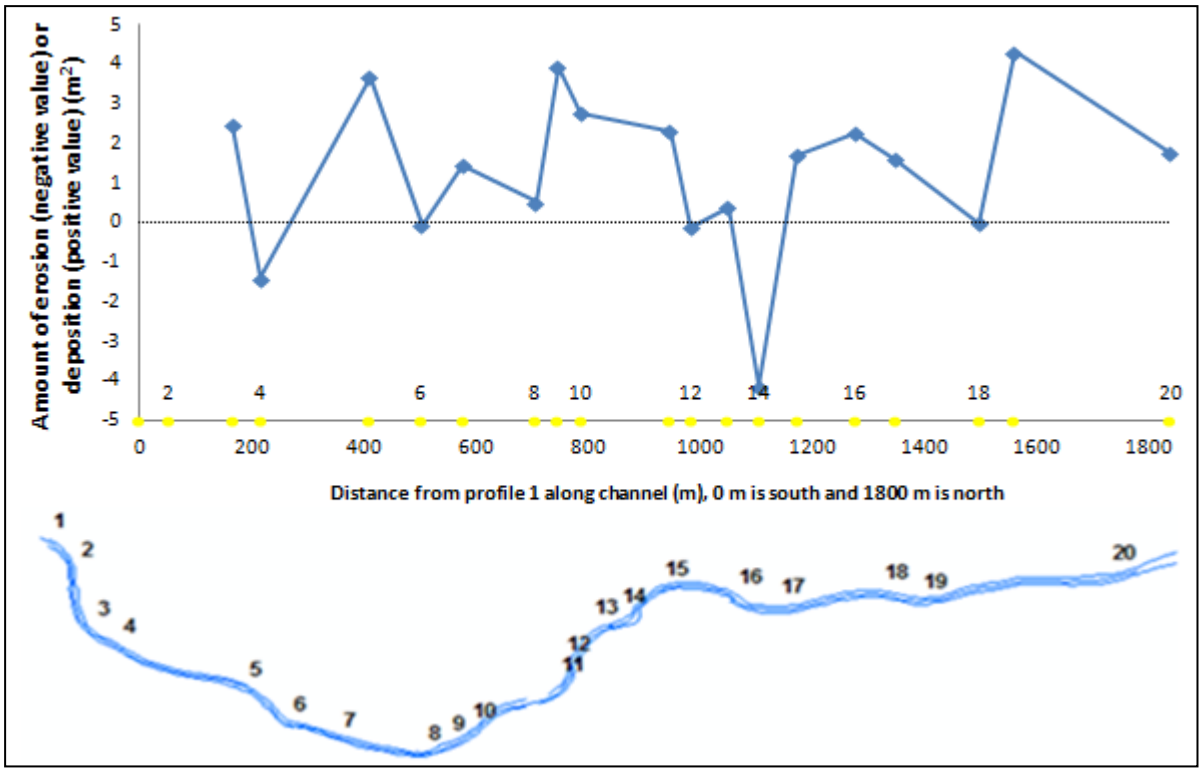

Figure 84: Amount of net erosion (negative value) or net deposition (positive value) (m^2) at each profile between 2008 and 2011. The amount of net erosion or net deposition is determined by the surface under the profile of 2011 minus the surface under the profile of 2008.

Chapter 12. Vegetation characteristics

This chapter is about the vegetation around the Groenlose Slinge. *Section 12.1.* is about the found vegetation species around the Groenlose Slinge, *Section 12.2.* is about vegetation patterns and the relation of vegetation to erosion and *Section 12.3.* is about root characteristics.

12.1. Vegetation species around the Groenlose Slinge

In *Appendix 10* a list of plant species found in the Groenlose Slinge is shown. In this list the vegetation names are in Latin, English and Dutch. In the field several vegetation species were present. Concerning trees, mainly young *Salix alba* (white willow), young *Alnus glutinosa* (black alder) and young *Alnus incana* (grey alder) were found. Also young *Betula Pubescens* (downy birch) and *Salix aurita* (eared willow) were present. The length of the young trees that were found can vary from a few centimetres to about four metres. Also young herbs were found, especially *Tanacetum vulgare* (tancy), *Urtica dioica* (common nettle) and *Conyza Canadensis* (Canadian horseweed) are common. Other herbs that were also found are: *Equisetum fluviatile* (horsetail), *Caltha palustris* (kingcup), *Sparganium erectum* (branched bur-reed), *Mentha aquatic* (water mint), *Rumex hydrolapthum* (great water dock) and *Jacobaea vulgaris* (ragwort). Concerning the grasses, many types were found, but the most common ones are *Phragmites australis* (common reed), *Typha* (bulrush) and *Glyceria maxima* (reed mannagrass). *Phragmites australis* (common reed) grows only near the waterline, not on top of the bank. At some locations mature forest was present. These forests contain besides the same species as the young trees, the young herbs and the young grasses, also *Quercus* (oak) and other tree-, shrub-, herb- and grass species. In *Figure 85* some of the most common vegetation species are shown.

Figure 85: Common vegetation species in and around the Groenlose Slinge.

Interesting features found at several locations in shallow water are old, short root stems (*Figure 86*). It is not possible to pull out those root stems because they break immediately. These root stems were also found during the fieldwork of 2008.

Figure 86: Old wood stems in the Groenlose Slinge.

From the observed vegetation a vegetation map was created. In *Appendix 7* the vegetation map can be found. Apart from observations, this map is also based on airphoto maps (airphoto map 2009 and airphoto map 2011 can be found in *Appendix 8*). Because of a smaller scale than reality, it was not possible to show all found species of vegetation on the maps. So, some categories were designed:

1) small trees
2) short grasses (<40 cm)
3) high grasses (>40 cm)
4) herbs
5) a combination of grasses, herbs and small trees
6) a combination of grasses and herbs
7) a combination of bare soil, grasses, herbs and small trees
8) bare soil
9) mature forest

The boundaries between the different categories on the vegetation map are not very strict. Two reasons can be called. The first reason is that not at every location the observed vegetation was noted in the field or could be clearly seen from the airphoto map. Consequently, assumptions had to be made. The second reason is that in nature often no strict boundaries between the different categories exist. There are often transitions from one category of vegetation to another category of vegetation. However, although the boundaries are not very strict, the vegetation map gives a good indication where what vegetation can be found.

12.2. Vegetation patterns and the relation of vegetation to erosion

The vegetation map (*Appendix 7*) was studied to find vegetation patterns. In longitudinal direction no patterns could be detected. Concerning the lateral direction, in the inner bends the sequence of common reed and/or bulrush at the water side, followed by young trees and then by mature forest is the most common sequence (33%) (*Figure 87*). A typical sequence in the outer bends is small trees at the water side followed by a mixture of grasses, herbs and small trees (33%) (*Figure 87*). In 73% of the inner bends reed and/or bulrush is present in contrast to 17% in the outer bends (*Figure 88*). In the outer bends mainly young trees were found (50%) and concerning the inner bends, in 20% of the bends young trees were found (*Figure 88*).

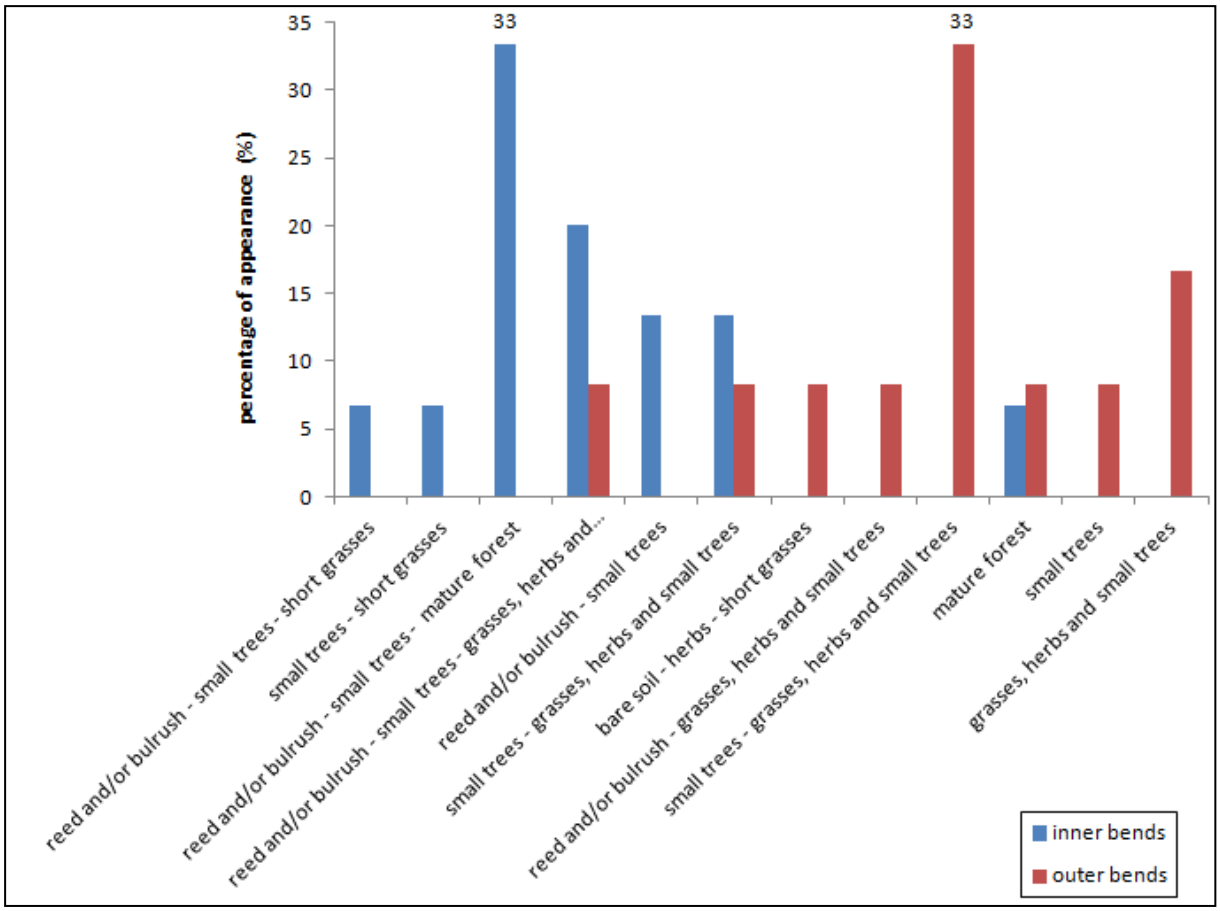

Figure 87: Occurrence of different lateral vegetation patterns.

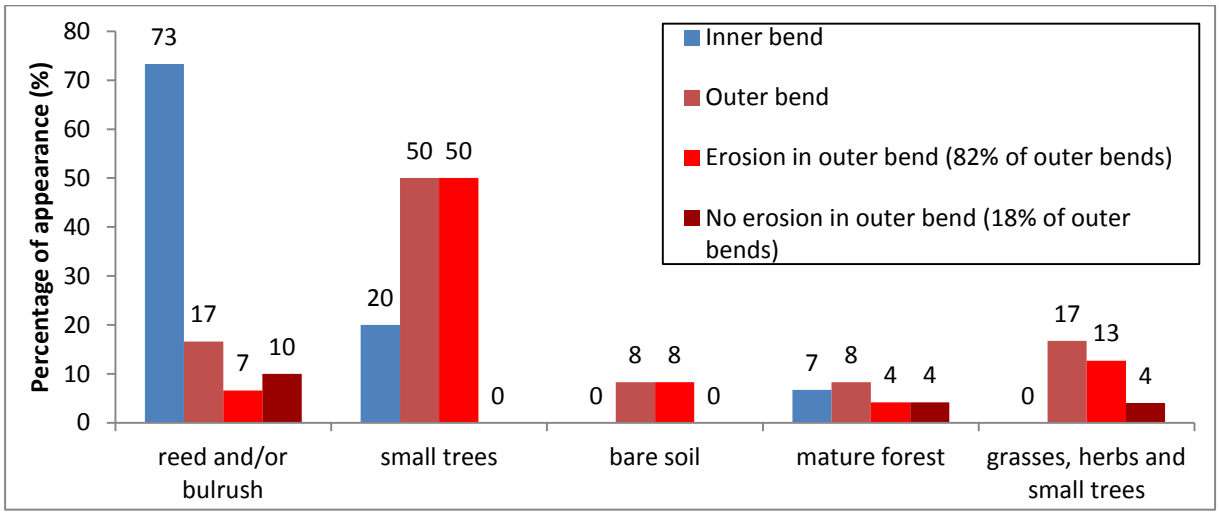

Figure 88: Occurrence of vegetation in inner bends and outer bends, occurrence of erosion in outer bends for each vegetation type and occurrence of no erosion in outer bends for each vegetation type. In the inner bends no erosion takes place.

When the locations of erosion (*Appendix 6*) were studied it was clearly visible that a relation exists with the presence of an inner bend or an outer bend. Each time erosion takes place, it is always in an outer bend. As never erosion takes place in an inner bend this indicates that the channel was dug wide enough. Because the erosion pattern reflects the pattern of outer bends and a relation between

vegetation and outer bends exists, also a relation exists between erosion and vegetation. However, as can be seen in *Figure 88*, this relation is different than the relation between outer bends and vegetation: in case of reed and/or bulrush in the outer bends, which is in 17% of the outer bends the case, just in 7% of all bends erosion takes place. In 10% no erosion takes place. Also in case of mature forest in the outer bends, just in 50% of these bends erosion is visible (4% in total). In case of small trees and bare soil in outer bends in all outer bends erosion takes place. Also in case of grasses, herbs and small trees nearly always erosion is visible in outer bends. Therefore, according to the fieldwork, grasses and small trees have the same effect on erosion because no relation can be found of more often erosion in case of small trees than in case of grasses (except reed) or the other way around.

Thus, in summary, erosion takes mostly place in outer bends where young, small trees are most common. There is never erosion in the inner bends where common reed is most common. In the outer bends where no erosion takes place, mature forest and reed and/or bulrush are most common. In the field there was a clear observation that the stream becomes suddenly narrower and erosion stops, exactly where presence of mature forest starts (*Figure 51* and *Figure 52*, *Section 11.1*). Concerning these results, it can be concluded that vegetation has effect on the erosion pattern, but that the location of outer bends has the overwhelming influence on the erosion pattern. The reason that erosion only in outer bends takes place is the specific flow pattern in outer bends (*Figure 6, Section 2.3.*). A relation between erosion and vegetation also exists because some vegetation prefers to grow in an outer bend where erosion takes place and other vegetation prefers to grow in an inner bend where deposition takes place. It is not the case that this relation exists because some vegetation species are more resistant for erosion than others. In this project, first the stream was re-meandered and thereafter the vegetation was going to grow. When a meandering stream forms in a naturally way, the effect of vegetation is probably larger.

12.3. Root characteristics

The observations show that the root distribution of grasses, herbs and trees differ from each other (*Figure 89* and *Figure 90*). Grasses have the largest density of roots and trees have the lowest density. Grasses have the smallest root diameter and trees the largest. Herbs have intermediate values. Concerning the young trees also a difference between the different species seems to exist. The root diameter distribution of *Salix alba* shows a decreasing trend: *Salix alba* has most roots with a small diameter and least roots with a relatively large diameter. In case of *Alnus* the root diameter distribution is more equally distributed. About each diameter class between zero and five mm is about equally represented. The root diameters of *Betula* are larger than the root diameters of *Salix alba* and *Alnus*. However, just three observations of the *Betula* root distribution were done.

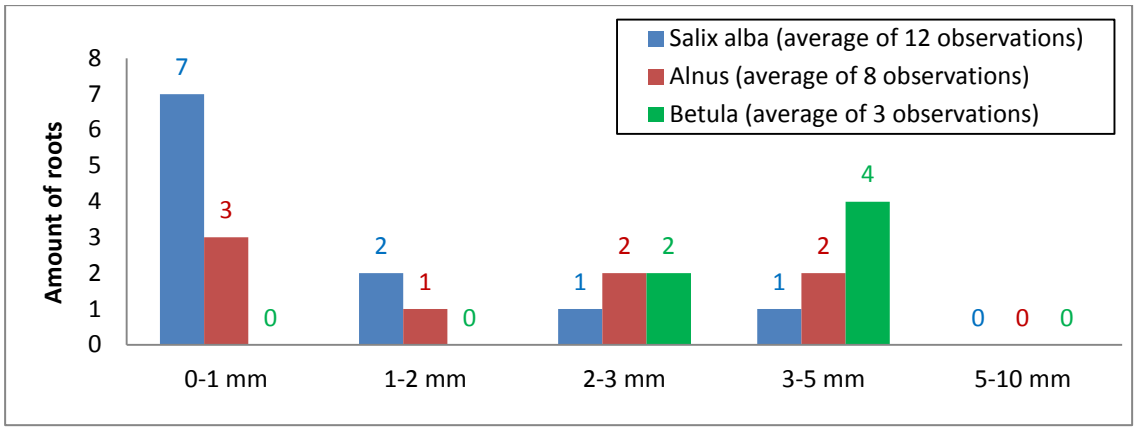

Figure 89: Root diameter distribution of small trees (Salix alba (white willow), Alnus (alder) and Betula (birch)).

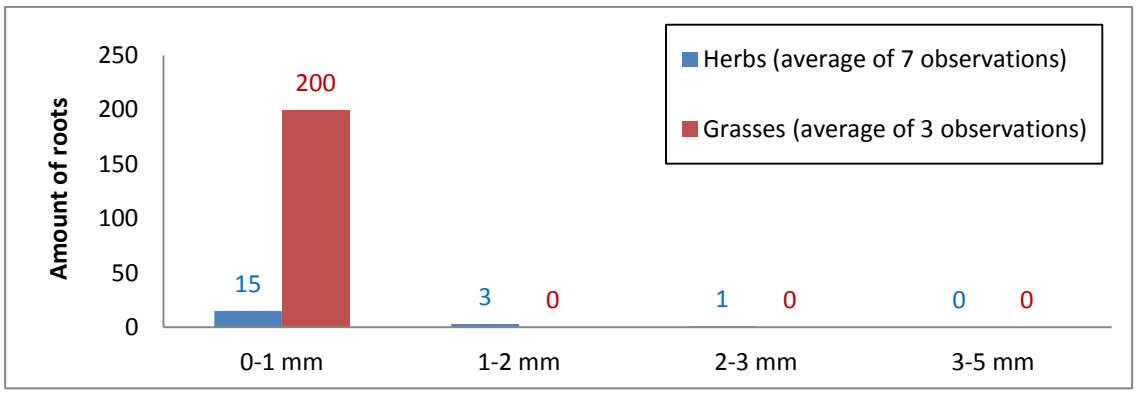

Figure 90: Root diameter distribution of herbs and grasses.

All young trees were rooted very shallow, about ten centimetres under the surface. Their longest roots have a length of at least four metres. The young trees have about five of these long roots. In *Figure 91* such a long root can be found. These long roots often contain runners of smaller roots. From the about five long roots, often one or two roots are thicker and longer than the other ones (*Figure 92*). When a long root is followed, it can be seen that it crosses other roots of other vegetation and it can be seen that a tangle of roots below the ground surface exists.

Figure 91: Long root of Salix alba (white willow).

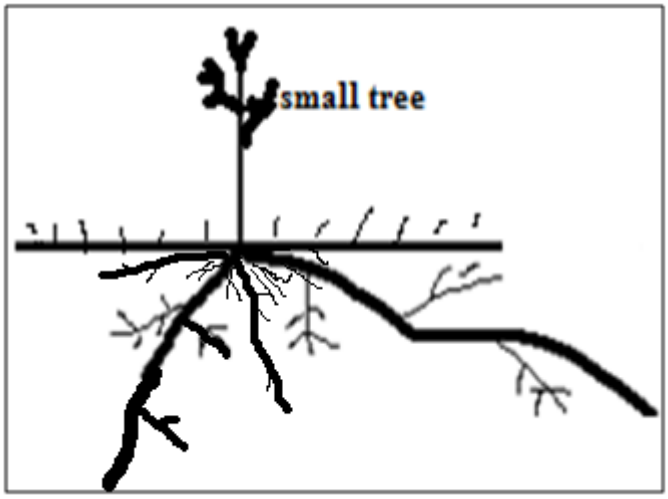

Figure 92: Small tree with about five longer roots of which one or two main roots.

The roots of herbs and grasses are shorter, denser and have a smaller diameter than the roots of small trees. The way of rooting of reed is different from most other herb- and grass species. In case of reed, root stems below the surface are present and thus the single reed stems that are above the surface are connected under the ground (*Figure 93)*. The root stems can have hairy small roots in wreaths around the root stems. Other grass species contain one wreath of many short, thin hair roots (*Figure 94*).

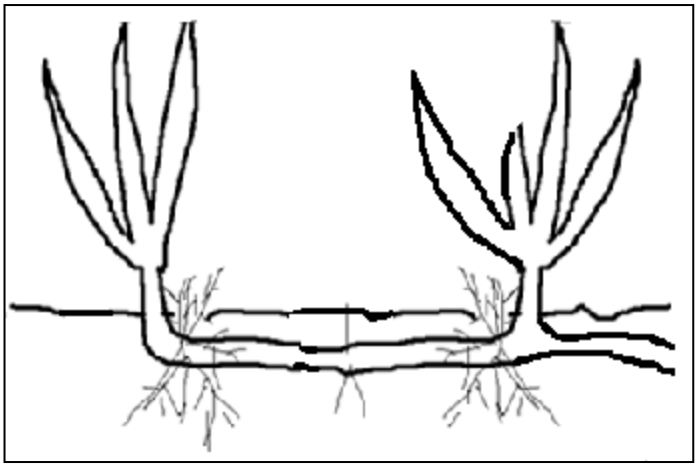

Figure 93: Reed. Note the connecting root stem below surface.

Figure 94: Grass species with one wreath of many short, thin hair roots.

Chapter 13. Bank Stability and Toe Erosion Model (BSTEM)

This chapter consists of six sections about results of the Bank Stability and Toe Erosion Model. *Section 13.1.* shows the results of added strength by vegetation roots, *Section 13.2.* is about the results of the bank stability model and *Section 13.3.* is about the toe erosion model. Next, *Section 13.4.* is about the modelled erosion and the comparison to measured erosion, *Section 13.5.* contains a sensitivity analysis and finally, *Sections 13.6.* gives a prediction of erosion between 2011 and 2012.

13.1. Added strength

According to the Bank Stability and Toe Erosion Model (BSTEM) the added strength by vegetation depends on the type and assemblage of vegetation, the age of vegetation, the material of the bank and the groundwater depth. In the Groenlose Slinge all these parameters could be changed in the period between 2008 and 2011. However, it is assumed that the type and assemblage of vegetation and the material of the bank and toe did not change. Actually, the assemblage of vegetation has changed between 2008 and 2011. When comparing (air)photos of 2009 and 2011 it can clearly be seen that the vegetation density has increased. Therefore, in BSTEM the assemblage of vegetation in 2011 should contain less bare soil than the assemblage of 2008. However, because just a rough estimation of the assemblage can be given, in the model it is assumed that the type and assemblage of vegetation has not changed.
Section 13.1.1. is about the added strength based on vegetation species, age and groundwater level. *Section 13.1.2.* is about the 'translation' between vegetation in the field and vegetation in BSTEM based on added strength and *Section 13.1.3.* contains the validation of added strength by roots.

13.1.1. Added strength based on vegetation species, age and groundwater level

In *Figure 95* the added strength of different vegetation species is plotted for different ages and for a low groundwater level and for a high ground water level. The low groundwater level is based on the measurements in the Groenlose Slinge in 2008 and the high water level is equal to the bankfull water level determined by the profiles of 2008. It can be noticed that for all types and ages the added strength in case of a large groundwater depth (low water, *Figure 95b* and *Figure 95d*) is larger than in case of a small groundwater depth (high water, *Figure 95a* and *Figure 95c*). The reason for this result can be that the increased matrix suction by vegetation at a large groundwater depth is larger than at a low ground water depth. In case of trees the added strength increases up to an age of 25 years and in case of herbs and grasses the added strength increases up to an age of ten years. After these ages the added strength remains constant.
The added strength is in all cases smaller than 3.5 kPa. Based on direct shear tests the cohesion of the soil without vegetation is equal to 5.8 kPa (Wytema, 2009). This means that the rate between added strength (kPa) due to vegetation and cohesion of soil (kPa) can increase to about 60%.
In *Figure 95* it can be seen that in case of mature vegetation, the added strength is least for meadow dry, second least for meadow wet and third least for canarygrass, reed. The added strength is highest in case of mature alder, followed by mature birch and black willow. As a result, it can be concluded that in case of the mature stage, the added strength of trees is larger than the added strength of grasses. However, studying the vegetation up to an age of five years old, it can be seen that the

added strength of grasses is larger than the added strength of trees. After about ten years the added strength by trees passes the added strength by grasses.

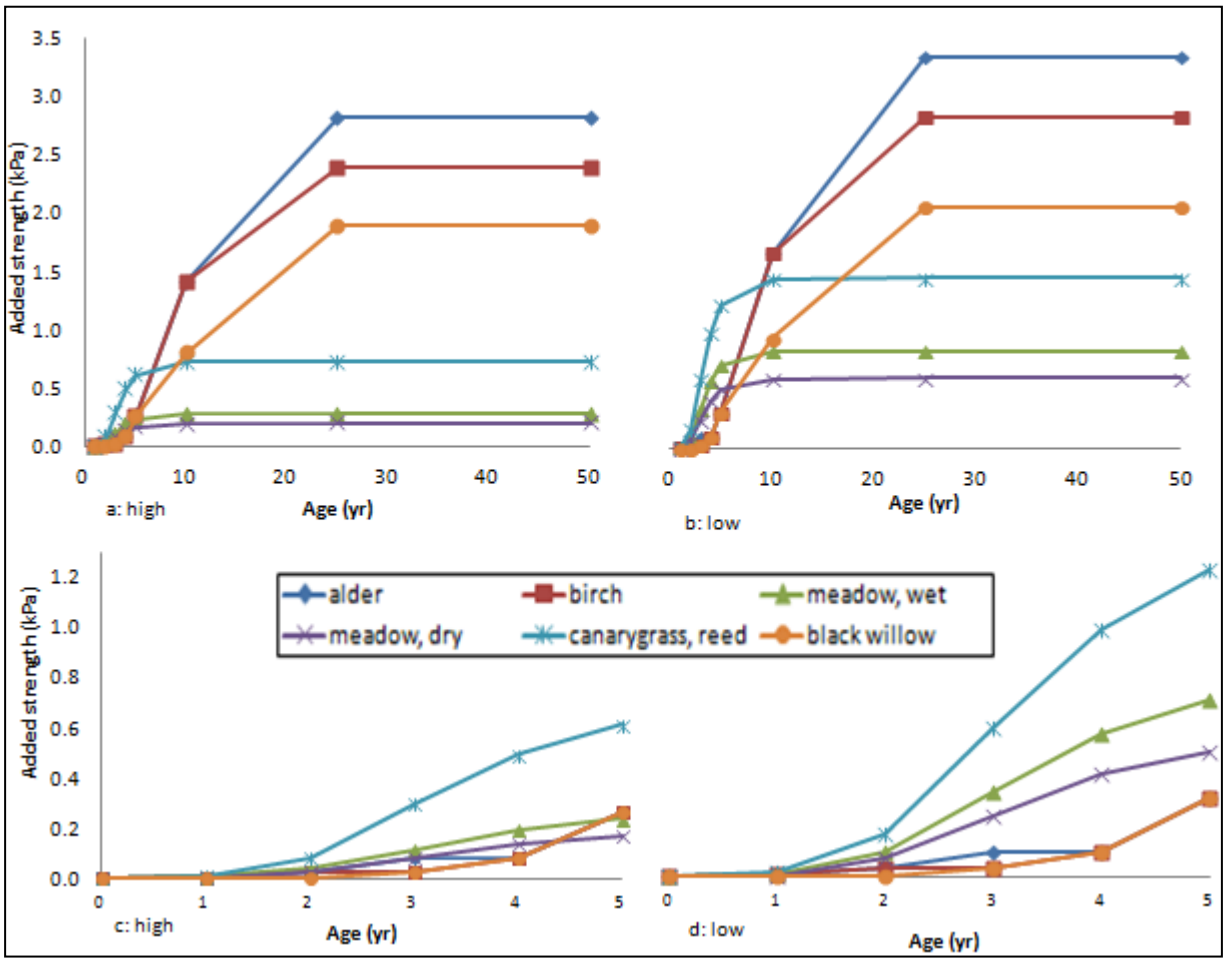

Figure 95: Added strength by vegetation roots (a=high water, up to 50 years, b=low water, up to 50 years, c=high water, up to five years, d=low water, up to five years.

13.1.2. 'Translation' between vegetation in field and vegetation in BSTEM

Most vegetation found in the field cannot be selected in the RipRoot model of BSTEM. In consequence, a 'translation' has to be made from the vegetation found in the field to the vegetation that can be chosen in BSTEM (*Table 7*). As can be seen, all trees found in the field are represented by alder. The reason for this representation is that according to BSTEM the added strength of trees hardly differs. However, the black willow differs from other trees in the mature stage and the added strength of mature black willow is between grasses and trees. It is assumed that herbs have a strength between grasses and trees. In consequence, in BSTEM the herbs are represented by black willow. Because it is assumed that the strength of high grasses like reed and bulrush is larger than the strength of short grass, high grass is represented by canarygrass, reed and short grass by meadow wet or meadow dry, depending on whether the short grass is close to the water or not.

Vegetation in field	Vegetation in BSTEM
birch	alder
alder	
white willow	
short grass (< 40 cm), at water side	meadow, wet
short grass (< 40 cm), not at water side	meadow, dry
high grass (>40 cm) (often reed)	canarygrass, Reed
herbs	black willow
bare soil / no vegetation	bare soil / no vegetation

Table 7: 'Translation' between vegetation in the field and vegetation in BSTEM.

13.1.3. Validation of added strength by roots

Apart from inserting the age of the vegetation to calculate the added strength which is the expected empirical added strength, in the RipRoot model of BSTEM also the root diameter distribution can be inserted to calculate the added strength. In *Figure 96* both methods for calculating the added strength are shown. On the x-axis, the upper row with vegetation names is the vegetation found in the field and the lower row with vegetation names is the vegetation in the RipRoot model that represents the vegetation in the field. It can be seen that the difference is added strength according to the two methods is small. On average, the added strength by inserting the root diameter distribution is 1.3 times higher than the expected empirical strength. Only in case of meadow wet, the method by inserting the root diameter distribution gives a bit smaller added strength than the expected empirical strength. It can be seen that in case of alder the added strength according to the root diameter distribution is 1.7 times higher than the expected empirical added strength. For birch this rate is equal to 1.8, for meadow wet this rate is 0.95, for meadow dry 1.3 and for black willow this rate is equal to 3.0. When the root distribution of *Salix alba* (white willow) that is found in the field is inserted in the alder option in BSTEM, the added strength is exactly the same as when the corresponding age at the 'alder option' is inserted. In case of mature alder and mature birch no observations could be done. However, an indication of the root distribution could be given based on the added strength according to the age. Based on their age, both, a 50-years old birch and a 50-years old alder give an added strength of 2.95 kPa. According to the model the following root distributions of alder and birch are possible, giving about the same added strength:

- 5 * 20 to 40 mm
- 4 * 20 to 40 mm and 12 * 10 to 20 mm
- 3 * 20 to 40 mm, 12 * 10 to 20 mm and 38 * 5 to 10 mm
- 3 * 20 to 40 mm, 12 * 10 to 20 mm, 30 * 5 to 10 mm and 105 * 3 to 5 mm

Besides these distributions also other distributions are possible. In the next chapters the empirical way to determine the added strength is applied and not the root diameter distribution, because the empirical method by inserting the age is an easier method and the differences in added strength between the two methods are negligible.

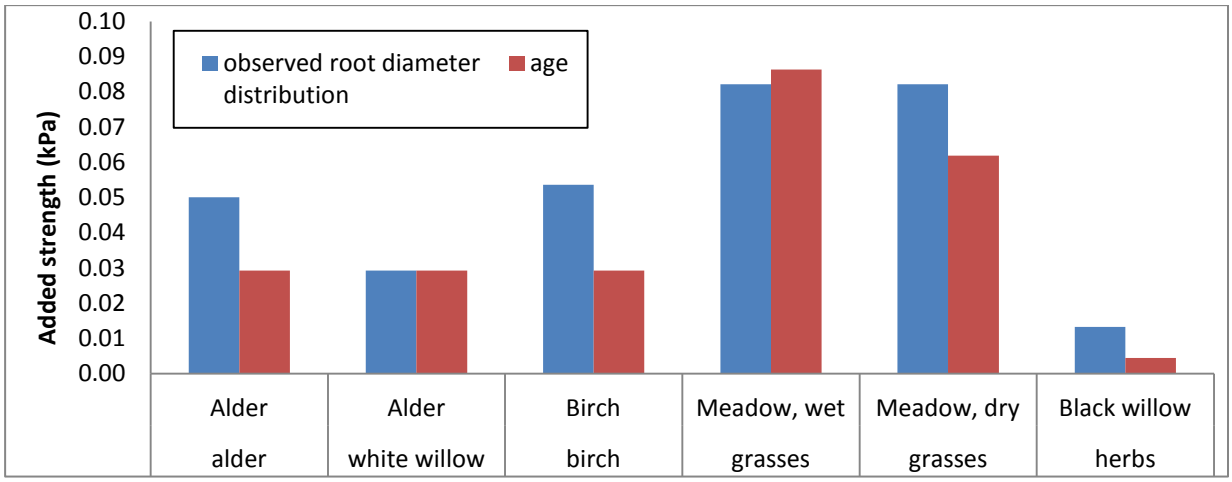

Figure 96: Modelled added strength based on age and based on observed root diameter distribution (profile 16w, 2008). On average, the modelled added strength based on age is 1.3 times larger than the modelled added strength based on root diameter distribution.

13.2. Bank stability model

In the bank stability model it was checked whether the bank profile is stable or not. When the factor of safety is larger than one, the bank is theoretically stable and no bank collapse takes place. When the factor of safety is smaller than one, the bank is unstable and bank collapse can take place. In that case also the failure width is calculated.

After having a close look to the bank stability model, it can be concluded that a high water level leads to a more stable profile and that a low groundwater depth leads to a less stable profile. It is assumed that in the Groenlose Slinge the groundwater level is equal to the water level in the channel and thus a high water level correlates to a low groundwater depth. Thus, on one hand profiles can become more stable due to an increased water level and on the other hand profiles can at the same time become less stable because of a decreased groundwater depth. However, a higher water level has much more influence on the stability than a lower groundwater depth. Hence, the bank becomes more stable in case of an increasing water level and a corresponding decreasing groundwater depth (*Table 8*). The bank stability model does not depend on the duration of flow, the reach slope and the reach length. Besides the water level and the groundwater depth, the bank stability also depends on the geometry of the profile. So, at one certain moment with equal water levels, some banks collapse while other banks do not. Also the bank material has influence on the stability: a clay-like bank is more stable than a sandy bank. This is because clay has a larger cohesion and thus a larger friction angle than sand. The failure width in case of failure does not depend on the factor of safety, but it depends on the bank geometry, the water level and the groundwater depth.

2008		Water level (m)	Groundwater depth (m)	Factor of safety	Failure width (m)
16W	High water level	16.27	0	2.59	-
	Low water level	15.24	1.03	0.70	0.10
18W	High water level	16.47	0	0.63	0.89
	Low water level	15.20	1.27	0.31	0.10

Table 8: The effect of water level and groundwater depth on the factor of safety. A factor of safety < 1 is an unstable situation and a Factor of Safety > 1 is a stable situation.

Also the type and age of vegetation have influence of the factor of safety (*Figure 97*). Comparing *Figure 95 (section 13.1.1)* and *Figure 97*, it can be seen that the factor of safety is directly related to the added strength because the pattern and shapes of the graphs are exactly the same. *Figure 97* represents profile 18W in 2008 and it can be seen that at this profile meadow wet and meadow dry can never really stabilize the profile because the maximal factor of safety is not larger than one. According to BSTEM, in this example canarygrass reed can cause a stable profile as youngest. Only this canarygrass reed can cause a safety profile in the first five years in case of high water.

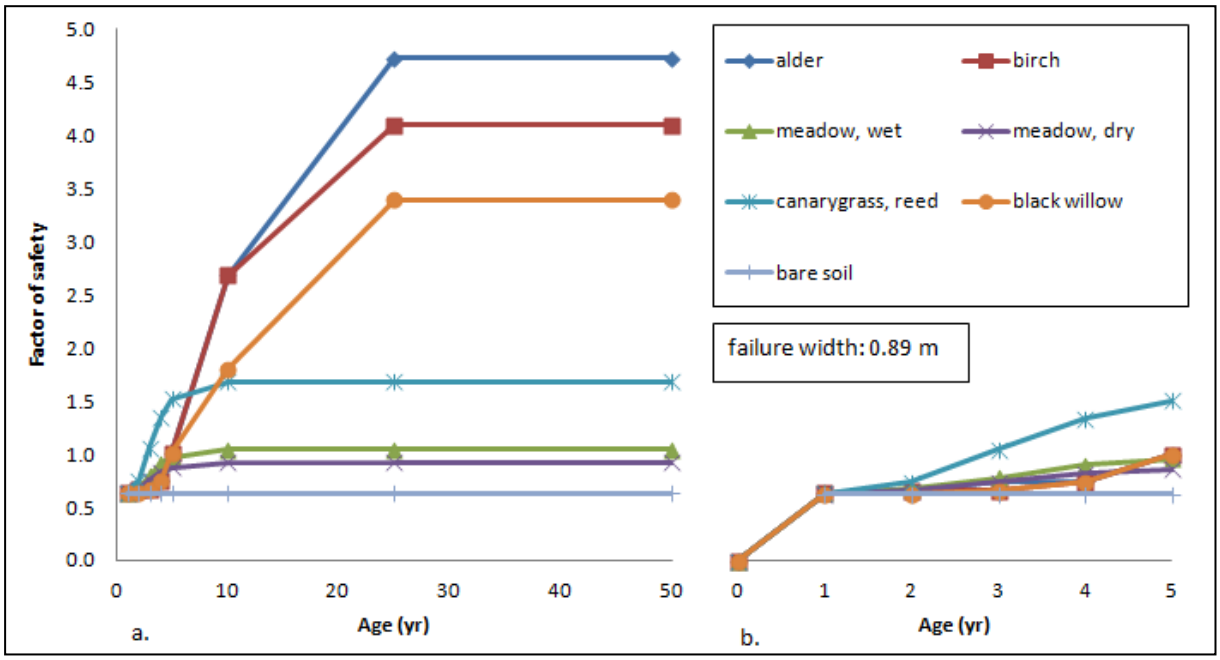

Figure 97: Factor of safety for different vegetation species as a consequence of age (high water, west part of profile 18, 2008).

13.3. Toe erosion model

Toe erosion depends on the duration of flow, the reach slope, the water level, the geometry and the toe material. The longer the duration of flow is and the steeper the slope is, the more toe erosion takes place. Also the higher the water level is, the more toe erosion takes place. Importantly, toe erosion does not depend on vegetation. It is assumed that the reach slope and toe material do not change over time. However, the water level and the duration of toe erosion (duration of flow) are no fix values in the Groenlose Slinge.

13.4. Modelled erosion and comparison to measured migration

In *Table 3* of *Section 9.2.1.* the general input values for BSTEM are shown. In the model an alternation of toe erosion (high water) and bank erosion (low water) was created. Also vegetation as found in the field was inserted. As noticed earlier, only the profiles 16W, 18W and 8E could be used for comparison, because only at these banks erosion took place over the whole height, from top bank to the lowest point. The geometry of each of these three profiles was inserted and models were run according to *Table 9. Table 9* is an example for profile 16W. Each row represents one run and after each run the new eroded or failed profile is inserted in the geometry. It is assumed that the profile fails below a factor of safety of one. In the table an alternation of high water and low water can be noticed. Also the age of the vegetation increases. In *Table 10* also the vegetation and water levels for profile 18W and profile 8E that were inserted are given. Also the top toe elevation, which has to be marked in BSTEM, is given. The failure width of each run can be summed and is equal to the total failure width during that period. The (maximal) toe lateral retreat can also be summed, but this is not equal to the total (maximal) retreat in that period. This is because the maximal lateral retreat is always at a different height and because the toe erosion overlaps with the bank failure. Thus, toe erosion is not a good chosen name, because not only erosion at the toe takes place. The model also calculates the total eroded area at the toe-erosion model. The sum of these values is also not suitable to compare with the measured eroded area, because in the toe erosion model the eroded area due to bank failure is not included.

Profile 16 W, bf water level = 16.27 m, low water level = 15.24 m, toe at = 14.5 m (+NAP)					
Duration (hr)	Water level (m + NAP)	Vegetation	Toe erosion (cm)	Failure width (m)	Factor of Safety
120	16.27	100% alder, 1.5 yr	46.264		
	15.24	100% alder, 1.5 yr		-	1.59
120	16.27	100% alder, 2.5 yr	64.140		
	15.24	100% alder, 2.5 yr		0.89	0.96
120	16.27	100% alder, 3.5 yr	107.194		
	15.24	100% alder, 3.5 yr		0.97	0.97
		Total (m):	217598	1.86	

Table 9: Three toe erosion runs and three bank stability runs for profile 16W.

	Profile 16 W	Profile 18 W	Profile 8 E
Vegetation assemblage	100% alder	40% canarygrass, reed 30% black willow 30% alder	33% meadow wet 33% black willow 34% alder
Toe level (m)	14.5	15.54	15.05
High water level (m)	16.27	16.47	16.26
Low water level (m)	15.24	15.203	15.142
Groundwater depth (m)	1.03	1.267	1.118

Table 10: Specific input values for profile 16W, 18W and 8E.

In *Figure 98 the* measured profiles of 2008, the modelled profiles for 2011 and the measured profiles of 2011 are shown for profile 16W, 18W and 8E. In *Figure 99* the amount of modelled and measured erosion is shown. Averaged over these three profiles, the modelled erosion is 2.1 times higher than the measured erosion. Notice that the geometry of the modelled eroded profile can be different than the measured eroded profile (*Figure 98*). For that reason the differences in lateral retreat are also useful to study. The lateral retreat at the toe is on average 1.7 times higher according to the model than measured. The lateral retreat at the beginning of the bank slope is on average 0.7 times higher according to the model than measured. Thus, the modelled toe retreat is larger than measured and the modelled bank retreat is less than measured, causing steeper modelled profiles than measured profiles.

Thus, on average, comparing the modelled erosion and the measured erosion, the modelled erosion is overestimated by a factor two. This is in contrast to Wytema (2009). According to him the model slightly underpredicts the erosion rate. The reason for this underprediction is not known and cannot be checked because of a lack of information about the model runs Wytem carried out. An important reason for the overestimation in this study is that in the Bank Stability and Toe Erosion Model no deposition can be modelled. In the profiles of *Appendix 2* it can be seen that in case of profile 16W between 2008 and between 2009 a little bit net deposition takes place. This net deposition is neglected in the model. Although profile 18W and profile 8E show no periods of deposition in *Appendix 2*, still periods of deposition can take place but the net result after each year is always erosion. Because in BSTEM no deposition is taken into account this can lead to more net erosion than in reality. Another reason for the overestimation can be that the duration of flow (the period of high water during which toe erosion takes place) is taken too large in the model. According to Waterschap Rijn en IJssel in the period 2008-2011 most erosion and corresponding overbank deposition took place in August 2010. According to the hydrograph of the Meibeek (*Appendix 9)* in August 2010 the water level was extremely high. Also in the profiles of *Appendix 2* the changes between the profiles of April 2010 and June 2011 show more changes than the profiles of September 2009 and April 2010. When it is assumed that the high water period in August 2010 causes by far most the largest part of the erosion measured between 2008 and 2011, it could have been better to model 120 hours of high water per three years instead of per year. This should result in less toe erosion and maybe better match with the measured profiles.

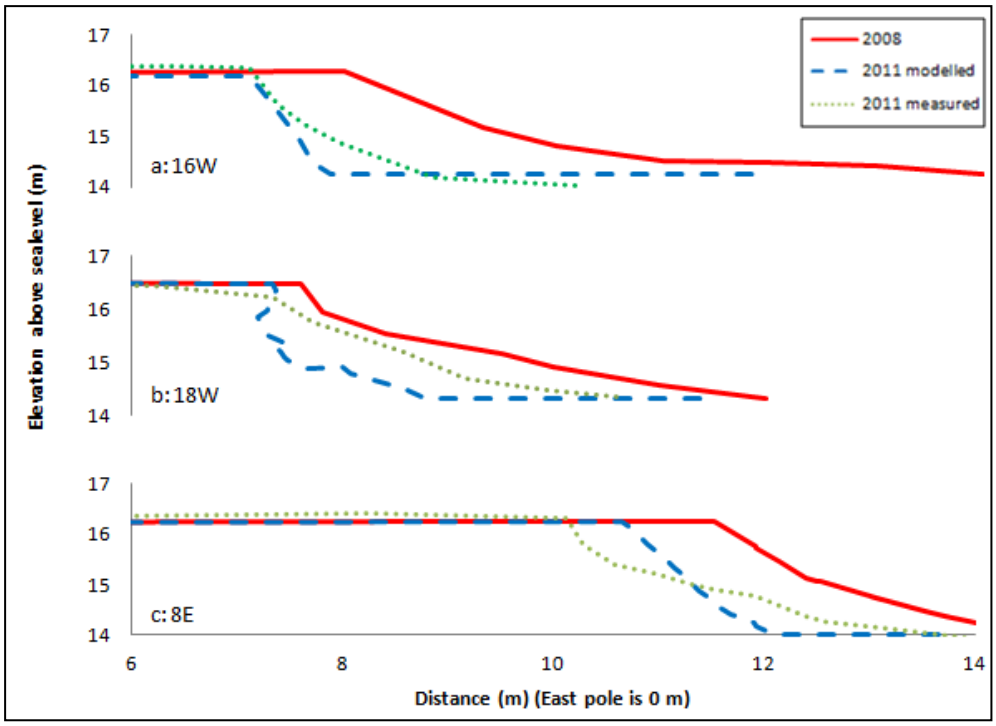

Figure 98: Measured profile of 2008, measured profile of 2011 and modelled profile of 2011 for profile 16W (a), 18W (b) and 8E (c).

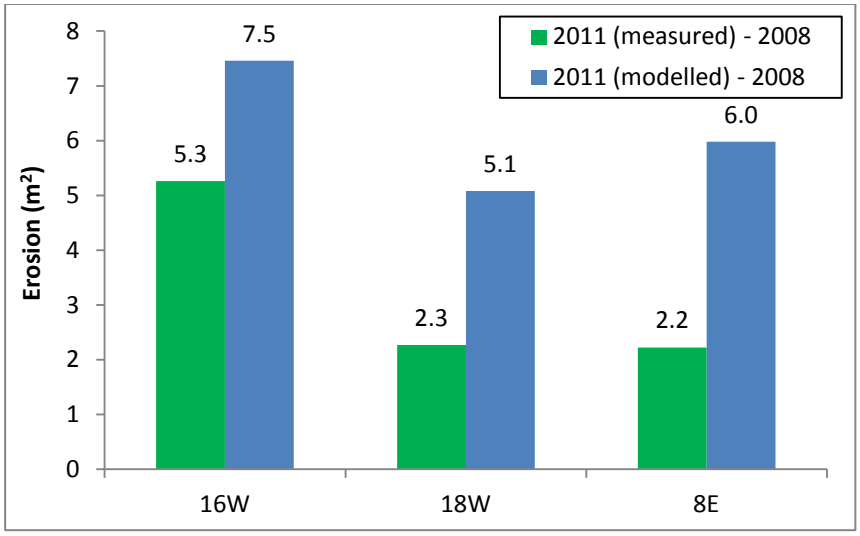

Figure 99: Measured and modelled erosion between 2008 and 2011 for profile 16W, 18W and 8E. The modelled erosion is on average 2.1. times higher than the measured erosion.

13.5. Sensitivity analysis

Sensitive parameters in BSTEM are reach slope, the duration of flow, the reach length, the water level, the groundwater level, the vegetation, the litholgy and the geometry. In this section the sensitivity of the vegetation (*Section 13.5.1.*), the sensitivity of the duration of flow (*Section 13.5.2.*) and the sensitivity of the groundwater level (*Section 13.5.3.*) are studied. *Section 13.5.4.* gives a conclusion about the sensitivity analysis.

13.5.1. Sensitivity analysis: Effect of vegetation

In this section the effect of vegetation is studied. Four scenarios are compared:
1) vegetation as found in the field (varying from 1.5 to 3.5 years old, most realistic situation)
2) mature trees, 50 years old
3) canary grass reed, 4 years old
4) alder, 4 years old
5) bare soil

In *Figure 101* the modelled profile for 2011 is shown for different vegetation types. In *Figure 100* the corresponding legend can be found. As noticed earlier, vegetation has no effect on toe erosion but only on bank failure. So, the migration of the toe is in all situations the same. As a result the failure width is representative for the amount of erosion in cubic metres. In *Figure 102* a diagram of the erosion for the modelling with different vegetation is shown. For each profile the maximal difference in erosion due to different vegetation species can be given as a percentage of the average erosion of the different scenarios: In profile 16W this percentage is equal to 24%, in profile 18W to 0% and in profile 8E this percentage is equal to 19%. This means an average maximal difference of 14%.

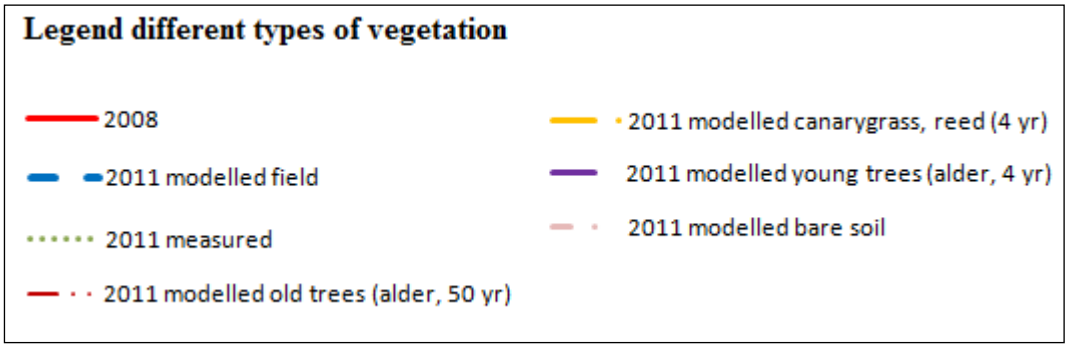

Figure 100: Legend for Figure 101.

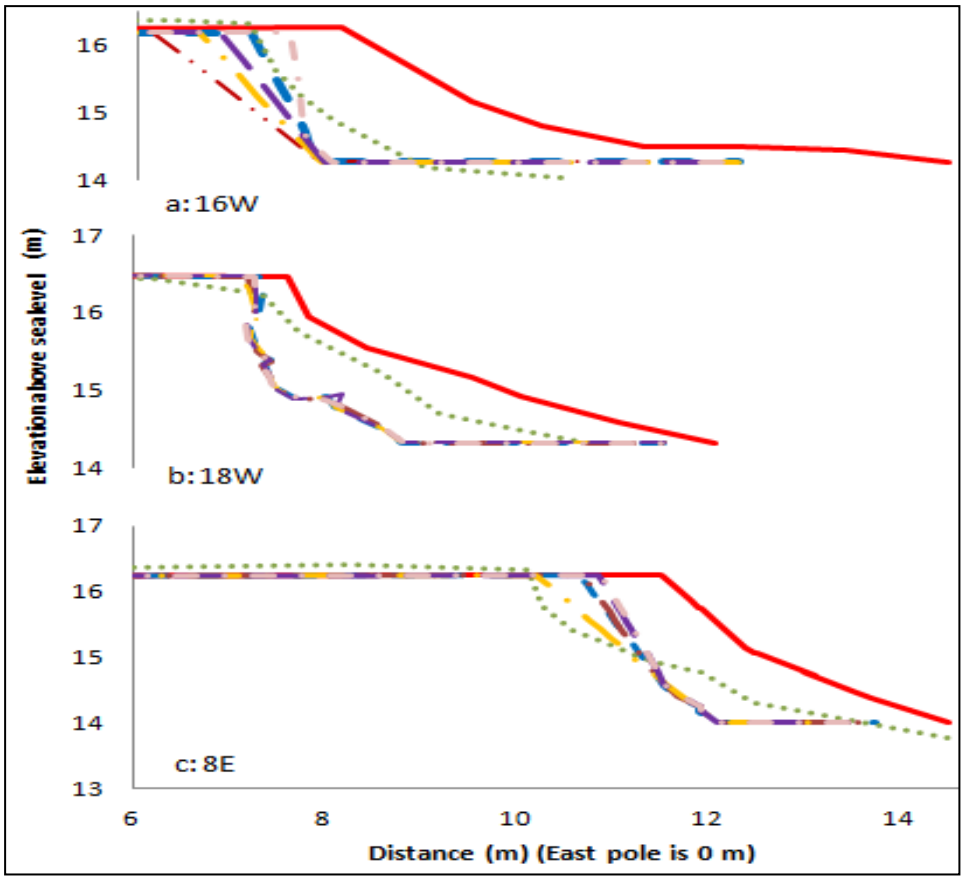

Figure 101: Measured profile of 2008, measured profile of 2011 and modelled profiles of 2011 as a consequence of different vegetation species for profile 16W (a), Profile 18W (b) and Profile 8E (c).

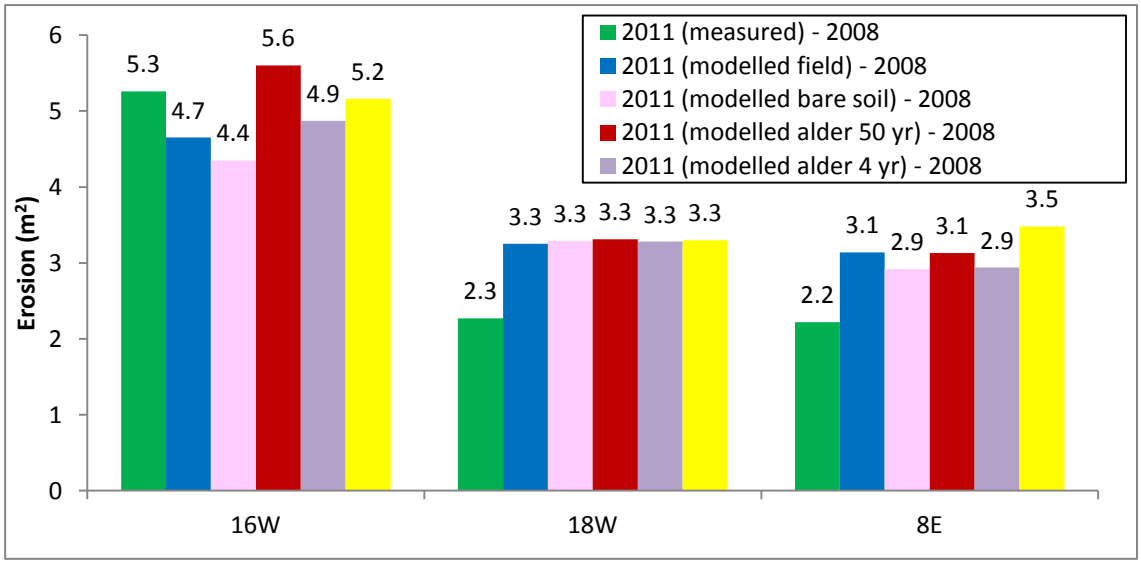

Figure 102: Measured erosion and modelled erosion as a consequence of different vegetation species. For each profile the maximal difference in erosion due to different vegetation species can be given as a percentage of the average erosion of the different scenarios: In profile 16W this percentage is equal to 24%, in profile 18W to 0% and in profile 8E this percentage is equal to 19%. This means an average maximal difference of 14%.

As can be seen in *Figure 101* and *Figure 102* the total failure width and the erosion do not automatically decrease when the added strength of the vegetation on the bank increases. The added strength of mature, old trees is largest, followed by canarygrass reed and young trees. Bare soil does not add any strength. In *Table 11* the failure width after each run is shown. Again, the total of the failure widths of each run corresponds to the lateral retreat of the bank top in the graphs. After analyzing these tables, it can be concluded that the amount of failures determines roughly the amount of total lateral retreat and total erosion. In case of less added strength, each time when low water takes place, a bit bank erosion takes place. In case of relatively much added strength, not each period of low water bank erosion takes place, but when after several low water periods bank erosion does take place, the bank erosion is relatively large. Thus, in general, the more often the bank fails, the less the total failure width and the less the erosion. It is thought that this is caused by relations between geometry and forces but why this exactly happens is not clear and needs more research. However, notice that when the bank does not fail over the whole observed period, the failure width is equal to zero. In case of an equal amount of bank failures, it can be seen that more bank retreat and more erosion takes place in case of more added strength. After studying the model, it is not exactly clear how this process works. A possible theory is that more strength due to vegetation can lead to larger clumps of sediment which cause more erosion in case of failing. It can be imagined that failing of a large, mature tree takes more sand away than failing of small grasses.
Thus, according to the model, vegetation only has an erosion restrictive effect when the added strength is large enough so that the bank does not fail over the whole observed period. When the added strength of vegetation is not large enough to overcome the unstable profile, even more bank erosion takes place in case of vegetation than in case of bare soil.

Profile 16W Failure width (m)	First run	Second run	Third run	Total
bare soil	0.10	0.10	0.30	0.50
young trees	0.13	0.54	0.53	1.19
canarygrass, reed	stable	0.68	0.72	1.40
old trees	stable	0.89	0.97	1.86

Profile 18W Failure width (m)	First run	Second run	Third run	Total
bare soil	0.01	0.07	0.27	0.35
young trees	0.08	0.09	0.18	0.35
canarygrass, reed	0.24	0.26	0.01	0.51
old trees	stable	stable	0.41	0.41

Profile 8E Failure width (m)	First run	Second run	Third run	Total
bare soil	0.10	0.10	0.44	0.64
young trees	0.13	0.13	0.41	0.67
canarygrass, reed	stable	0.67	0.65	1.32
old trees	stable	stable	0.84	0.84

Table 11: Failure width after each run for different species (different added strength).

A comparison between the effect of vegetation in the field and the effect of vegetation according to BSTEM can be made. In the field no differences in erosion resistance between grasses, herbs and young trees were found. As could be seen in *Figure 97 (Section 13.2.)* only the factor of safety of reed and mature trees is above one in case of profile 18W (2008). Assuming that this modelled situation of profile 18W (2008) also occurs at other profiles where erosion takes place, the observations in the field are confirmed by BSTEM: when the factor of safety is below one, it does not matter which vegetation is present, because in spite of the vegetation, the bank does fail. When the young trees become older, the factor of safety of profiles comes above one, leading to more stable profiles.

13.5.2. Sensitivity analysis: Effect of alternation of toe erosion and bank failure

In the former sections the duration of flow was equal to 120 hours and the toe erosion model as well as the bank stability model were run three times. That means that each year contains one period of toe erosion. The smaller the duration of flow, the more runs have to be done. In this section it is checked what happens when the duration of flow increases to 360 hours (15 days) and decreases to 60 hours. In *Figure 103* and *Figure 104* it can be seen that the profiles in case of different flow durations are different. This is because the geometry of the profiles after toe erosion depends on the duration of toe erosion (high water). Accordingly, the geometry of the eroded profiles can differ from each other. Therefore also the factors of safety can be different after different durations of toe erosion. Studying *Figure 103* and *Figure 104* no relation between the duration of flow and the amount of erosion seems to exist. Again, for each profile the maximal difference in erosion due to different durations of flow can be given as a percentage of the average erosion of the different scenarios: in profile 16W this percentage is equal to 44% and in profile 18W to 38%. In profile 8E this percentage is equal to 20%. This means an average maximal difference of 34%.

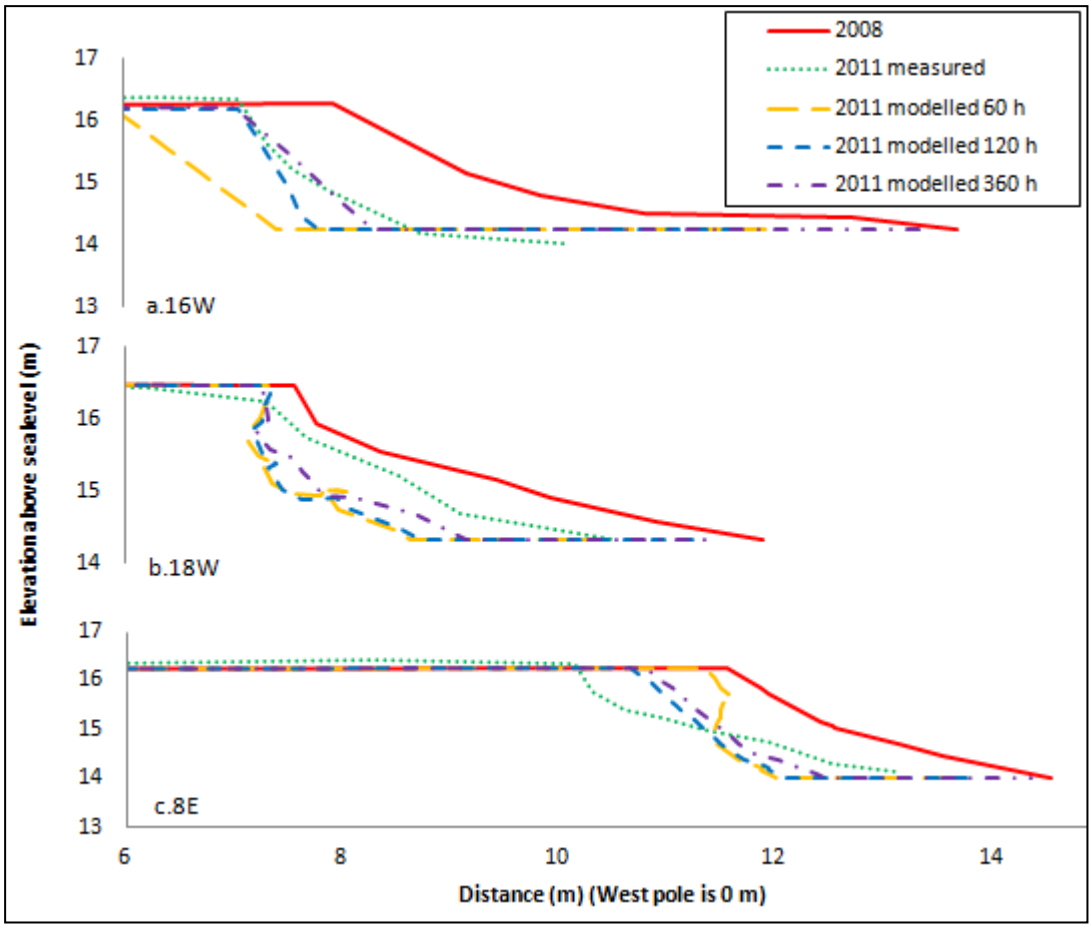

Figure 103: Measured profile of 2008, measured profile of 2011 and modelled profiles of 2011 as a consequence of different durations of flow for profile 16W (a), 18W (b) and 8E (c).

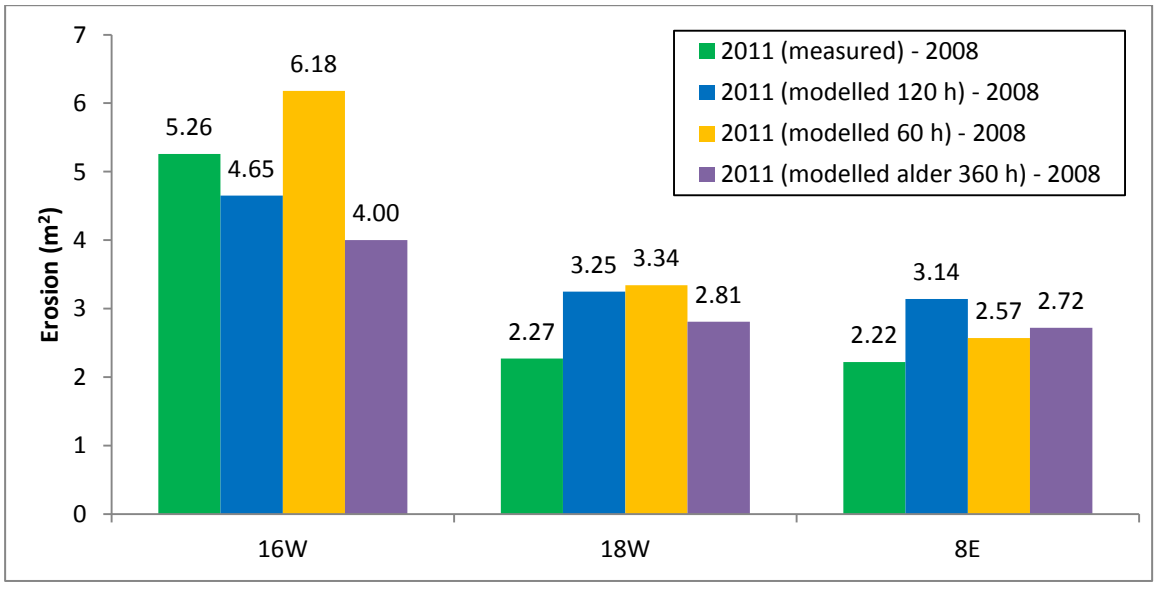

Figure 104: Measured erosion and modelled erosion as a consequence of different durations of flow. For each profile the maximal difference in erosion due to different durations of flow can be given as a percentage of the average erosion of the different scenarios: in profile 16W this percentage is equal to 44%, in profile 18W to 38% and in profile 8W this percentage is equal to 20%. This means an average maximal difference of 34%.

13.5.3. Sensitivity analysis: Effect of groundwater depth

In the former sections the groundwater level was equal to the water level in the channel. However, in reality the groundwater level can be higher or lower than the water level in the channel and can also vary. To the following scenarios a closer look was had to:

1) the groundwater level is equal to the water level in the channel (former sections) (depth ≈ 1 m)
2) the groundwater level is at the bank top
2) the groundwater level is two metres below bank top
3) the groundwater level is three metres below bank top

In *Figure 105* and in *Figure 106* these situations are shown. In all three profiles it can be seen that the erosion is larger in case of a higher groundwater level. Concerning the maximal difference in erosion due to different groundwater depths as a percentage of the average erosion of the different scenarios, in profile 16W this percentage is equal to 67%, in profile 18W to 55% and in profile 8E this percentage is equal to 91%. This leads to an average maximal difference of 71%.

The lower the groundwater level is, the less times the bank fails. In case of a groundwater depth of two metres as well as in case of a groundwater depth of three metres the bank is stable after each run and no bank failure takes place. Consequently, only toe erosion takes place and the modelled geometry of these profiles is the same. In each situation the modelled profile is most close to the measured profile in case that the groundwater level is equal to the water level in the channel. This level was also used to predict erosion in *Section 13.4.*

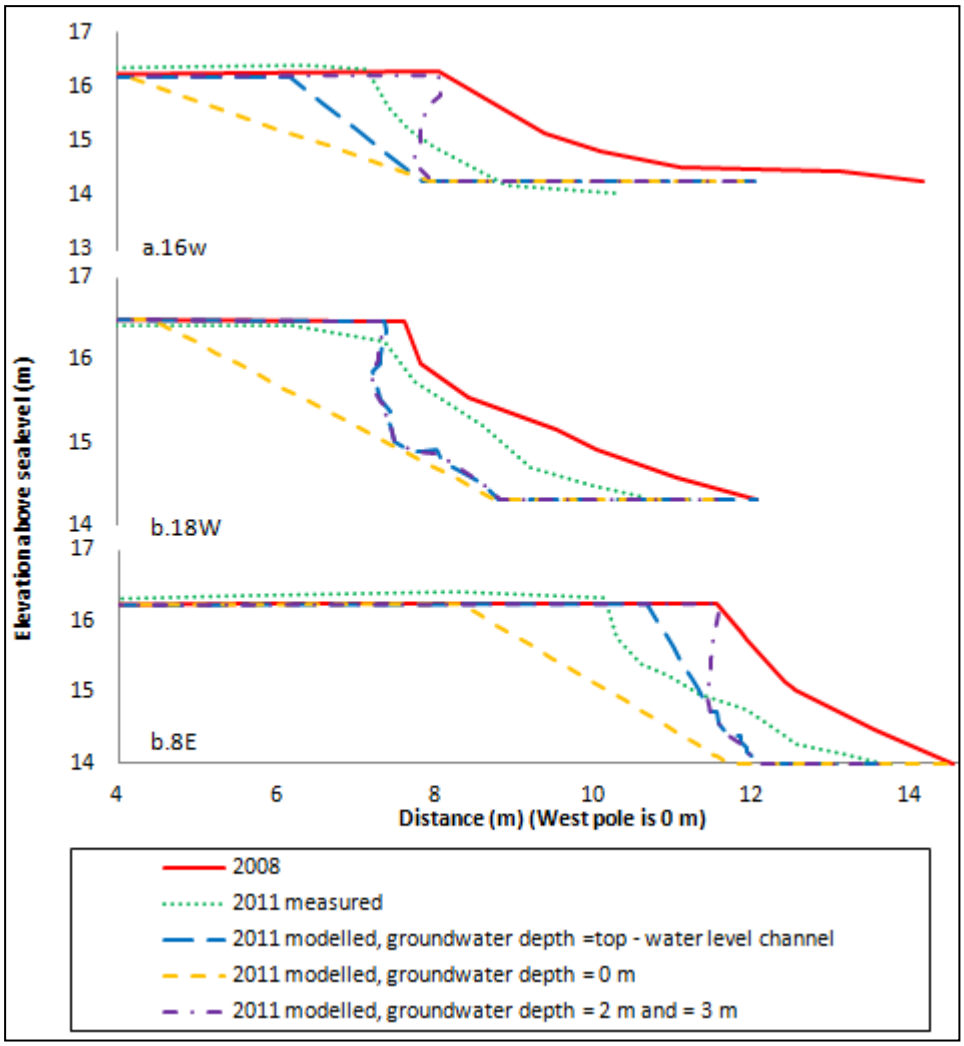

Figure 105: Measured profile of 2008, measured profile of 2011 and modelled profiles of 2011 as a consequence of different groundwater depths for profile 16W, 18W and 8E.

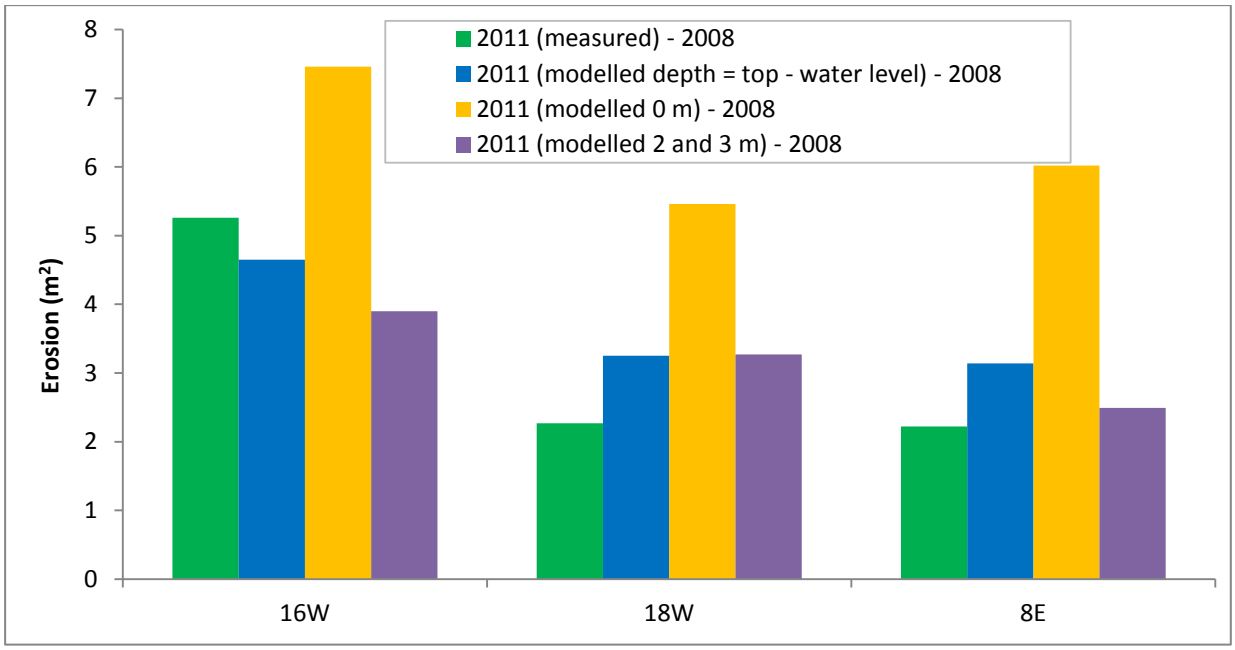

Figure 106: Measured erosion and modelled erosion as a consequence of different groundwater depths. For each profile the maximal difference in erosion due to different groundwater depths can be given as a percentage of the average erosion of the different scenarios: in profile 16W this percentage is equal to 67%, in profile 18W to 55% and in profile 8E this percentage is equal to 91%. This means an average maximal difference of 71%.

13.5.4. Conclusion sensitivity analysis

The sensitivity of the vegetation, the duration of flow and the groundwater level to the amount of erosion is studied in BSTEM. From those three parameters vegetation is least sensitive (14% maximal variation) and groundwater is most sensitive (71% maximal variation). The high sensitivity of groundwater was also noticed in the literature review as according to Pollen-Bankhead and Simon (2010) streambank stability is particularly sensitive to changes in water table elevation and therefore in soil matrix suction. The duration of flow and the corresponding amount of runs have an intermediate sensitivity; the maximal variation in amount of erosion is on average equal to maximal 34%. In this research it was assumed that the groundwater level was equal to the water level in the channel. Although a groundwater level equal to the water level in the channel delivers the best prediction for erosion between 2008 and 2011, because of the high sensitivity more research is necessary to the groundwater level around the Groenlose Slinge.

13.6. Prediction of erosion

Using BSTEM also predictions for the geometry of the profiles in June 2012, one year after the measured profiles in 2011, could be done. It was assumed that the same vegetation assemblage is present as in 2011, but that the vegetation is one year older (4.5 years). The duration of flow is 120 hours, the water levels of 2011 are used and the groundwater table is the same as the water level in the channel. Also the other general inputs are the same (*Table 3, Section 9.2.1.*). In *Figure 107* the predicted profiles for June 2012 are given. It can be seen that in all three profiles only toe erosion takes place and no bank failure. As noticed earlier, toe erosion is a wrong name, because erosion over the whole height of the profile that is under water can take place during high water. Also for the profiles 11E and 14W a prediction could be done, because at these profiles also observations of only

erosion (and no deposition) are visible. In *Figure 108* the predicted profiles are given. Also at these profiles it is modelled that only toe erosion takes place and no bank failure. In the field, observations of tension cracks and undercut banks were done. Thus, in contrast to the model, in the field there were indications that bank failures are going to take place between June 2011 and June 2012. In *Figure 109* the amount of predicted erosion is given and also the predicted erosion per year for the period 2008 to 2011 is included. According to the results of *Section 13.4.* the modelled erosion was about two times as high as the measured erosion. Consequently, the values of erosion in *Figure 109* can be divided by two to obtain the best predictions. The figure shows that the on average the modelled erosion per year in the period 2008 to 2011 is 2.1 times higher than the modelled erosion in the period 2011 to 2012. The reason for this difference in erosion is that according to BSTEM at all profiles no bank failure takes place in the period 2011-2012. The reason for these stable banks could be an increased added strength due to vegetation or the more stable geometry of the profiles. In this case the stable geometry of the profiles is the reason for the more stable banks because the bank stability model noticed that the bank angle is less than the friction angle and that for that reason no bank failure can take place.

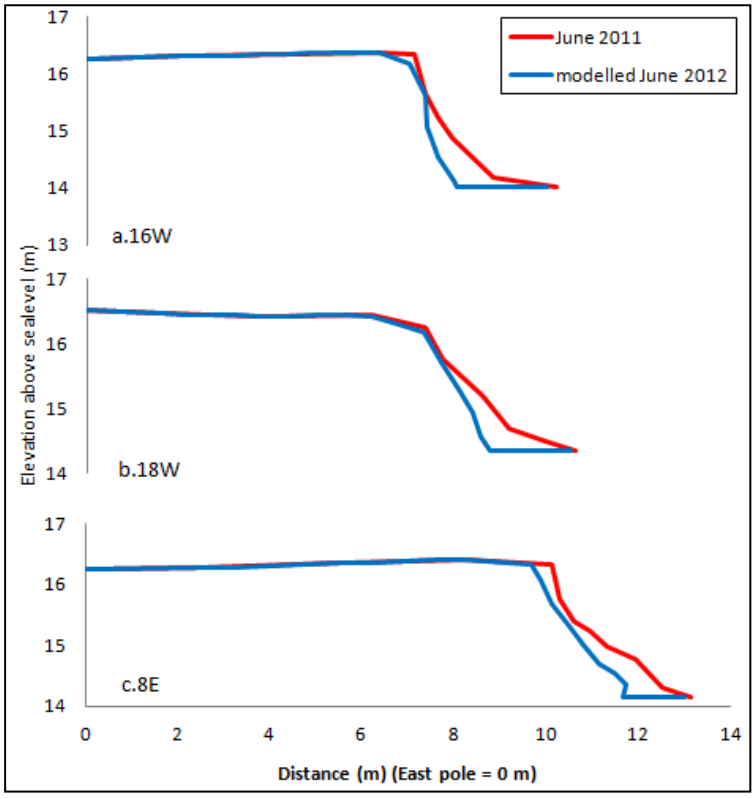

Figure 107: Measured profiles of June 2011 and modelled profiles for June 2012 for profile 16W (a), profile 18W (b) and profile 8E (c).

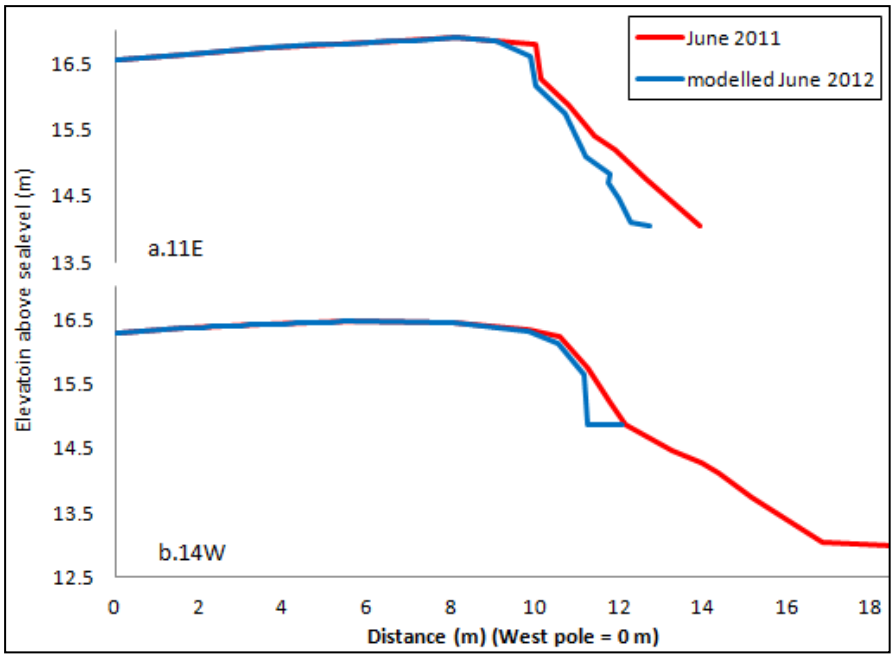

Figure 108: Measured profiles of June 2011 and modelled profiles for June 2012 for profile 11E (a) and profile 14W (b).

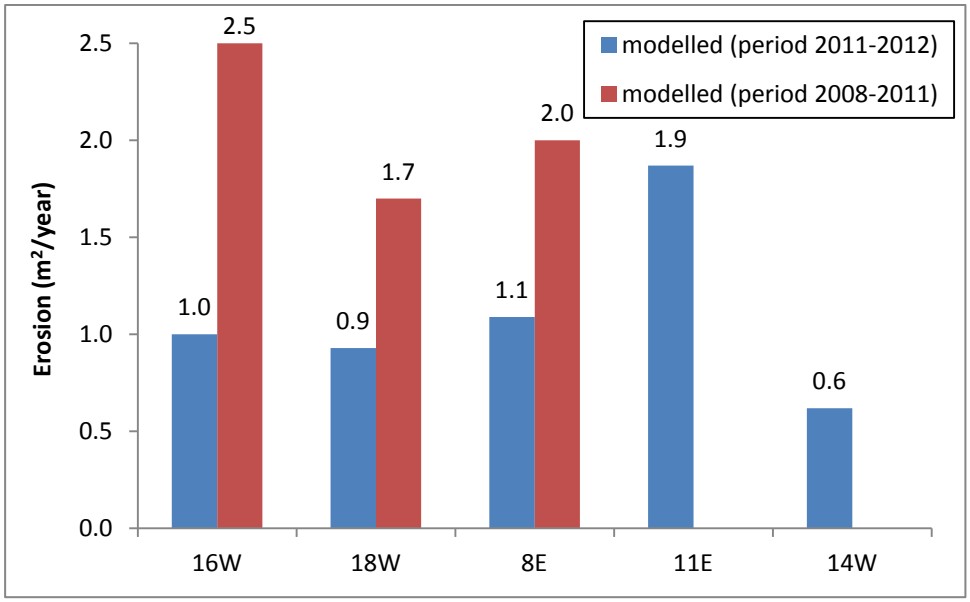

Figure 109: Modelled erosion per year for the period between June 2011 and June 2012 and for the period between 2008 and 2011. On average the modelled erosion per year in 2008-2011 is 2.1. times as high as the modelled erosion in 2011-2012.

Part IV: Discussion and conclusion

In this last part, *Chapter 14* contains some discussion subjects and *Chapter 15* contains the conclusions of this research.

Chapter 14: Discussion

In this chapter *Section 14.1.* discusses the optimum migration rate, *Section 14.2.* discusses sharp bends, *Section 14.3.* discusses the effect of different vegetation on erosion, *Section 14.4.* is about recommendations for BSTEM and *Section 14.5.* discusses the quality of the ecology in the Groenlose Slinge.

14.1. Optimum migration rate

According to literature, the migration of bends is largest in case that $2 < r_c / w < 3$. r_c is the radius of curvature and w is the bankfull width. In this research the optimum is about four instead of between two and three. A reason for the observation that the optimum r_c/w according to *Figure 41* is slightly higher than according to the literature can be that in the field vegetation is present on the banks. The theory does not take vegetation into account. Due to vegetation, the bankfull width can be narrower than without vegetation. When no vegetation was present, r_c/w could lead to a lower value because the width (w) increases. This could lead to a lower optimum of r_c/w.

Jansen (2009) determined the migration for the Groenlose Slinge between 2007 and 2008. In *Figure 110* the average migration rate divided by the width is plot against the radius of curvature divided by de width for the period 2007-2008. Comparing this figure with *Figure 41* (*Section 10.8.*) it can be seen that the plotted pattern of the studied profiles is about the same: in both figures the profiles 3, 13 and 16 show the same order of increase in average migration rate divided by the width. Profile 14 is an exception. In *Figure 41* (2008-2011) the average migration rate of profile 14 was relatively low and in *Figure 110* (2007-2008) the average migration rate is relatively high. This is confirmed by the bank lines map (*Appendix 4*) and the waterlines map (*Appendix 5*). This means that the theory of a low migration rate in case of sharp bends could not be applied in the period between 2007 and 2008. The reason for this finding can be that in the period 2007-2008 the bend was not sharp enough for flow separation and the ratio of r_c/w was closer to ratio where the migration rate is maximal. Although in the bank lines map (*Appendix 4*) and the waterlines map (*Appendix 5*) it can clearly be seen that the bend became sharper between 2007/2008 to 2011, in the figures the ratio between radius of curvature and the width is about the same. On the contrary, the order of average migration rate divided by the width is in *Figure 110* (2007-2008) a order of ten larger than the average migration rate divided by the width in *Figure 41* (2008-2011). This means that the migration rate between 2007 and 2008 is about ten times as high as the migration rate between 2008 and 2007. As was discussed earlier, this is probably caused by the loose sand that has not yet settled just after constructing the re-meandered stream.

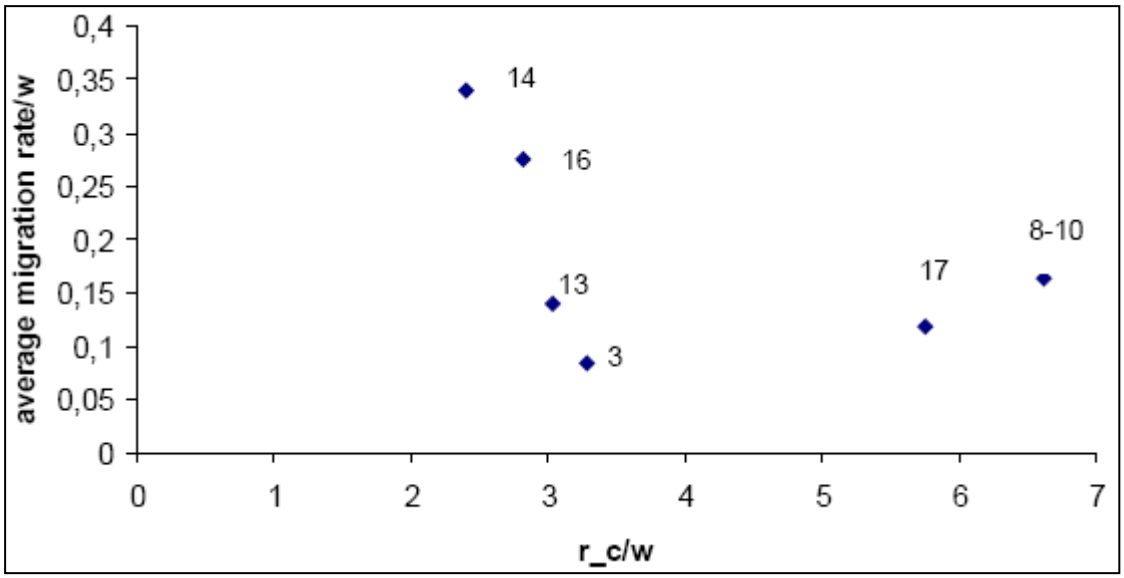

Figure 110: Relation between migration, radius of curvature and bankfull width for 2007-2008 (Jansen, 2009). (See Figure 32 in Section 10.6. for the period 2008-2011 and see Figure 17 in Section 7.1. for overall locations of profiles.)

14.2. Sharp bends

According to Friedkin (1945) and Ferguson (1987) only in case of strong banks, sharp bends can exist (*Section 2.4*). However, it is concluded that the migration rate of sharp bends is small. For that reason the strength of the bank is not needed to be very high. Also in case of the sharp bend in the Groenlose Slinge, the added strength of the vegetation on the bank is not higher than on the other banks.

Because of the variety in hydrological and morphological characteristics in meandering streams that cause different habitats, a meandering stream with a sinuosity of at least 1.5 is assumed to have a positive effect on the ecology (Van de Kruijs, 2010). The Groenlose Slinge and many other re-meandering streams have a lower sinuosity, often because streams with a higher sinuosity are associated with more space as a consequence of the higher migration rates. That space is often not available. An idea that has positive influence on the ecology but does not take much space is digging sharp bends. Concerning the Groenlose Slinge, Profile 14 is located downstream of the apex of a sharp bend. This bend is deeper and wider than the other bends. Also a striking stream pattern occurs, leading to a variation in velocities (*Figure 8*). The variation in velocities in this sharp bend could lead to different habitats which has a positive effect on the ecology. According to theory and according to measurements in the Groenlose Slinge, sharp bends have a low migration rate. Accordingly, the advantage of sharp bends is that not much space has to be reserved for migration and nevertheless a high curvature is created with a positive effect on the ecology. Thus, digging sharp bends should be a good alternative to create a positive effect on the ecology.

14.3. Effect of different vegetation on erosion

According to literature (*Section 3.3.3.*), each vegetation species has a different effect on erosion. This is partly confirmed by this research. Although no differences on the effect of erosion between grasses, herbs and small trees can be detected in the fieldwork area, on a smaller scale it is observed that *Alnus* (alder) and *Salix alba* (white willow) have a different effect on erosion because *Salix alba* is

more found in the water due to erosion (87%) than *Alnus* (13%). A reason for this difference is that the roots of *Alnus* cause a larger added strength than the roots of *Salix Alba*. This is confirmed by Wu (1979) how says that the added strength of mature *Alnus* is between 32 and 52 mPa and the added strength of mature *Salix alba* is between 18 and 37 mPa. However, notice that this is about mature vegetation. Also in BSTEM it can be seen that the added strength of mature willows is smaller than the added strength of mature alder. However, in BSTEM this difference is only the case at mature vegetation. Up to an age of four years the added strength of willows is the same as the added strength of alder. However, notice that the specific species of willow, *Salix alba*, cannot be selected in the model. It is also known that the roots of *Alnus* are water proof and in consequence *Alnus* can root in the water. Because *Alnus* roots grow often to the waterline and because there the erosive power is strong, the *Alnus* roots have much influence on erosion restriction. According to literature, the larger the reaching depth, the larger the stability effect is. However, this example of *Alnus* that has roots growing to the waterline shows that not necessarily a large reaching depth is important but that the root density distribution in relation to the erosive power of the water is important. As well *Alnus* as *Salix alba* were often found direct at the water side. This is because the seeds come into the water and stay at the water side.

According to BSTEM (Simon et al, 2009), the added strength of grasses is larger than the added strength of young trees. A straight forward reason for this difference is that, although the tensile strength of one single young tree root is larger than the tensile strength of a grass root, the density of grass roots is much larger than the density of small tree roots, leading to a larger total strength. When the age of trees increases, the density of tree roots increases and also the strength of each tree root increases leading to a higher total added strength than grasses. According to BSTEM (Simon, 2009) streambank stability is particularly sensitive to changes in water table elevation and therefore to soil matric suction. For that reason in a next research to the effect of vegetation on bank stability, the groundwater depth should be measured.

14.4. Recommendations for BSTEM

This section discusses possible improvements of the Bank Stability and Toe Erosion Model. *Section 15.8.1.* is about changing from a two dimensional model into a three dimensional model and *Section 15.8.2.* is about improvements of the RipRoot model of BSTEM.

14.4.1. Changing from a two dimensional model into a three dimensional model

According to the results, the radius of curvature, the pattern of outer bends and the width are the key parameters that determine the locations of erosion and the migration rate. Therefore, a real improvement of the model should be when the model is changed from two dimensional into three dimensional, so that also the pattern of the stream including inner and outer bends can be inserted. Another improvement that is related to the change from two dimensional into three dimensional should be when the model is also able to model deposition. To construct a three dimensional model, the model Jansen (2009) used, called JPI, can be combined with BSTEM. BSTEM is a two dimensional model that takes the x and z direction into account and the JPI model is an one dimensional model that only takes the y direction into account. Together these models form a three dimensional model.

14.4.2. Improvements of the RipRoot model of BSTEM

In this research the added strength was determined by selecting a vegetation species in the RipRoot model of BSTEM. However, not each vegetation species found in field can be selected in the model. To overcome this problem, in the RipRoot model also an equation exists that can calculate the added strength by vegetation roots. This equation is given in *Equation 25*. α and β are no fixed values and should be determined. Also D, the root diameter distribution, has to be inserted. In a next research it can be studied what the values for α and β are for each found species, so that this equation can be used to calculate the added strength. Also more research should be done to the root diameter distribution. When more knowledge is present about α, β and the root diameter distribution, this equation can be applied. Applying this equation should be better than selecting a species in RipRoot because in case of the equation no 'translation' between species has to be made.

(Eq. 25) added strength (MPa) = $\alpha * D^{\beta}$

The added strength by vegetation roots at the bank toe is more important for bank stability than added strength on the bank top since hydraulic shear stress increases with stream depth. Hence, another point to improve the RipRoot model in BSTEM is to include the possibility to insert vegetation also on the toe and not only at the top one metre of the bank.
Another shortcoming of the RipRoot model of BSTEM is that concerning the effect of vegetation only the added strength of roots is included. However, as can be found in the literature review (*Section 3.3.2.*), there are also other effects of vegetation on bank erosion. Some effects stabilize banks and other effects destabilize banks. From those other effects, the destabilizing effect of surcharge seems to play the largest role in the Groenlose Slinge. This surcharge effect is the effect of bank collapse due to the mass of vegetation in relation to the bank slope. In the outer bends with mature forest on the bank where erosion takes place, besides the stabilizing effect of added strength by roots, the destabilizing surcharge effect can play a role. In case of erosion in the outer bends with mature forest, often undermining of the bank is visible in the field. It can be imagined that in this way of mass failure the surcharge effect plays a role.

14.5. Quality of the ecology in the Groenlose Slinge

The Europe Water Framework Directive (European WFD) (in Dutch: Europees Kader Richtlijn Water (Europees KRW)), ensures that organizations like Waterboards or community boards take care of their water systems. The aim of the WFD is to achieve 'good water status' for all waters, including water quality and ecological quality. One way to achieve this goal is re-meandering. There are too less observations or measurements to conclude already that the ecology in and around the Groenlose Slinge has improved after re-meandering. However, the improvement of the morphodynamica is already clearly visible and this morphodynamica is a motor to improve the ecology. The WFD-score of fish, of macrofauna and of vegetation is determined in 2010 (three years after re-meandering) and also before re-meandering. According to this monitoring the WFD-score of fish decreased from two to one, the WFD-score of macrofauna remains the same and the WFD-score of vegetation increased from three to four. The decrease of fish can be caused by bad sampling or by the dam Beekvliet which is still not able for fish to pass (Waterschap Rijn en IJssel). For the Groenlose Slinge is should be difficult to achieve the ecological quality wished by the Europe Water Framework

Directive. This difficulty exists because the stream velocity is the Groenlose Slinge is too low for some fauna. So, a significant group of fauna would not be found in the Groenlose Slinge.
Often (small) trees fall into the Groenlose Slinge as a consequence of erosion. Because these fallen trees create different stream velocities, it could have a positive effect on the ecology. Thus, from an ecological point of view, fallen trees should have to take out of the water only when they cause significant damming up of water that can lead to floods.

Chapter 15. Conclusions

The main aim of this research was to determine the effect of vegetation on the bank erosion pattern and the lateral migration rate of the Groenlose Slinge. A second aim was to study the morphological evolution of this stream. By answering the research questions of this thesis that are repeated below, the aim of this research is achieved. In this chapter short answers on the research questions are given:

What are the morphological and hydrological characteristics of the Groenlose Slinge? How did these characteristics change between 2008 and 2011?

Although the Groenlose Slinge has been re-meandered, strictly seen the Groenlose Slinge is not a meandering stream as the sinuosity is equal to 1.2 which is smaller than 1.5. Although according to this definition the Groenlose Slinge is not a meandering stream, the stream shows some characteristics of a meandering stream: there is one major channel, there are pools and there are scroll bars. The sharp bend of the Groenlose Slinge shows flow separation. The Groenlose Slinge has a width varying between 8.2 m and 15.9 m and a depth varying between 0.9 m and 1.8 m depending on the water level. Between 2008 and 2011 the high water width seems to be slightly increased, probably due to floods. The banks of the Slinge have increased and the low water width has decreased due to the net deposition of 1.5 m^2 per metre length between 2008 and 2011. Also the radius of curvature of the bends has decreased as a result of erosion in outer bends and deposition in inner bends. This research shows that the higher the decrease in radius of curvature, the larger the increase in depth. This is caused because sharper bends cause more damming up of the water than gentle bends. Therefore, the sharper bends are the reason for the higher water depths in 2011 than in 2008.

What vegetation and what vegetation patterns do occur around the Groenlose Slinge? What are the characteristics of this vegetation? What is known about their roots and their added strength?

Concerning the vegetation in the outer bends, a sequence of young, small trees like *Alnus* (alder) and *Salix alba* (white willow) at the water side, followed by a mixture of grasses, herbs and small trees are most common. In the inner bends a sequence of reed/bulrush at the water side followed by small trees and mature forest is most common. The added strength of *Alnus* (alder) is larger than the added strength of *Salix alba* (white willow). In the mature stage, trees have the largest added strength and grasses the least. However, young grasses have a larger added strength than young trees.

How does stream bank erosion work? What processes and what factors do play a role?

Steam bank erosion and lateral migration consists of two steps: first, bank undercutting takes place by toe erosion due to fluvial erosion during high water, secondly, bank failure takes place due to mass wasting during low water. The flow strength and the bank strength determine the amount of erosion. The factors that determine the flow strength are: valley slope, discharge and the properties and the form of bends including the curvature of bends. Factors determining the bank strength are:

lithology, groundwater level, bank elevation, bank slope and vegetation. According to the bank stability and toe erosion model, the groundwater level seems to be the most sensitive parameter in case of the Groenlose Slinge.

Where does erosion take place and what is the lateral migration rate? Does a relation between erosion and vegetation and a relation between the lateral migration rate and erosion exist?

The measured lateral migration averaged over the length is equal to 0.92 m between 2008 and 2011. As well the lateral migration rate is higher between 2007 and 2008 than between 2008 and 2011. Erosion only takes place in outer bends and never in inner bends, indicating that the channel was dug wide enough. The rate of migration depends on the ratio of radius of curvature to width. In case of the Groenlose Slinge the migration is largest in case that r_c / w is about four. In case of lateral migration no different effect of vegetation can be detected. Only reed, bulrush and mature forest affect the erosion pattern reflected in the pattern of outer bends.

What are the differences between the prediction of the 2011 profile by the Bank Stability and Toe Erosion Model based on the profile of 2008 and the measured profile of 2011? What are the sensitive parameters of BSTEM and how sensitive are they? And what is the prediction of the bank erosion of 2012?

The modelled erosion is overpredicted by a factor two compared to the measured erosion. Concerning the prediction of erosion in 2012, in no case bank failure takes place, but only toe erosion. However, according to observations of tension cracks and undercut banks it is not likely that no bank failures will take place between June 2011 and June 2012. The toe erosion model of BSTEM depends on the duration of flow, the reach slope, the water level and the toe material and the bank stability model depends on the water level, the groundwater depth, the geometry and the bank material. In this research the sensitivity of vegetation, of duration of flow and of groundwater depth are researched. From these parameters the most sensitive parameter is the groundwater depth. The assemblage vegetation is not very sensitive to the amount of erosion.

What are hydrological and morphological characteristics in the sharp bend of the Groenlose Slinge and what is the role of vegetation in this sharp bend?

The geometry of the sharp bend in the Groenlose Slinge is different than the geometry of gentle bends. Also the stream pattern is different because two upward going flows are present. Because the migration of the sharp bend is low, the role of vegetation in this sharp bend is not different than in gentle bends.

Chapter 16. Samenvatting van de belangrijkste resultaten ten behoeve van beheer voor Waterschap Rijn en IJssel / Summary of the most important results concerning maintanance for waterboard Rijn and IJssel

In dit hoofdstuk wordt een samenvatting gegeven (in het Nederlands) van de belangrijkste resultaten ten behoeve van beheer van de Groenlose Slinge

Doel

Het doel van het onderzoek was het bepalen van het effect van vegetatie op de het oevererosiepatroon en de laterale migratiesnelheid van de Groenlose Slinge. Een tweede doel was het bepalen van de morfologische ontwikkeling van de Groenlose Slinge tussen 2007 en 2011.

Methodes

Voor dit onderzoek is veldwerk uitgevoerd in een traject van de Groenlose Slinge. Ook is het Bank Stability and Toe Erosion Model (BSTEM) gebruikt om erosie te modeleren. Voor het bepalen van de morfologische veranderingen zijn naast twintig dwarsprofielen ook de locaties van de insteeklijnen en de waterlijnen bepaald. Men moet ervan bewust zijn dat het bepalen van de insteeklijnen erg interpretatiegevoelig is. In *Appendix 3* kan het verschil in interpretatie van de insteeklijn worden waargenomen. In tegenstelling tot de waterlijnen is de locatie van de waterlijnen niet interpretatiegevoelig, maar gevoelig voor de hoogte van het water op dat moment. Dus, vanwege de verschillen in interpretatie en verschillende waterhoogtes, moet men bij analyseren van de insteeklijnen en de waterlijnen voorzichtig zijn met het trekken van conclusies. Aangezien deze metingen jaarlijks al vanaf 2007 plaatsvinden, kunnen er analyses worden gedaan wat betreft ontwikkelingen in de morfologie en migratie van de Groenlose Slinge. Ook is er een vegetatiekaart en een erosie- en depositiekaart gemaakt. Tot slot zijn worteleigenschappen zoals diameter, dichtheid en lengte genoteerd.

Resultaten

De morfologische ontwikkeling tussen 2007 (aanleg) en 2011

In de periode tussen 2008 en 2011 vond er aanzienlijke netto depositie van gemiddeld 1.5 m^2 per meter lengte plaats. Echter, doordat er tussen 2007 en 2008 veel erosie plaatsvond liggen de profielen van 2011 over het algemeen nog steeds lager dan de aangelegde profielen in 2007. De breedte van de Groenlose Slinge bij hoog water lijkt ongeveer 30 cm te zijn toegenomen tussen 2008 en 2011. Dit zou het resultaat kunnen zijn van hoogwaterperiodes. Als een gevolg van de netto depositie tussen 2008 en 2011 is de breedte van de beek bij laag water gemiddeld met ongeveer één meter afgenomen en is de hoogte van de oevers gemiddeld toegenomen met 17 centimeter. Ook de gemiddelde waterdiepte lijkt ongeveer vier cm te zijn toegenomen. De bochten in de Groenlose Slinge zijn scherper geworden waardoor het water waarschijnlijk meer opgestuwd wordt. Dit zou de reden kunnen zijn van de grotere waterdiepte in 2011 vergeleken met 2008.

Laterale migratie en vegetatie
De berekende laterale migratie tussen 2008 en 2011 is 0.92 m., dus 0.31 meter per jaar. Het is meer regel dan uitzondering dat niet het gehele profiel met dezelfde snelheid migreert en ook de richting van migratie van verschillende delen van het profiel kan verschillen. Dit betekent dat bijvoorbeeld de thalweg naar het oosten kan migreren terwijl de westelijke oever naar het westen migreert of dat de oostelijke oever sneller migreert dan de westelijke oever.
Uit het onderzoek komt naar voren dat de mate van laterale migratie wordt bepaald door de verhouding van de kromtestraal en de breedte. Wanneer deze verhouding gelijk is aan ongeveer vier is de migratie per meter breedte het grootst. Uit het onderzoek blijkt dat vegetatie geen effect heeft op de snelheid van migreren.

Erosie en vegetatie
Als er erosie wordt waargenomen is dit altijd in een buitenbocht. Alleen riet, lisdodde en oud bos kunnen invloed hebben op dit patroon. De toegevoegde sterkte van grassen, kruiden en jonge boompjes is te klein om invloed te hebben op dit erosiepatroon wat bepaald wordt door de locatie van de buitenbochten.

Toevoegende sterkte van vegetatie
De toegevoegde sterkte van vegetatie aan de oever neemt toe als de vegetatie ouder wordt. In het geval van bomen wordt de maximale toegevoegde sterkte na ongeveer 25 jaar bereikt en in het geval van grassen en kruiden na ongeveer tien jaar. Tot en met een leeftijd van vijf tot tien jaar is de toegevoegde sterkte van grassen groter dan de toevoegende sterkte van bomen. Na die periode wordt de toevoegende sterkte van bomen groter dan de toevoegende sterkte van grassen. De toevoegende sterkte van els is groter dan de toevoegende sterkte van schietwilg. Dit heeft tot gevolg dat de schietwilg vaker in het water wordt aangetroffen als gevolg van erosie dan de els.

Scherpe bochten
In het geval van scherpe bochten is de migratiesnelheid klein. Er wordt verwacht dat de variatie in hydrologie en morfologie in scherpe bochten groter is dan in normale, flauwe bochten. Dit zou leiden tot verschillen in habitat wat weer een rijke variatie in flora en fauna zou opleveren. De migratiesnelheid van scherpe bochten is klein, waarschijnlijk omdat de stroming in scherpe bochten zich splitst (Eng: flow separation). Dus omdat scherpe bochten een gunstig effect op de ecologie zouden kunnen hebben, zou het invoeren van scherpe bochten een ideale oplossing zijn voor het verbeteren van de ecologie wanneer niet veel migratie gewenst is in verband met andere belangen.

Conclusie van het onderzoek
De conclusie van het onderzoek is dat het oevererosiepatroon van de Groenlose Slinge over het algemeen wordt gereflecteerd door het patroon van buitenbochten en dat vegetatie geen verschillend effect heeft op de mate van laterale migratie van de Groenlose Slinge. Wat betreft de morfologische ontwikkeling is depositie de meest kenmerkende observatie.

Conclusie voor wat betreft beheer
Dit onderzoek kan bijdragen bij het bepalen van het beheer van (her)meanderende beken. Als een vrij meanderende beek gewenst is, zouden volwassen bomen, riet en lisdodde die aanwezig zijn in de

buitenbochten verwijderd moeten worden om erosie in de buitenbochten niet tegen te houden. Wat de beste manier van verwijderen is (bijv. grazen of maaien), zou nog onderzocht moeten worden. Het zou immers kunnen zijn dat maaien zou zorgen voor vertakkingen van de wortels wat juist tot versterking van de oevers zou leiden. Wanneer men wil dat erosie voorkomen moet worden, moet er juist voor gezorgd worden dat er volwassen bomen, riet en lisdodde aanwezig zijn op de oevers. Deze vegetatie hoeft alleen maar in de buitenbochten worden geplaatst, omdat in principe alleen hier erosie plaats vindt. Met name els (Alnus) heeft een sterk erosieresistent karakter.

Chapter 17. References

Abernethy, B. and Rutherfurd, I.D., 1998. *Where along a river's length will vegetation most effectively stabilize streambanks?* Geomorphology, vol. 23(1), p. 55-75.

Allen, J.R.L., 1964. Sedimentology 3, Figure 4, p.168.

Allen, J.R.L. and Van Bendegom, L., 1978. *A neglected innovator in meander studies*. In Miall, A.D., editor. *Fluvial sedimentology*. Canadian Society of Petroleum Geologists Memoir, vol. 5, p. 199-209.

Andrle, R., 1994. *Flow structure and development of circular meander pools*. Geomorphology, vol. 9, p. 261-270.

Bathurst, J.C., Thorne, C.R. and Hey, R.D., 1979. *Secondary flow and shear stress at river bends*. Journal of Fluid Mechanics, vol. 536, p. 27-48.

Blanckaert, K. and Graf, W., 2001. *Mean flow and turbulence in open-channel bend.* Journal of Hydraulic Engineering, vol. 127, p. 835-847.

Blanckaert, K. and Vriend, H.J.D., 2003. *Nonlinear modelling of mean flow redistribution in curved open channels.* Water resources research, vol. 39(12), p.1375.

Blanckaert, K.[1], Kleinhans, M.G.[2], McLelland, S.J.[3], Uijttewaal, W.S.J.[4], Murphy, B.J.[3], Van der Kruijs, A.[2], Parsons, D.R.[5]., 2010. *Flow separation and morphology in sharp meander bends*. 1: Ecole Polytechnique Fédérale Lausanne, Switzerland, 2: Universiteit Utrecht, 3: University of Hull, 4: Delft University of Technology, 5: University of Leeds.

Bollen Weide, E., 2011. *Interview Groenlose Slinge with Ellen Bollen Weide*

Bourke, P., 1990. *Equation of a circle from 3 points (2 dimensions).* (http://paulbourke.net/geometry/circle from3/)

Bridges, P. and Leeder, M., 1976. *Sedimentary model for intertidal mudflat channels, with examples from the Solway Firth, Scotland.* Sedimentology, vol. 23, p. 533-552.

BRIDGIS BV, Tiel, 2008. Edited by Jansen, 2009.

Brooker, A., 1988. *Channelized rivers: Perspectives for Environmental Management*. John Wiley & sons, Chichester.

Camporeale, C., Perona, P., Porporato, A. and Ridolf, L., 2005. *On the long-term behaviour of meandering rivers.* Water Resources Research, vol. 41, issue 12, p. 13.

Coppin, N.J. and Richards, I.J., 1990. *Use of vegetation in civil engineering.* CIRIA. In Norris, J.E., Stokes, A., Mickovski, S.B., Cammeraat, E., Van Beek, R. and Nicoll, B.C. (Eds.), *Slope stability and erosion control.* Ecotechnological solutions p. 65-118. Dordrecht, The Netherlands: Springer.

Crosato, A., 1990. *Simulation of meandering river processes, Communications on Hydraulic and Geotechnical Engineering*. Report No. 90-3, Faculty of Civil Engineering, Delft University of Technology.

Crosatio, A., 2007. *Effects of smoothing and regridding in numerical meander migration models*, Water Resources Research, vol. 43, p. 10.

Darby, S.E., Gessler, D. and Thorne, C.R., 2000. *A computer program for stability analysis of steep, cohesive riverbanks.* Earth Surface Processes and Landforms, vol. 25, p. 175-190.

Darby, S.E., Alabyan, A.M. and Van de Wiel, M.J., 2002. *Numerical simulation of bank erosion and channel migration in meandering rivers.* Water Resources Research, vol. 38, p. 21.

Davies-Colley, R.J., 1997. *Stream channels are narrower in pasture then in forest.* In Wynn, T., Mostaghimi, S., Burger, J.A., Harpold, A.A., Henderson, M.B. and Henry, L., 2004. *Variation in root*

density along streambanks. Journal of environmental quality, vol. 33, p. 2030-2039.

De Grote Bosatlas, 2001. 52nd edition, Wolters-Noordhoff Atlasproducties Groningen

De Kramer, J.[1], Wilbers, A.[2], Van den Berg, J.[2] and Kleinhans, M.G.[2], 2000. *De Allier als morfologisch voorbeeld voor de Grensmaas.* 1: Dienst Landelijk Gebied Gelderland, 2:Universiteit, afdeling Fysische geografie, Utrecht. Natuurhistorisch maandblad, Augustus 2000, Jaargang 89.

De Vriend, H., 1977. *A mathematical model of steady flow in curved shallow channels*. Journal of Hydraulic Research, vol. 15, p.37-54.

Fagherazzi, S., Gabet, E and Furbisch, D., 2004. *The effect of bidirectional flow on tidal channel planforms.* Earth Surface Processes and Landforms, vol. 29, p. 295-309.

Ferguson, R., 1987. *Hydraulic and sedimentary controls of channel patterns.* Inst. British Geographers Special Publication, vol. 18., chapter. 6, p 129-158. Blackwell, Oxford, UK.

Ferguson, R., Parsons, D., Lane, S. and Hardy, R., 2003. *Flow in meander bends with recirculation at the inner bank.* Water Resources Research, vol. 39, p 1322-1333.

Friedkin, J.F., 1945. *A laboratory study of the meandering of alluvial rivers.* U.S. Waterways Experiment Station, Vicksburg, Mississippi, U.S.A., p. 40

Gautier, E., Brunstein, D., Vauchel, P., Roulet, M., Fuertes, O., Guyot, J.L., Darozzes J. and Bourrel L.,2007. *Temporal relations between meander deformation, water discharge and sediment fluxes in the floodplain of the Rio Beni (Bolivian Amazonia).* Earth Surface Processes and Landforms, vol. 32, p. 230-248.

Gran, K. and Paola, C., 2001. *Riparian vegetation controls on braided stream dynamics*. Water Resources Research, vol. 37, issue 12, p.3275 – 3283.

Gray, D.H. and Leiser, A.T., 1982. *Biotechnical slope protection and erosion control.* In Wynn, T., Mostaghimi, S., Burger, J.A., Harpold, A.A., Henderson, M.B., Henry, L., 2004. *Variation in root density along streambanks*. Journal of environmental quality, vol. 33, p. 2030-2039.

Gray, D.H. and Sotir, R.B., 1996. *Biotechnical and soil bioengineering slope stabilization: A practical guide for erosion control.* In Norris, J. E., Stokes, A., Mickovski, S. B., Cammeraat, E., Van Beek, R. and Nicoll, B.C. (Eds.), *Slope stability and erosion control.* Ecotechnological solutions, p. 65-118. Dordrecht, The Netherlands: Springer.

Greenway, D.R., 1987. *Vegetation and slope stability*. In *Slope stability*, edited by Anderson, M.G. and Richards, K.S., chap. 6, p. 187–230, Wiley, J. and Hoboken, N.J. in Pollen, N. and Simon, A. (2005). *Estimating the mechanical effects of riparian vegetation on streambank stability using a fiber bundle model*. Water resources research, vol. 41, W07025.

Hodskinson, A. and Ferguson, R., 1998. *Numerial modeling of separated flow in river bends: model testing and experimental investigation of geometric controls on the extent of flow separation at the concave bank.* Hydrological Prossess, vol. 12, p. 1323-1338.

Hooke, J., 2006: *Hydromorphological adjustment in meandering river systems and the role of flood events.* Sediment Dynamics and the Hydromorphology of FluvialSystems (Proceeding of a symposium held in Dundee, UK, July 2006), IAHS Publication, vol. 306, p. 127-135.

Hughes, M.L., McDowell, P.F. and Andrew Marcus, W., 2006. *Accuracy assessment of georectified aerial photographs: implications for measuring lateral channel movement in GIS*, Geomorphology, vol. 74, issue 1-4, p. 1-6.

Jansen, M., July 2009. *Long term meandering trends in the Groenlose Slinge, the Netherlands, in response to discharge regime and the presence of vegetation.* Master thesis, supervised by Dr. M.G. Kleinhans. Utrecht University, Department of Physical Geography, Faculty of Geosciences.

Johnson, W., 1994. *Woodland expansion in the Platte River, Nebraska: patterns and causes.* Ecological monographs, vol. 64, p. 45-84.

Julian, J.P. and Torres, R., 2006. *Hydraulic erosion of cohesive riverbanks.* Geomorphology, vol. 76, p. 193-206.

Kleinhans, M.G., Schuurman, F., Bakx, W. and Markies, H., 2009. *Meander channel dynamics in highly cohesive sediment on an intertidal mud flat in the Westerschelde estuary, the Netherlands.* Faculty of Geosciences, Department of Physical Geography, Utrecht University. Elsevier B.V..

Kleinhans, M.G., 2011. *Sorting out river channel patterns.* Progress in Physical Geography, vol. 34(3), p. 287-326. DOI: 10.1177/0309133310365300. Utrecht University, The Netherlands.

Kleinhans, M.G. and Van den Berg, J.H., 2010. *River channel and bar patterns explained and predicted by an empirical and physics-based method.* Department of Physical Geography, Faculty of Geosciences, Utrecht University, Utrecht, The Netherlands. DOI: 10.1002/esp.2090.

Knighton, D., 1998. *Fluvial forms and processes.* Oxford University Press Inc., New York, p. 383

Lanzoni, S.[1], Federici, B.[2] and Seminara, G.[2], 2006. *On the convective nature of bend instability*.1)Dept. of Hydraulic, Maritime, Environmental and Geotechnical Engineering University of Padova, Italy, 2) Dept. of Environmental Engineering, University of Genova, Italy. River, Coastal and Estuarine Morphodynamics: RCEM 2005 – Parker & Garcia (eds) 2006 Taylor & Francis Group, London, ISBN 0415392705

Lawler, D.M., 1992. *Process dominance in bank erosion systems*. In P.A. Carling, and Petts, G.E. (Eds.), *Lowland floodplain rivers: Geomorphology and river management: Applications of the river styles framework*. Oxford (UK): Blackwell Publications.

Lawler, D.M., 1993. *The measurement of riverbank erosion and lateral channel change: A review.* In Brierley, G. J. and Fryirs, K. A. (Eds.), *Geomorphology and river management: Applications of the river styles framework.* Oxford (UK): Blackwell Publications.

Lawler, D.M., Thorne, C.R. and Hooke, J.M., 1997. *Bank erosion and instability.* In Thorne, C.R., Hey,R.D. and Newson M.D. (Eds.), *Applied fluvial geomorphology for river engineering and management*, p.137-172. Chichester (UK): John Wiley and Sons Ltd.

Lawler, D.M., 2004. *The importance of high-resolution monitoring in erosion and deposition dynamics studies: Examples from estuarine and fluvial systems.* Geomorphology, vol. 64(1-2), p. 1-23. DOI:10.1016/j.geomorph.2004.04.005.

Lawler, D.M., 2005. *Defining the moment of erosion: The principle of thermal consonance timing.* Earth Surface Processes and Landforms, vol. 30(13), p.1597-1615. DOI: 10.1002/esp.1234.

Leeder, M. and Bridges, P., 1975. *Flow separation in meander bends*. Nature, vol. 253, p. 338-339 (January 31).

Leopold, L.B, Wolman, M.G., 1960. *River Meanders.* Geological Society of America Bulletin 1960, vol. 71, p.769-793. DOI: 10.1130/0016-7606(1960)71[769:RM]2.0C);2

Leopold, L.B., Wolman, M.G. and Miller, L.P., 1964. *Fluvial processes in geomorphology*. Freeman and Co., San Francisco.

Mamo, M. and Bubenzer, G.D., 2001a. *Detachment rate, soil erodibility, and soil strength as influenced by living plant roots, part I: Laboratory study.* In Wynn, T. watershed update – streambank retreat: Aprimer, vol. 4 AWRA hydrology & watershed management technical committee.

Mamo, M. and Bubenzer, G.D., 2001b. *Detachment rate, soil erodibility, and soil strength as influenced by living plant roots, part I: Field study*. Transactions of the ASAE, vol. 44(5), p. 1175-

1181. In Wynn, T. watershed update - streambank retreat: Aprimer, vol. 4. AWRA hydrology & watershed management technical committee.

Micheli, E.R. and Kirchner, J.W., 2002. *Effects of wet meadow riparian vegetation on streambank erosion. 1. Remote sensing measurements of streambank migration and erodibility.* Earth surface processes and landforms, vol. 27, p. 627-239.

Moorhead, K.K., Professor of Evironmental Studies, UNC Asheville. http://facstaff.unca.edu/moorhead/scholarship.htm, visited at 7th June, 2011.

Morgenstern, N.R. and Price, V.R., 1965. *The analysis of the stability of general slip surfaces*.Geotechnique, vol. 15, p. 79-93.

Osman, A and Thorne, C.R., 1988. *Riverbank stability analysis. I: Theory.* Journal of Hydraulic Engineering, vol. 114, p. 134-150.

Perucca, E., Camporeale, C. and Ridolfi, L., 2007. *Significance of the riparian vegetation dynamics on meandering river morpholdynamics*. Water Resources Research, vol. 43, p. 10.

Pollen, N., Simon, A. and Collision, A.J.C., 2004. *Advances in assessing the mechanical and hydrologic effects of riparian vegetation on streambank stability*. In *Riparian vegetation and fluvial geomorphology*. *Water science and applications 8*, S., Bennett and A., Simon (eds). AGU; 125–139.In Pollen-bankhead, N.L., and Simon, A. (2008). *Enhanced application of root-reinforcemen algorithms for bank-stability modelling.* Earth surface processes and landforms, DOI: 10.1002/esp.

Pollen, N., 2007. *Temporal and spatial variability in root reinforcement of streambanks: accouting for soil shear strength and moisture*. Catena, vol. 29, p.197-205.

Pollen-Bankhead, N. and Simon, A., 2009. *Enhanced application of root-reinforcement algorithms for bank-stability modelling.* Earth Surface-Processes and Landforms, vol. 34(4), p. 471-480. DOI: 10.1002/esp.1690.

Pollen-Bankhead, N. and Simon, A., 2010. *Hydrologic and hydraulic effects of riparian root networks on streambank stability: Is mechanical root-reinforcement the whole story?.* Geomorphology 116(2010)353-362 *USDA-USR National Sedimentation Laboratory, P.O. Box 1157, Oxford, ms 38655, USA.

Simon, A. and Darby, S., 1999. *The nature and significance of incised river channels*. In Darby, S.E. and Simon, A. eds., *Incised river channels: Processes, forms, engineering, and management.* John Wiley & sons: New York. p. 3-18. In Wynn, T. watershed update - streambank retreat: A primer, vol. 4 AWRA hydrology & watershed management technical committee.

Simon, A. Curini, A, Darby, S.E. and Langendoen, E.J., 2000. *Bank and near-bank processes in an incised channel*. Geomorphology, vol. 35, p. 183-217.

Simon, A and Collison, A.J.C., 2002. *Quantifying the mechanical and hydrologic effects of riparian vegetation on streambank stability.* Earth Surface Processes and Landforms, vol. 27(5), p.527-546. DOI:10.1002/esp.325.

Simon, A., Thomas., R., Curini, A. and Bankhead, N., 2009: They developed the Bank Stability and Toe Erosion Model, version 5.2.

Struiksma, N., Olesen, K.W., Flokstra, C. and De Vriend, H.J., 1985. *Bed deformation in curved alluvial channels*. Journal of hydraulic Research, vol. 23(1), p. 57-79.

Tal, M. and Paola, C., 2007. *Dynamics single-thread channels maintained by theminteraction of flow and vegetation*. Geology, vol. 35(4), p. 347-350.

Thorne, C.R. and Tovey, N.K., 1981. *Stability of composite riverbanks*. Earth Surface Processes and Landforms, vol. 6, p. 469-484.

Thorne, C.R., 1982. *Processes and mechanisms of riverbank erosion*. In Hey, R.D., Bathurst J. C. and Thorne C.R. (Eds.), *Gravel-bed rivers*. p. 227-271. Chichester, United Kingdom: John Wiley.

Thorne, C.R. et al., 1985. *Direct measurements of secondary currents in a meandering sand-bad river*. Nature, vol. 315(27), p. 746-747.

Thorne, C.R. and Osman, A., 1988. *Riverbank stability analysis, II: Applications.* Journal of Hydraulic Engineering, vol. 114, p. 151-172.

Thorne, C.R., 1990. *Effects of vegetation on riverbank erosion and stability.* p. 125–144. In Thornes, J.B. (ed.) *Vegetation and erosion processes and environments.* In Wynn, T., Mostaghimi, S.,Burger, J. A., Harpold, A. A., Henderson, M. B. and Henry, L., 2004. *Variation in root density along stream banks*. Journal of environmental quality, vol. 33, p. 2030–2039.

Thorne, C.R., Hey, R.D. and Newson, M.D., 1997. *Applied fluvial geomorphology for river engineering and management.* Wiley, Chichester, p. 376.

Tufekcioglu, A., Raich, J.W. and Isenhart, R.C.T.M.S., 1999. *Fine root dynamics, coarse root biomass, root distribution, and soil respiration in a multispecies riparian buffer in central iowa, USA.* In Wynn, T., Mostaghimi, S., Burger, J.A., Harpold, A.A., Henderson, M.B. and Henry, L., 2004. *Variation in rootdensity along streambanks*. Journal of environmental quality, vol. 33, p. 2030–2039. U.S. Fish & Wildlife Service Digital Library System, http://image.fws.gov/, visited at 7th June, 2011.

Van Bendegom, L., 1947. *Eenige beschouwingen over riviermorphologie en rivierverbetering*. De Ingenieur, vol. 59, p. 1-11.

Van de Kruijs, A., July 2010. *Flow separation in sharp bends*. Master thesis, supervised by Dr. M.G. Kleinhans. Utrecht University, Department of Physical Geography, Faculty of Geosciences.

Van der Vossen, J. and Verhagen, D., 2009. *Handreiking natuurvriendelijke oevers: Een hulpmiddel bij het proces van ontwerp tot aanleg van een natuurvriendelijke oever.* Stichting Toegepast Onderzoek Waterbeheer, Utrecht.

VT-BSE-TMDL Center, 2006. http://www.tmdl.bse.vt.edu/stream_restoration/C115/

Waldron, L.J., 1977. *The shear resistance of root-permeated homogeneous and stratified soil*. In Pollen-bankhead, N. and Simon, A., 2008. *Enhanced application of root-reinforcement algorithms for bank-stability modeling.* Earth surface processes and landforms. DOI: 10.1002/esp.

Waldron, L.J. and Dakessian, S., 1981. *Soil reinforcement by roots: calculation of increased soil shear resistance from root properties.* Soil Science, vol. 132(6), p. 427-435.

Wolfert, H.P., 2001. *Geomorphological Change and River Rehabilitation. Case Studies on Lowland Fluvial Systems in the Netherlands.* Alterra scientific contributions. Alterra green world research, Wageningen.

Wonnacott, T.H. and Wonnacott, R.J., 1990. *Introductory Statistics*. Fifth edition. University of Western Ontario. John Wiley & Sons.

Wu, T.H., McKinnel, W.P. and Swanston, D.N., 1979. *Strength of tree roots and landslides on Price of Wales Island, Alaska.* Canadian Geotechnical Journal, vol. 16(1), p. 19-33.

Wytema, H.J.S., July 2009. *The influence of vegetation on riverbank instability in a recently renaturalized river*. Master thesis, supervised by Dr. M.G. Kleinhans. Utrecht University, Department of Physical Geography, Faculty of Geosciences.

Internet: www.ahn.nl/viewer

Appendices

Appendix 1: Bank Stability and Toe Erosion Model, version 5.2.

The Bank Stability and Toe Erosion model version 5.2. (BSTEM-5.2.) is a sophisticated, physically-based two dimensional bank erosion model, programmed in Excel and is primarily intended for use in studies where bank toe erosion threatens bank stability. The model estimates boundary shear stress from channel geometry and considers critical shear stress and erodibility of the bank and bank toe, which are two separate zones with potentially different material. The effect of erosion protection on the bank and the bank toe can be incorporated in this model to show the effects of erosion control measures. Also the RipRoot model, that is part of the bank-stability and toe erosion model, is specially designed to include the effect of vegetation on erosion.

History of the Bank Stability and Toe Erosion model

Since the late 1990's, a physical-deterministic (sensitive to initial conditions) bank-stability model was developed at the USDA-ARS National Sedimentation Laboratory to model planar failures. Now, it is one of the most sophisticated erosion models available and already eleven versions of the model exist. The newest version of the model is version 5.2 (June, 2011), but there are no significant differences between this version and version 5.1. and 5.0. and just a few details were changed. However, version 5.0 is very different with reference to the former versions because the RipRoot model from Pollen and Simon (2005) is added. Due to the RipRoot model, the accuracy of added strength improves in relation to the former versions. RipRoot (Pollen and Simon, 2005) builds on earlier work by Waldron (1977), Wu et al. (1979) and Waldron and Dakessian (1981).

How the Bank Stability and Toe Erosion model works

As its name already suggests, the bank-stability and toe-erosion model consists of two parts: A bank stability model and a toe erosion model. The model partly uses the theories described in the literature review, like the different types of mass failures (*Section 2.1.2.*) and the Mohr-Coulomb criterion (*Section 3.2.2., Equation 2).* The model also uses equations like streambank stability algorithms, equations to calculate the average boundary shear stress, equations to calculate the erodibilty, equations to calculate the critical shear stress and equations to determine the erosion rates and amounts. The bank stability model part combines three models that calculate the factor of safety (Fs) for multi-layer streambanks. These applied methods are horizontal layers (Simon et al., 2000), vertical slices with tension cracks (Morgenstern and Price, 1965) and cantilever failures (Thorne and Tovey, 1981). For more information about the technical background of the model is referred to the technical background of the run-toe erosion model 5.2. (Simon et al., 2000; Simon and Collison, 2002 and Pollen-Bankhead and Simon, 2009).

In the model some assumptions have to be made. For example, it is assumed that there are hydrostatic conditions below the water table and that a linear interpolation of matric suction above the water table exists. It is also assumed that the parameterization is right. The model has been parameterized with literature values for variables corresponding to different vegetation, soil types and sediment types. However, in reality these values will change from site to site and from time to time. Finally, it is assumed that the bed elevation is fixed. This is because the model assumes that erosion is not transport limited and does not incorporate the simulation of sediment transport. In

reality, the bed can be eroded preferentially to the bank if the relative resistance of the bed and bank materials are such that the bed is more erodible than the toe or bank material.

Several parameter values can be put in BSTEM-5.2.: bank elevation (m), bank angle (deg), input bank toe length (m), input bank toe angle (deg), input shear surface angle (deg), bank layer thickness (m), reach length (m), input reach slope (m), elevation of flow (m), duration of flow (hours), bank material, toe material, vegetation, protection measures, water table depth (m) and the presence of cracks. From these input values, the input of bank toe angle, the input of shear surface angle, the input of vegetation or protection and the input of cracks are not necessary to put in. The bank stability model gives the factor of safety (Fs) as output. According to *Section 2.1.2*, the bank is stable if Fs > 1. However, according to this model, the bank is stable if Fs is larger than 1.3 to provide a safety margin for uncertain or variable data. Banks with an Fs value between 1.0 and 1.3 are said to be 'conditionally stable', i.e. stable but with little safety margin. Slopes with an Fs value less than 1.0 are unstable. The output of the toe erosion model is the average applied boundary shear stress (Pa), the maximal lateral retreat (cm), the eroded area of the bank (m^2), the eroded area of the bank toe (m^2), the eroded area of the bed (m^2) and the total eroded area (m^2).

Including vegetation in the model

The vegetation is included in the model by the RipRoot model. The RipRoot model can calculate the added strength caused by roots from different vegetation species and from different assemblages of vegetation. In the RipRoot model several species can be selected and each species delivers a different additional strength. The age of maximum added strength is different for each species.

Appendix 2: Profiles Groenlose Slinge 2007-2011

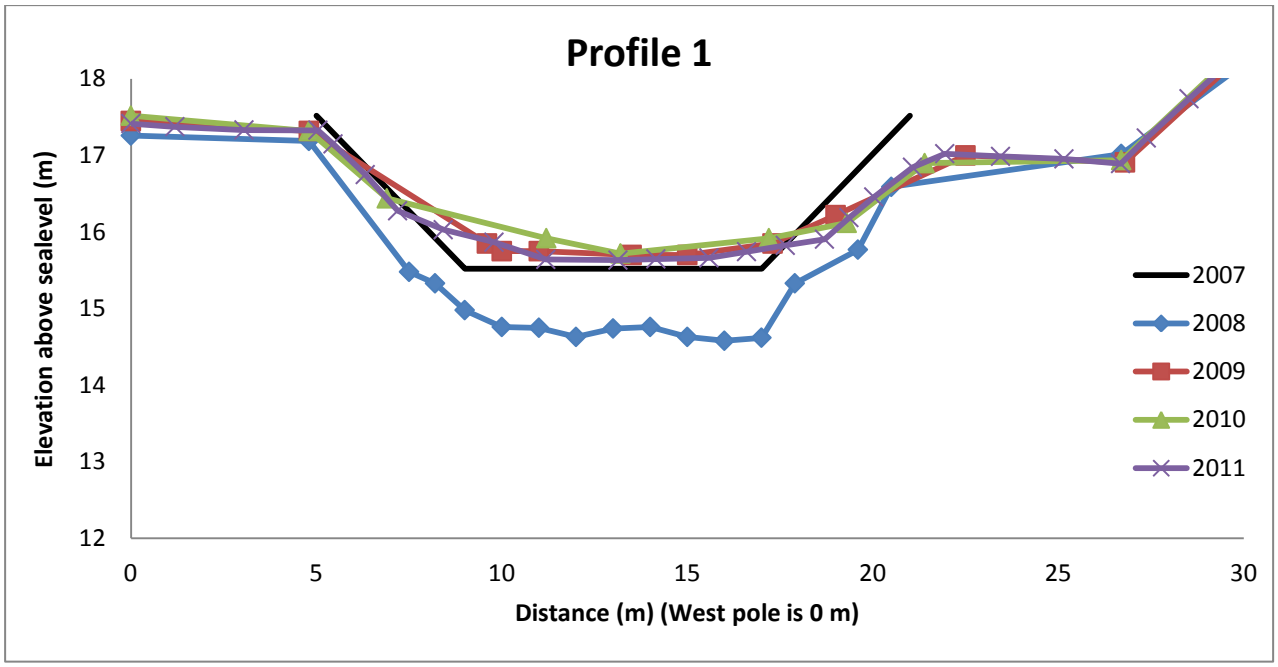

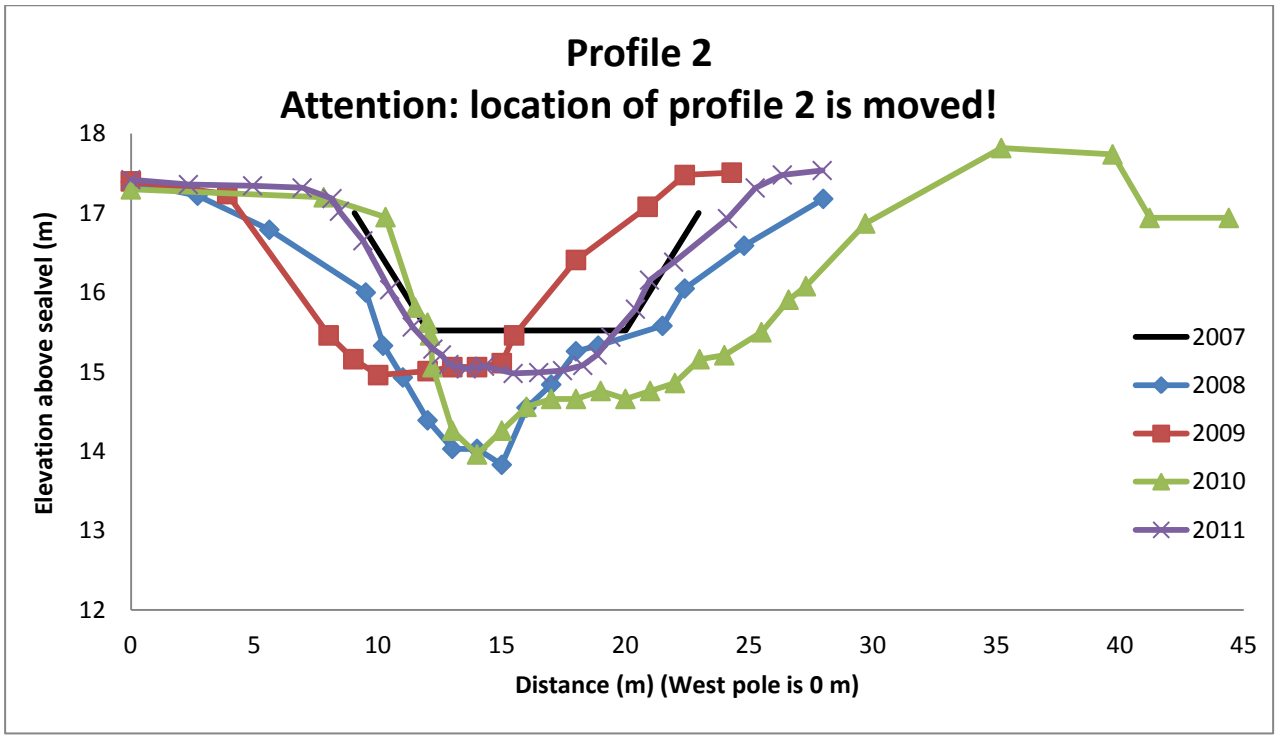

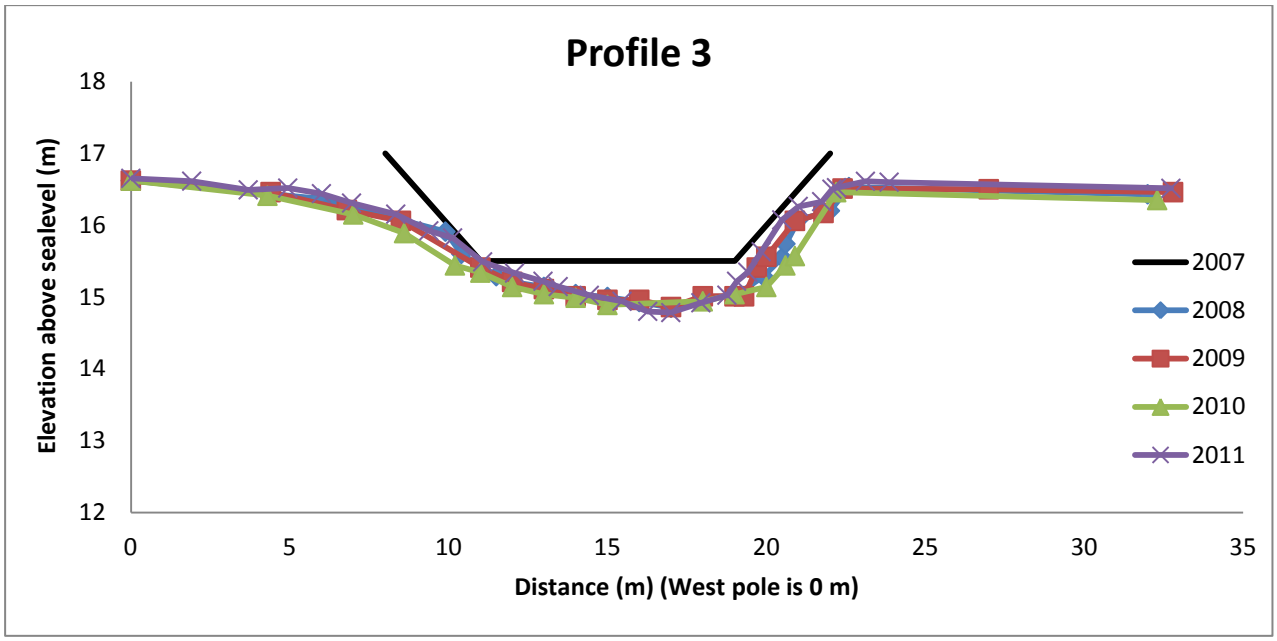
Profile 3
Elevation above sealevel (m)
18
17
16
15
14
13
12
0
5
10
15
20
25
30
35
Distance (m) (West pole is 0 m)
2007
2008
2009
2010
2011

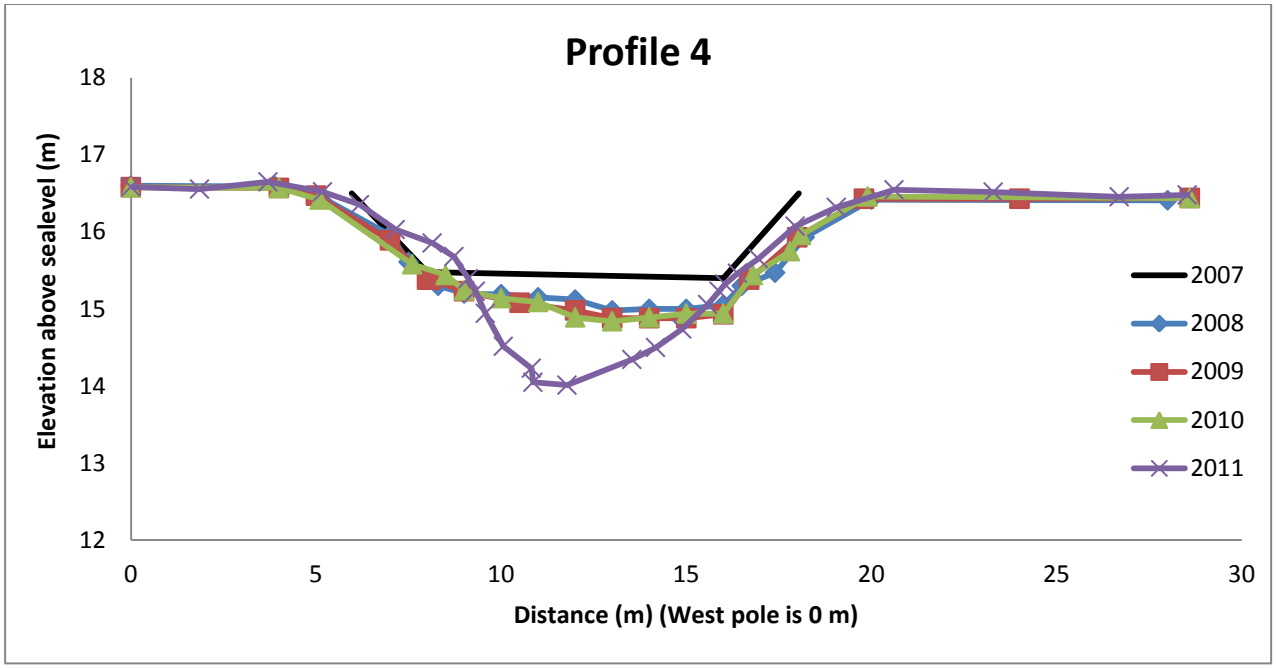
Profile 4
Elevation above sealevel (m)
18
17
16
15
14
13
12
0
5
10
15
20
25
30
Distance (m) (West pole is 0 m)
2007
2008
2009
2010
2011

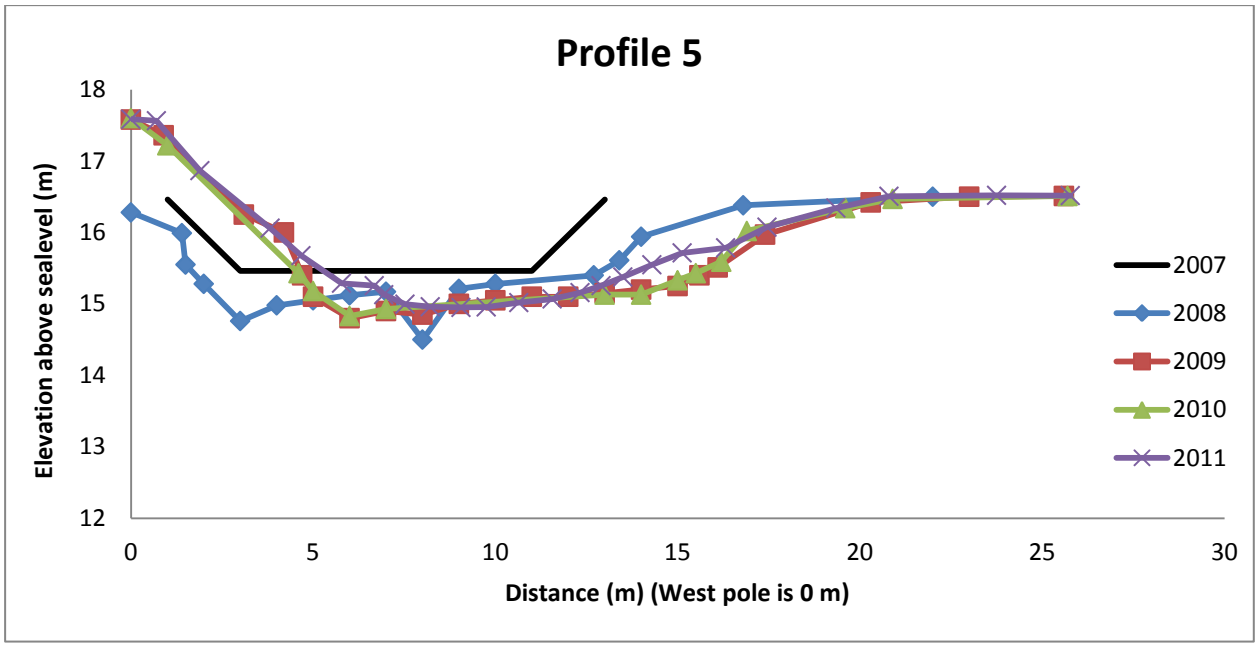
Profile 5
Elevation above sealevel (m)
18
17
16
15
14
13
12
0
5
10
15
20
25
30
Distance (m) (West pole is 0 m)
2007
2008
2009
2010
2011

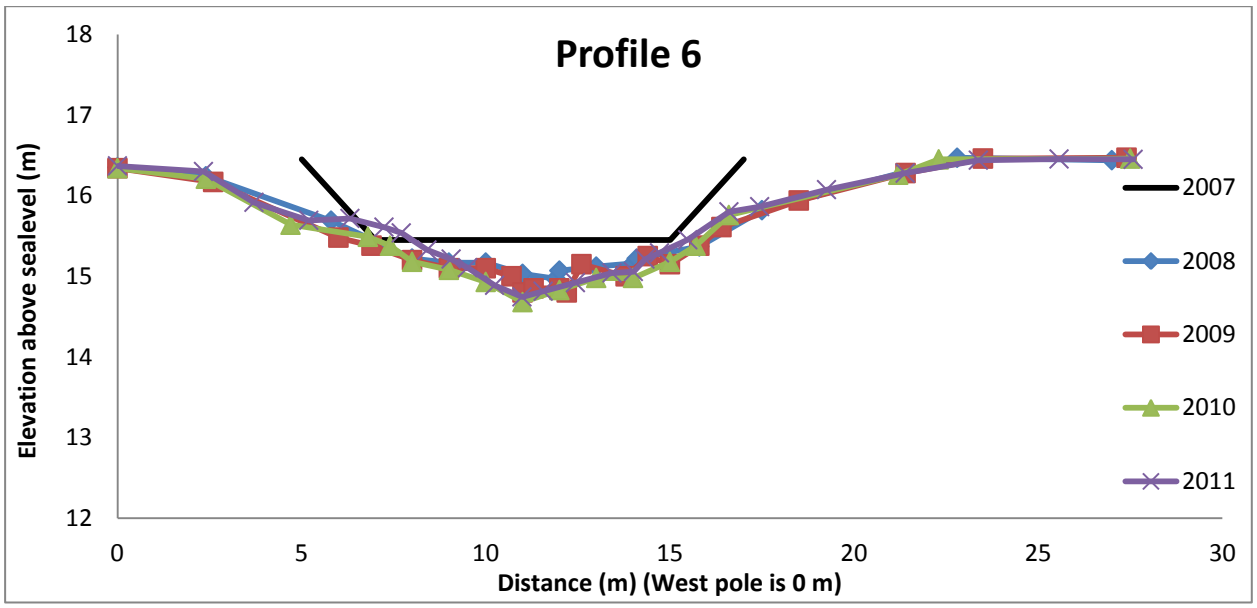
Profile 6
Elevation above sealevel (m)
18
17
16
15
14
13
12
0
5
10
15
20
25
30
Distance (m) (West pole is 0 m)
2007
2008
2009
2010
2011

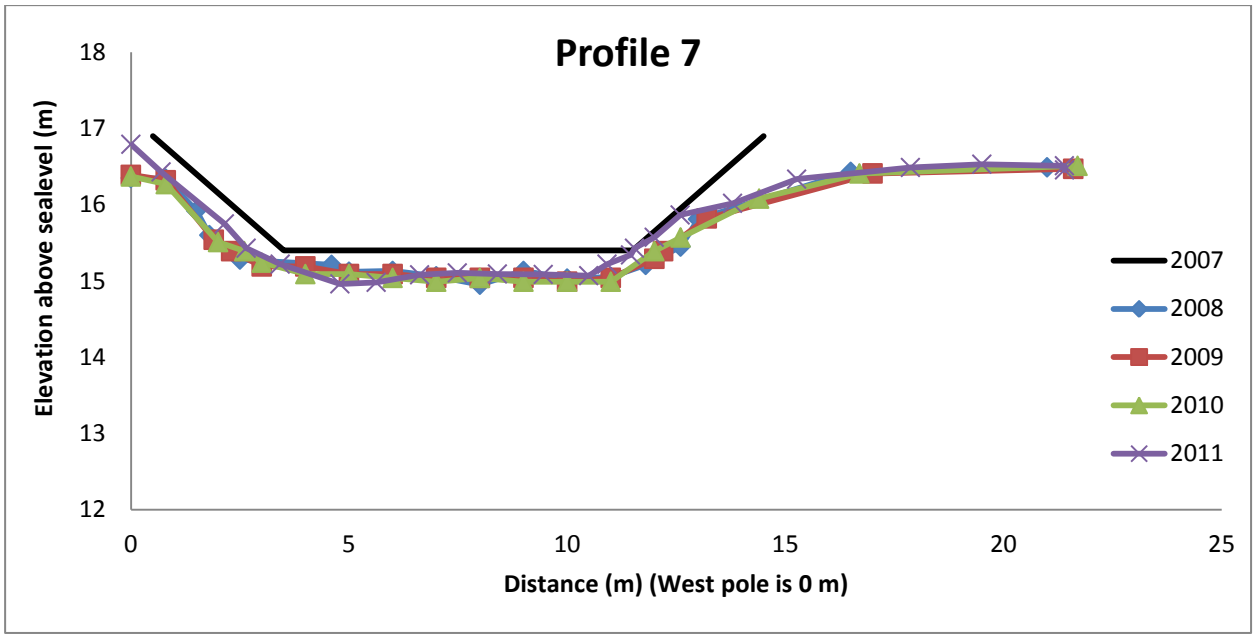
Profile 7
Elevation above sealevel (m)
18
17
16
15
14
13
12
0
5
10
15
20
25
Distance (m) (West pole is 0 m)
2007
2008
2009
2010
2011

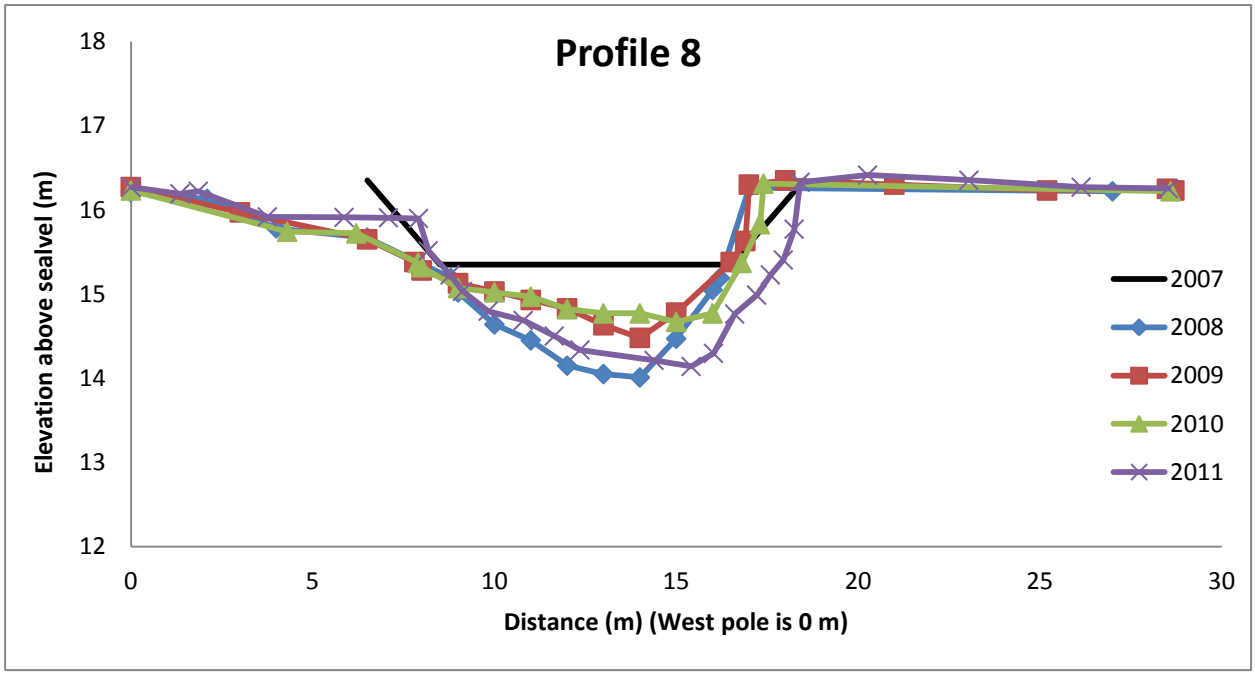
Profile 8
Elevation above sealvel (m)
18
17
16
15
14
13
12
0
5
10
15
20
25
30
Distance (m) (West pole is 0 m)
2007
2008
2009
2010
2011

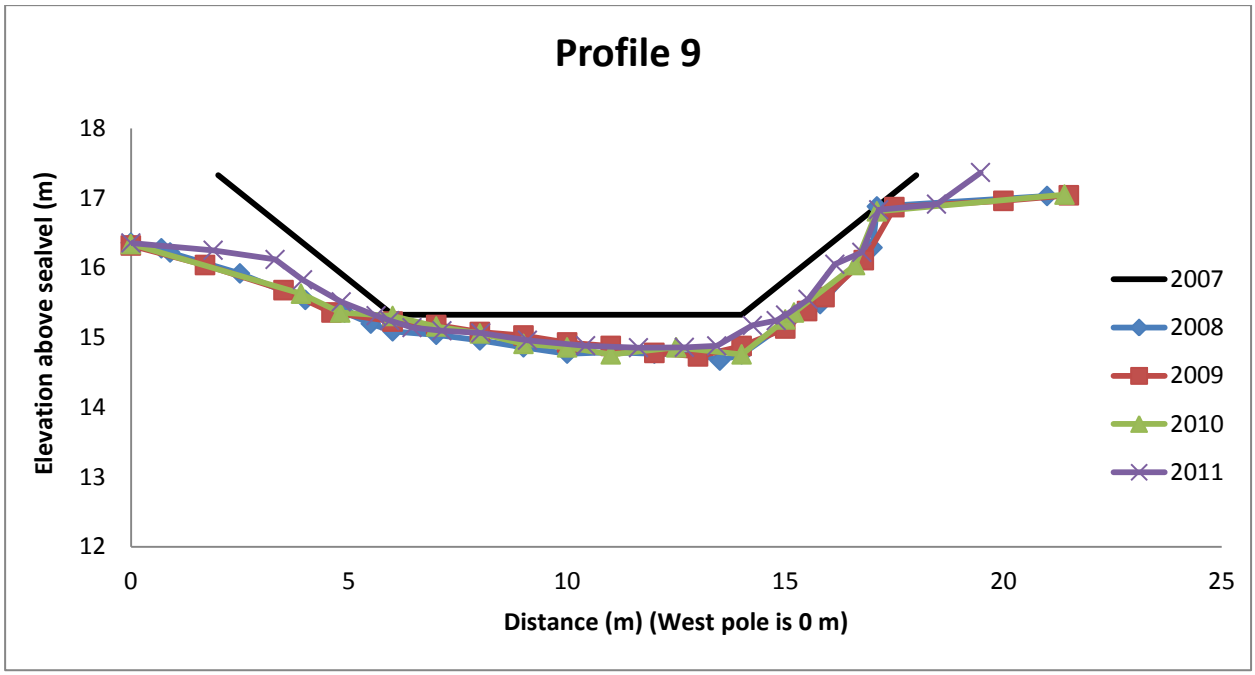
Profile 9
Elevation above sealvel (m)
18
17
16
15
14
13
12
0
5
10
15
20
25
Distance (m) (West pole is 0 m)
2007
2008
2009
2010
2011

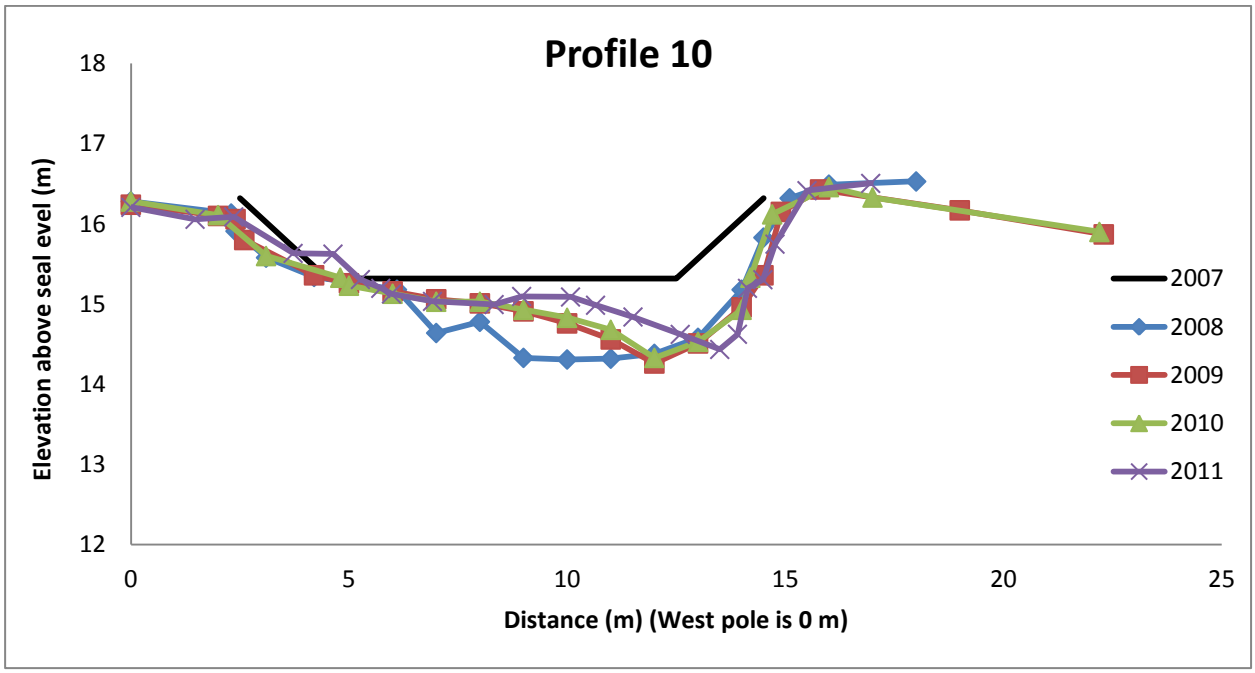
Profile 10
Elevation above seal evel (m)
18
17
16
15
14
13
12
0
5
10
15
20
25
Distance (m) (West pole is 0 m)
2007
2008
2009
2010
2011

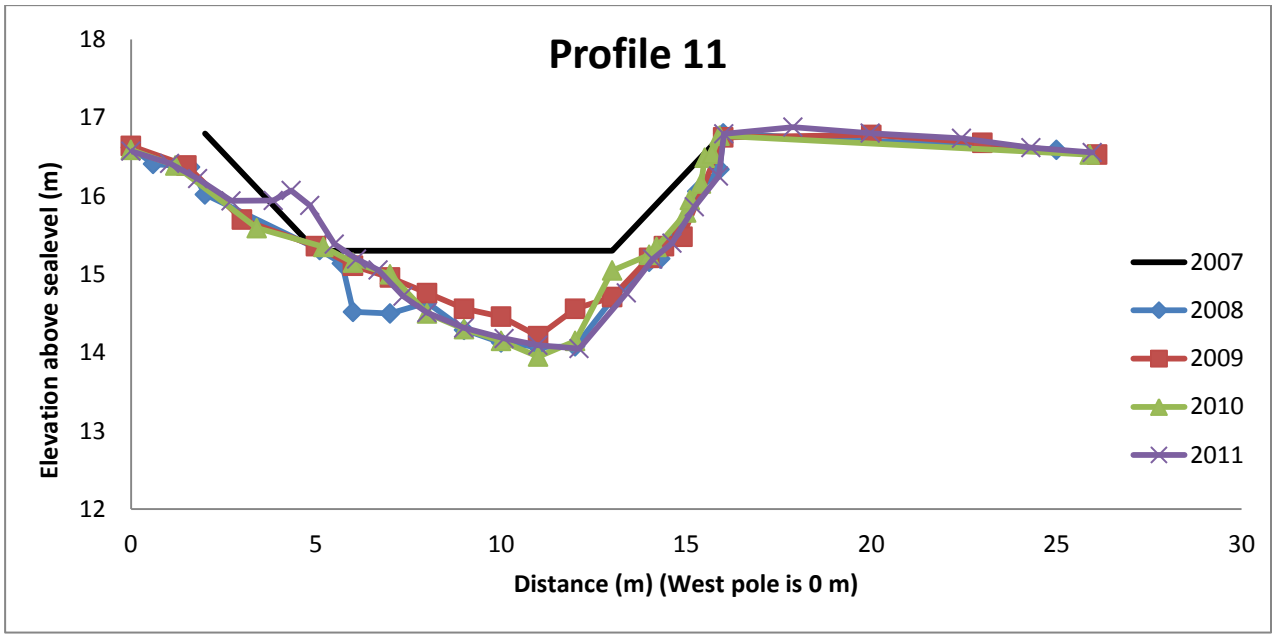
Profile 11
Elevation above sealevel (m)
18
17
16
15
14
13
12
0
5
10
15
20
25
30
Distance (m) (West pole is 0 m)
2007
2008
2009
2010
2011

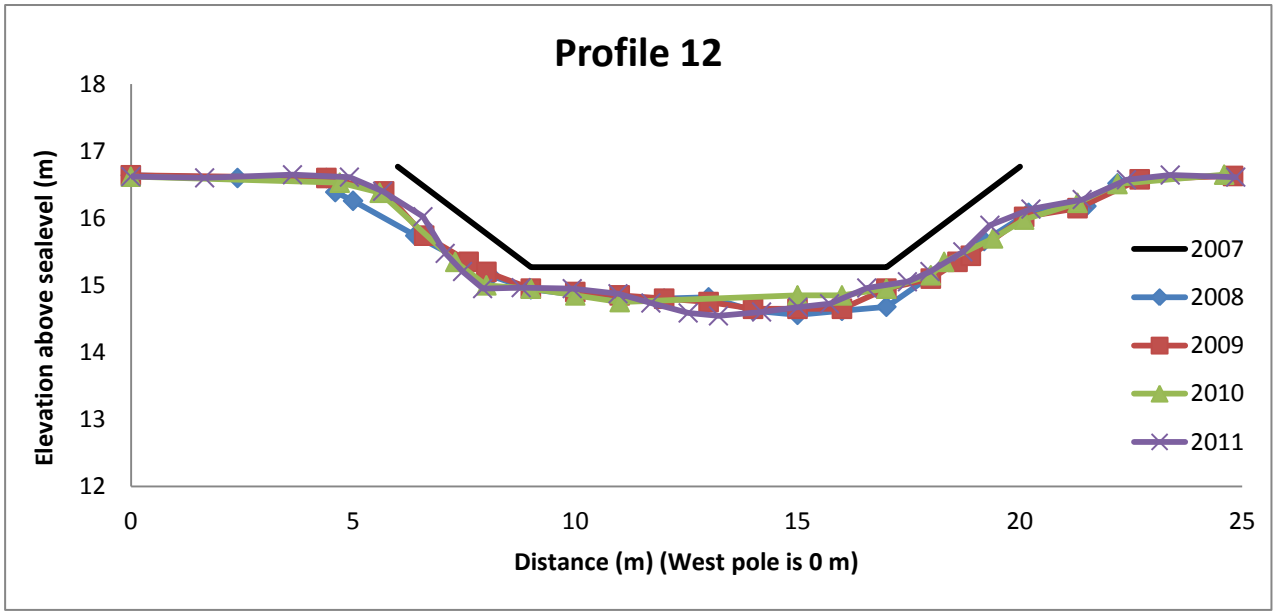
Profile 12
Elevation above sealevel (m)
18
17
16
15
14
13
12
0
5
10
15
20
25
Distance (m) (West pole is 0 m)
2007
2008
2009
2010
2011

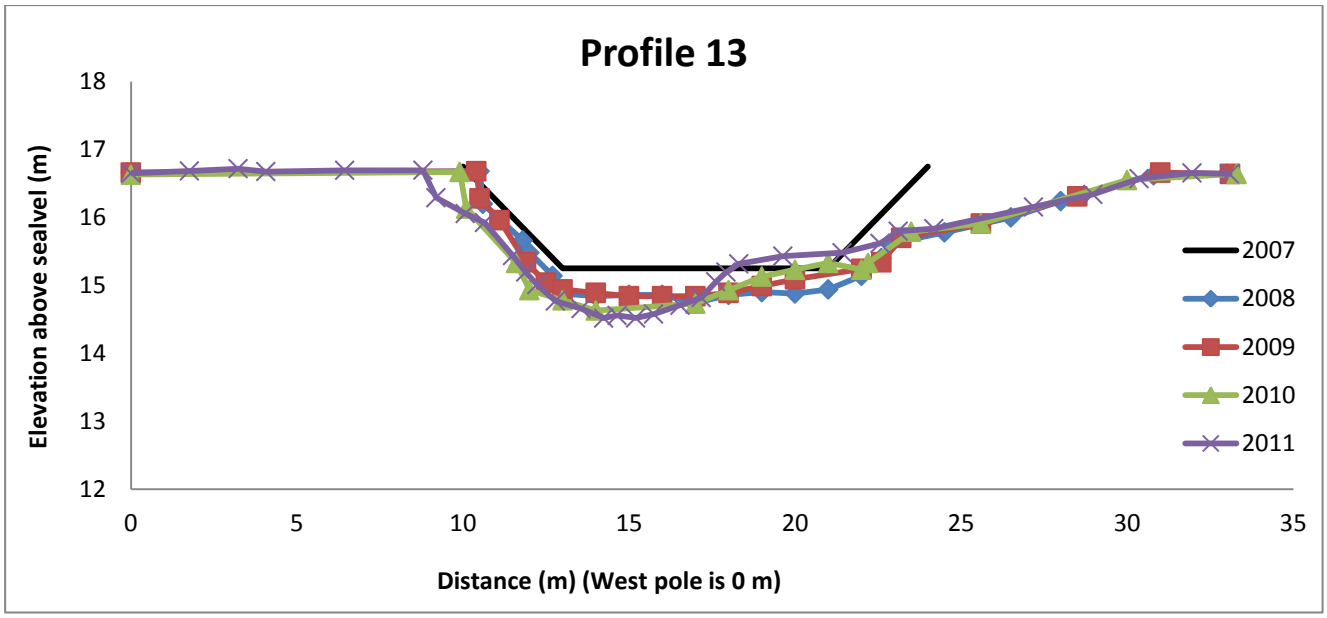
Profile 13
Elevation above sealvel (m)
18
17
16
15
14
13
12
0
5
10
15
20
25
30
35
Distance (m) (West pole is 0 m)
2007
2008
2009
2010
2011

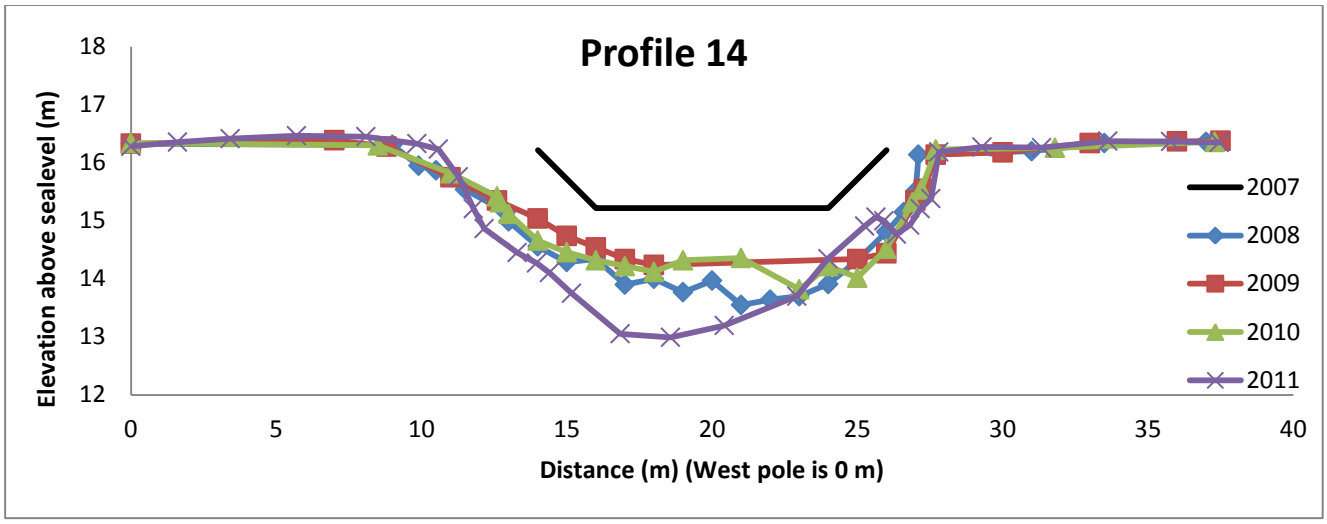
Profile 14
Elevation above sealevel (m)
18
17
16
15
14
13
12
0
5
10
15
20
25
30
35
40
Distance (m) (West pole is 0 m)
2007
2008
2009
2010
2011

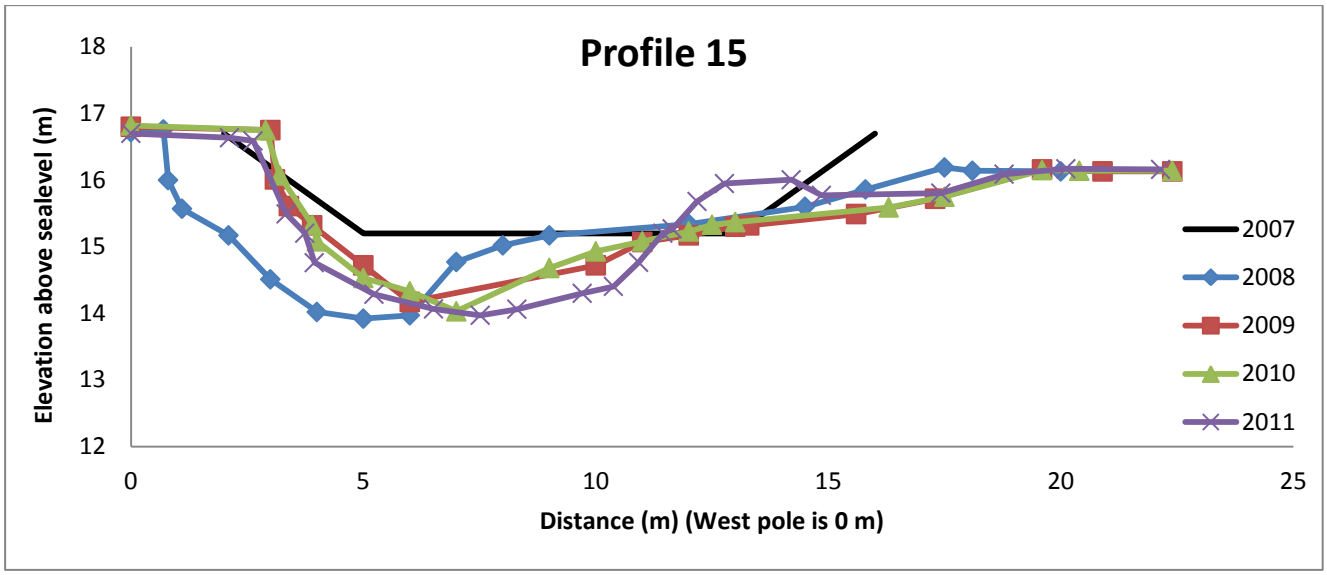
Profile 15
Elevation above sealevel (m)
18
17
16
15
14
13
12
0
5
10
15
20
25
Distance (m) (West pole is 0 m)
2007
2008
2009
2010
2011

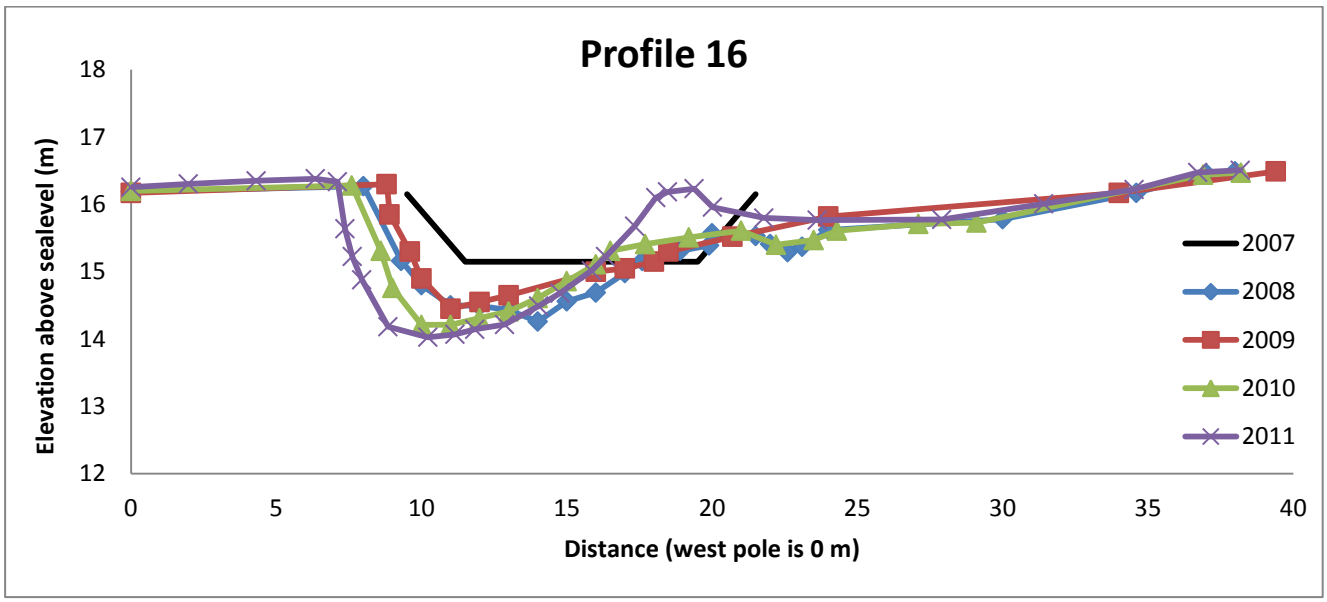
Profile 16
Elevation above sealevel (m)
18
17
16
15
14
13
12
0
5
10
15
20
25
30
35
40
Distance (west pole is 0 m)
2007
2008
2009
2010
2011

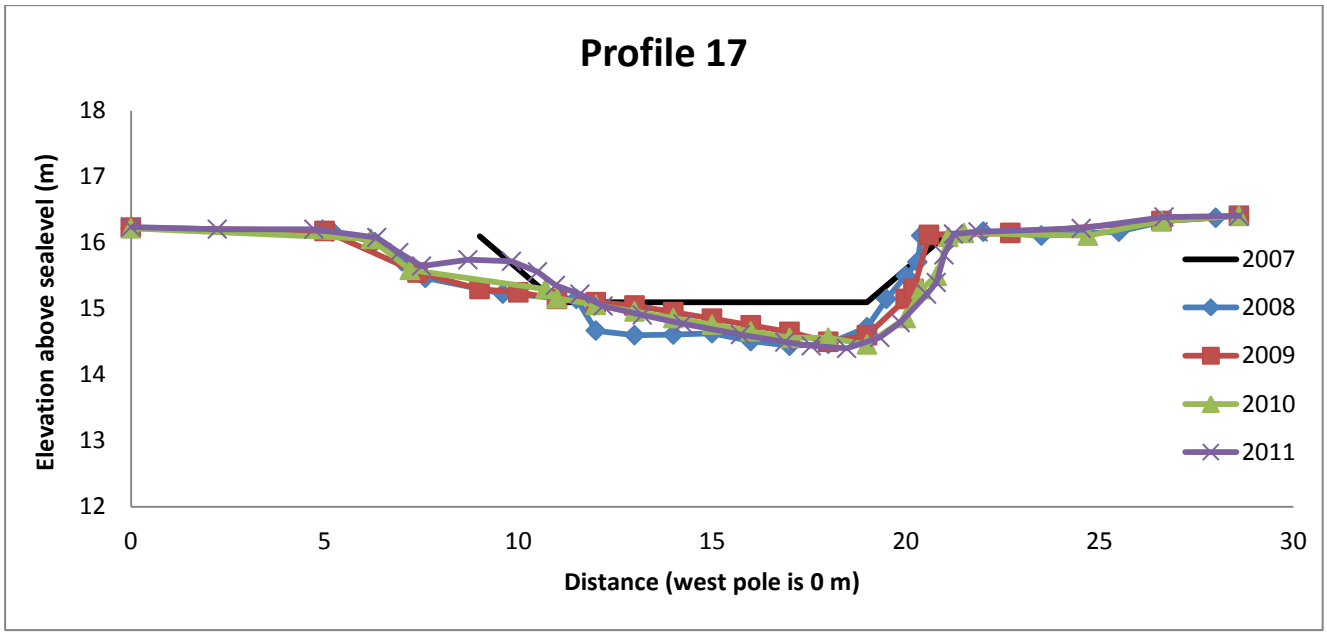
Profile 17
Elevation above sealevel (m)
18
17
16
15
14
13
12
0
5
10
15
20
25
30
Distance (west pole is 0 m)
2007
2008
2009
2010
2011

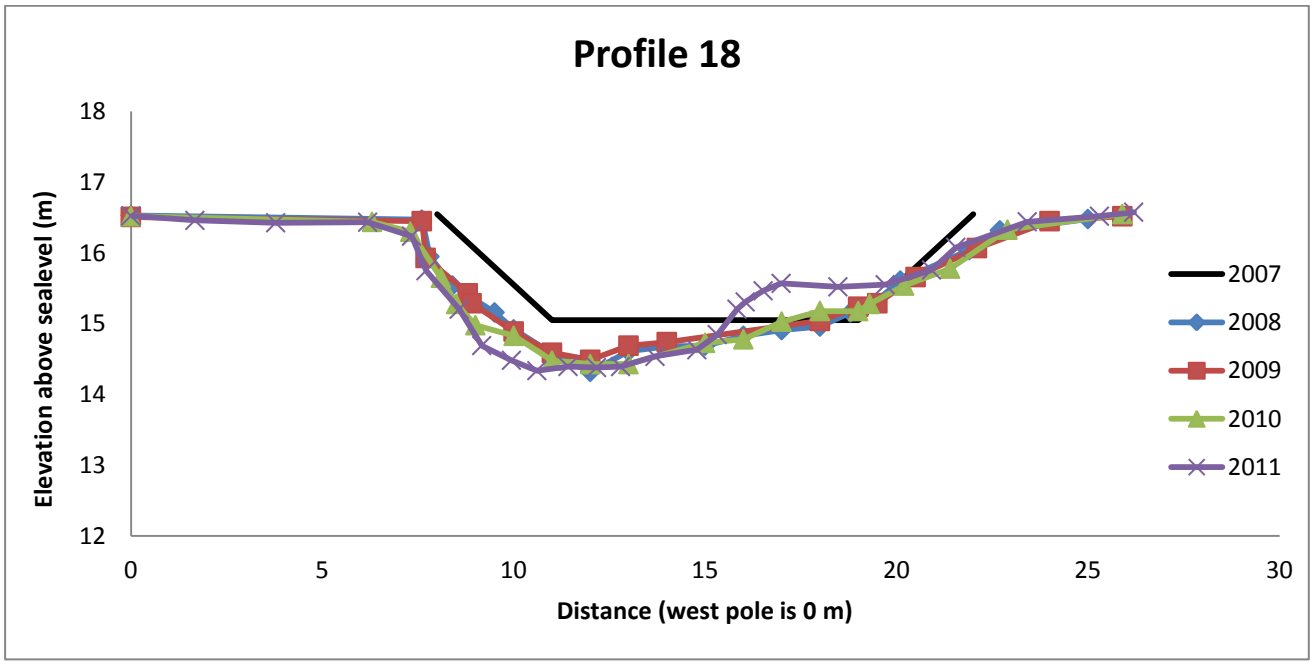
Profile 18
Elevation above sealevel (m)
18
17
16
15
14
13
12
0
5
10
15
20
25
30
Distance (west pole is 0 m)
2007
2008
2009
2010
2011

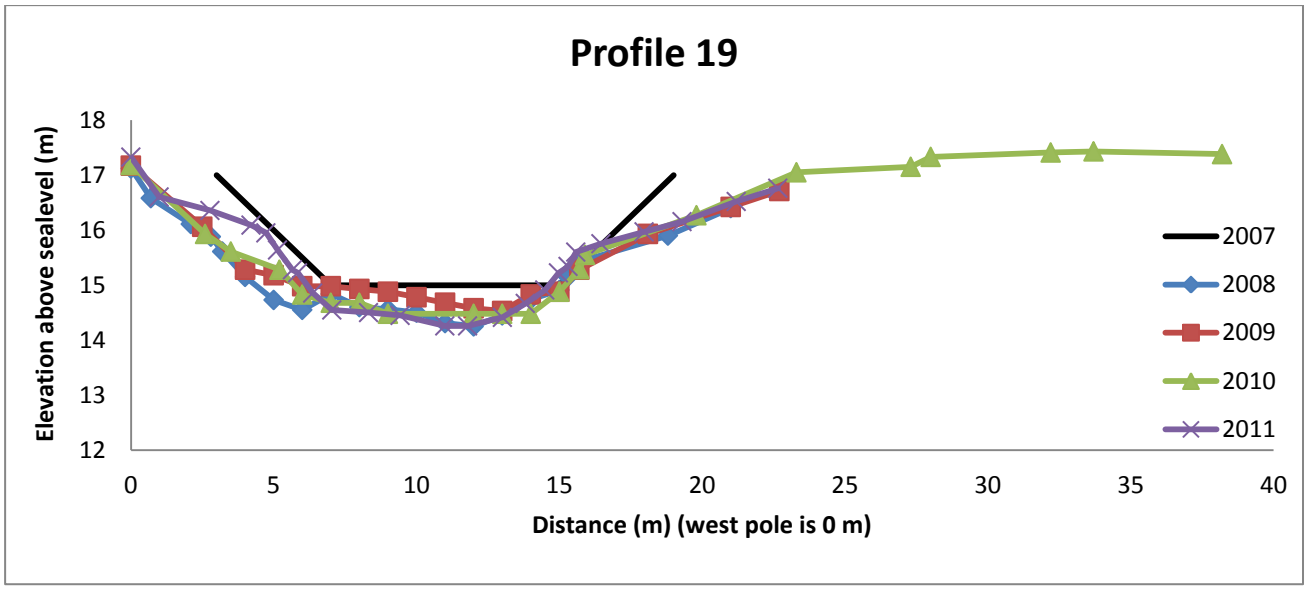
Profile 19
Elevation above sealevel (m)
18
17
16
15
14
13
12
0
5
10
15
20
25
30
35
40
Distance (m) (west pole is 0 m)
2007
2008
2009
2010
2011

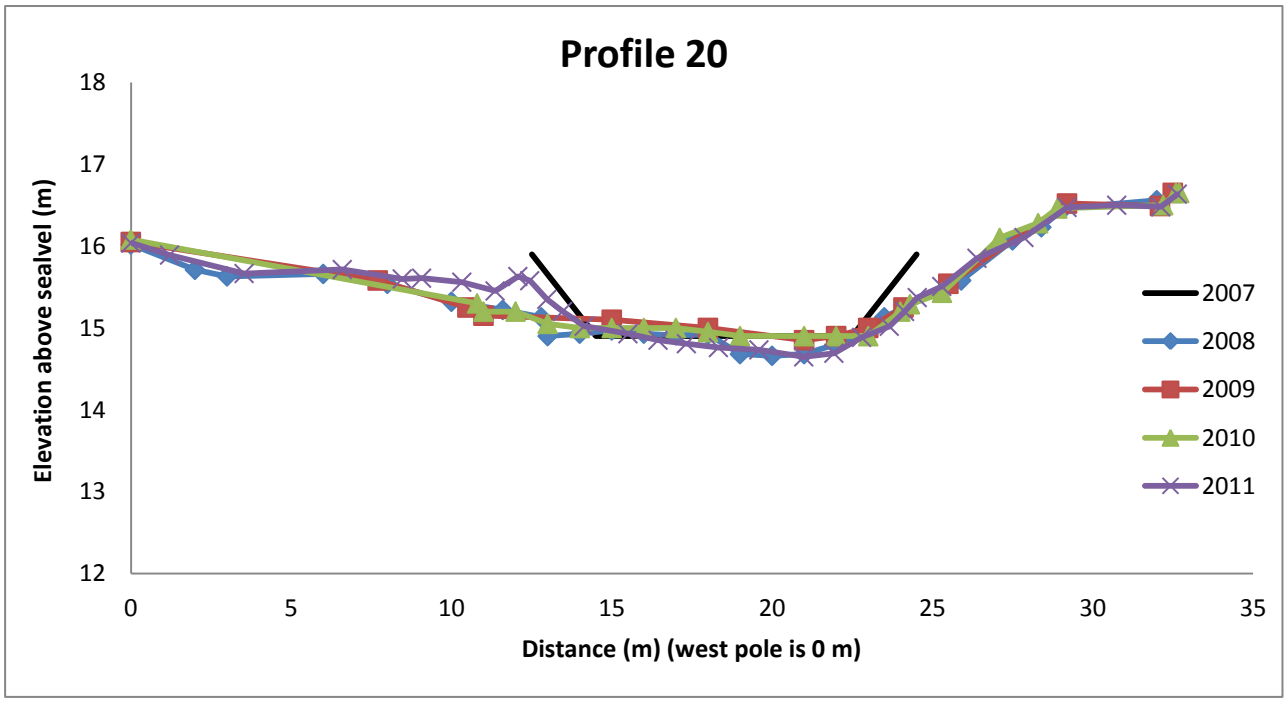
Profile 20
Elevation above sealevel (m)
18
17
16
15
14
13
12
0
5
10
15
20
25
30
35
Distance (m) (west pole is 0 m)
2007
2008
2009
2010
2011

Appendix 3: Profiles Groenlose Slinge 2008 and 2011, including waterlines

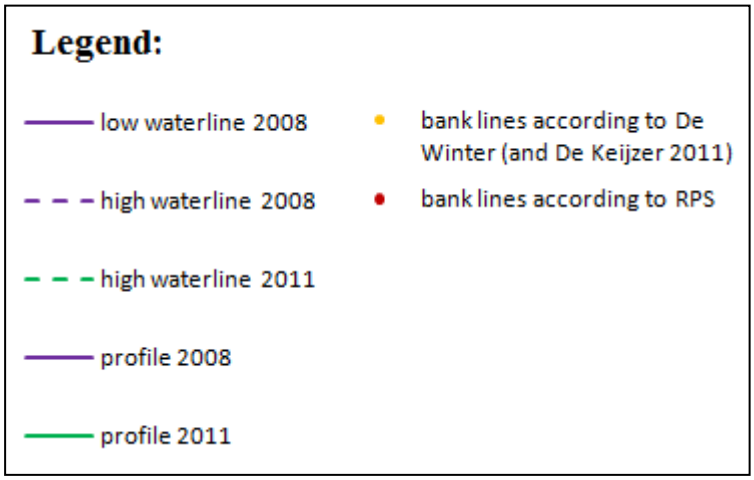

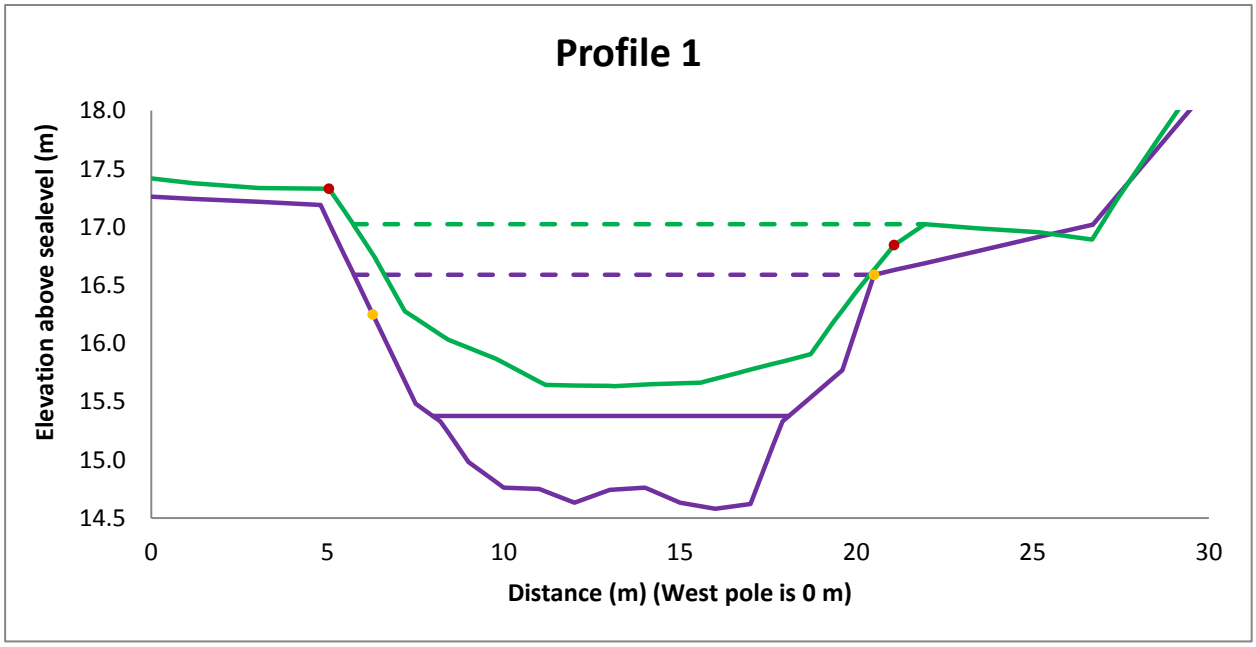

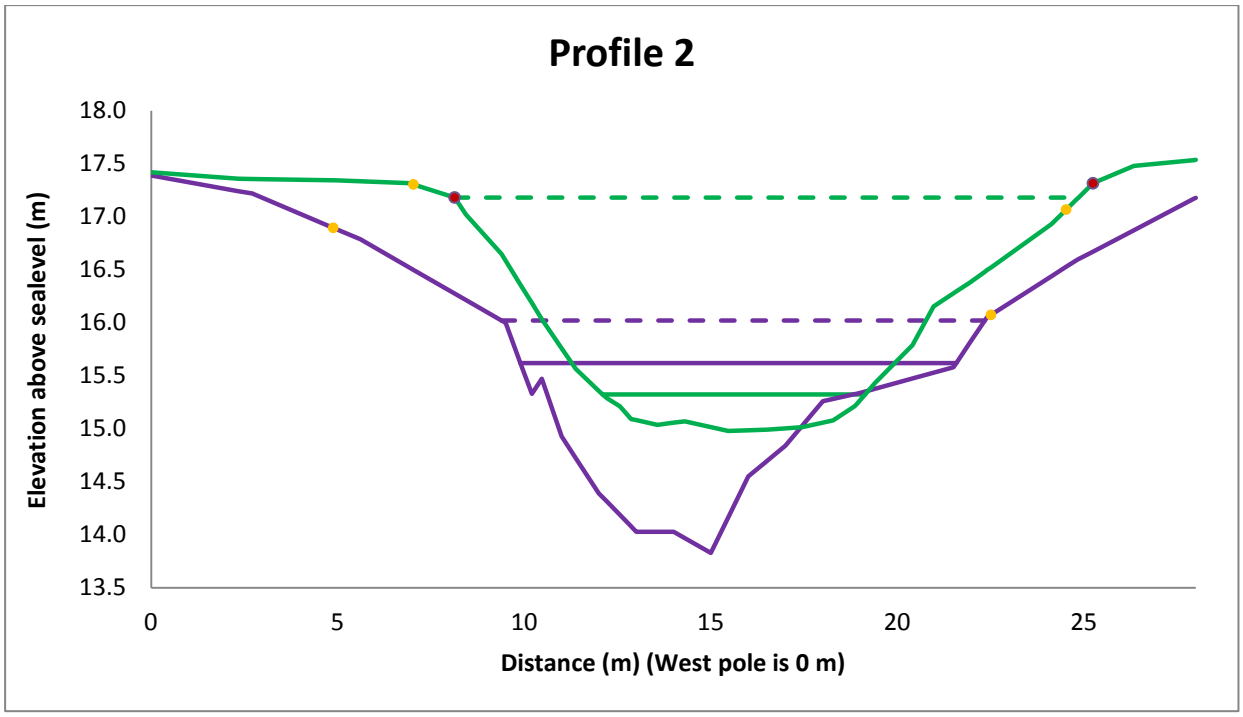
Profile 2
Elevation above sealevel (m)
18.0
17.5
17.0
16.5
16.0
15.5
15.0
14.5
14.0
13.5
0
5
10
15
20
25
Distance (m) (West pole is 0 m)

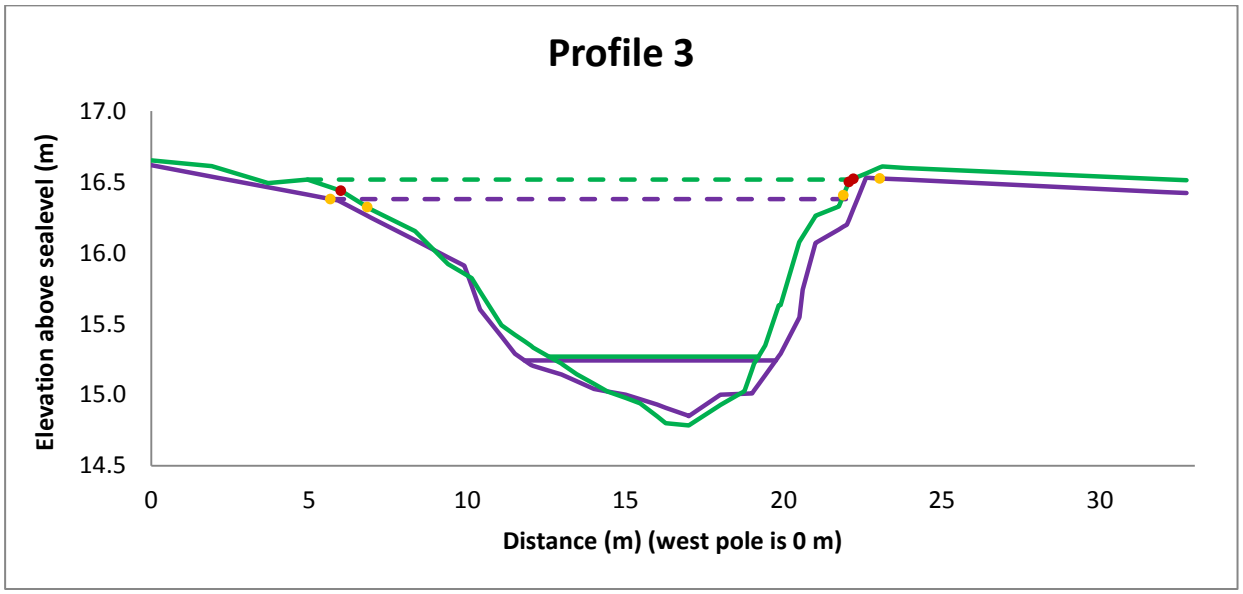
Profile 3
Elevation above sealevel (m)
17.0
16.5
16.0
15.5
15.0
14.5
0
5
10
15
20
25
30
Distance (m) (west pole is 0 m)

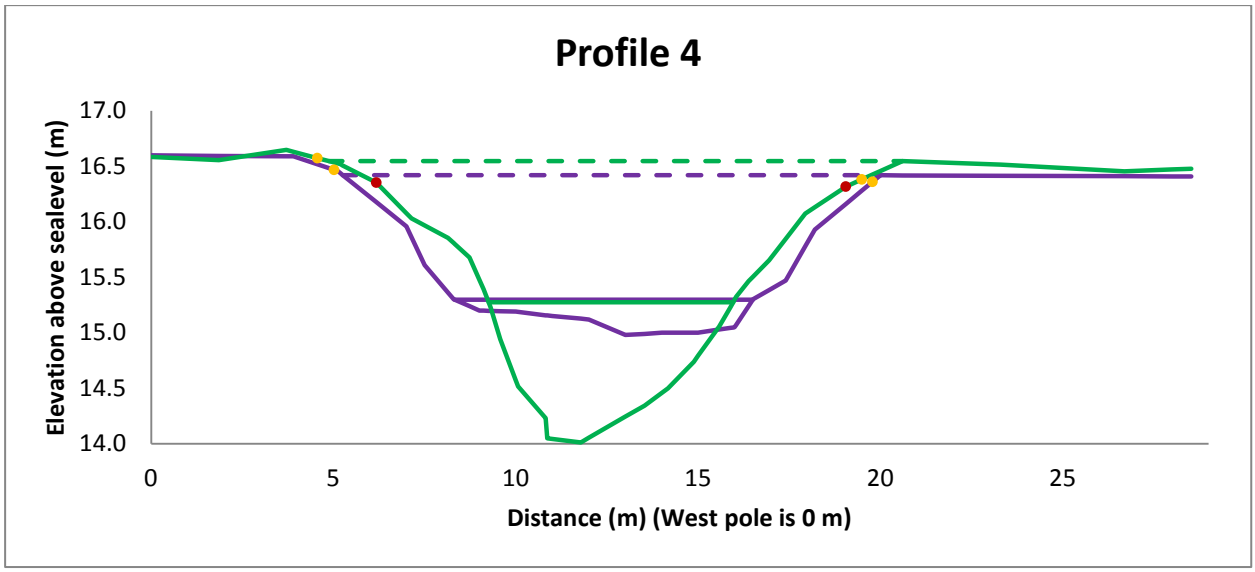
Profile 4
Elevation above sealevel (m)
17.0
16.5
16.0
15.5
15.0
14.5
14.0
0
5
10
15
20
25
Distance (m) (West pole is 0 m)

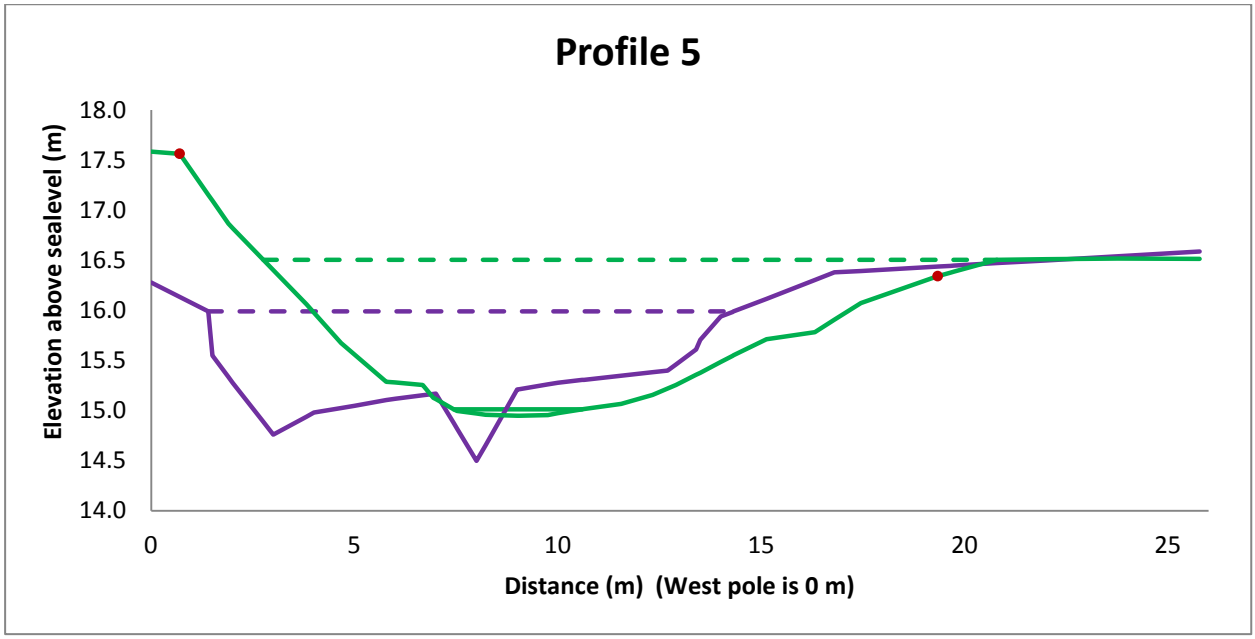
Profile 5
Elevation above sealevel (m)
18.0
17.5
17.0
16.5
16.0
15.5
15.0
14.5
14.0
0
5
10
15
20
25
Distance (m) (West pole is 0 m)

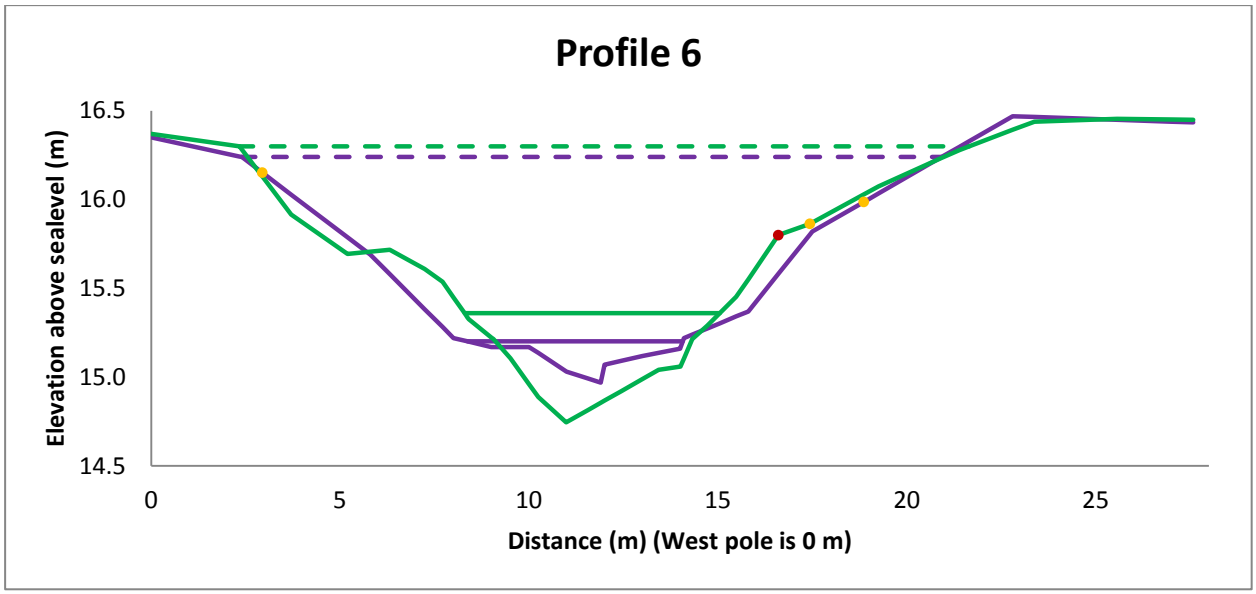
Profile 6
Elevation above sealevel (m)
16.5
16.0
15.5
15.0
14.5
0
5
10
15
20
25
Distance (m) (West pole is 0 m)

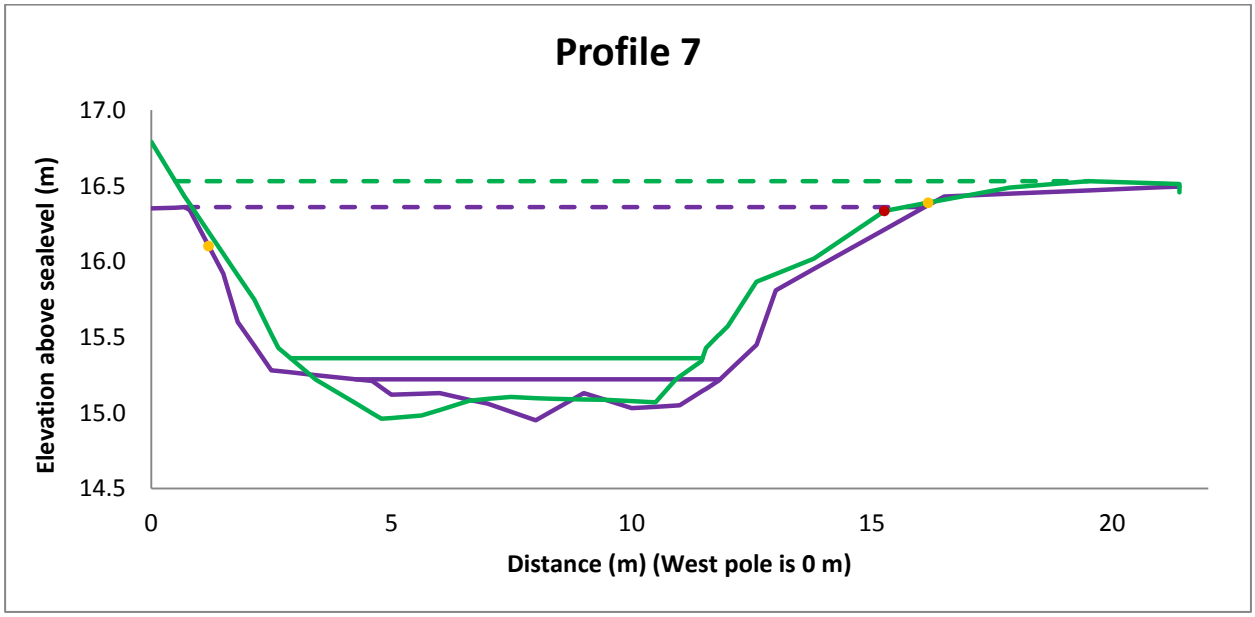
Profile 7
Elevation above sealevel (m)
17.0
16.5
16.0
15.5
15.0
14.5
0
5
10
15
20
Distance (m) (West pole is 0 m)

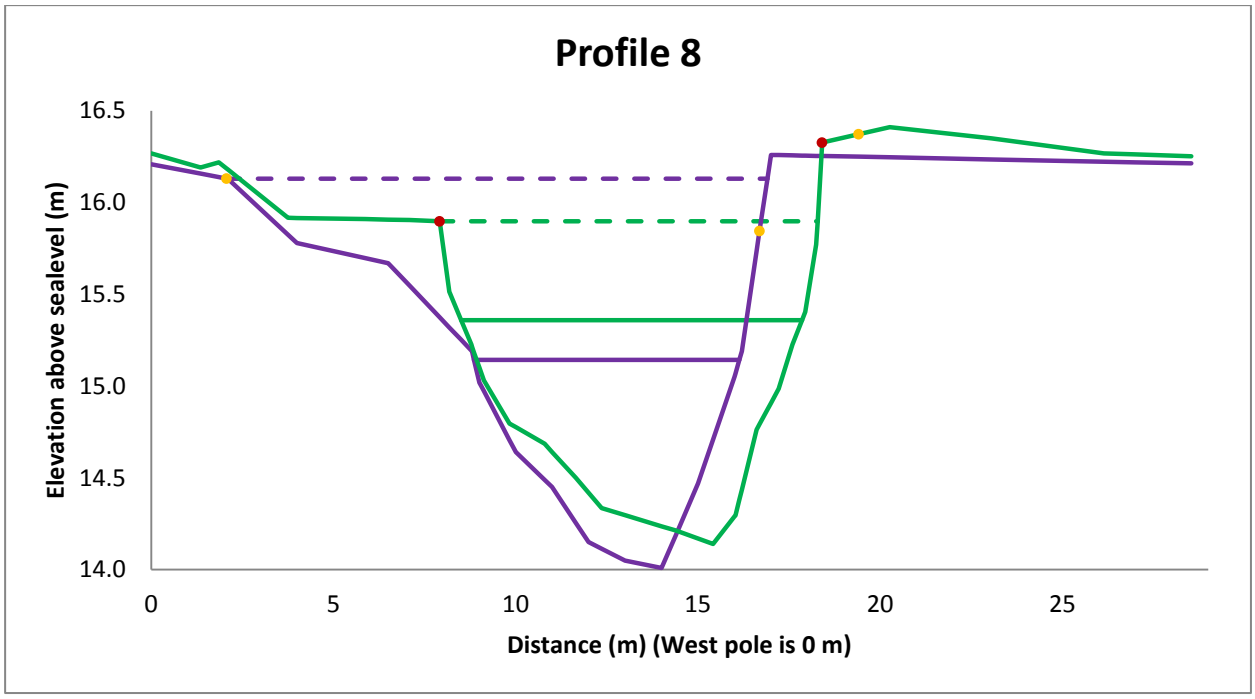
Profile 8
16.5
16.0
15.5
15.0
14.5
14.0
Elevation above sealevel (m)
0
5
10
15
20
25
Distance (m) (West pole is 0 m)

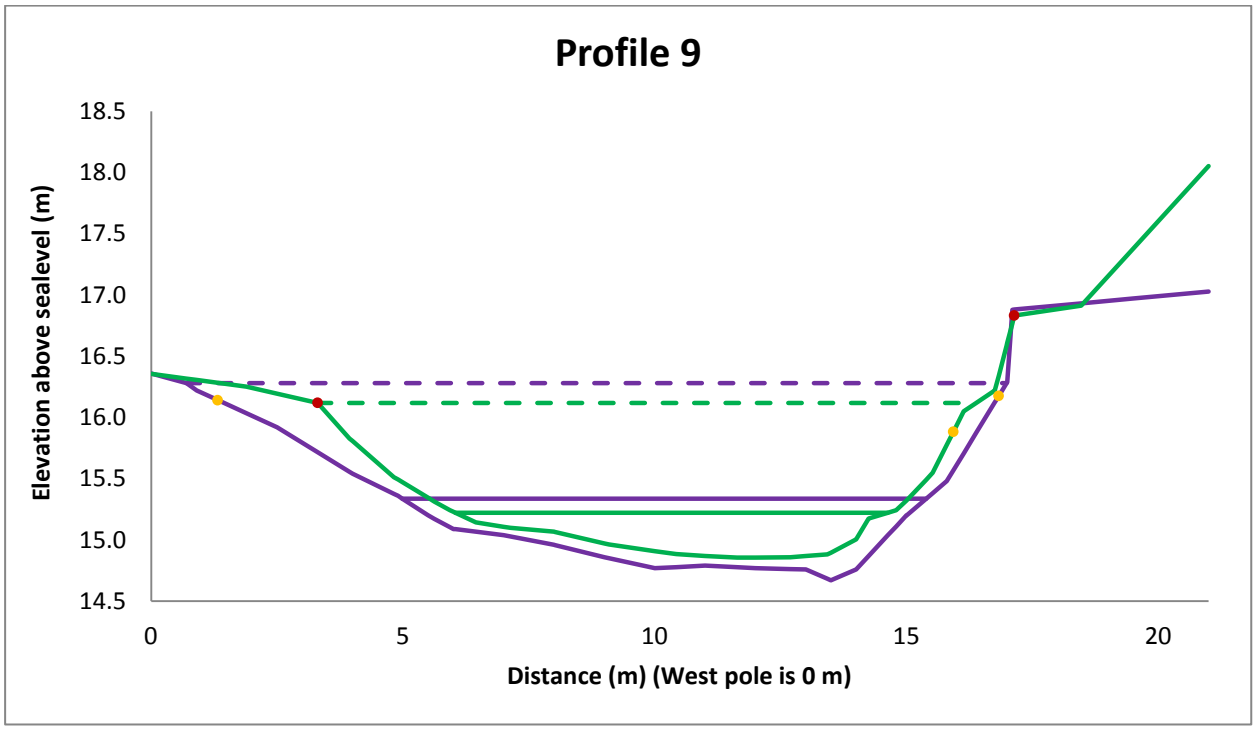
Profile 9
18.5
18.0
17.5
17.0
16.5
16.0
15.5
15.0
14.5
Elevation above sealevel (m)
0
5
10
15
20
Distance (m) (West pole is 0 m)

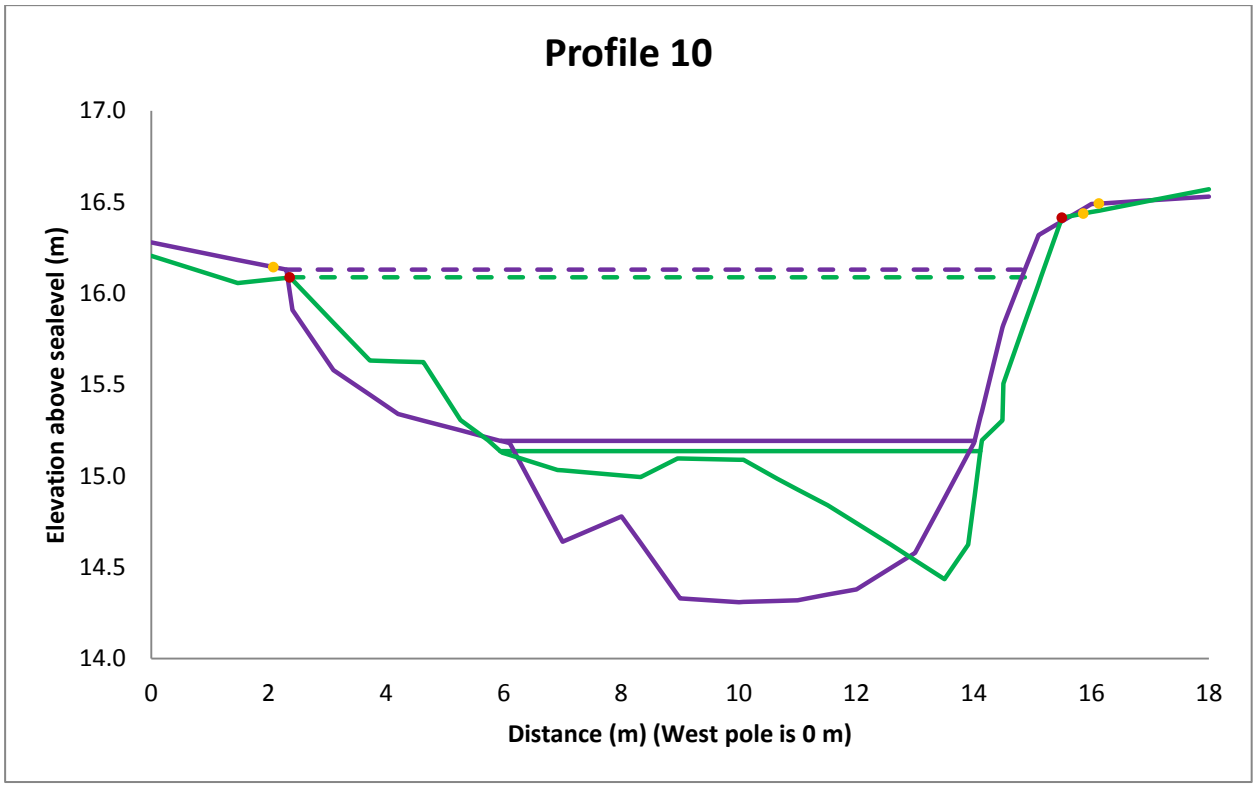
Profile 10
17.0
16.5
16.0
15.5
15.0
14.5
14.0
Elevation above sealevel (m)
0
2
4
6
8
10
12
14
16
18
Distance (m) (West pole is 0 m)

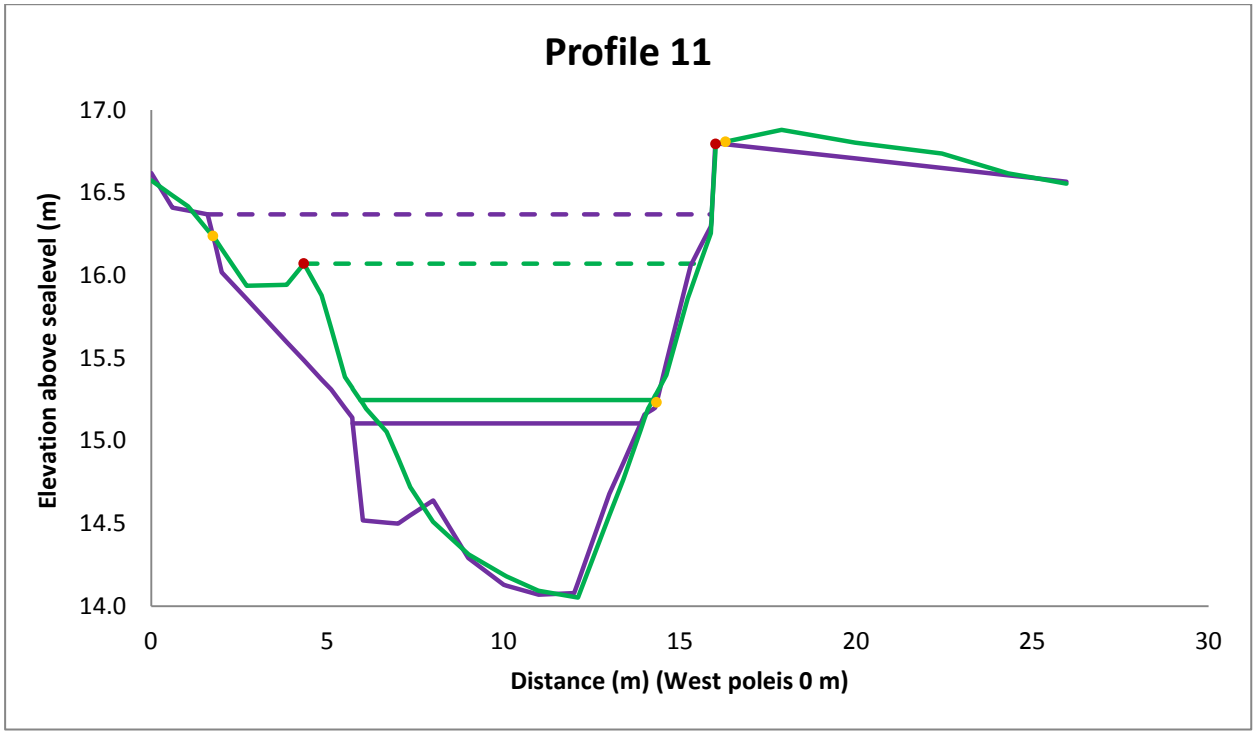
Profile 11
17.0
16.5
16.0
15.5
15.0
14.5
14.0
Elevation above sealevel (m)
0
5
10
15
20
25
30
Distance (m) (West poleis 0 m)

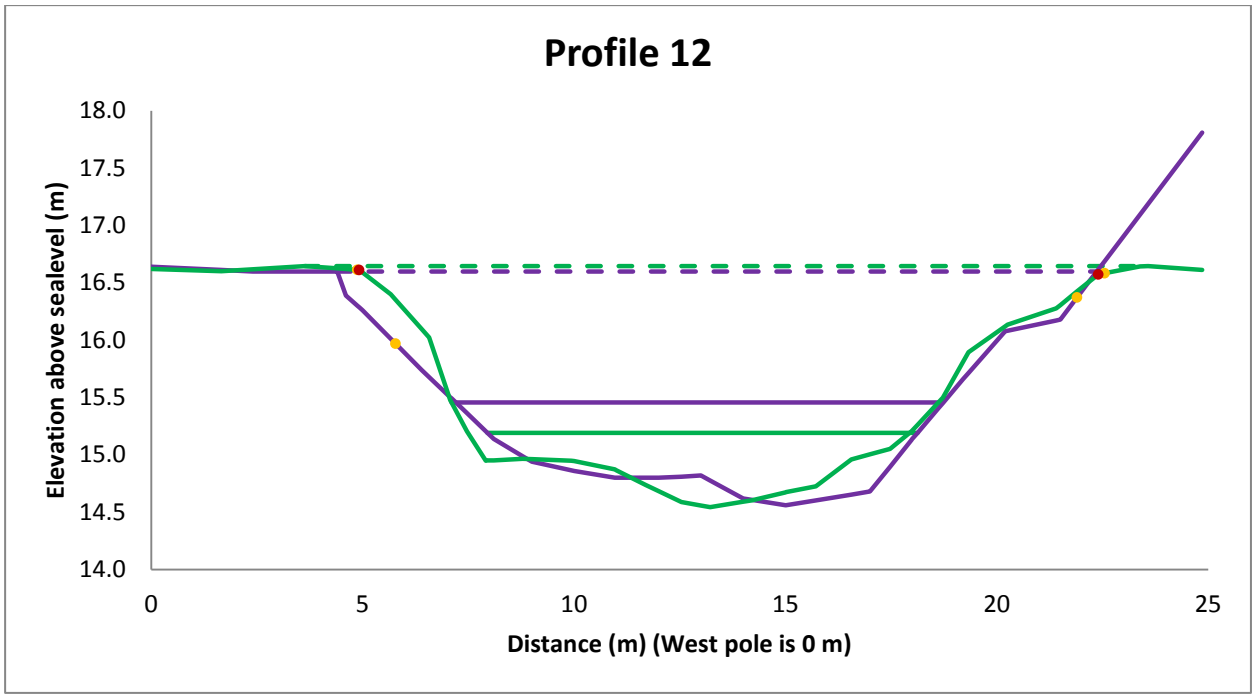
Profile 12
Elevation above sealevel (m)
18.0
17.5
17.0
16.5
16.0
15.5
15.0
14.5
14.0
0
5
10
15
20
25
Distance (m) (West pole is 0 m)

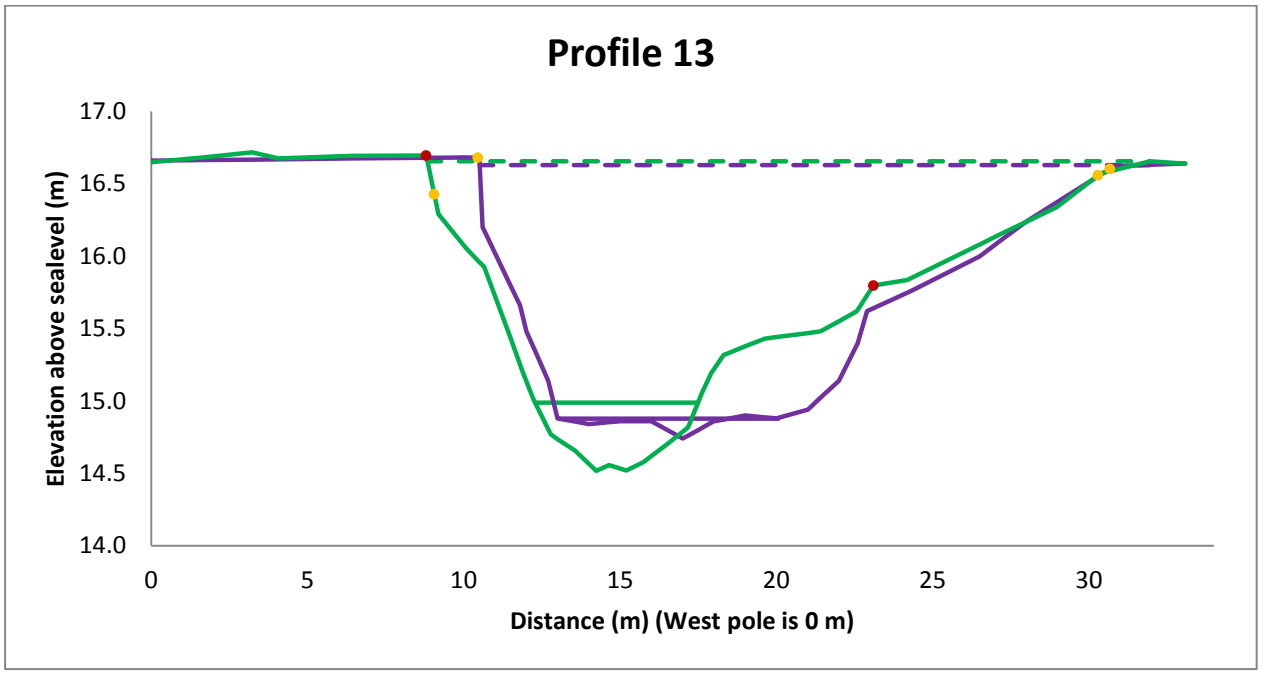
Profile 13
Elevation above sealevel (m)
17.0
16.5
16.0
15.5
15.0
14.5
14.0
0
5
10
15
20
25
30
Distance (m) (West pole is 0 m)

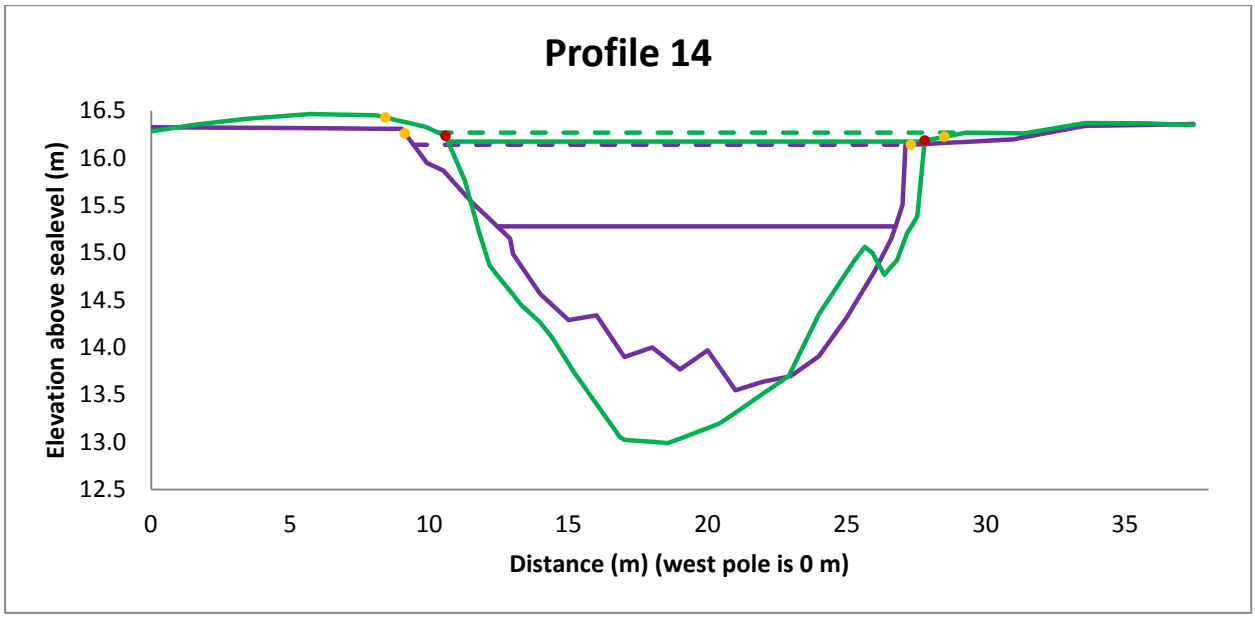
Profile 14
Elevation above sealevel (m)
16.5
16.0
15.5
15.0
14.5
14.0
13.5
13.0
12.5
0
5
10
15
20
25
30
35
Distance (m) (west pole is 0 m)

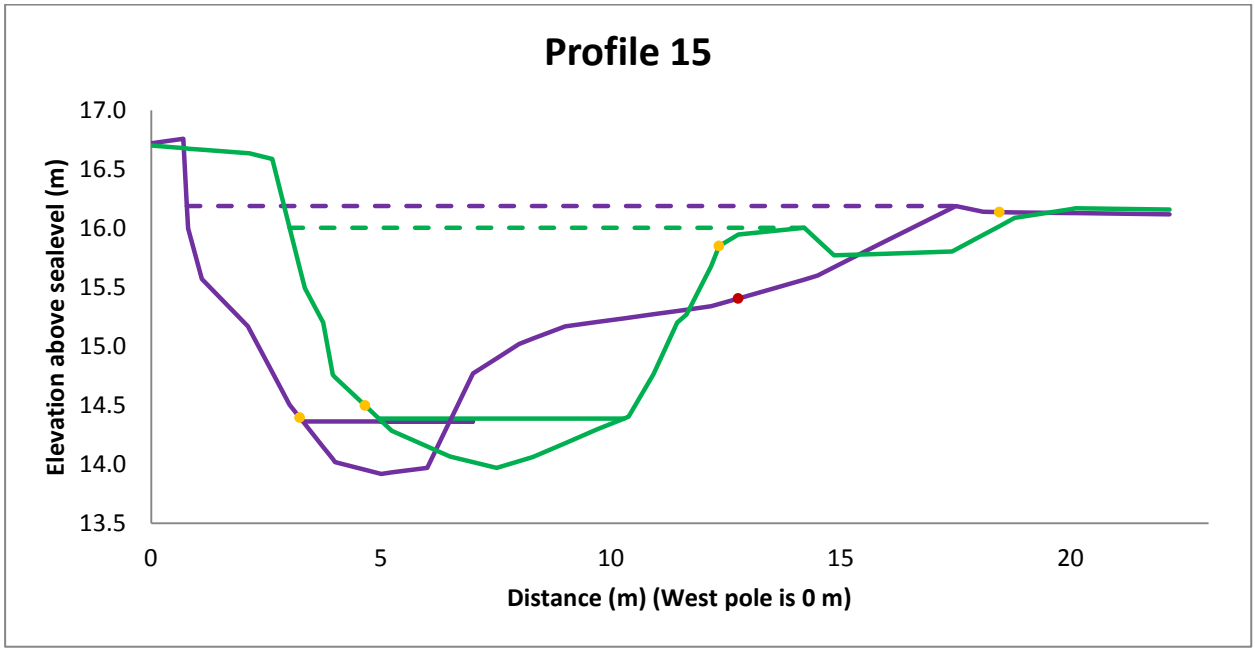
Profile 15
Elevation above sealevel (m)
17.0
16.5
16.0
15.5
15.0
14.5
14.0
13.5
0
5
10
15
20
Distance (m) (West pole is 0 m)

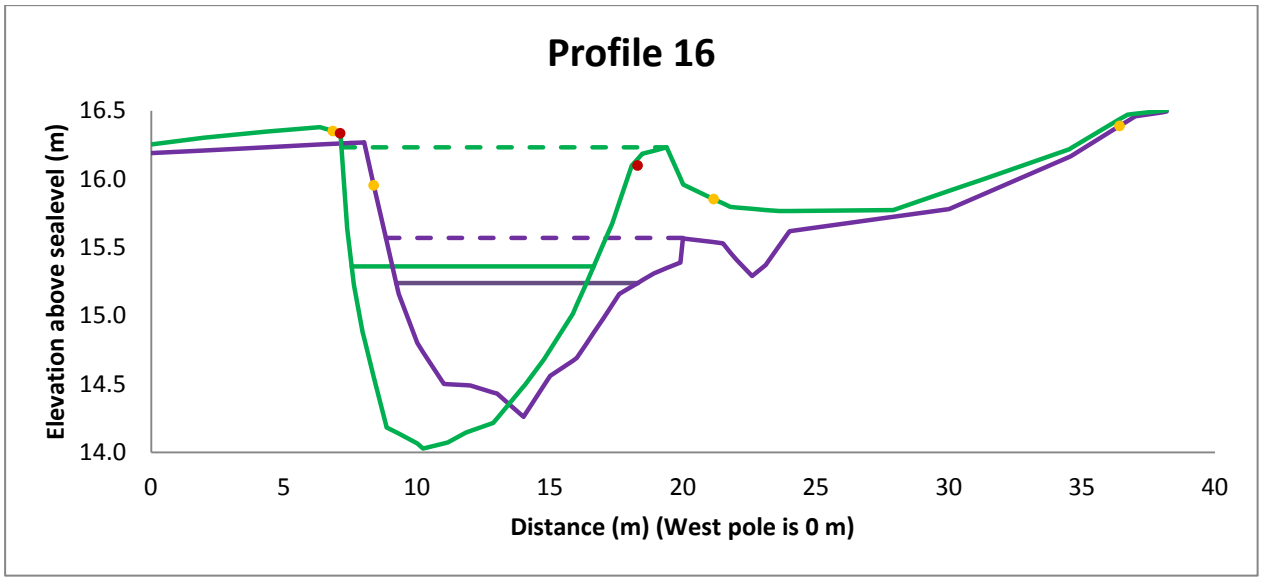
Profile 16
Elevation above sealevel (m)
16.5
16.0
15.5
15.0
14.5
14.0
0
5
10
15
20
25
30
35
40
Distance (m) (West pole is 0 m)

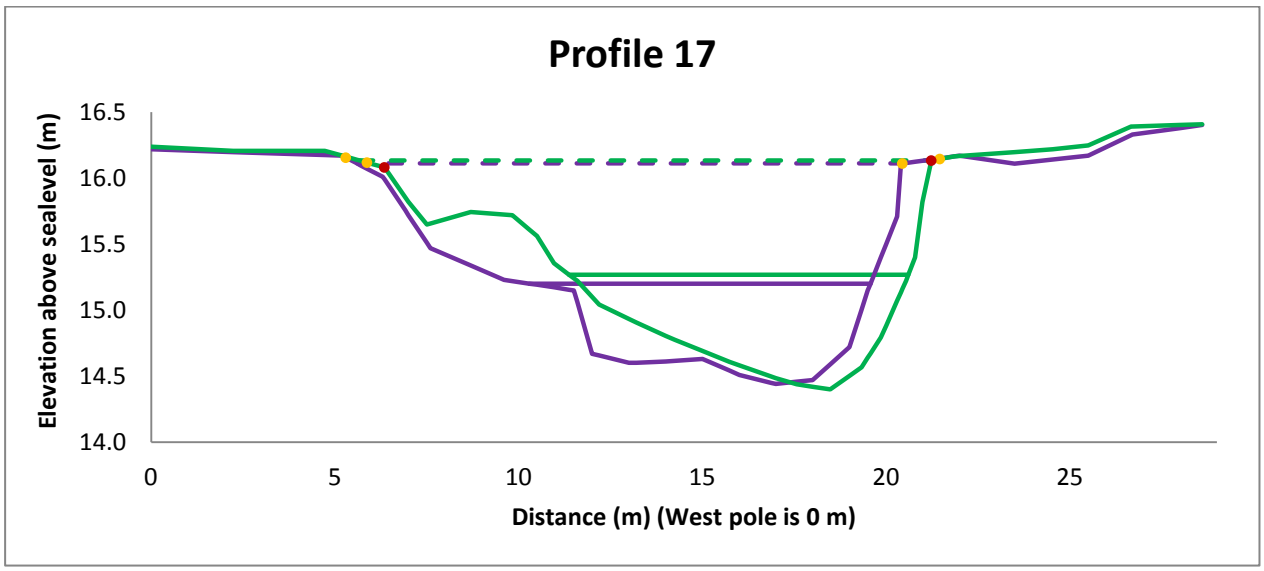
Profile 17
Elevation above sealevel (m)
16.5
16.0
15.5
15.0
14.5
14.0
0
5
10
15
20
25
Distance (m) (West pole is 0 m)

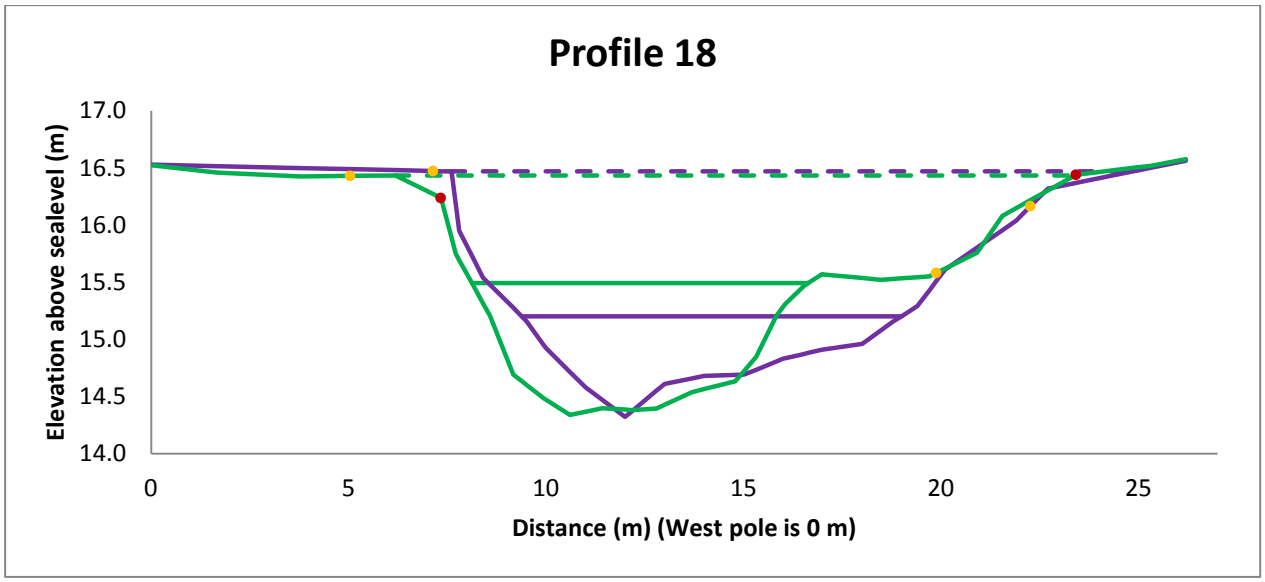
Profile 18
Elevation above sealevel (m)
17.0
16.5
16.0
15.5
15.0
14.5
14.0
0
5
10
15
20
25
Distance (m) (West pole is 0 m)

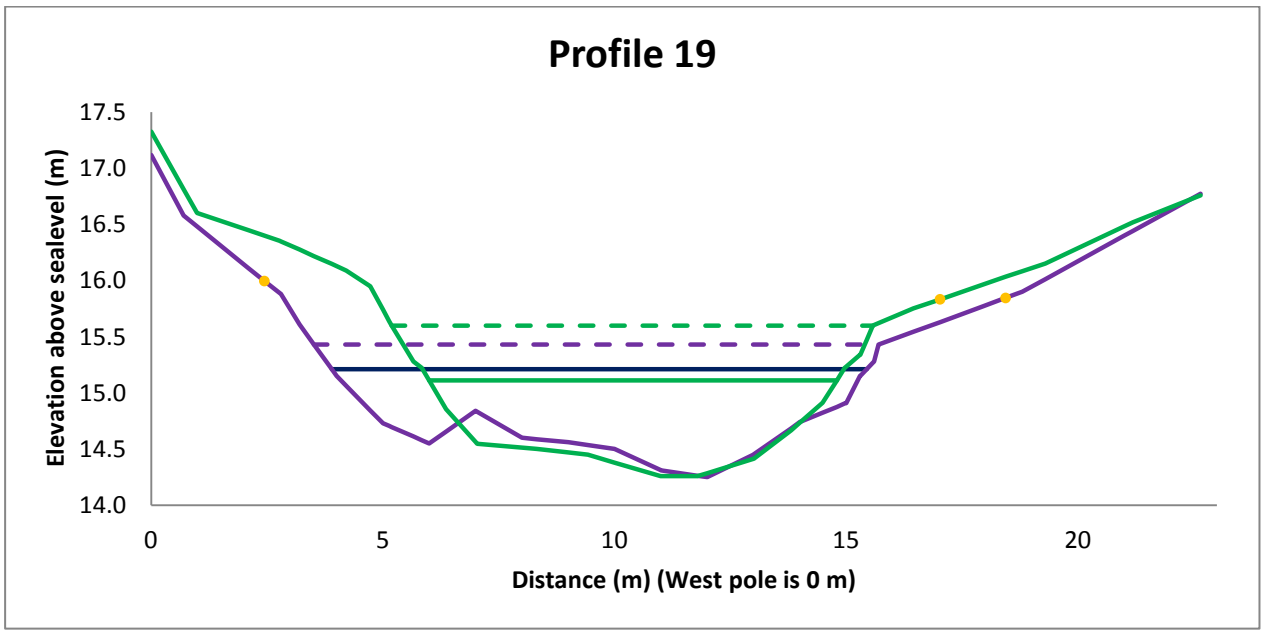
Profile 19
Elevation above sealevel (m)
17.5
17.0
16.5
16.0
15.5
15.0
14.5
14.0
0
5
10
15
20
Distance (m) (West pole is 0 m)

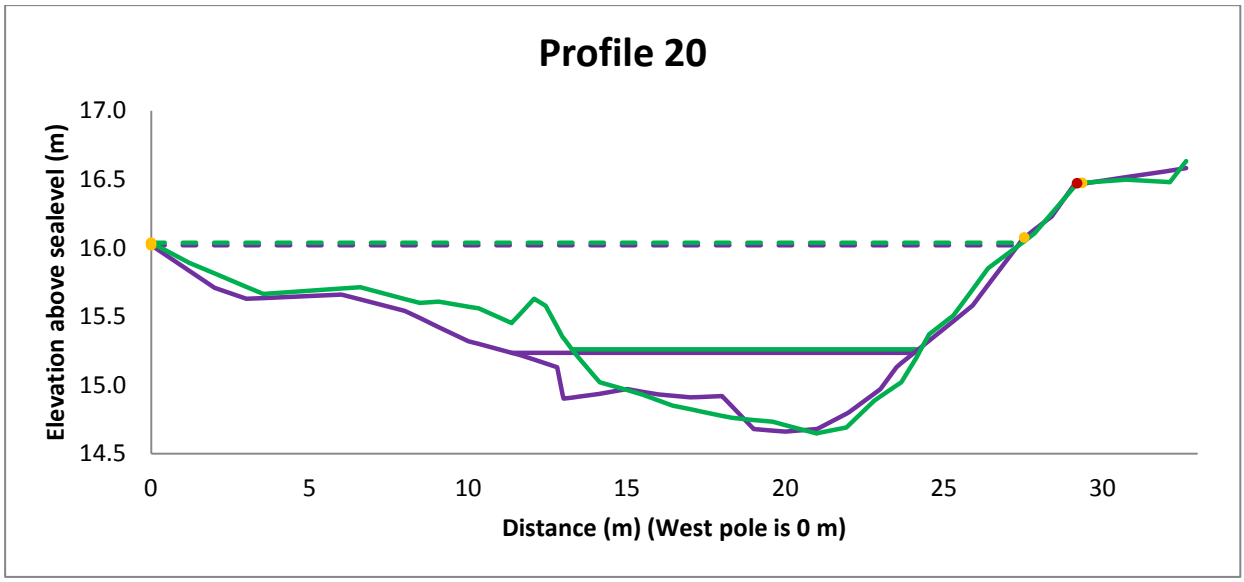
Profile 20
Elevation above sealevel (m)
17.0
16.5
16.0
15.5
15.0
14.5
0
5
10
15
20
25
30
Distance (m) (West pole is 0 m)

Appendix 4: Bank lines map

The bank lines map is split up into ten pages.

See next pages!

The digital version can be found on CD2.

Bank lines Groenlose Slinge 2007 - 2011
Page 1

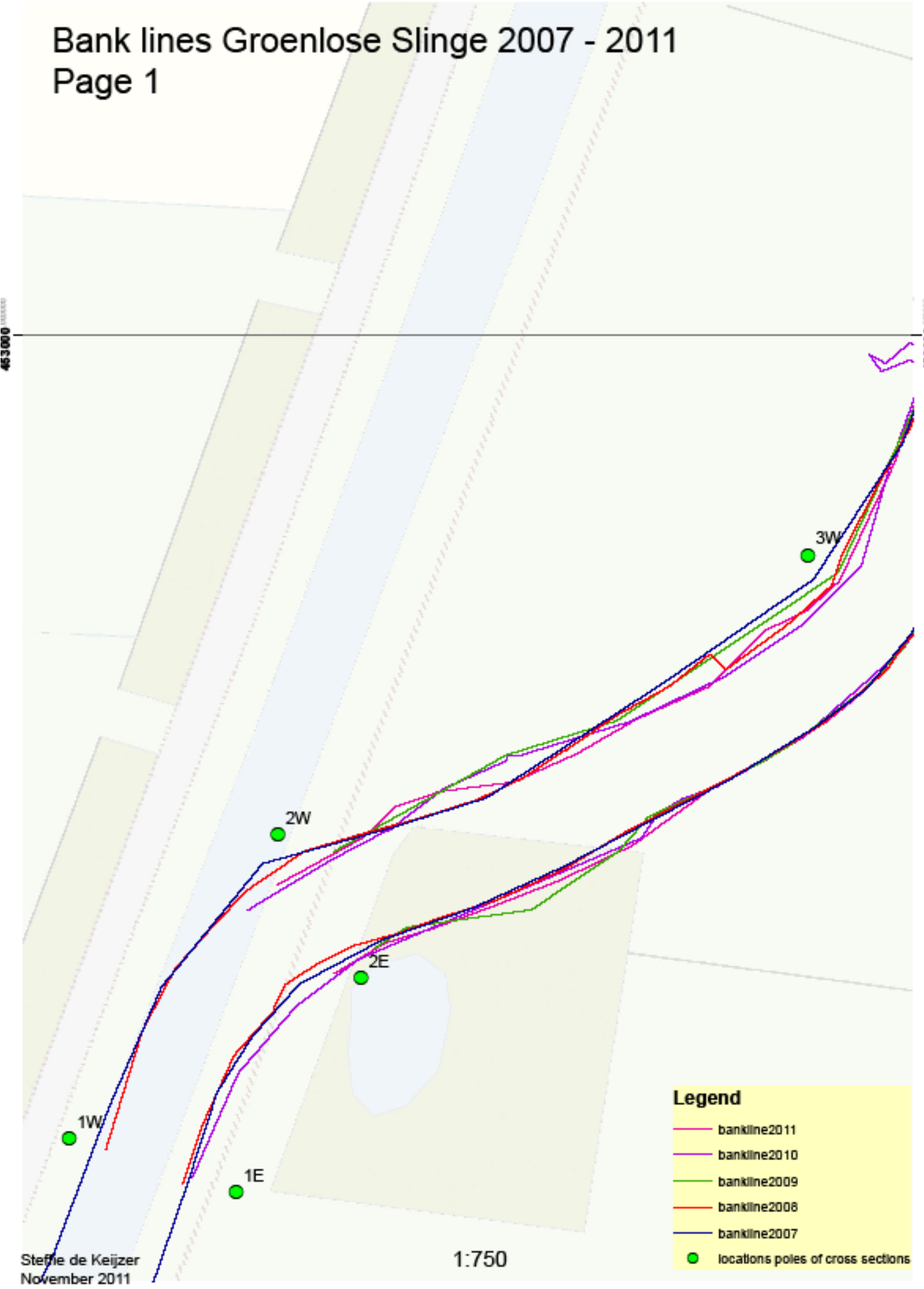

Steffie de Keijzer
November 2011

Bank lines Groenlose Slinge
2007 - 2011
Page 2

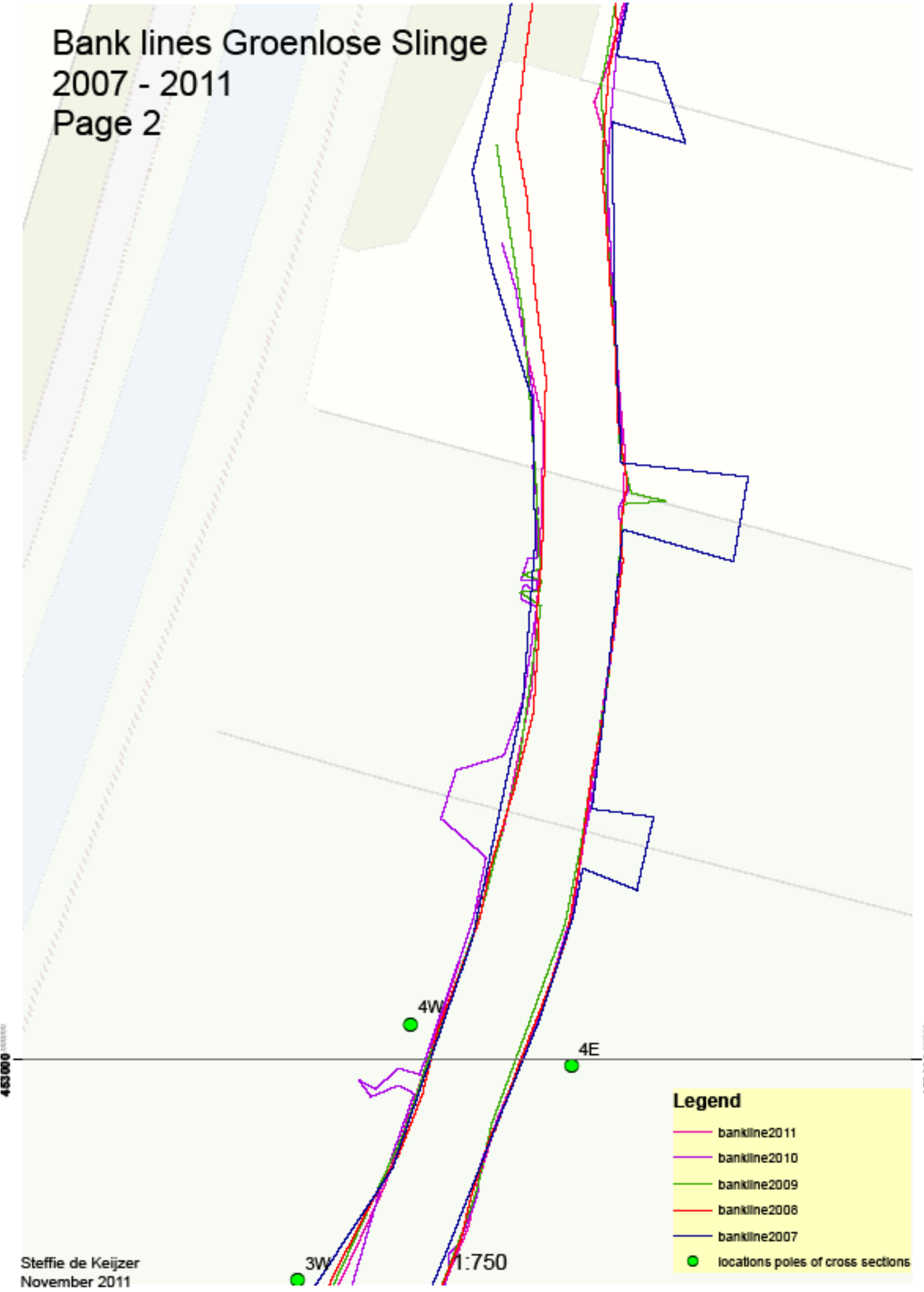

Steffie de Keijzer
November 2011

Bank lines Groenlose Slinge
2007 - 2011
Page 3

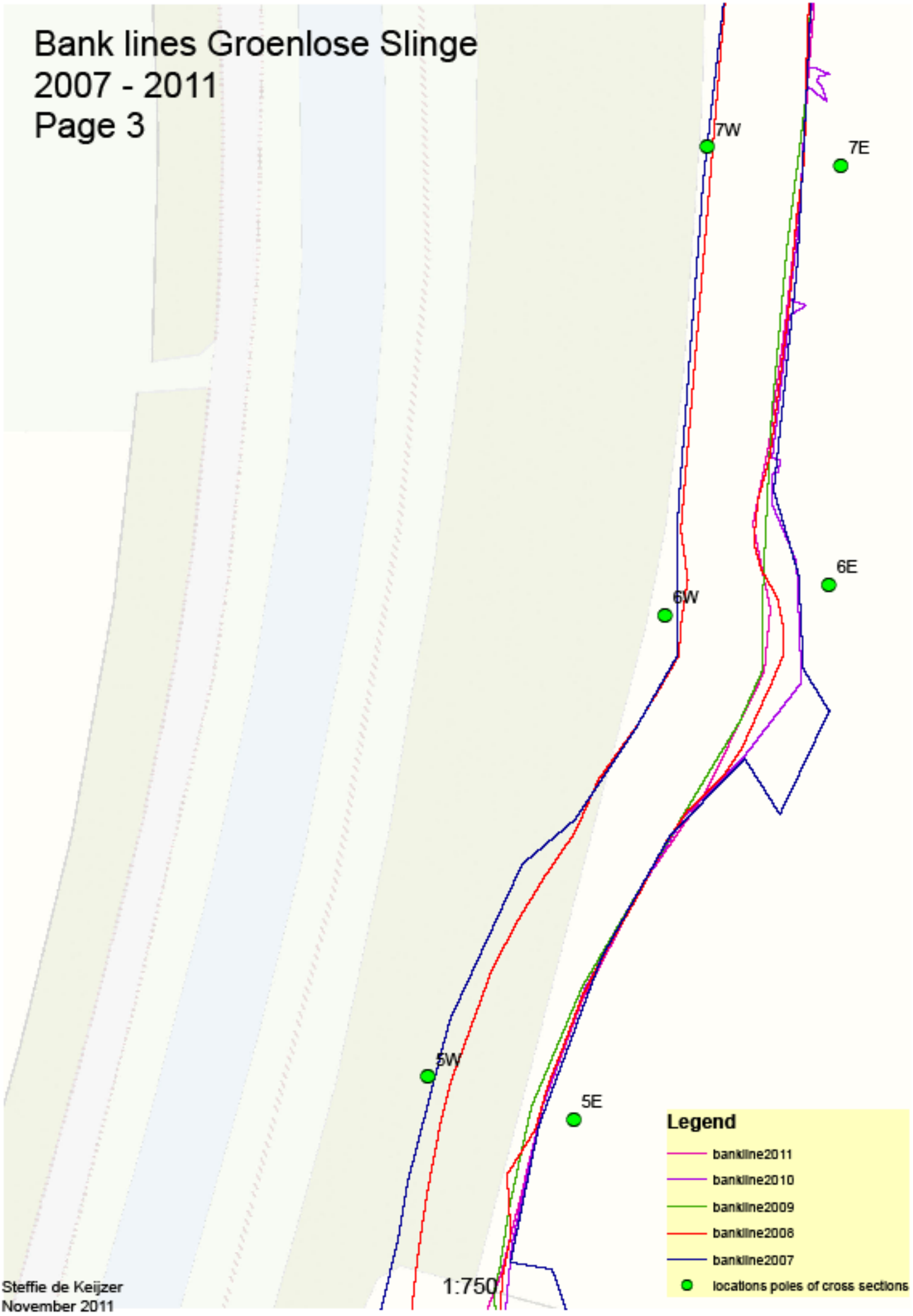

Steffie de Keijzer
November 2011

Bank lines Groenlose Slinge 2007 - 2011
Page 4

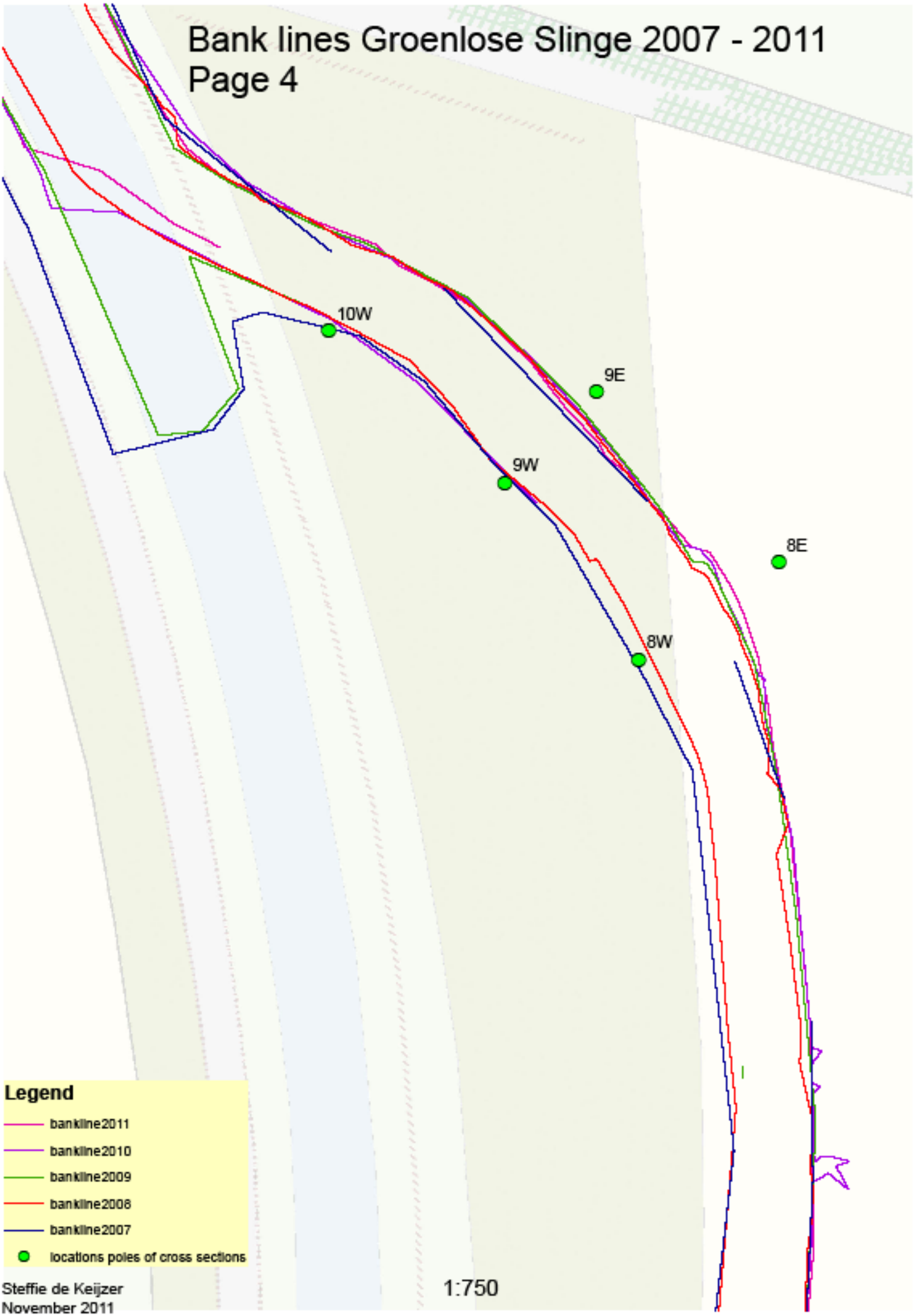

Steffie de Keijzer
November 2011

Bank lines Groenlose Slinge 2007 - 2011
Page 5

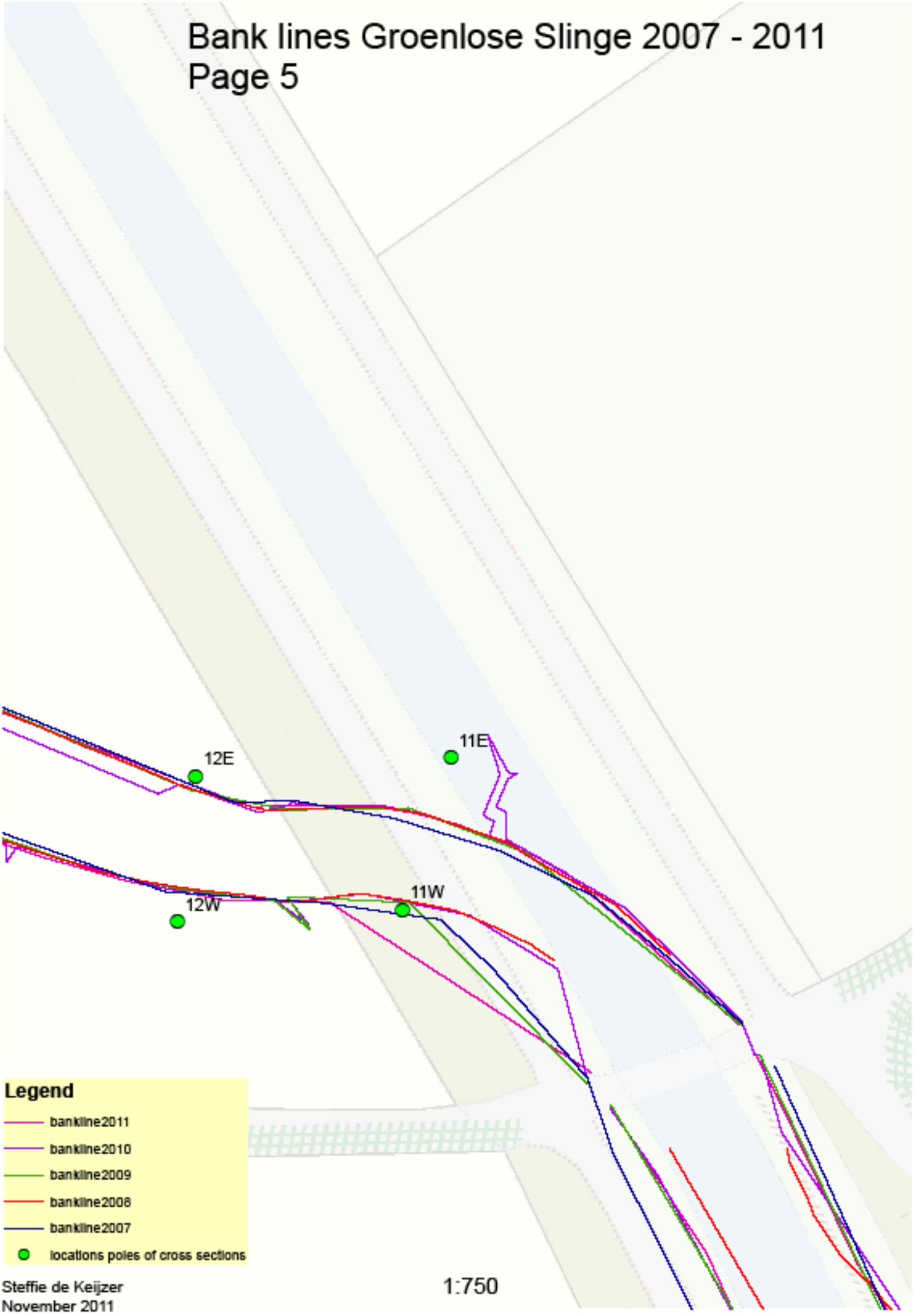

Steffie de Keijzer
November 2011

1:750

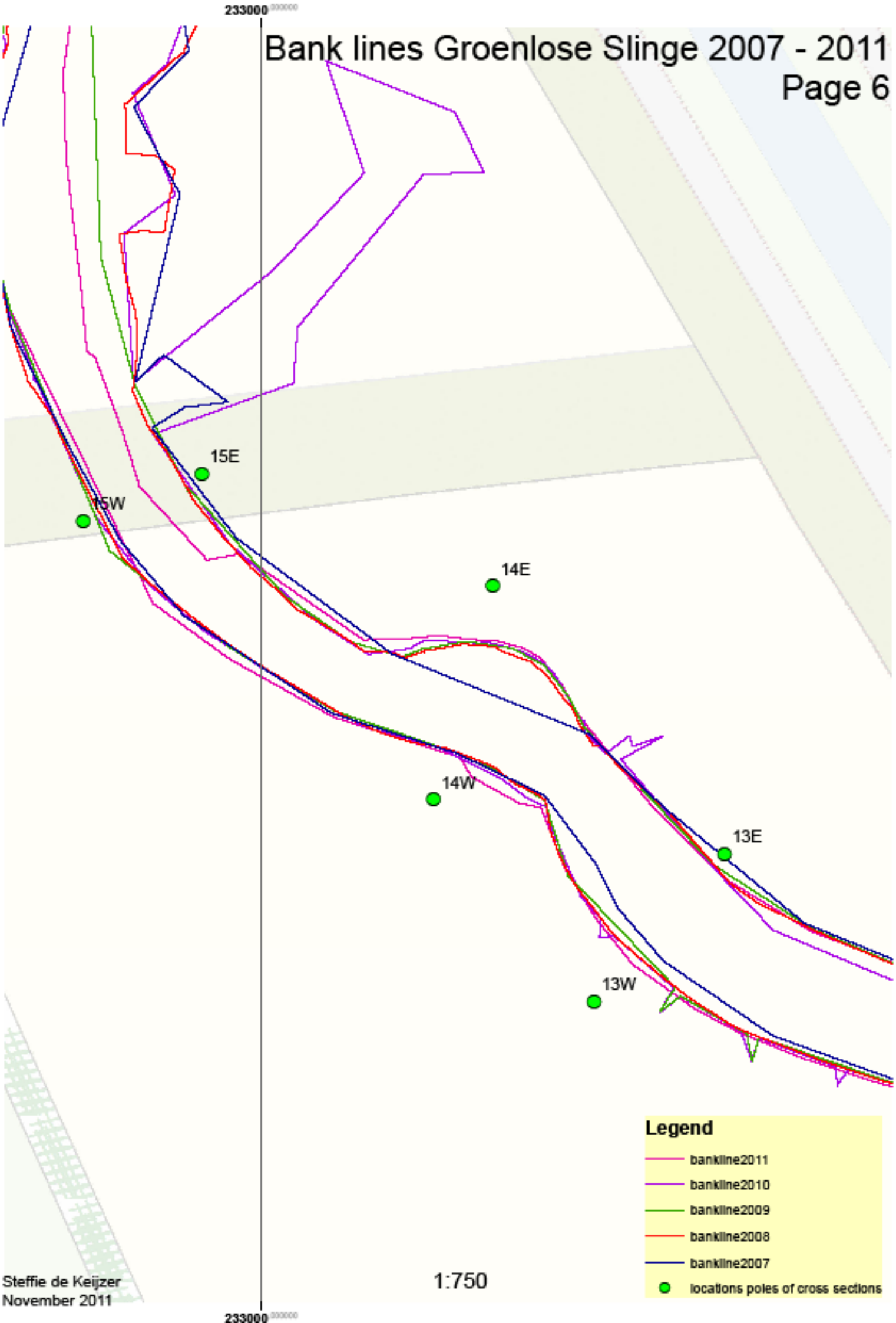
233000
Bank lines Groenlose Slinge 2007 - 2011
Page 6
15E
15W
14E
14W
13E
13W
Legend
bankline2011
bankline2010
bankline2009
bankline2008
bankline2007
locations poles of cross sections
Steffie de Keijzer
November 2011
1:750
233000

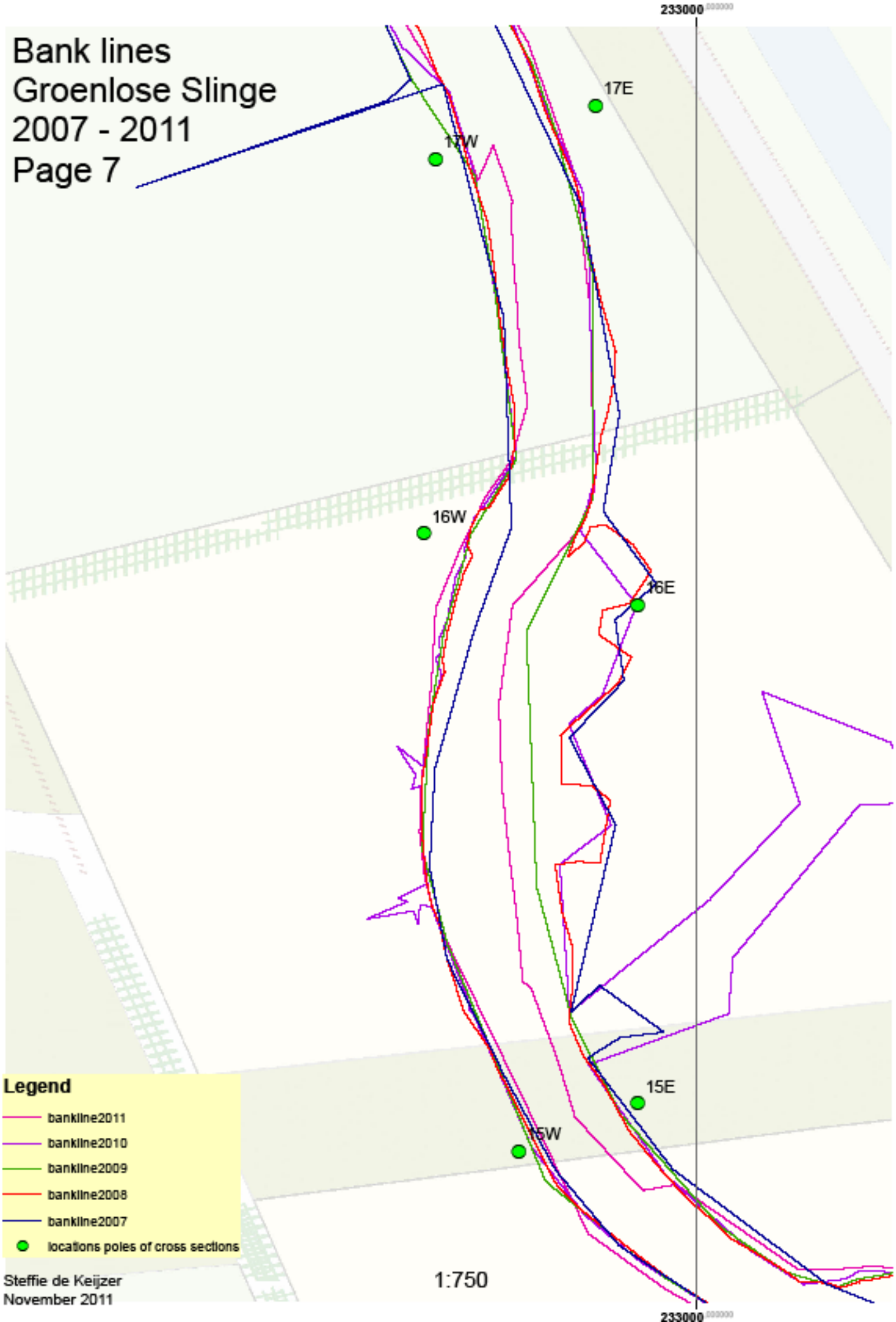
Bank lines
Groenlose Slinge
2007 - 2011
Page 7
233000
17E
17W
16W
16E
15E
15W
233000
Legend
bankline2011
bankline2010
bankline2009
bankline2008
bankline2007
locations poles of cross sections
Steffie de Keijzer
November 2011
1:750

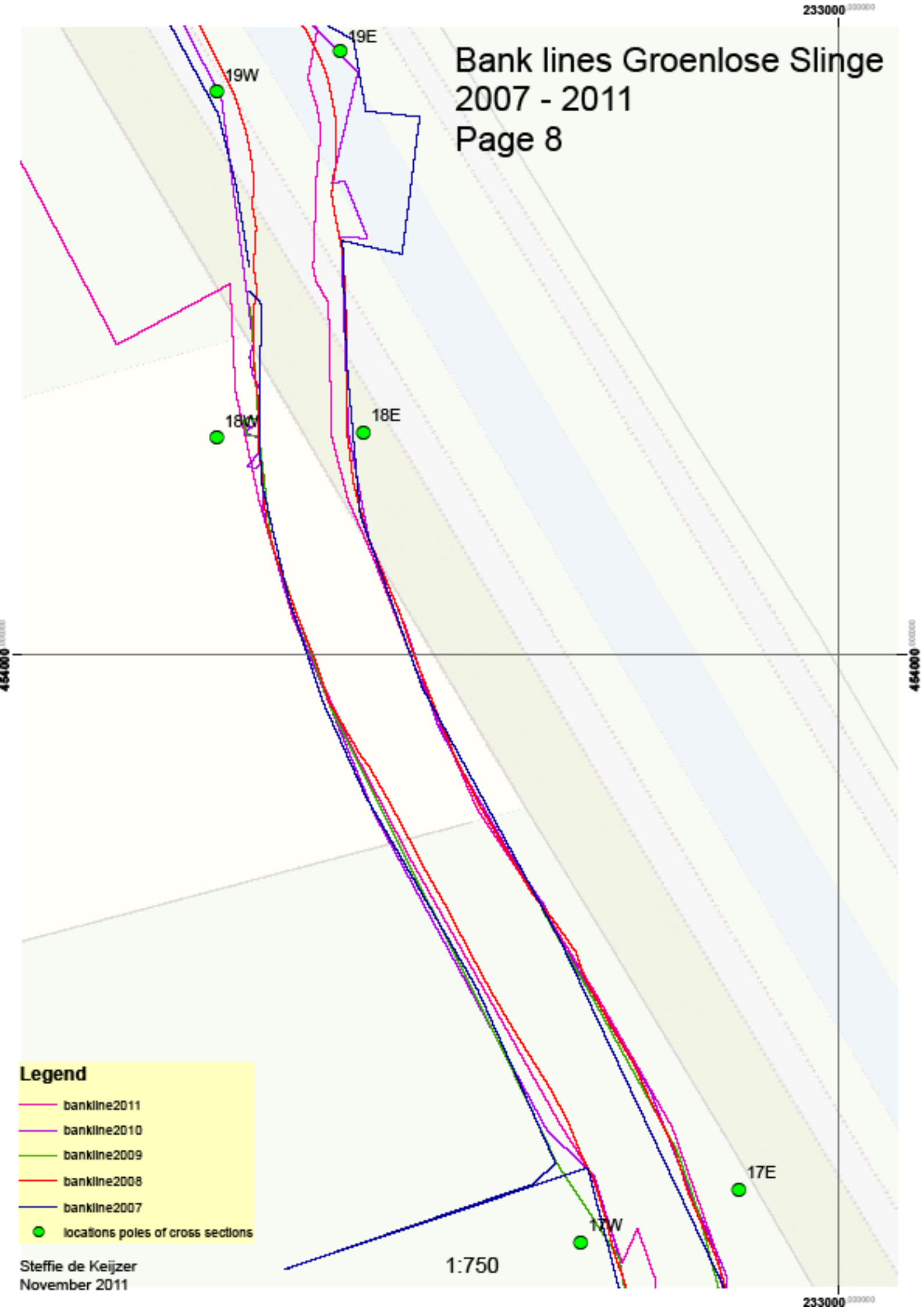
Bank lines Groenlose Slinge
2007 - 2011
Page 8
19E
19W
18E
18W
17E
17W
233000
454000
Legend
bankline2011
bankline2010
bankline2009
bankline2008
bankline2007
locations poles of cross sections
Steffie de Keijzer
November 2011
1:750

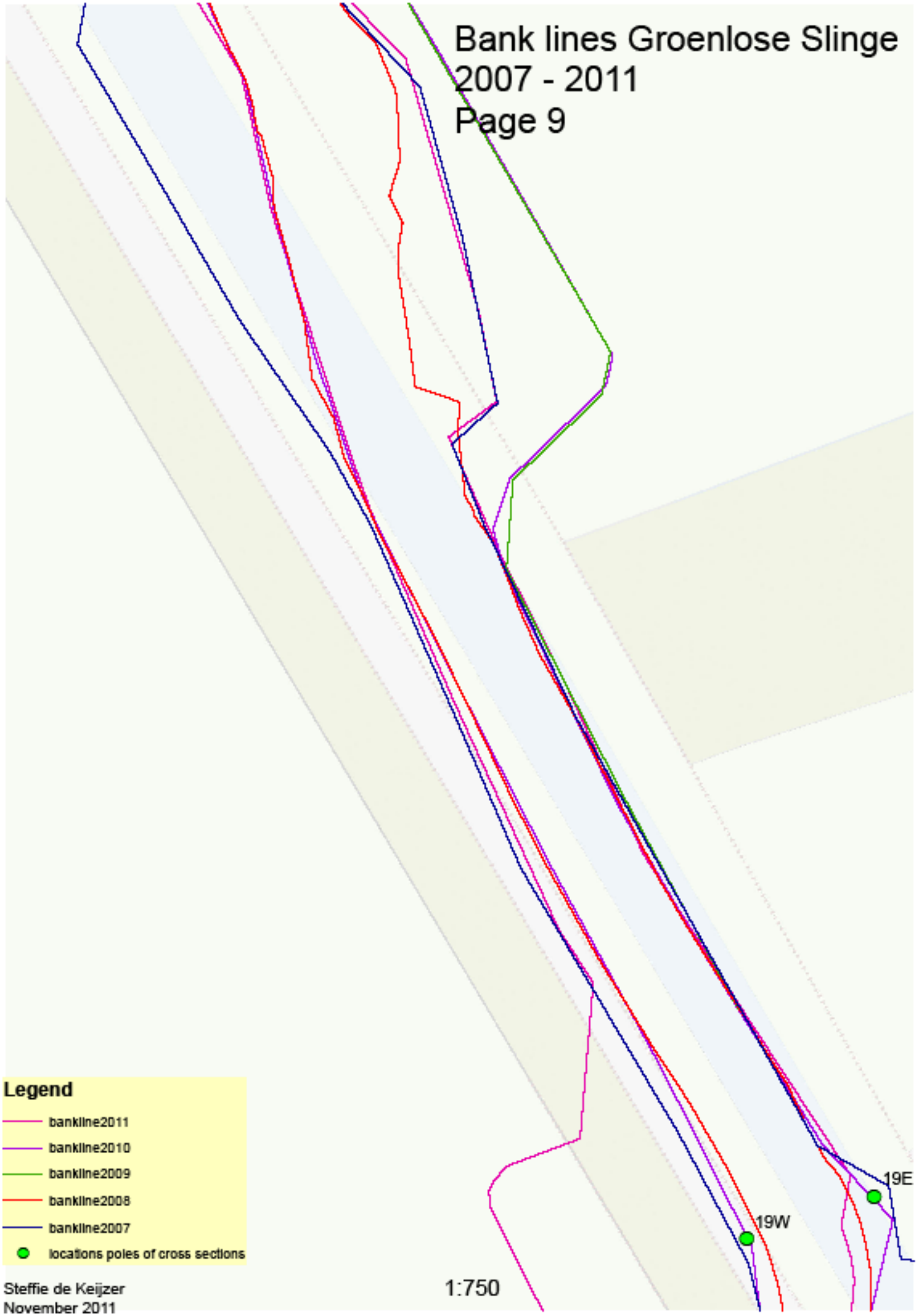
Bank lines Groenlose Slinge
2007 - 2011
Page 9
Legend
bankline2011
bankline2010
bankline2009
bankline2008
bankline2007
locations poles of cross sections
19E
19W
1:750
Steffie de Keijzer
November 2011

Bank lines Groenlose Slinge 2007 - 2011
Page 10

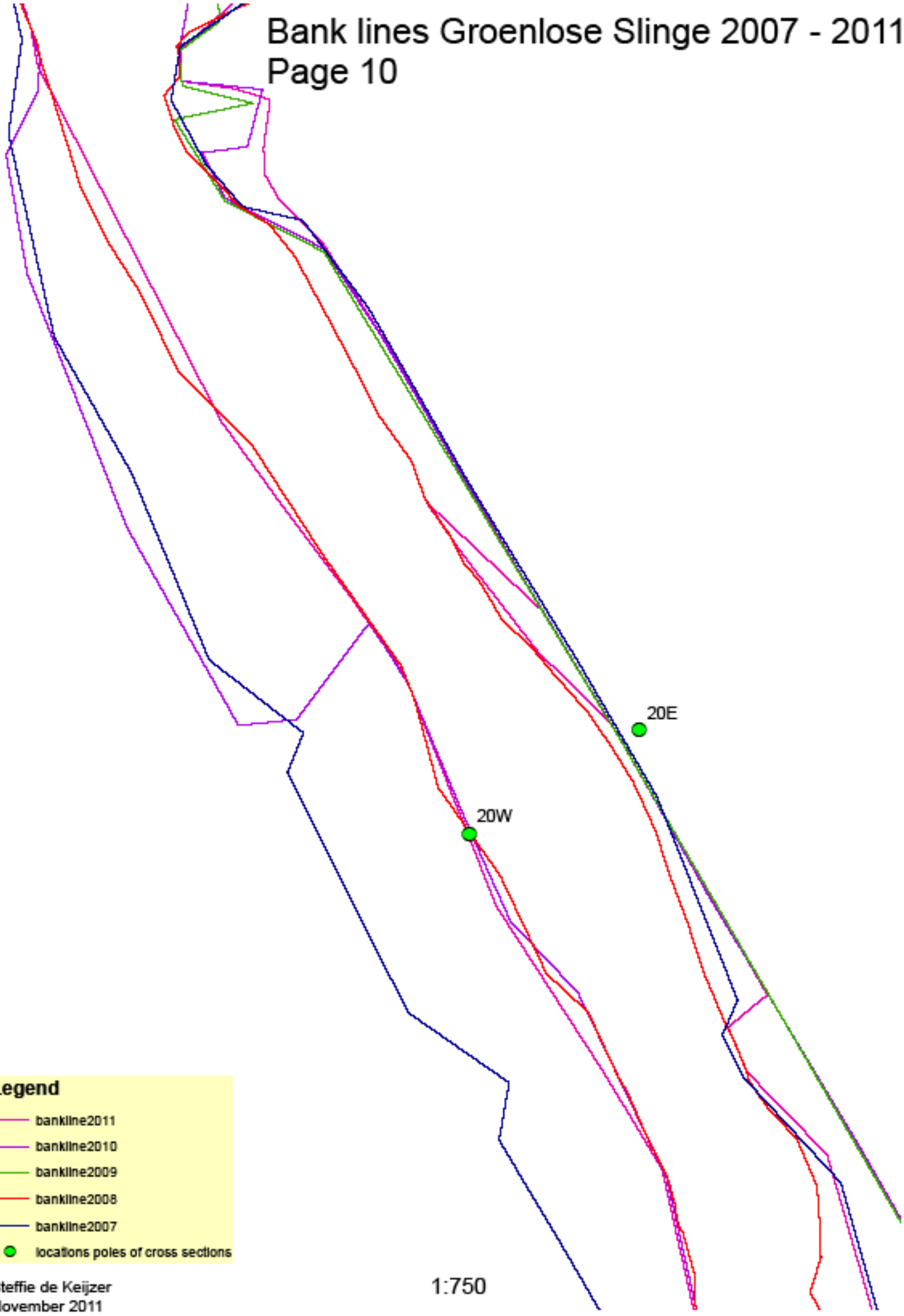

Steffie de Keijzer
November 2011

1:750

Appendix 5: Waterlines map

The waterlines map is split up into ten pages.

See next pages!

The digital version can be found on CD2.

Waterlines Groenlose Slinge 2007 - 2011
Page 1

Steffie de Keijzer
November 2011

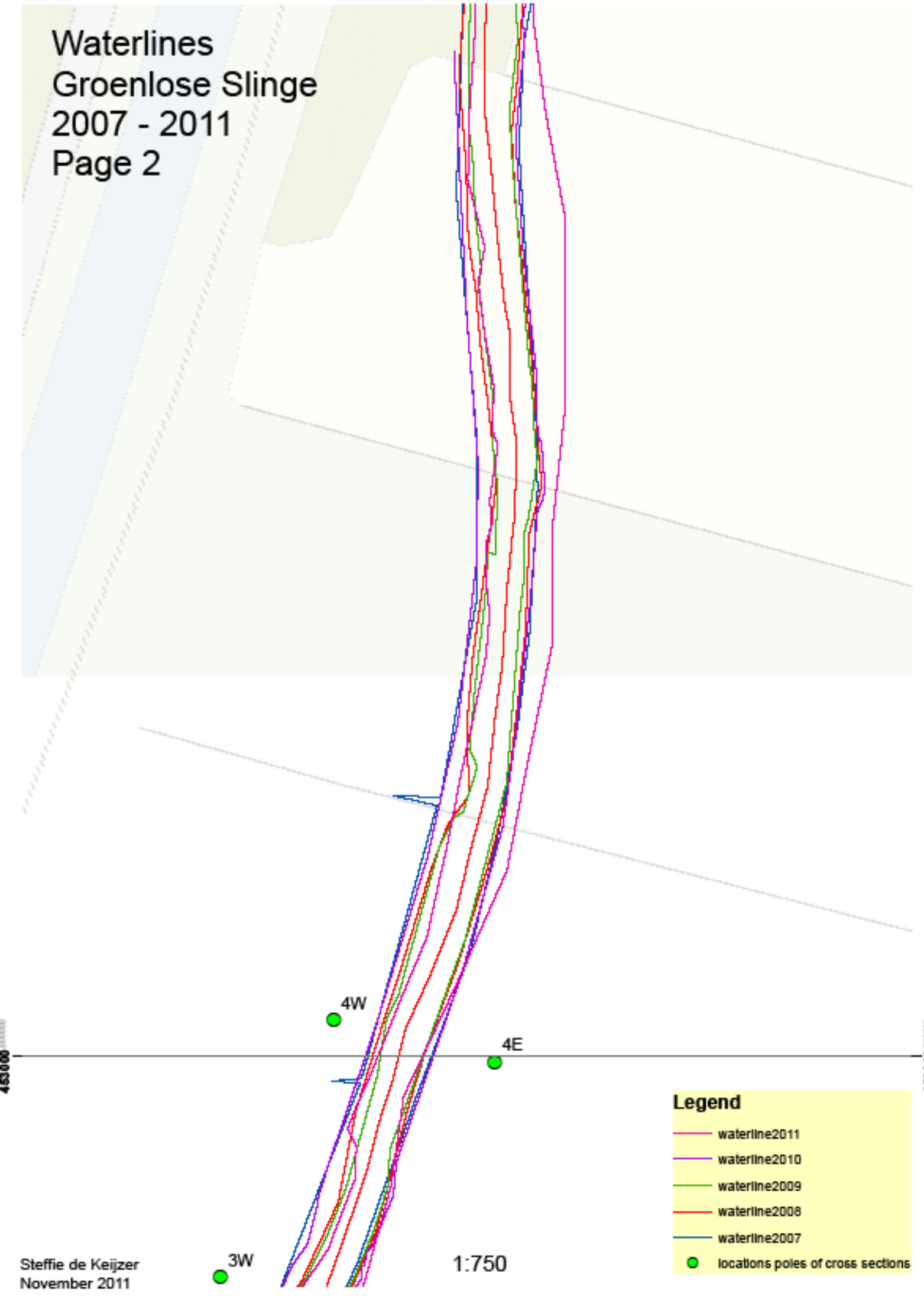
Waterlines
Groenlose Slinge
2007 - 2011
Page 2
4W
4E
3W
453000
453000
Legend
waterline2011
waterline2010
waterline2009
waterline2008
waterline2007
locations poles of cross sections
Steffie de Keijzer
November 2011
1:750

Waterlines Groenlose Slinge 2007 - 2011
Page 3

Steffie de Keijzer
November 2011

Waterlines Groenlose Slinge 2007 - 2011
Page 4

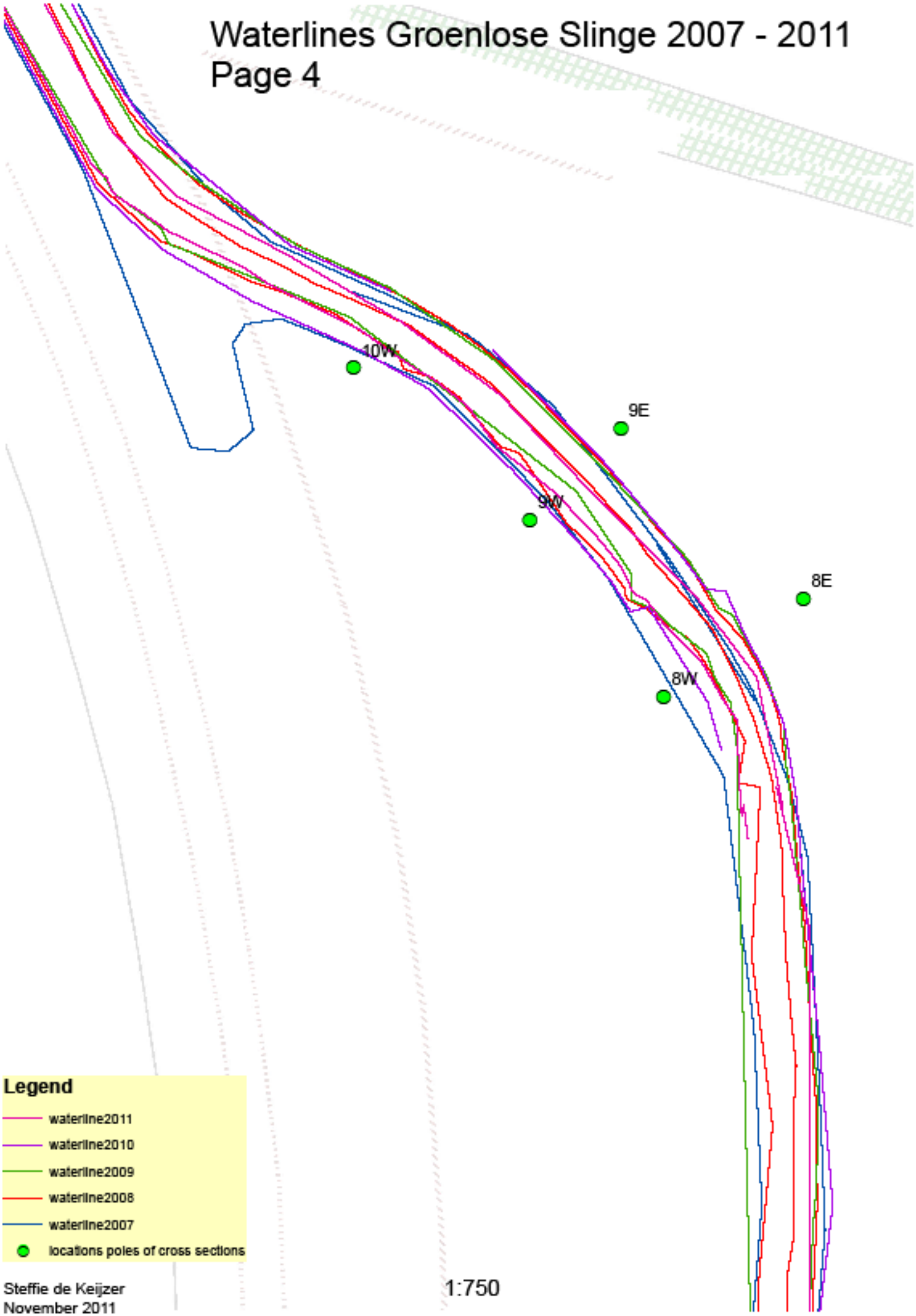

Steffie de Keijzer
November 2011

1:750

Waterlines Groenlose Slinge 2007 - 2011
Page 5

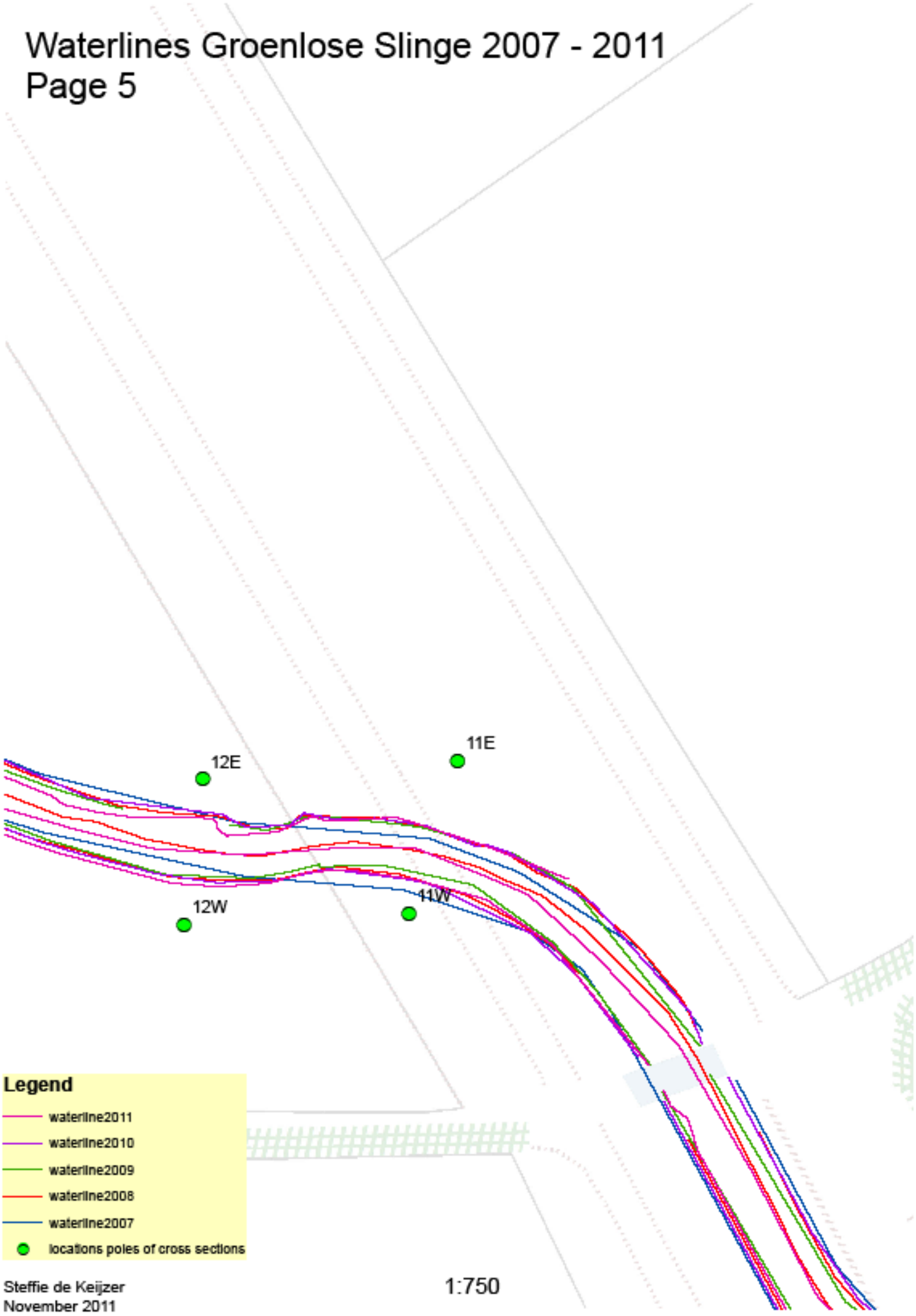

Steffie de Keijzer
November 2011

1:750

Waterlines Groenlose Slinge 2007 - 2011
Page 6

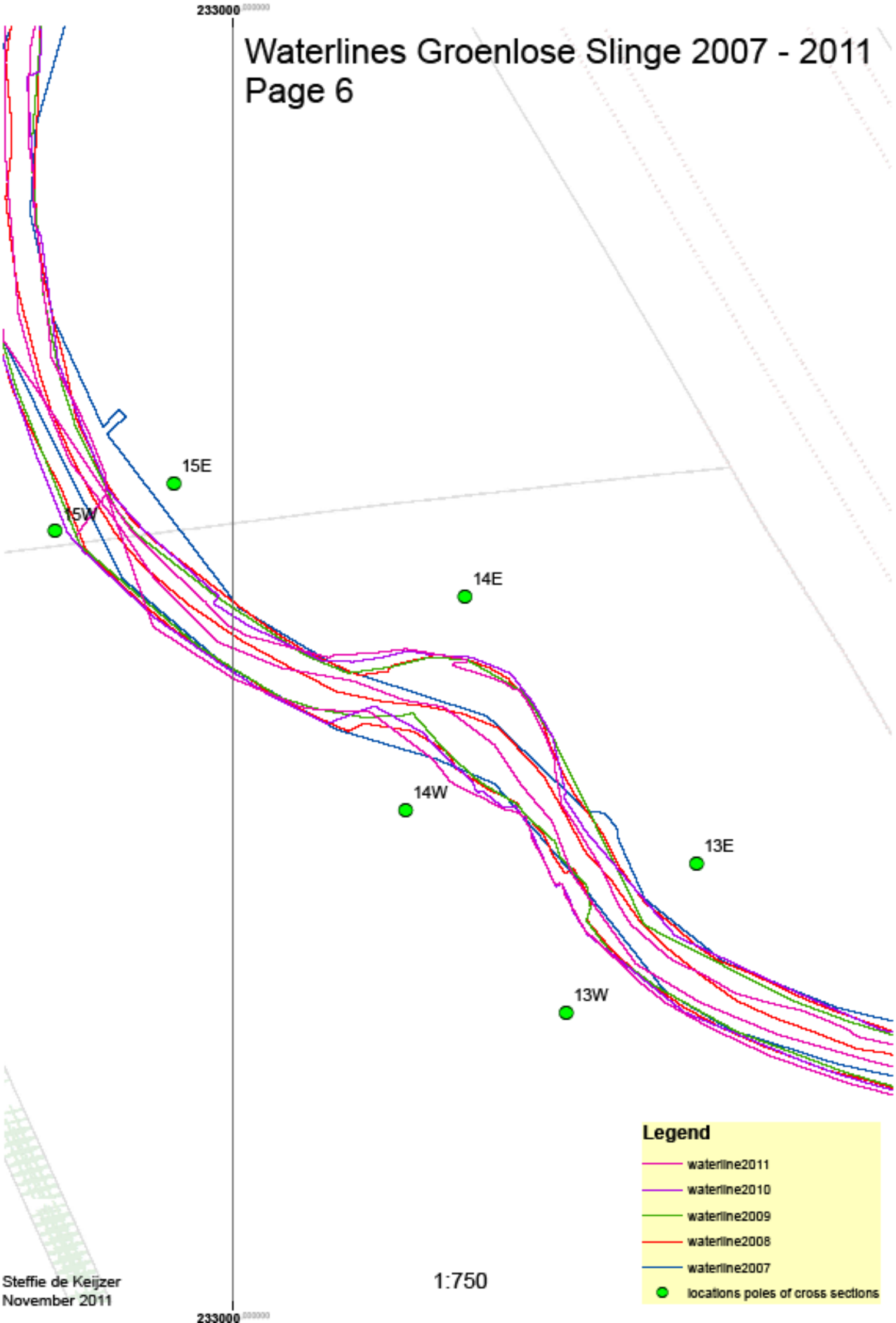

Steffie de Keijzer
November 2011

Waterlines Groenlose Slinge
2007 - 2011
Page 7

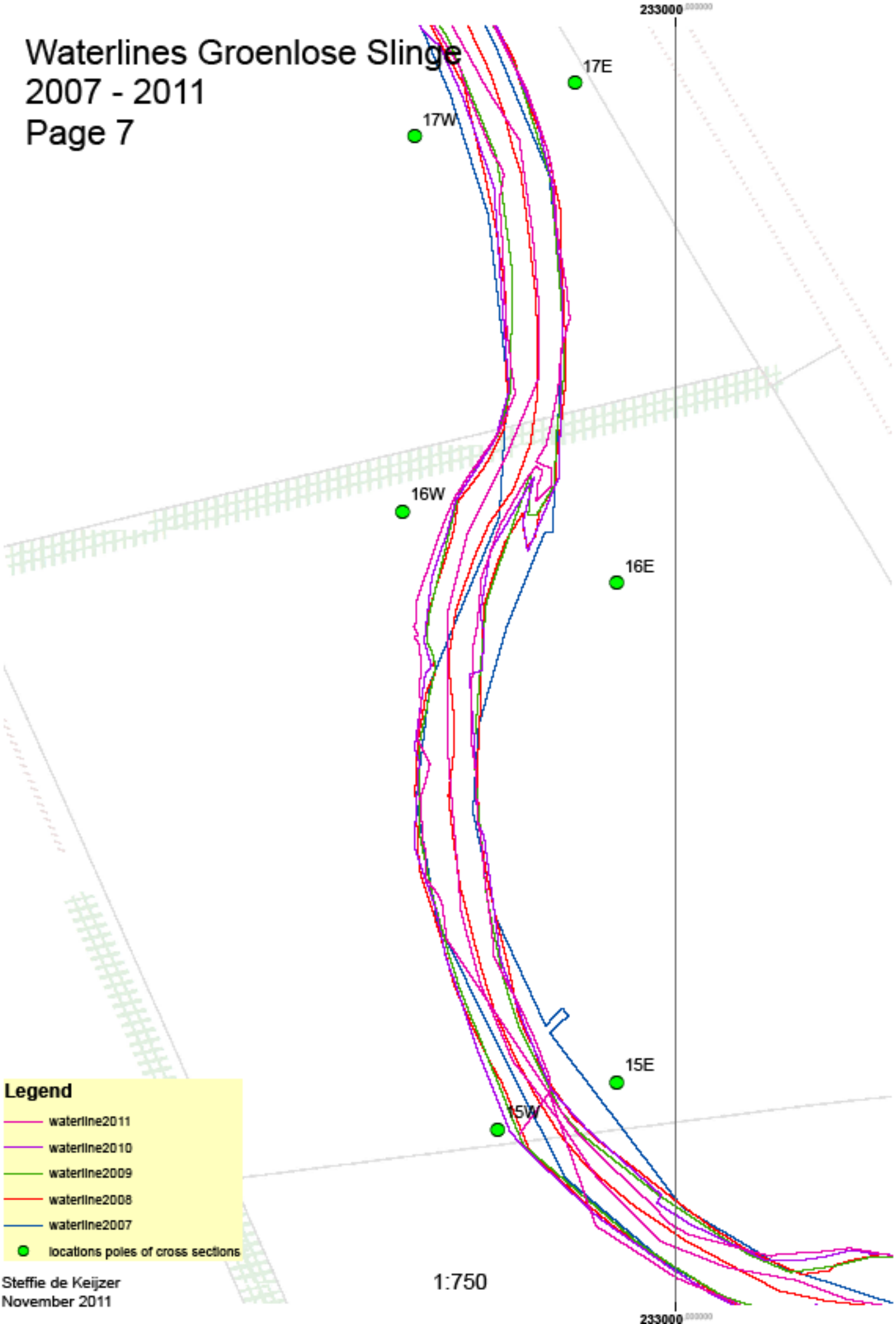

Legend

- waterline2011
- waterline2010
- waterline2009
- waterline2008
- waterline2007
- locations poles of cross sections

Steffie de Keijzer
November 2011

1:750

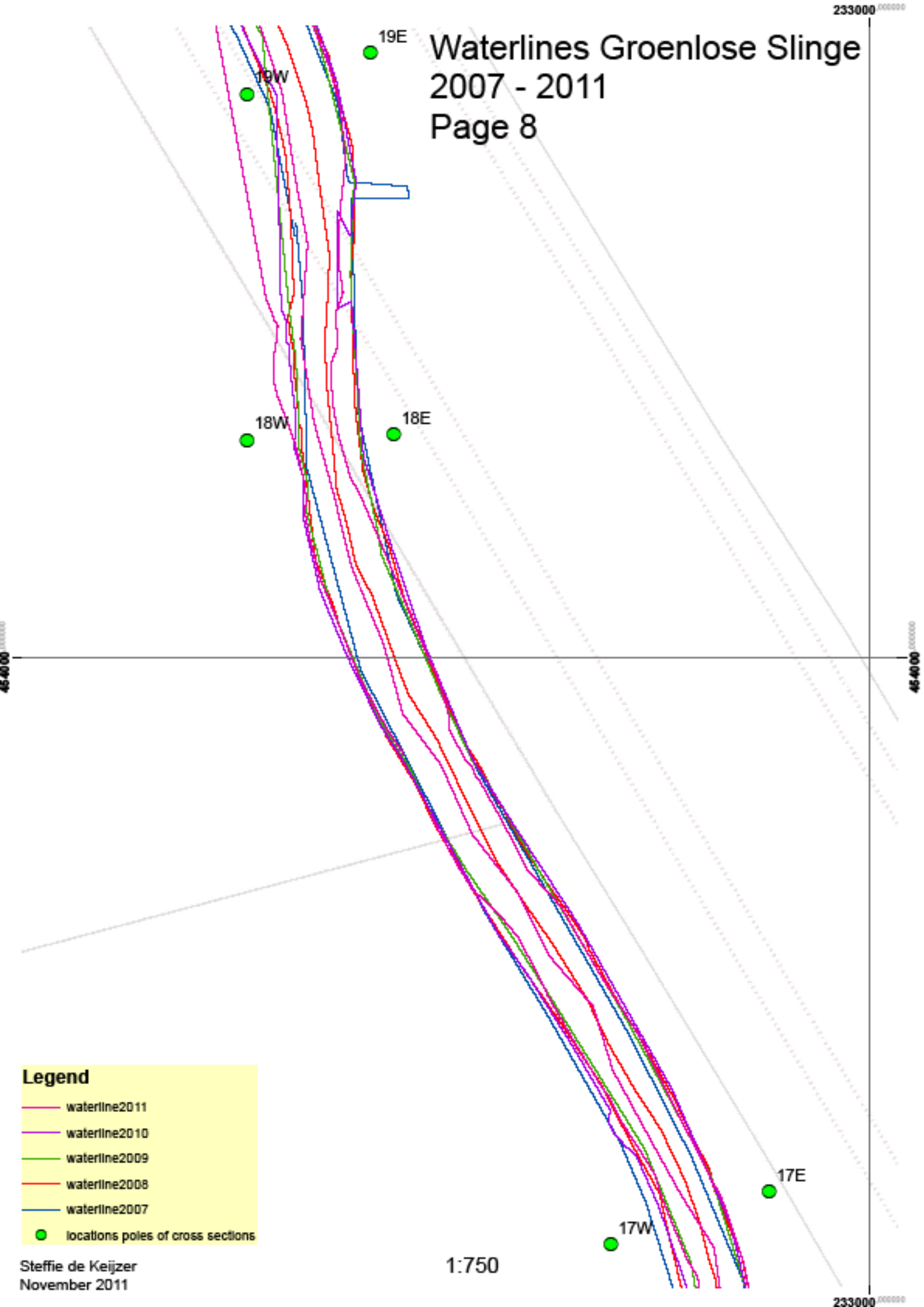
Waterlines Groenlose Slinge
2007 - 2011
Page 8
19E
19W
18E
18W
17E
17W
233000
454000
Legend
waterline2011
waterline2010
waterline2009
waterline2008
waterline2007
locations poles of cross sections
Steffie de Keijzer
November 2011
1:750

Waterlines Groenlose Slinge
2007 - 2011
Page 9

Legend

- waterline2011
- waterline2010
- waterline2009
- waterline2008
- waterline2007
- locations poles of cross sections

Steffie de Keijzer
November 2011

1:750

Waterlines Groenlose Slinge 2007 - 2011
Page 10

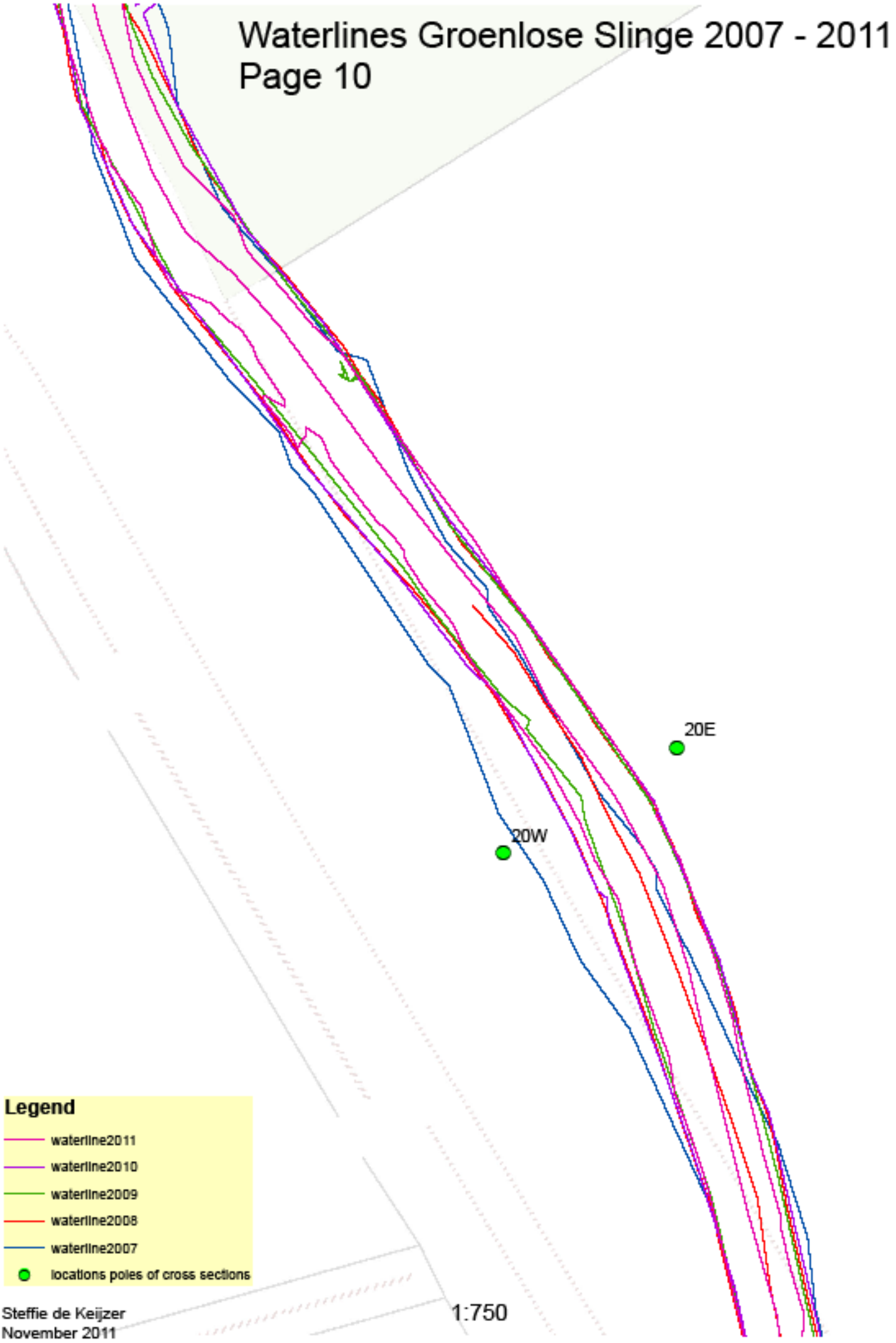

Steffie de Keijzer
November 2011

1:750

Appendix 6: Erosion - Deposition map 2011

The erosion – deposition map is split up into ten pages.

See next pages!

The digital version can be found on CD2.

Erosion - Deposition map 2011
Page1

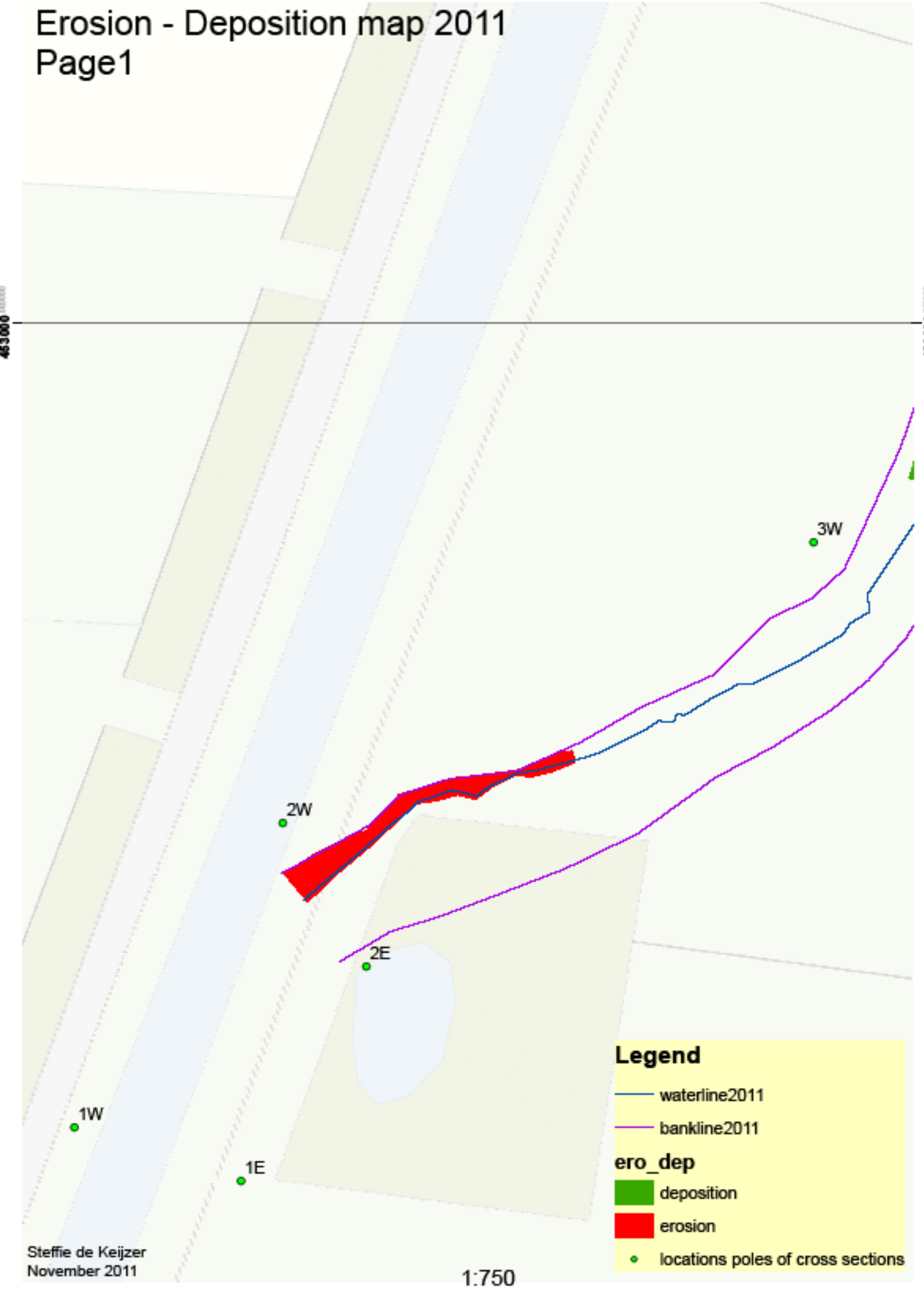

Steffie de Keijzer
November 2011

1:750

Erosion - Deposition map 2011
Page 2

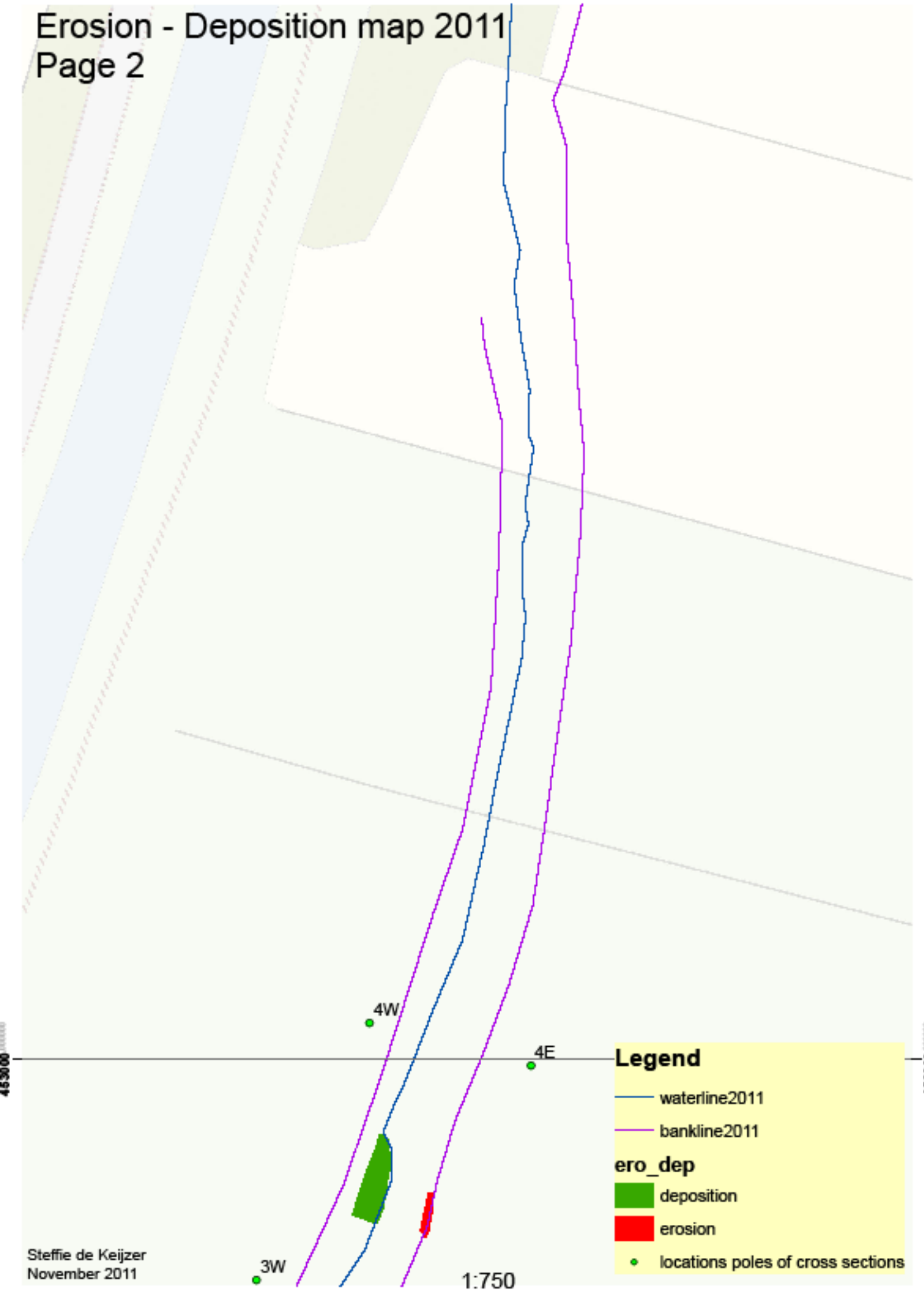

Steffie de Keijzer
November 2011

Erosion - Deposition map 2011
Page 3

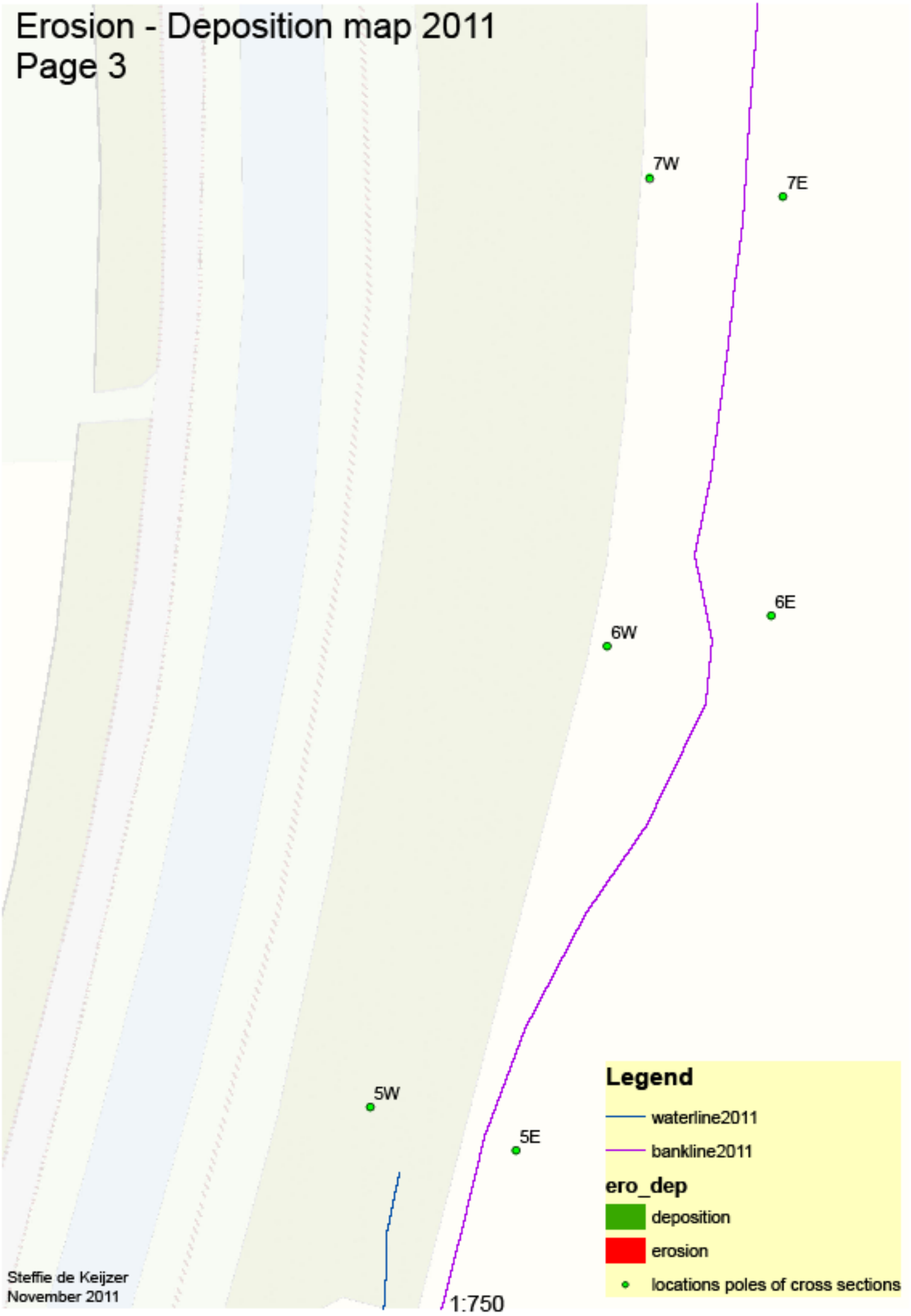

Steffie de Keijzer
November 2011

Erosion - Deposition map 2011
Page 4

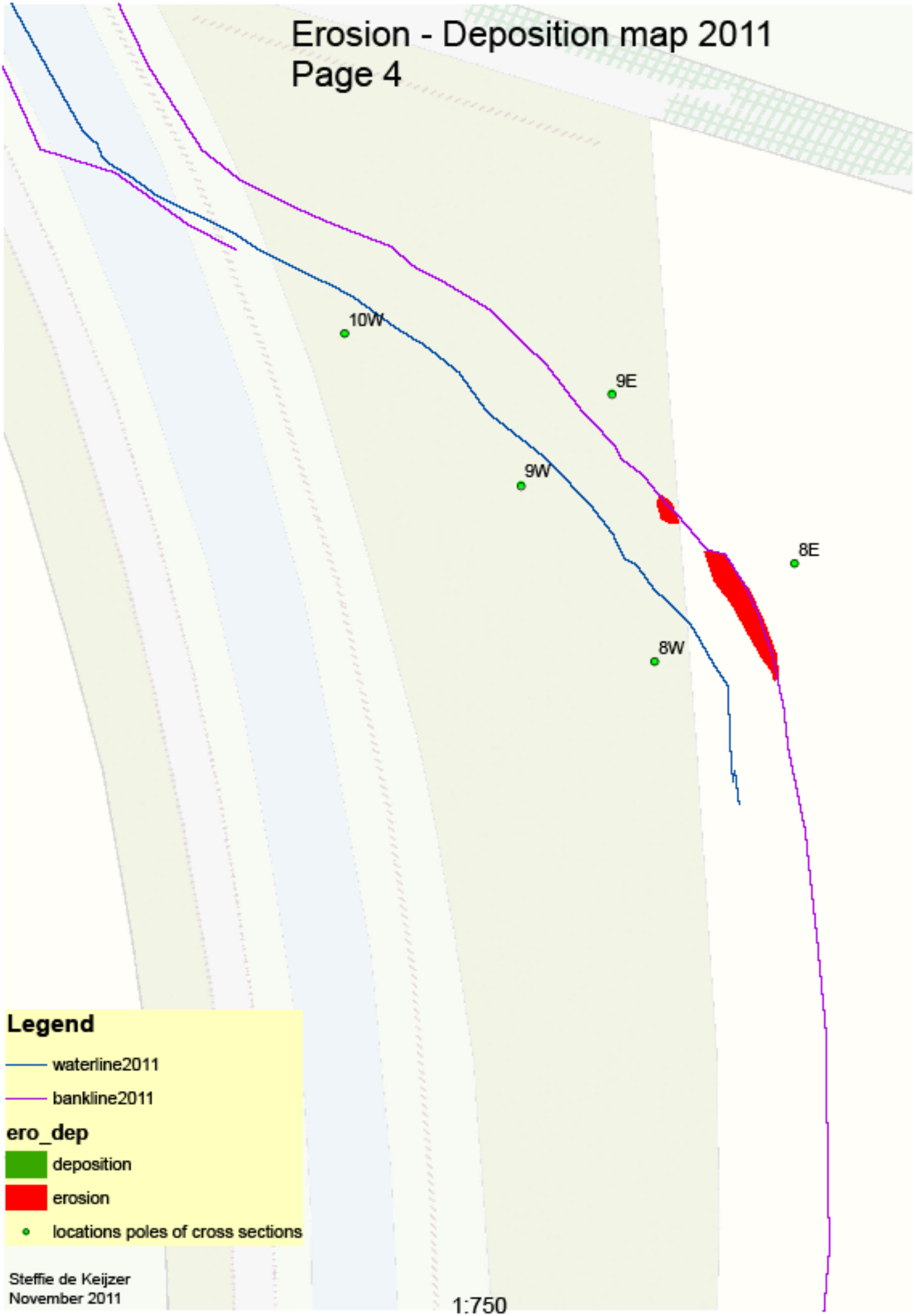

Erosion - Deposition map 2011
Page 5

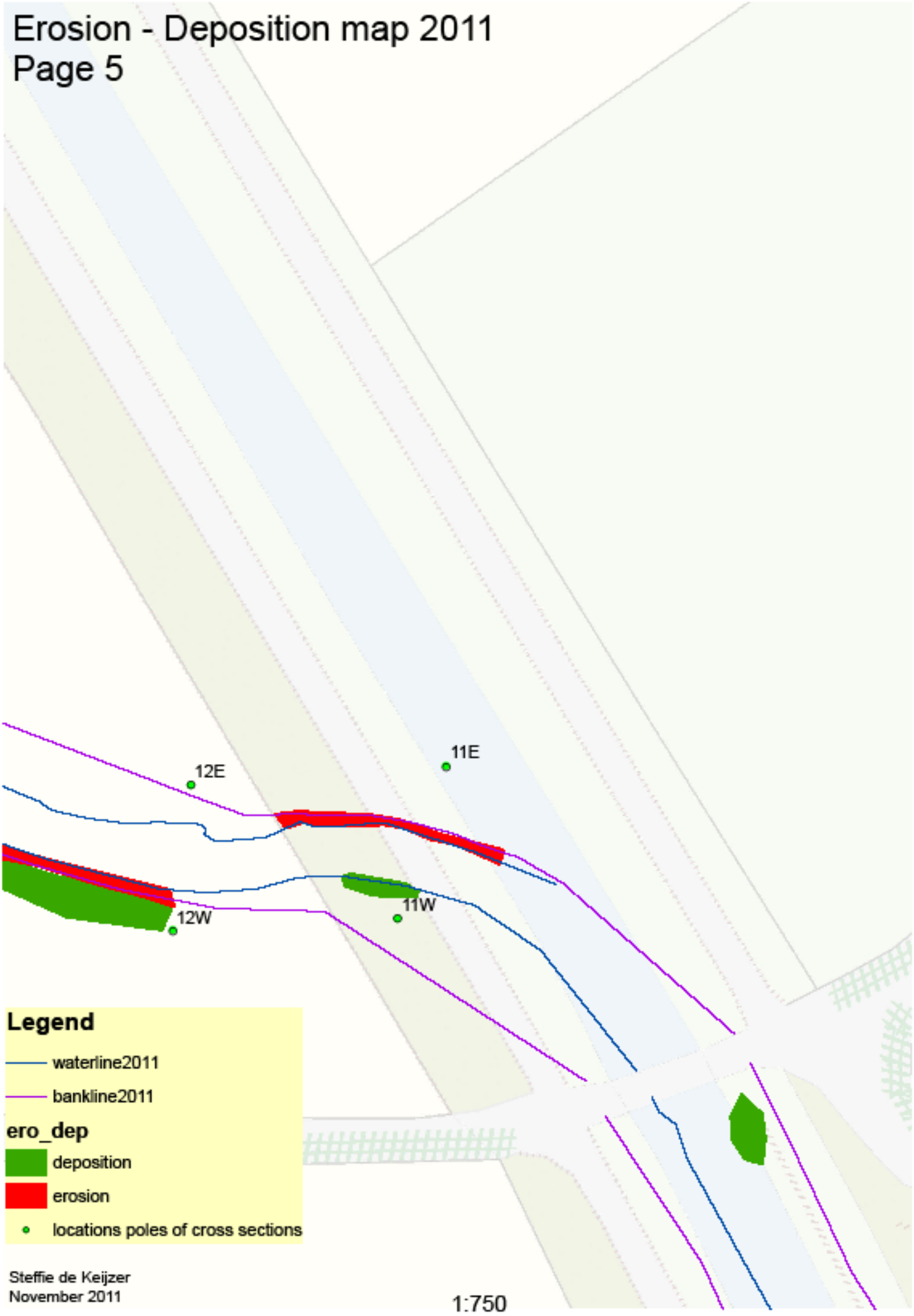

Steffie de Keijzer
November 2011

1:750

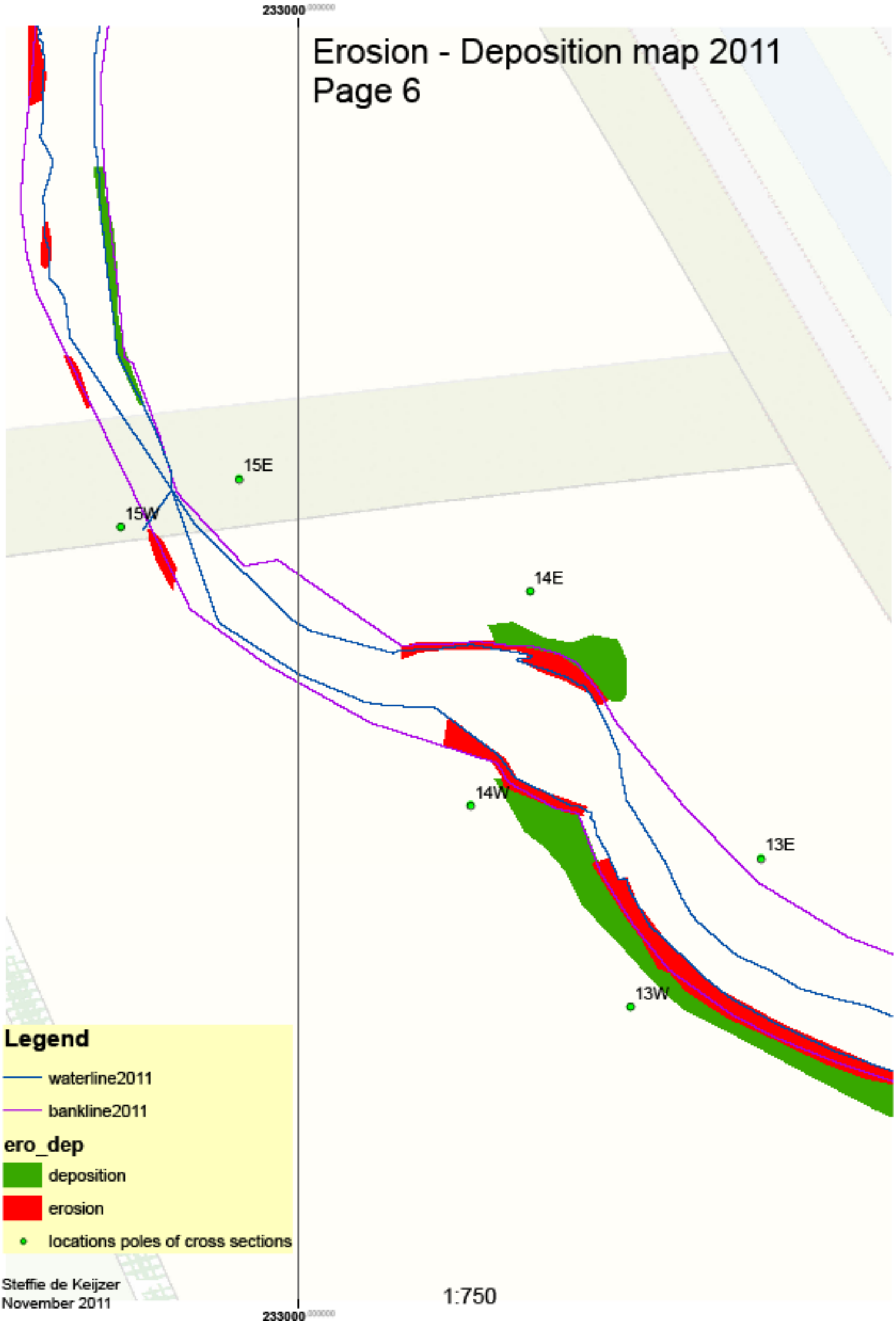
233000
Erosion - Deposition map 2011
Page 6
15E
15W
14E
14W
13E
13W
Legend
waterline2011
bankline2011
ero_dep
deposition
erosion
locations poles of cross sections
Steffie de Keijzer
November 2011
1:750
233000

Erosion - Deposition map 2011 Page 7

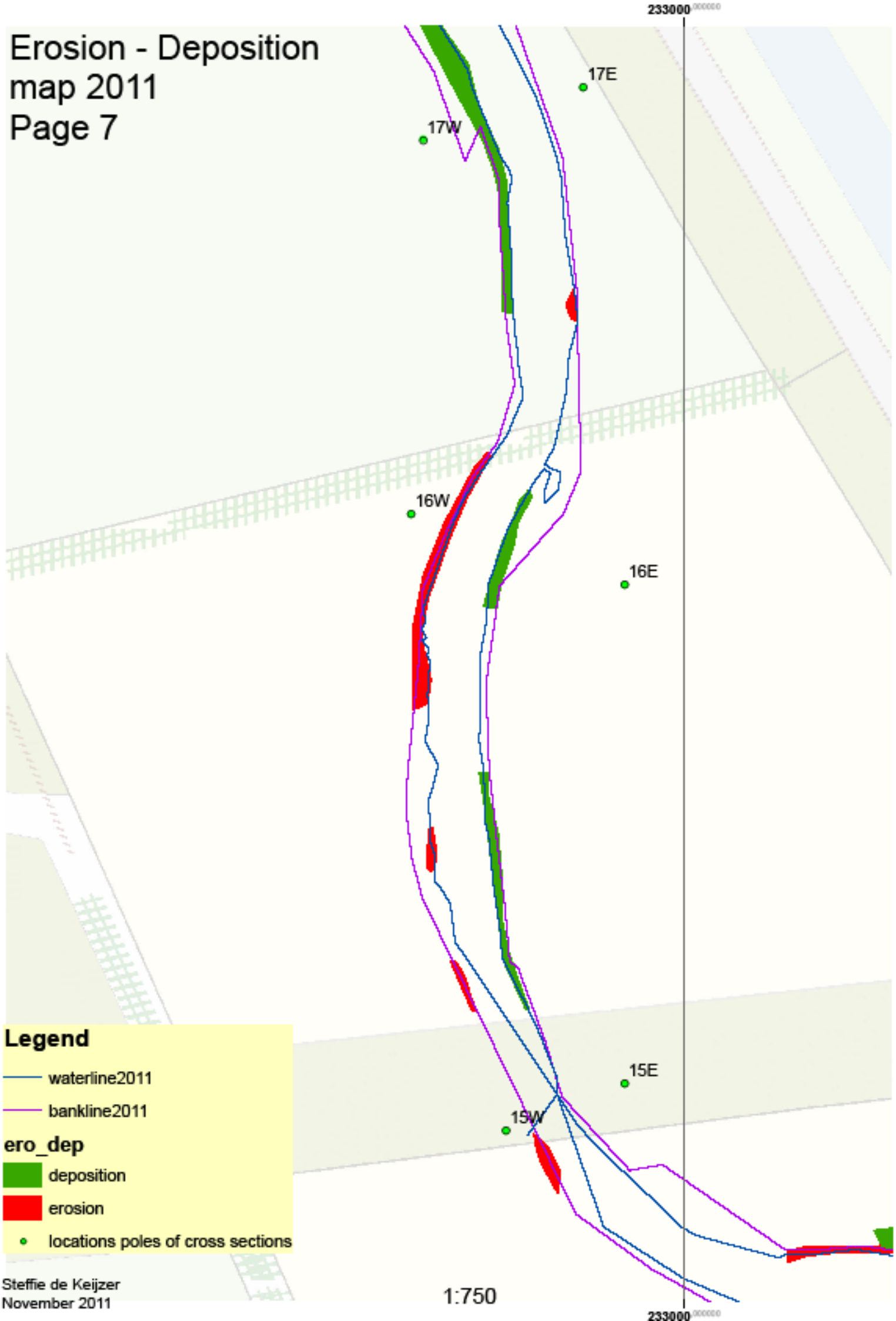

Legend

- waterline2011
- bankline2011

ero_dep

- deposition
- erosion
- locations poles of cross sections

Steffie de Keijzer
November 2011

1:750

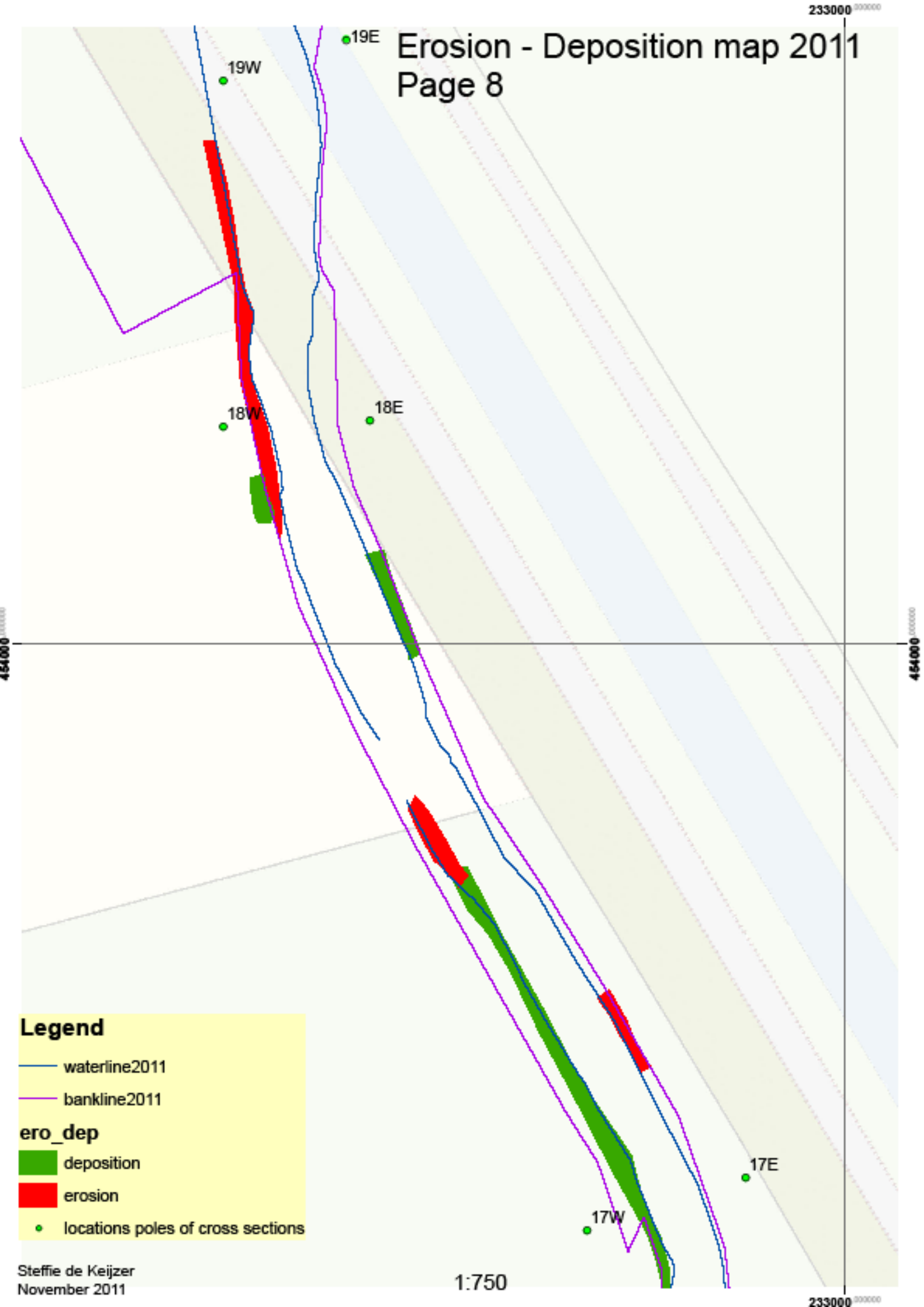
Erosion - Deposition map 2011
Page 8
19E
19W
18W
18E
17E
17W
233000
464000
Legend
waterline2011
bankline2011
ero_dep
deposition
erosion
locations poles of cross sections
Steffie de Keijzer
November 2011
1:750

Erosion - Deposition map 2011
Page 9

Steffie de Keijzer
November 2011

Erosion - Deposition map 2011
Page 10

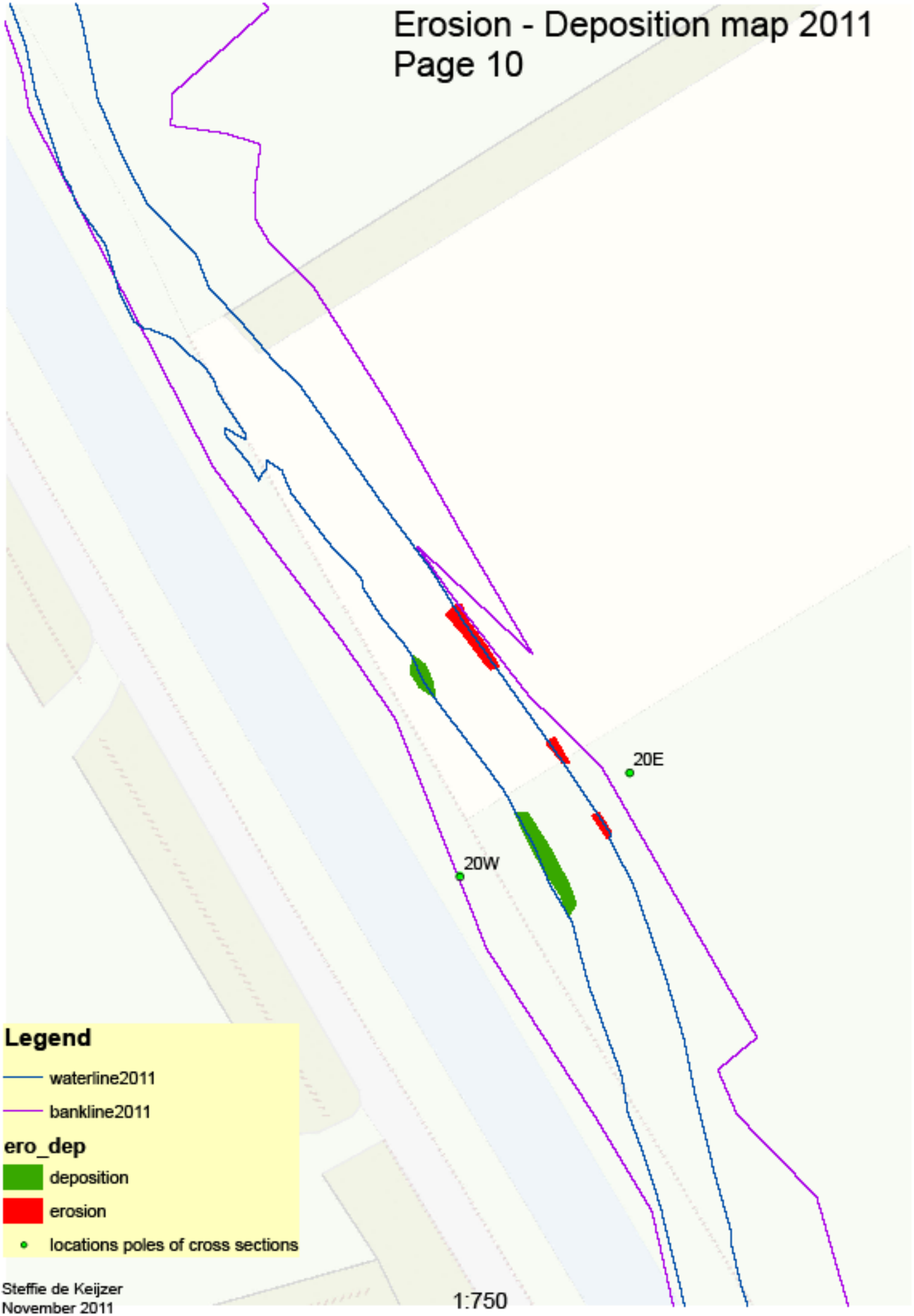

Steffie de Keijzer
November 2011

1:750

Appendix 7: Vegetation map

The vegetation map is split up into ten pages.

See next pages!

The digital version can be found on CD2.

Vegetation Groenlose Slinge 2011, page 1

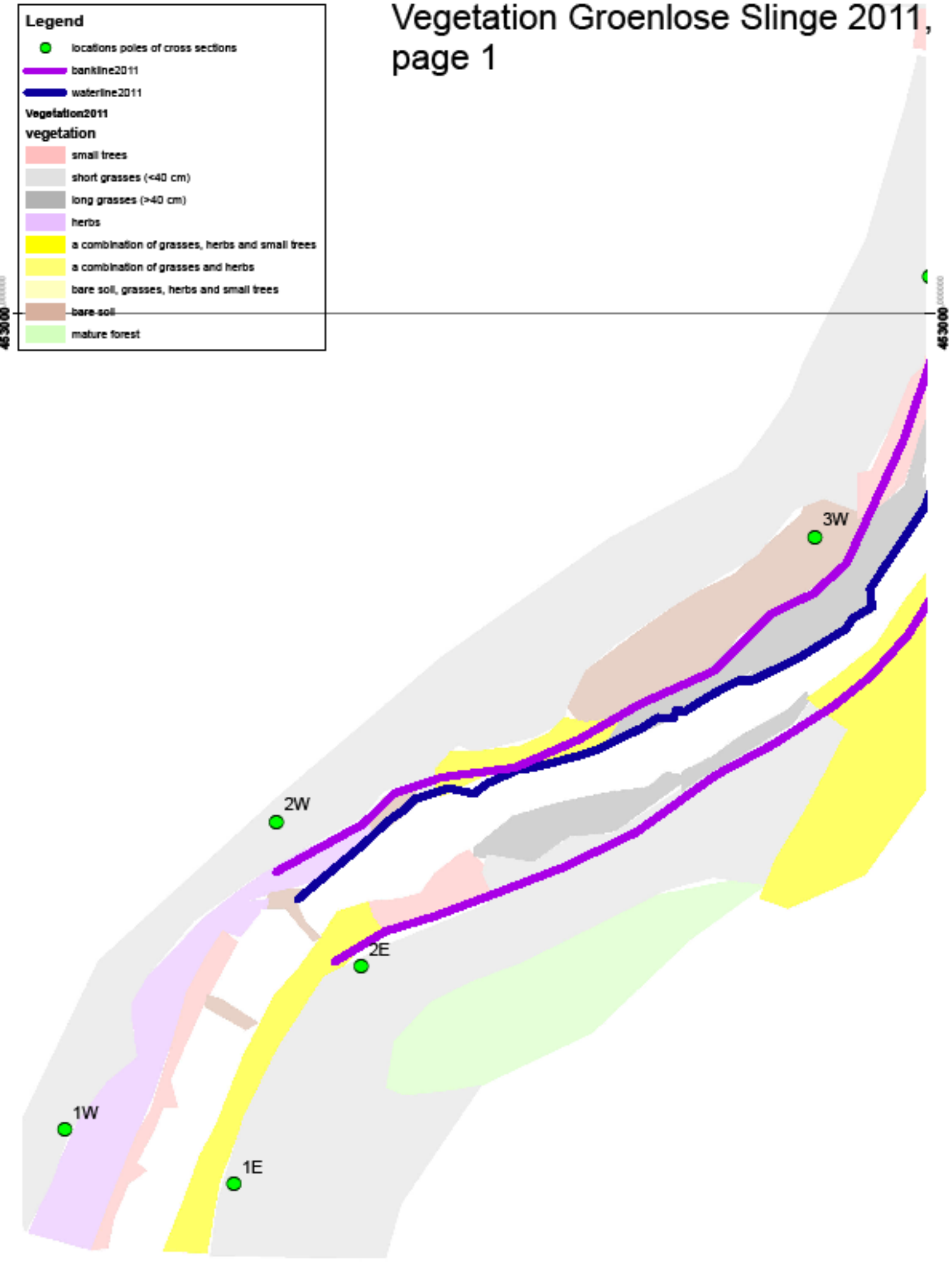

Steffie de Keijzer
December 2011

1:750

Vegetation Groenlose Slinge 2011, page 2

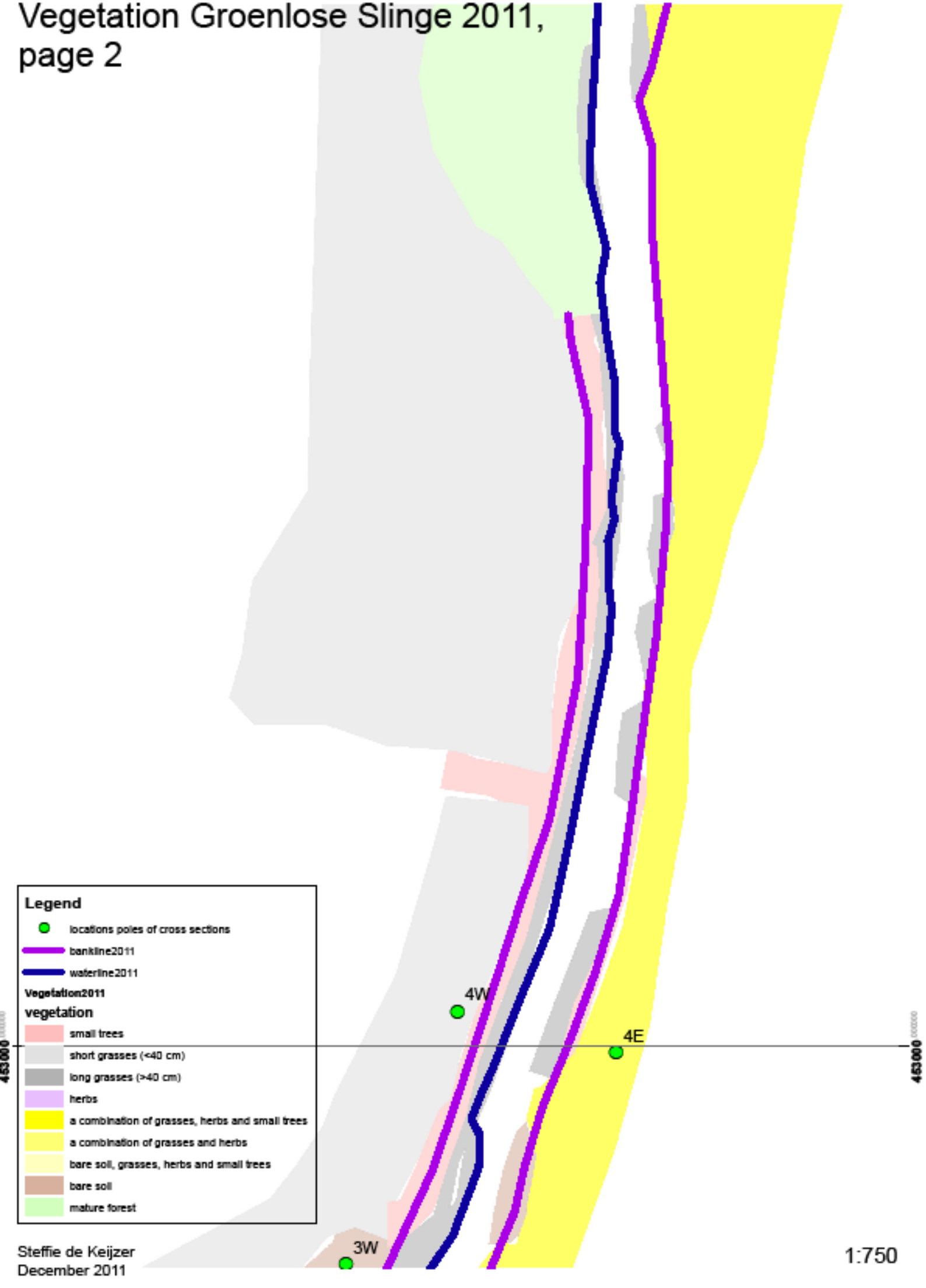

Steffie de Keijzer
December 2011

1:750

Vegetation Groenlose Slinge 2011, page 3

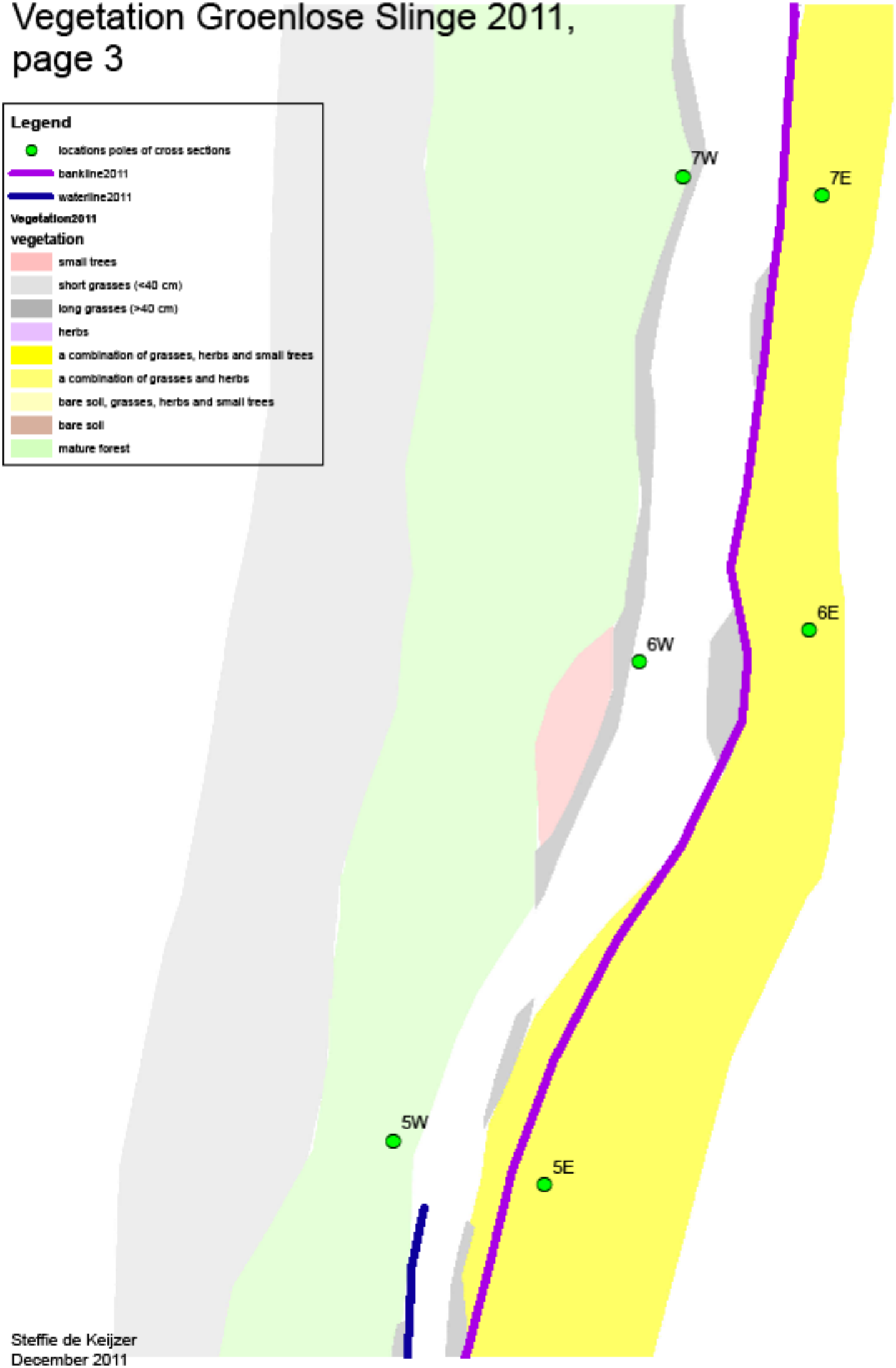

Steffie de Keijzer
December 2011

1:750

Vegetation Groenlose Slinge 2011, page 4

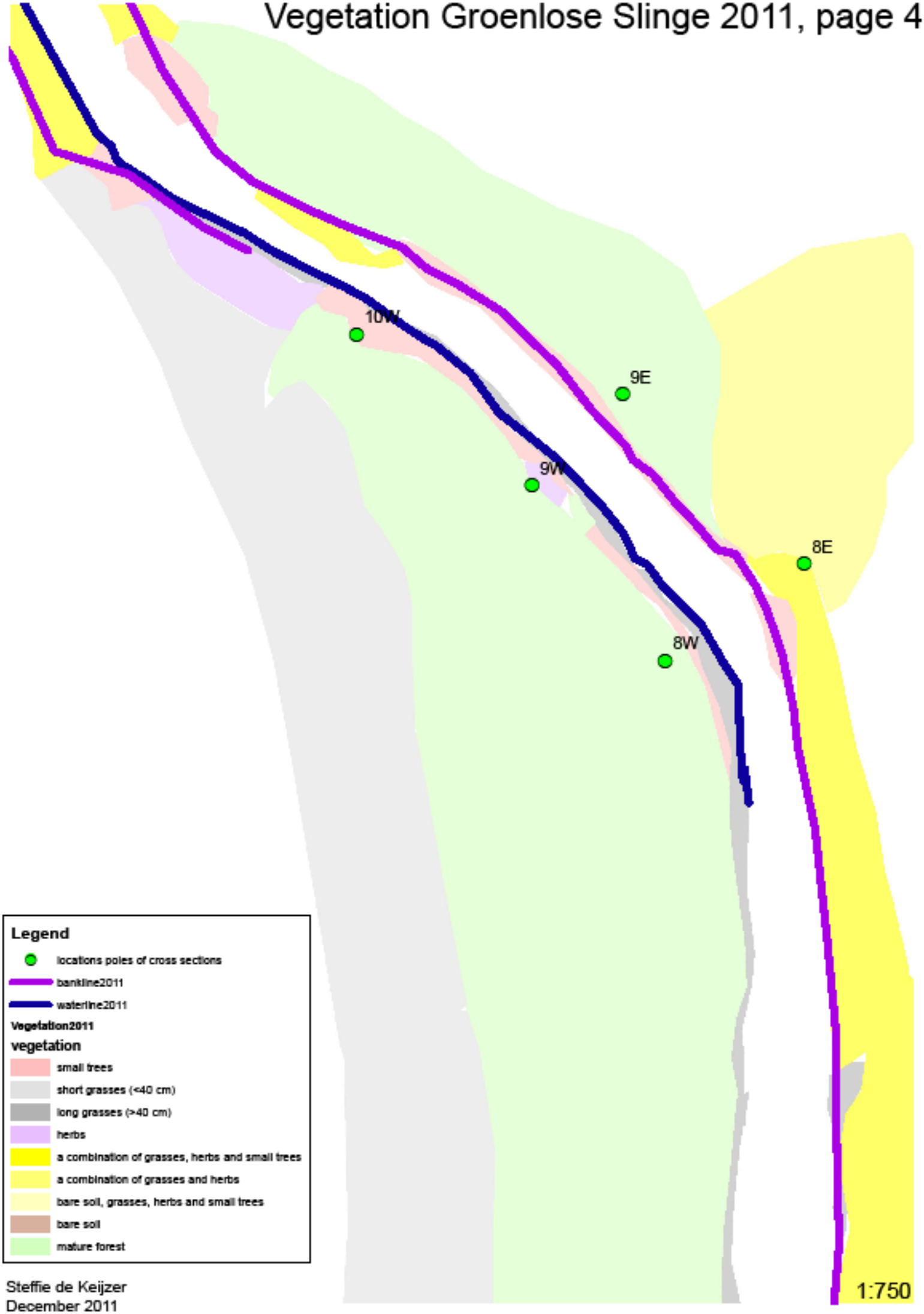

Steffie de Keijzer
December 2011

Vegetation Groenlose Slinge 2011, page 5

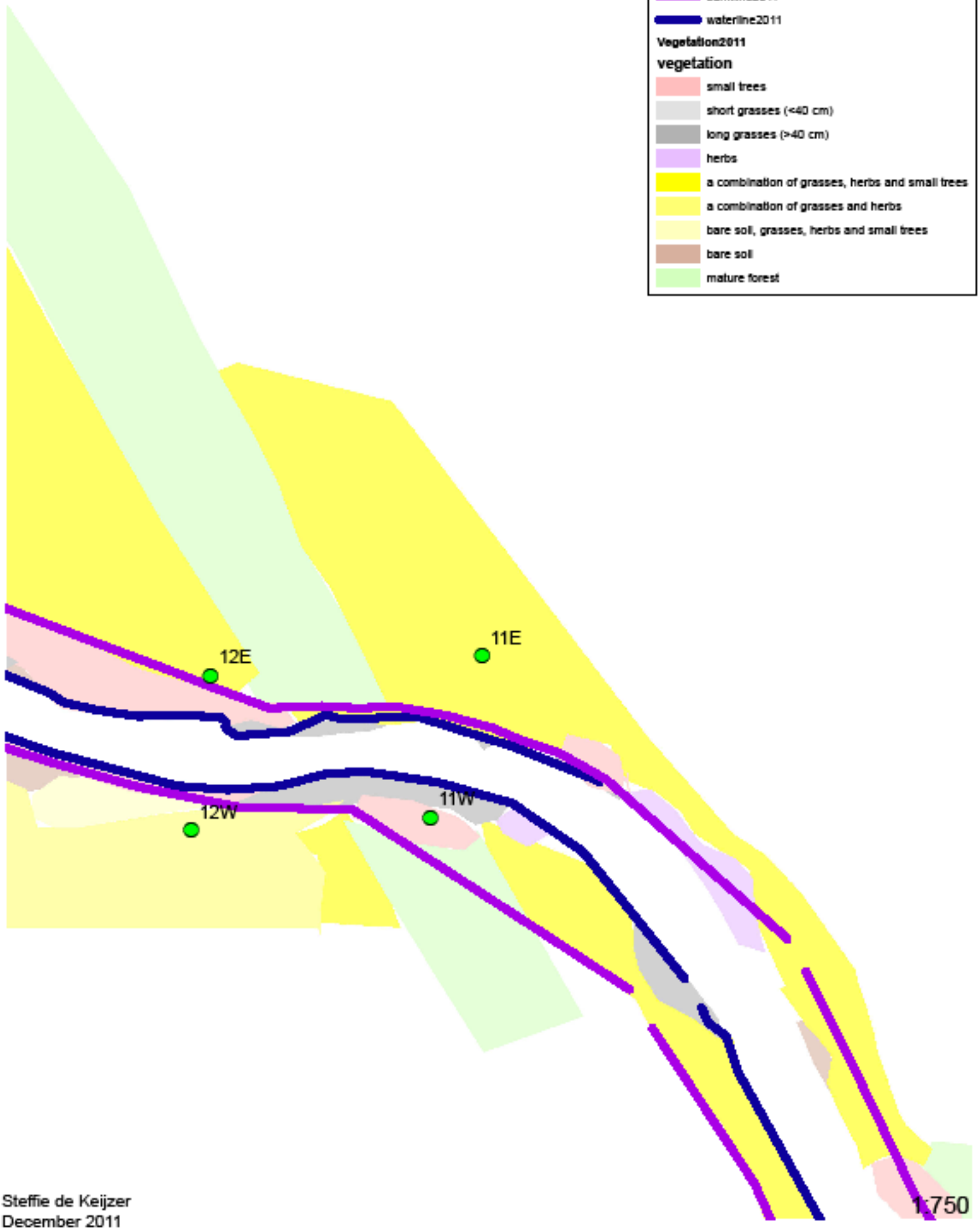

Steffie de Keijzer
December 2011

1:750

Vegetation Groenlose Slinge 2011, page 6

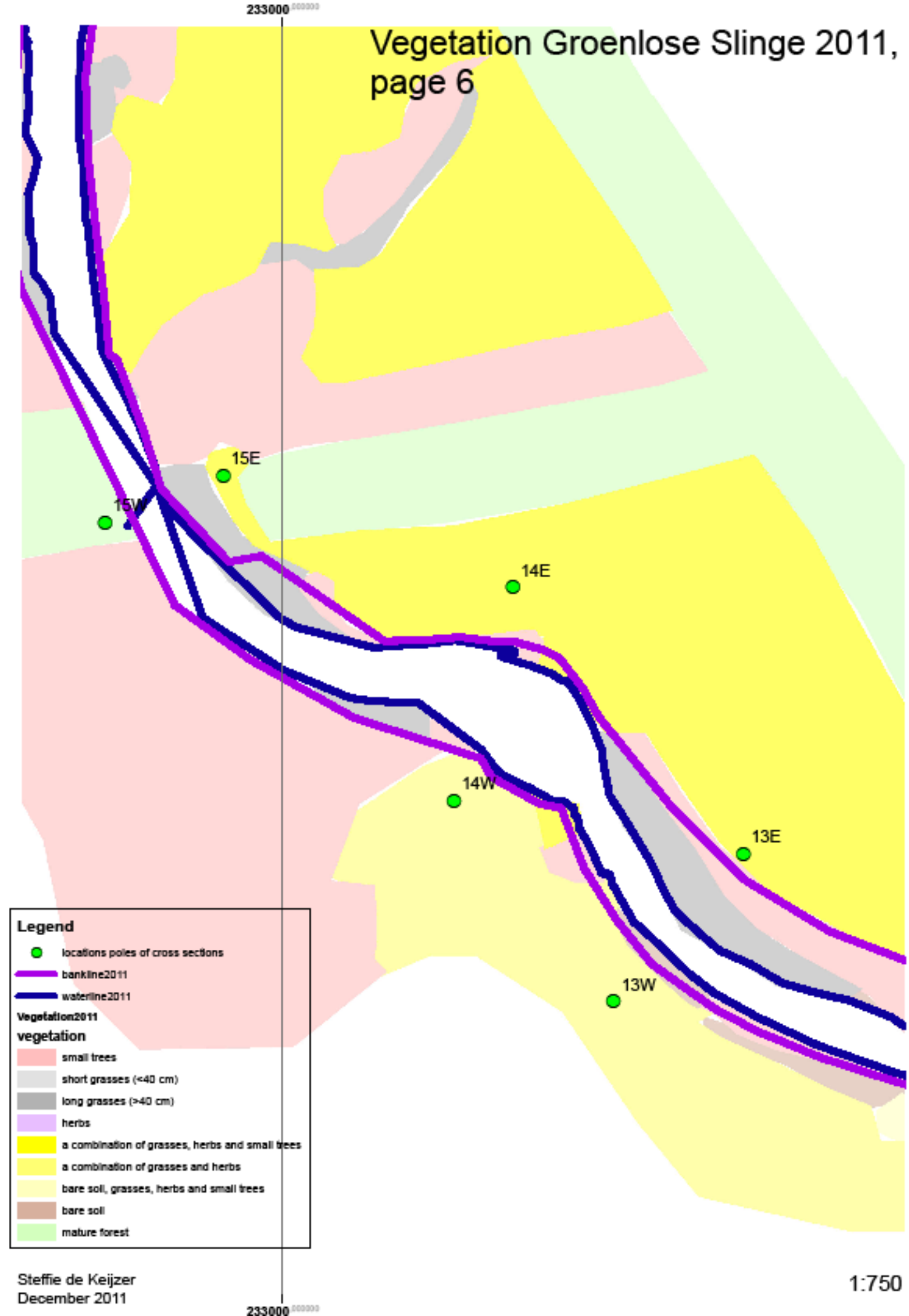

Steffie de Keijzer
December 2011

1:750

Vegetation Groenlose Slinge 2011, page 7

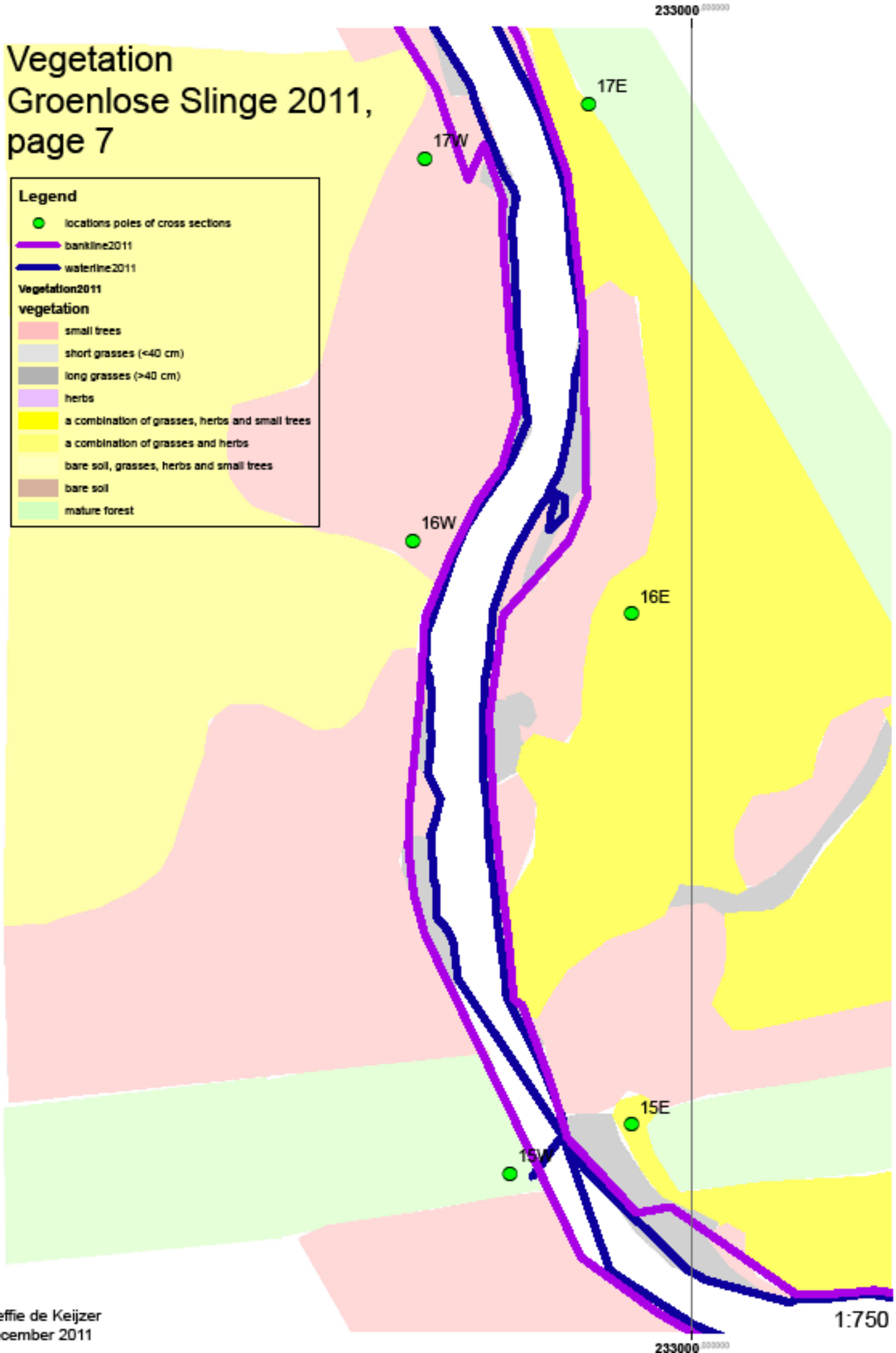

Steffie de Keijzer
December 2011

Vegetation Groenlose Slinge 2011, page 8

Steffie de Keijzer
December 2011

1:750

Vegetation
Groenlose Slinge 2011, page 9

Legend

- locations poles of cross sections
- bankline2011
- waterline2011

Vegetation2011

vegetation

- small trees
- short grasses (<40 cm)
- long grasses (>40 cm)
- herbs
- a combination of grasses, herbs and small trees
- a combination of grasses and herbs
- bare soil, grasses, herbs and small trees
- bare soil
- mature forest

Steffie de Keijzer
December 2011

Vegetation
Groenlose Slinge 2011, page 10

Steffie de Keijzer
December 2011

1:750

Appendix 8: Airphoto maps 2009 and 2011

The airphoto maps of 2009 and 2011 are split up into twice ten pages.

See next pages!

The digital version can be found on CD2.

Legend:

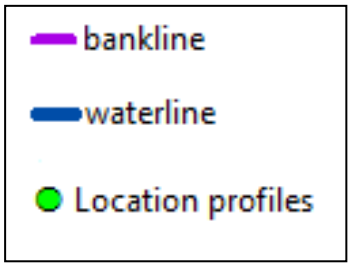

Airphoto Groenlose Slinge 2011, page 1

1:750

Steffie de Keijzer
December 2011

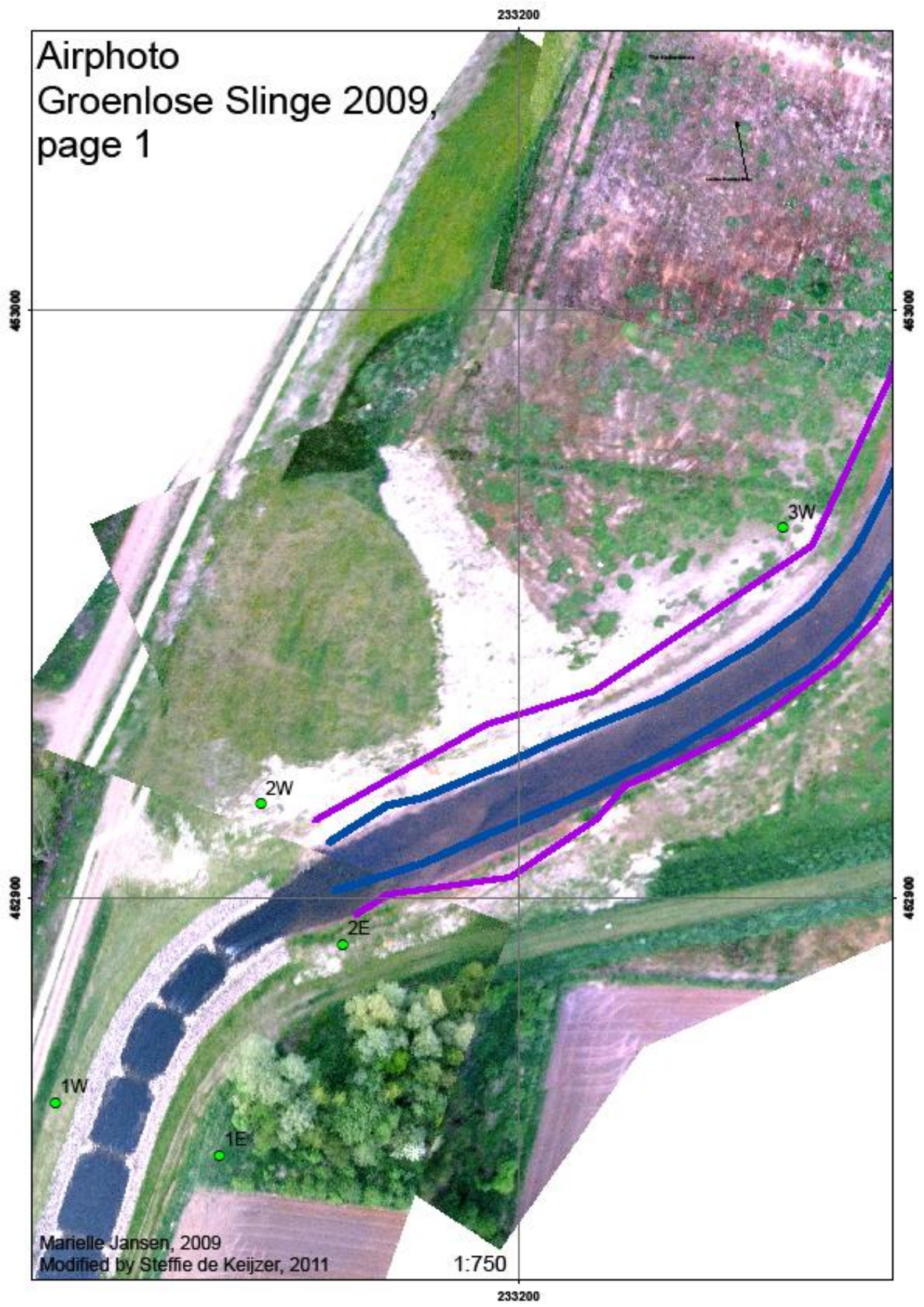
Airphoto
Groenlose Slinge 2009,
page 1
233200
453000
452900
3W
2W
2E
1W
1E
Marielle Jansen, 2009
Modified by Steffie de Keijzer, 2011
1:750

Airphoto Groenlose Slinge 2011, page 2

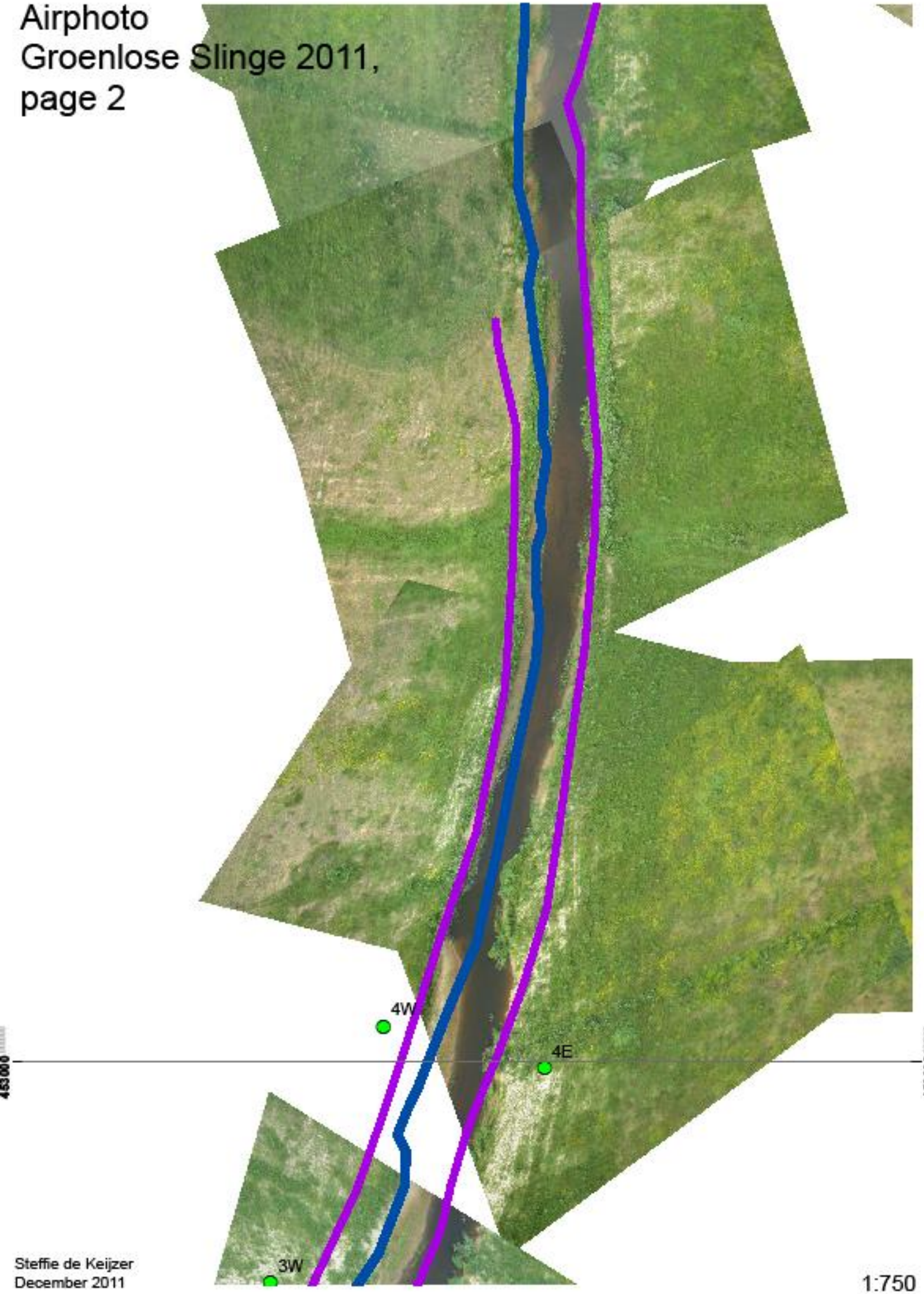

Steffie de Keijzer
December 2011

1:750

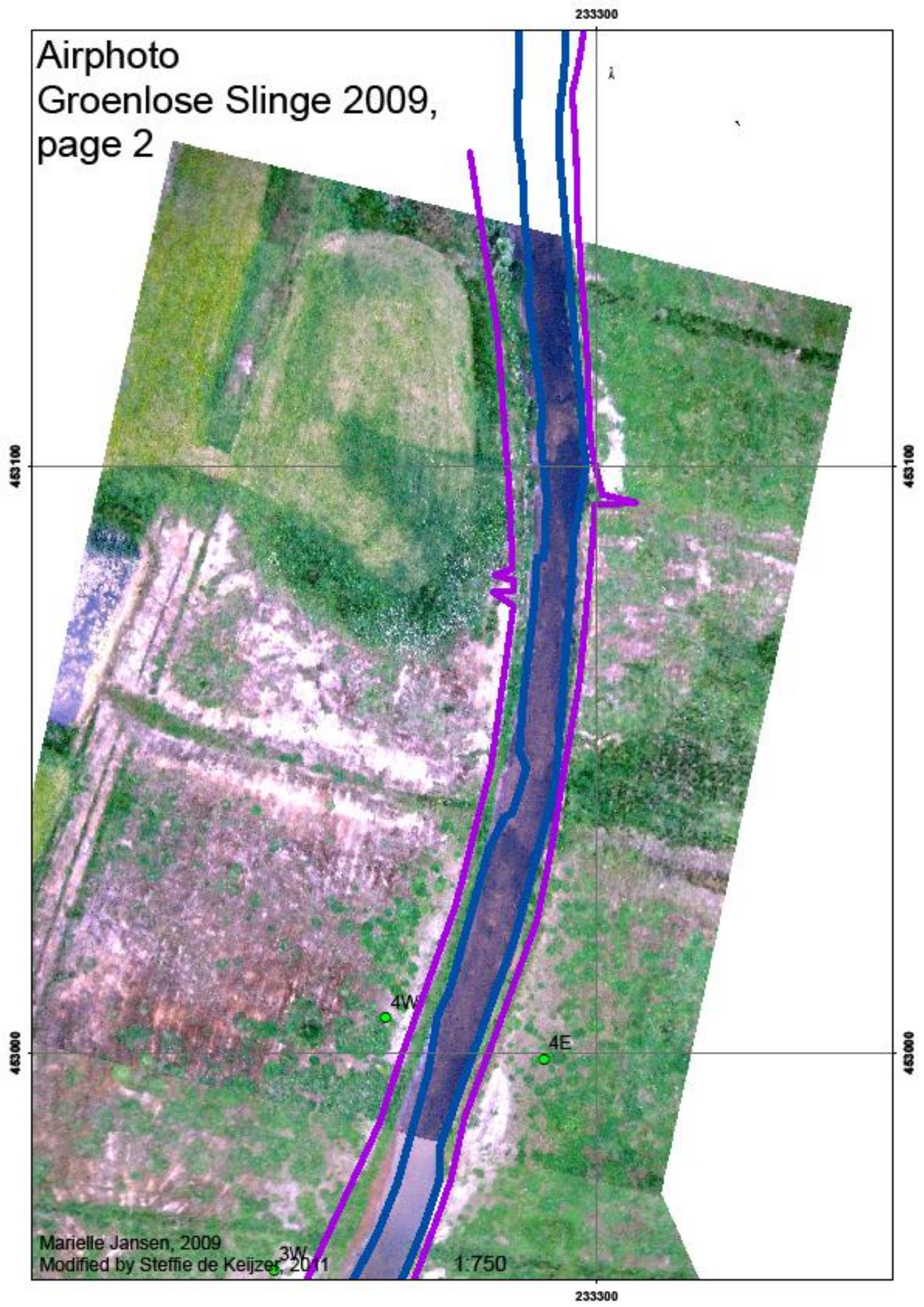
Airphoto
Groenlose Slinge 2009,
page 2
233300
453100
453000
4W
4E
3W
Marielle Jansen, 2009
Modified by Steffie de Keijzer, 2011
1:750

Airphoto Groenlose Slinge 2011, page 3

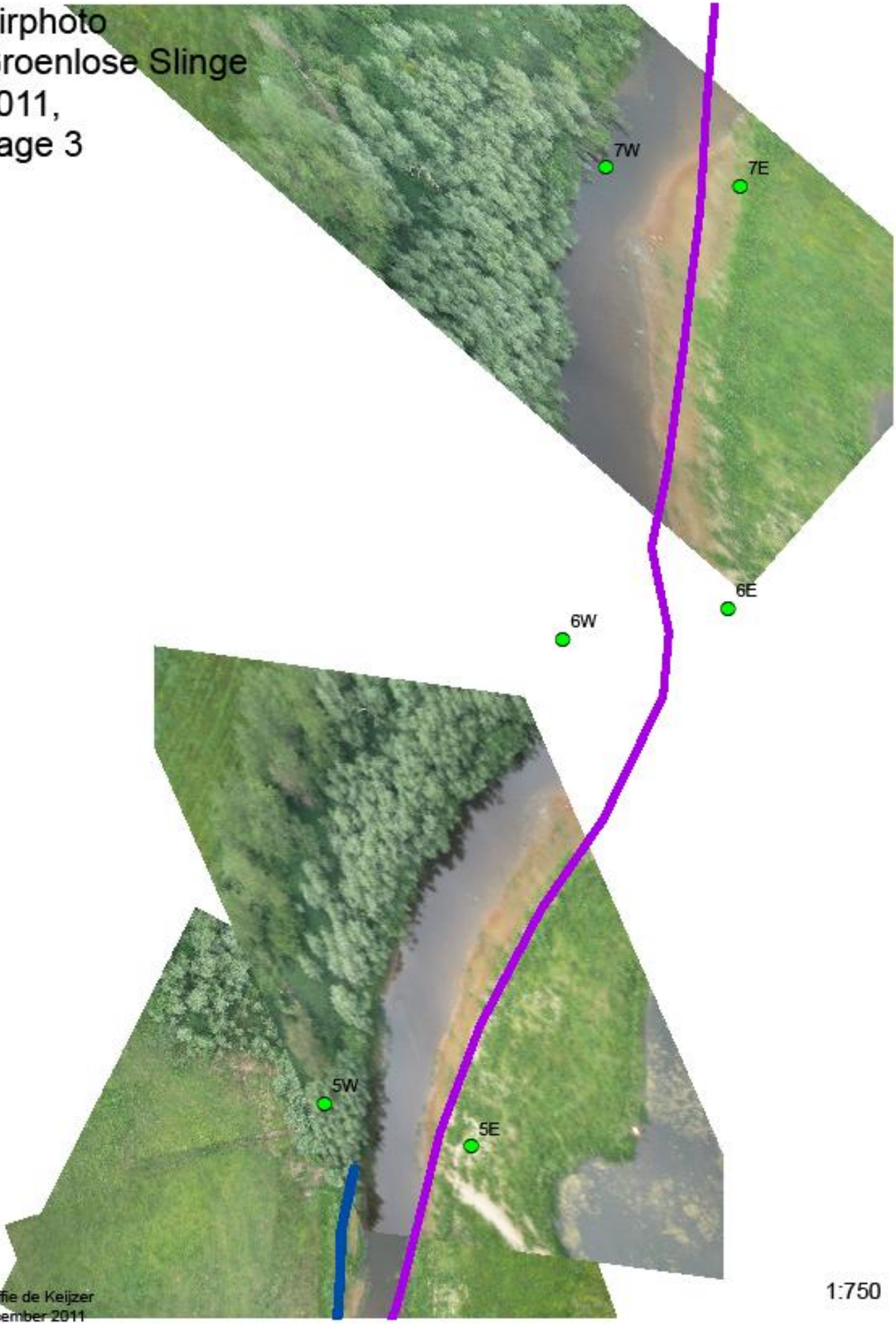

Steffie de Keijzer
December 2011

1:750

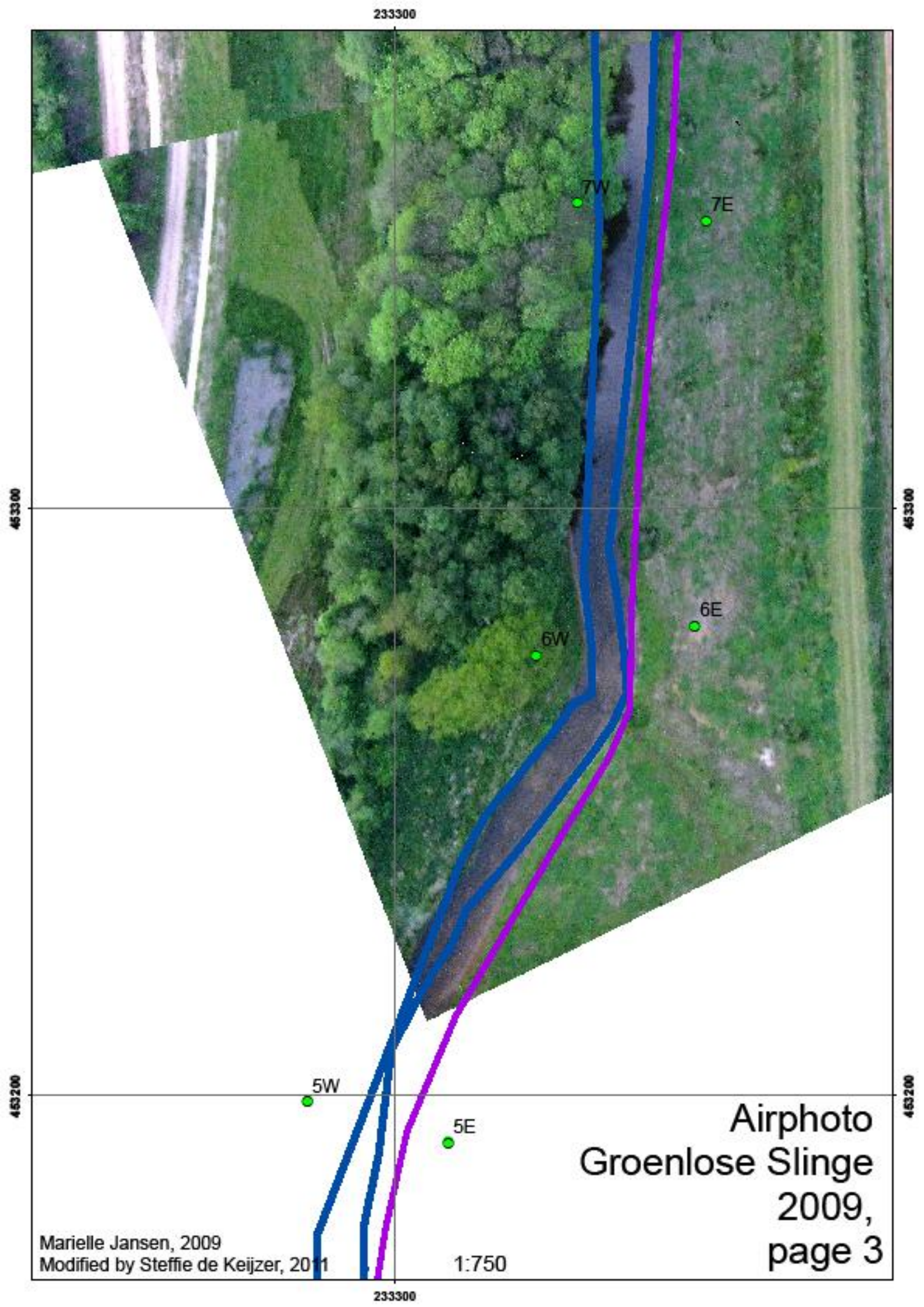
233300
453300
453200
7W
7E
6W
6E
5W
5E
Airphoto
Groenlose Slinge
2009,
page 3
Marielle Jansen, 2009
Modified by Steffie de Keijzer, 2011
1:750

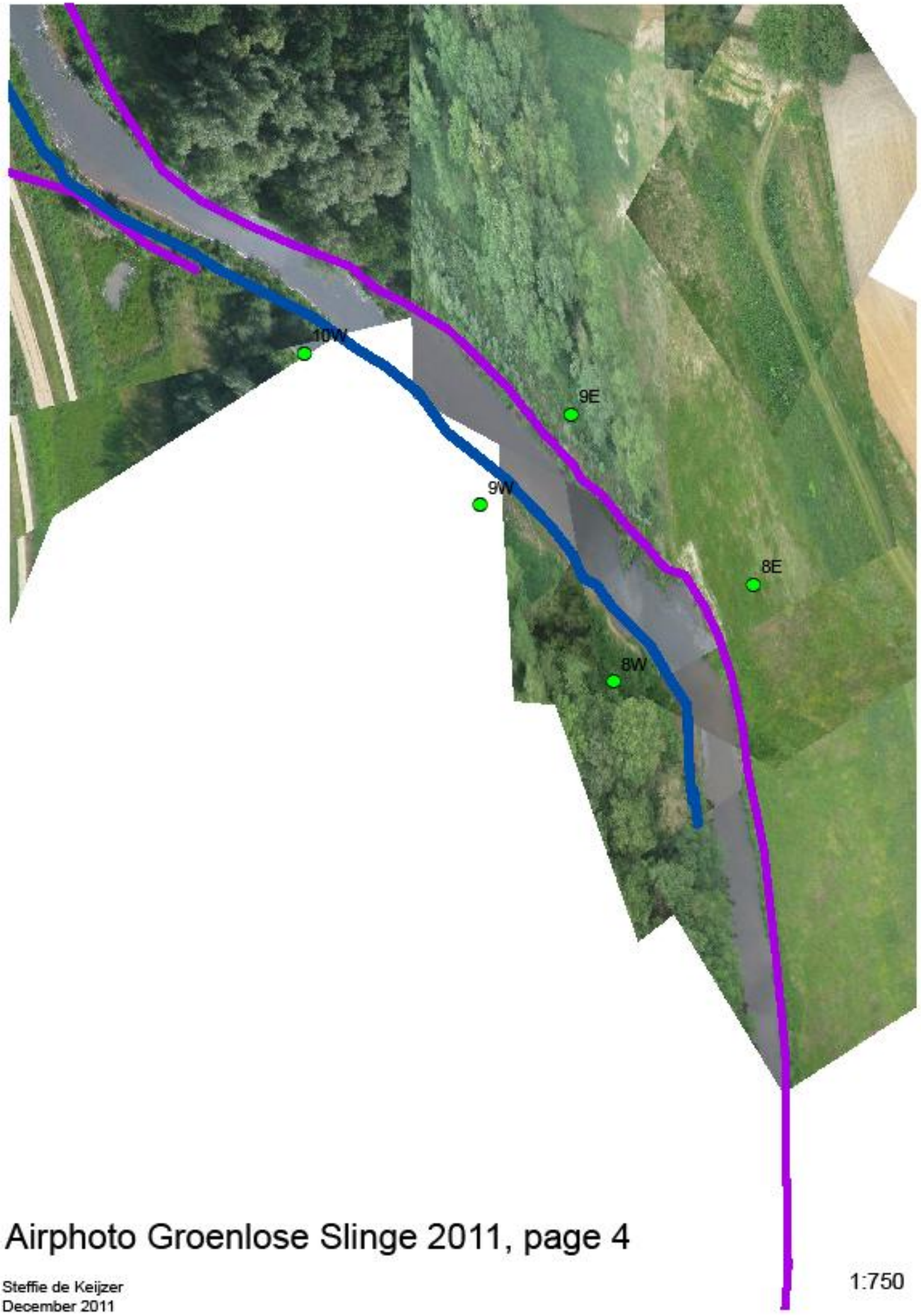

Airphoto Groenlose Slinge 2011, page 4

Steffie de Keijzer
December 2011

1:750

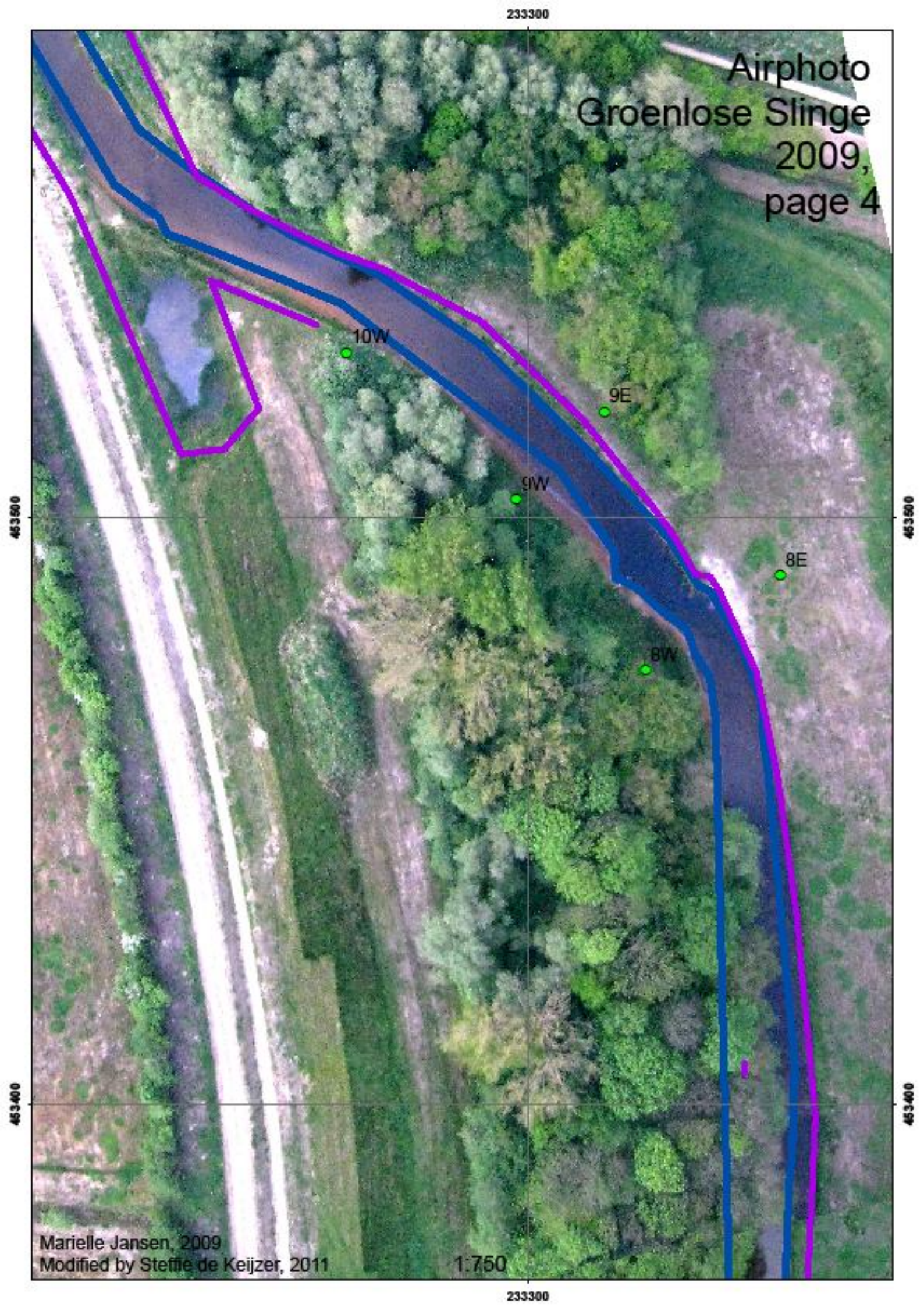
233300
Airphoto
Groenlose Slinge
2009,
page 4
10W
9E
9W
8E
8W
453500
453400
Marielle Jansen, 2009
Modified by Steffie de Keijzer, 2011
1:750
233300

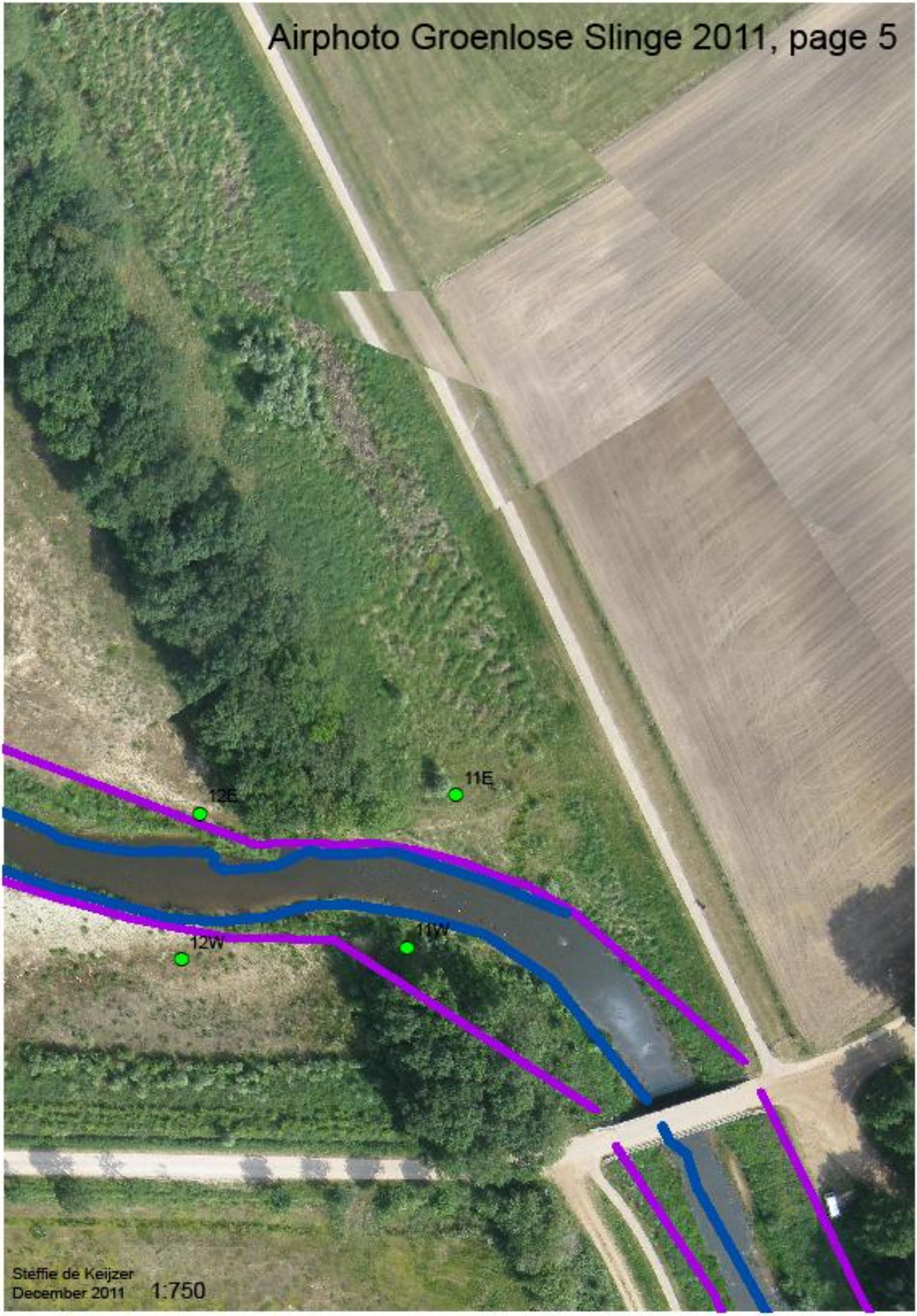
Airphoto Groenlose Slinge 2011, page 5
11E
12E
11W
12W
Steffie de Keijzer
December 2011
1:750

233100 233200

Airphoto Groenlose Slinge 2009, page 5

453700 453700

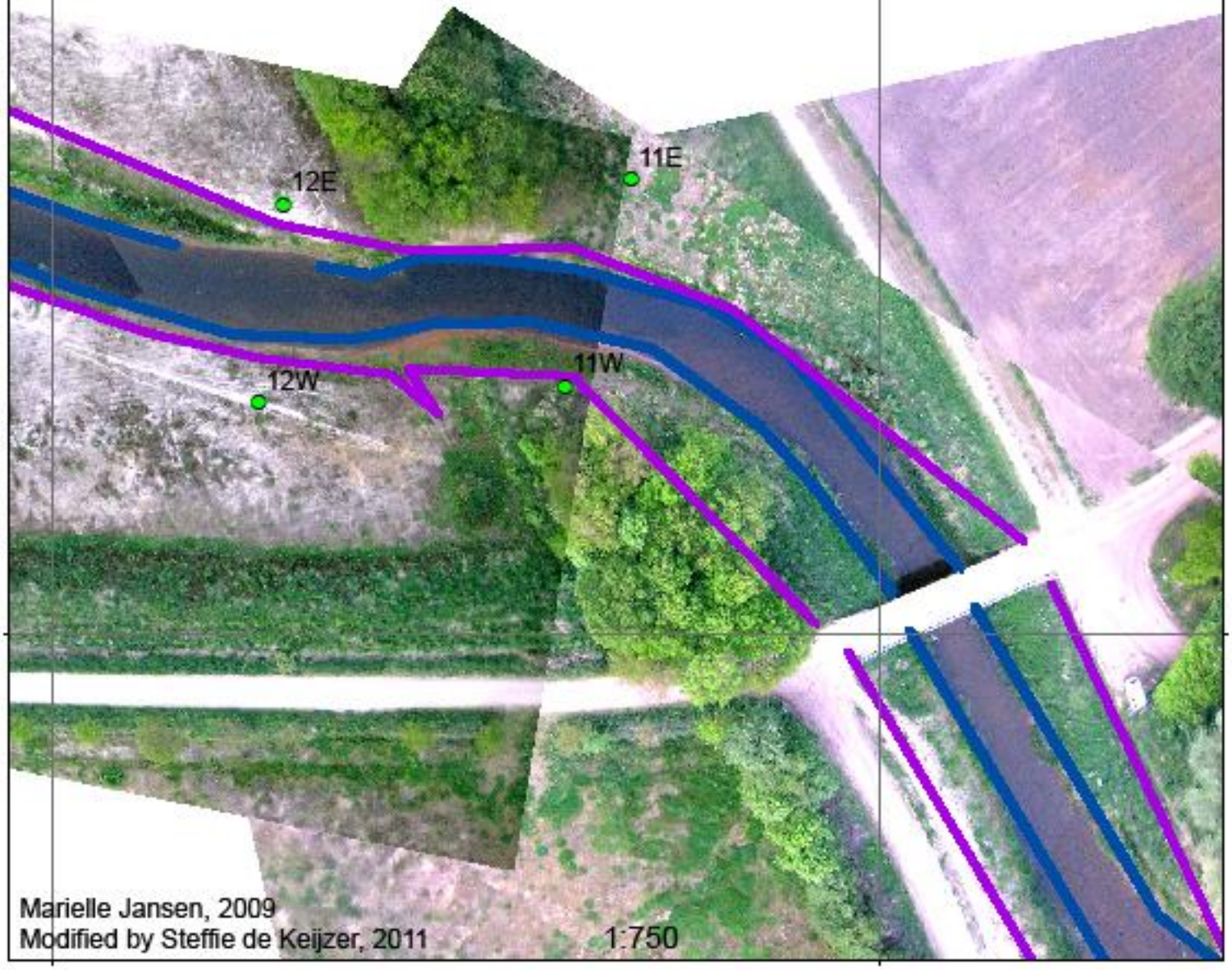

453600 453600

Marielle Jansen, 2009
Modified by Steffie de Keijzer, 2011

1:750

233100 233200

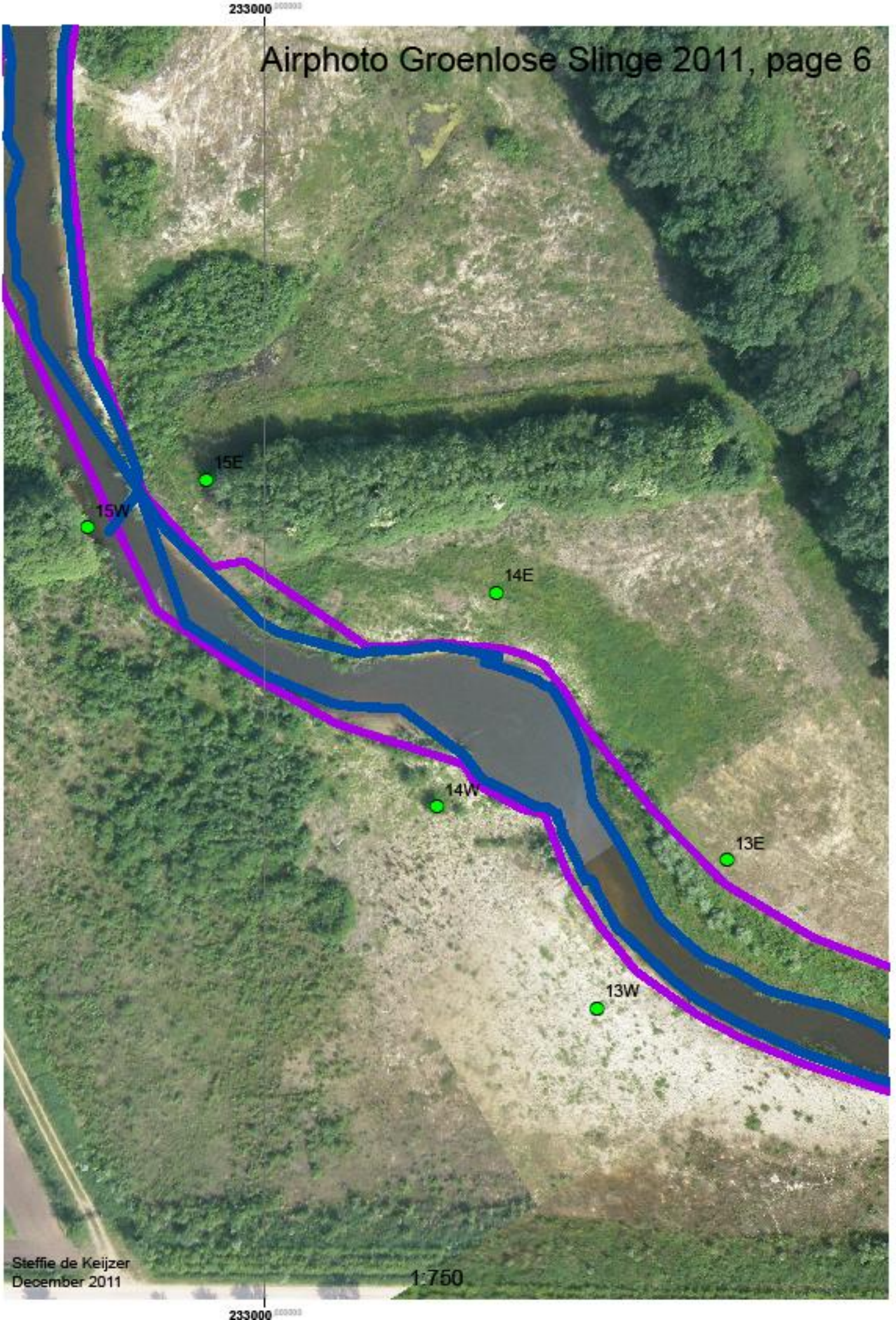
233000
Airphoto Groenlose Slinge 2011, page 6
15E
15W
14E
14W
13E
13W
Steffie de Keijzer
December 2011
1:750
233000

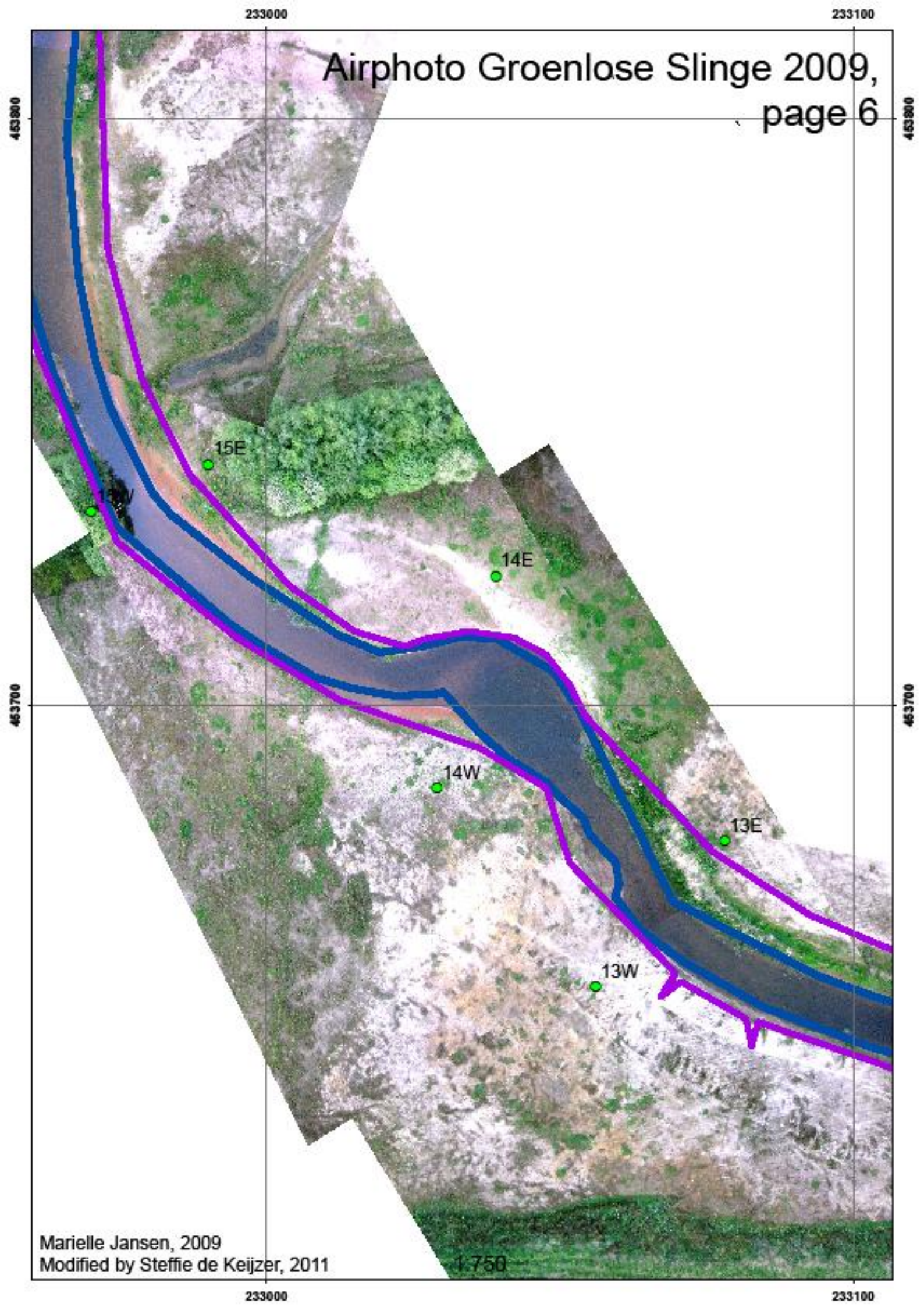
Airphoto Groenlose Slinge 2009,
page 6
233000
233100
453800
453700
15E
14E
14W
13E
13W
Marielle Jansen, 2009
Modified by Steffie de Keijzer, 2011
1:750

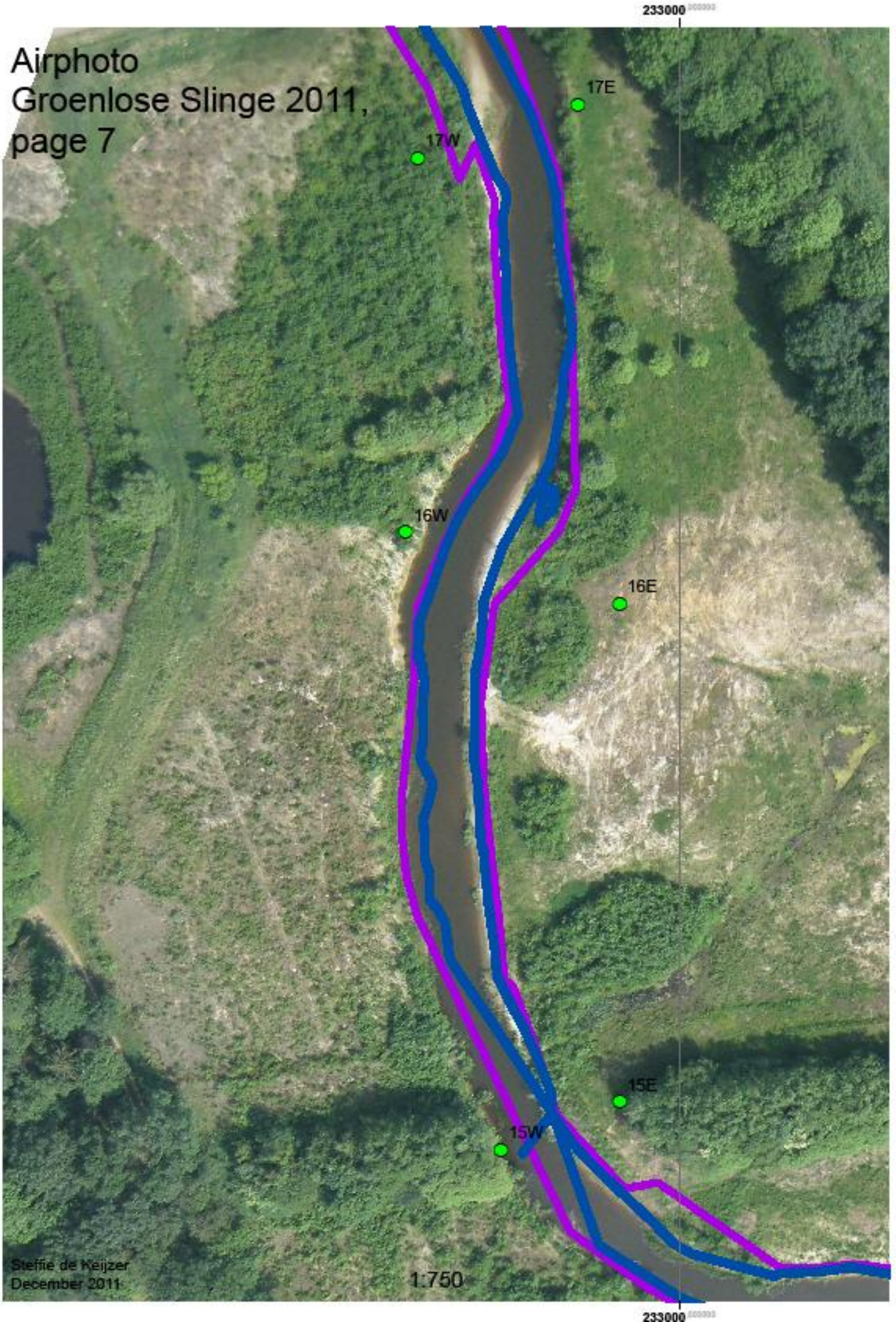
Airphoto
Groenlose Slinge 2011,
page 7
233000
17E
17W
16W
16E
15E
15W
Steffie de Keijzer
December 2011
1:750
233000

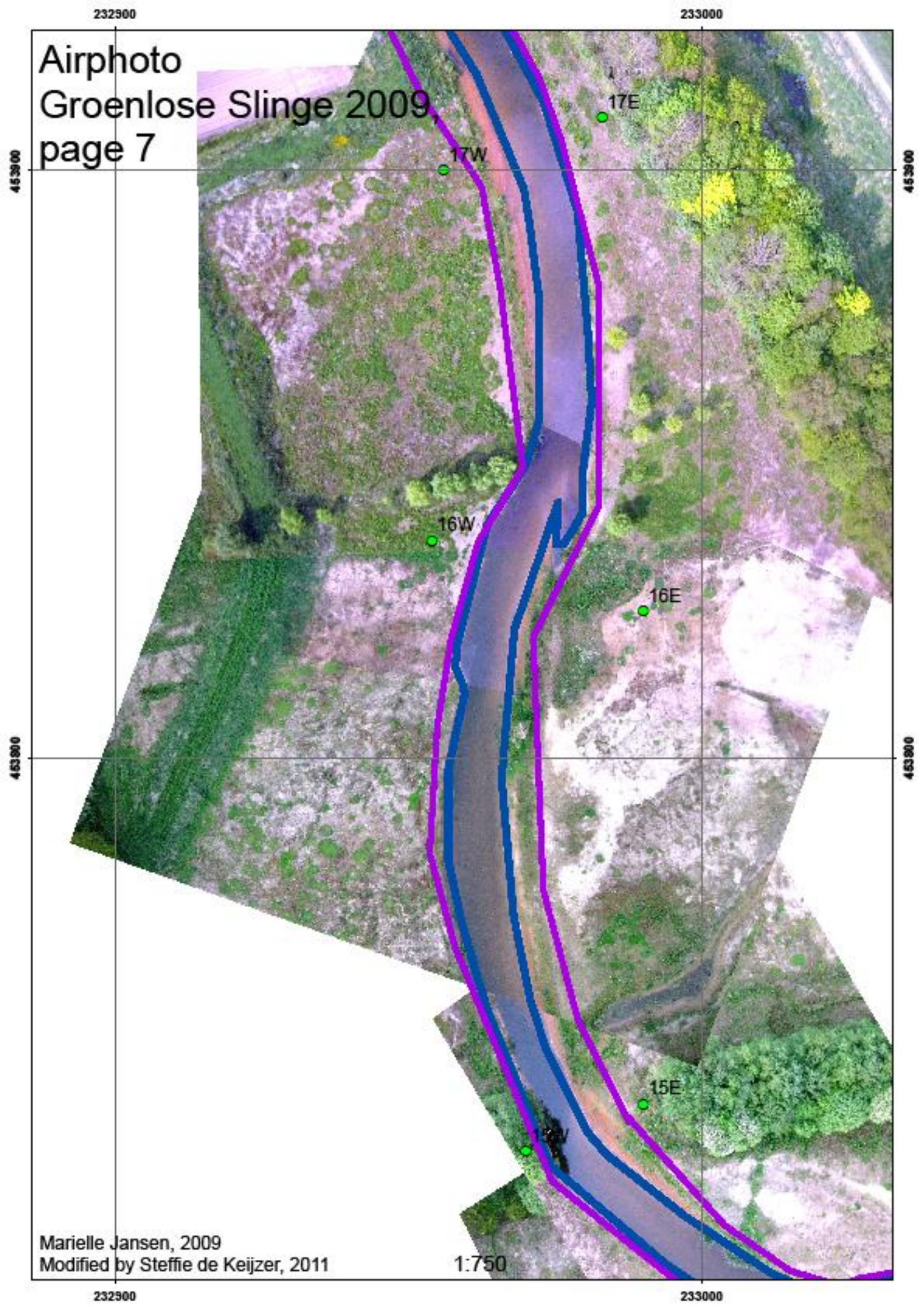
Airphoto
Groenlose Slinge 2009,
page 7
232900
233000
453900
17E
17W
16W
16E
15E
Marielle Jansen, 2009
Modified by Steffie de Keijzer, 2011
1:750

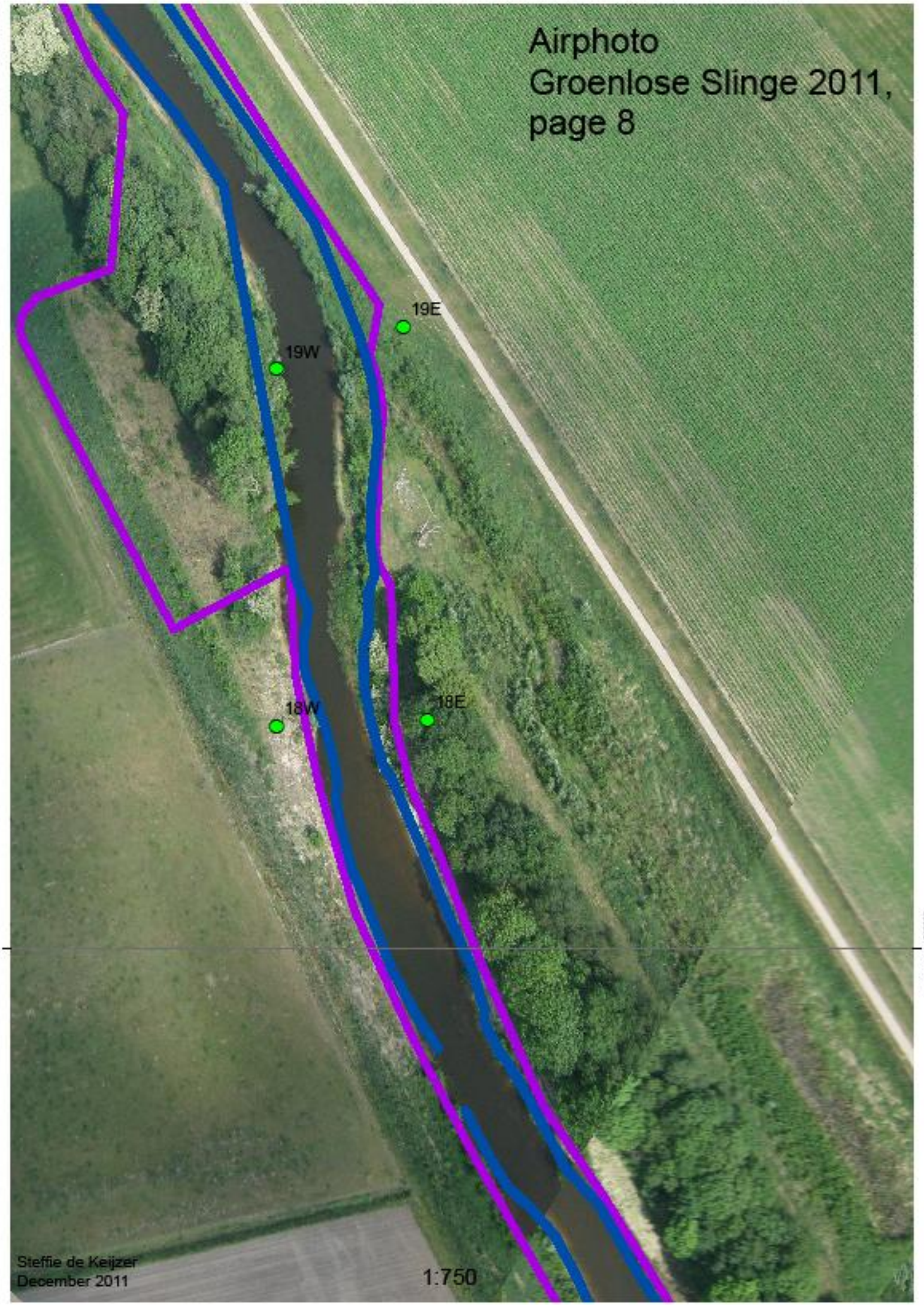
Airphoto
Groenlose Slinge 2011,
page 8
19E
19W
18E
18W
454000
454000
Steffie de Keijzer
December 2011
1:750

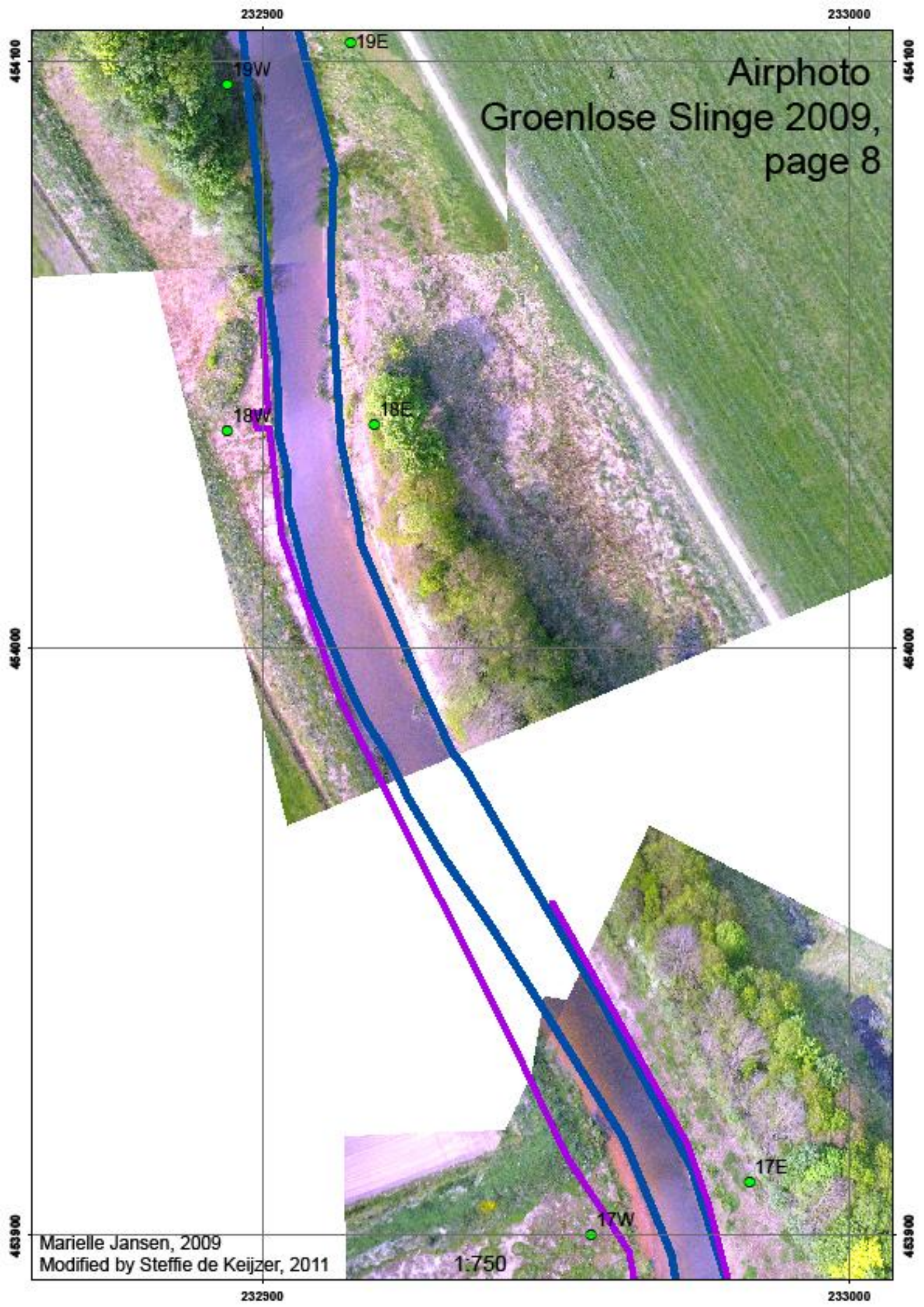
232900
233000
454100
454000
453900
19E
19W
18W
18E
17E
17W
Airphoto
Groenlose Slinge 2009,
page 8
Marielle Jansen, 2009
Modified by Steffie de Keijzer, 2011
1:750

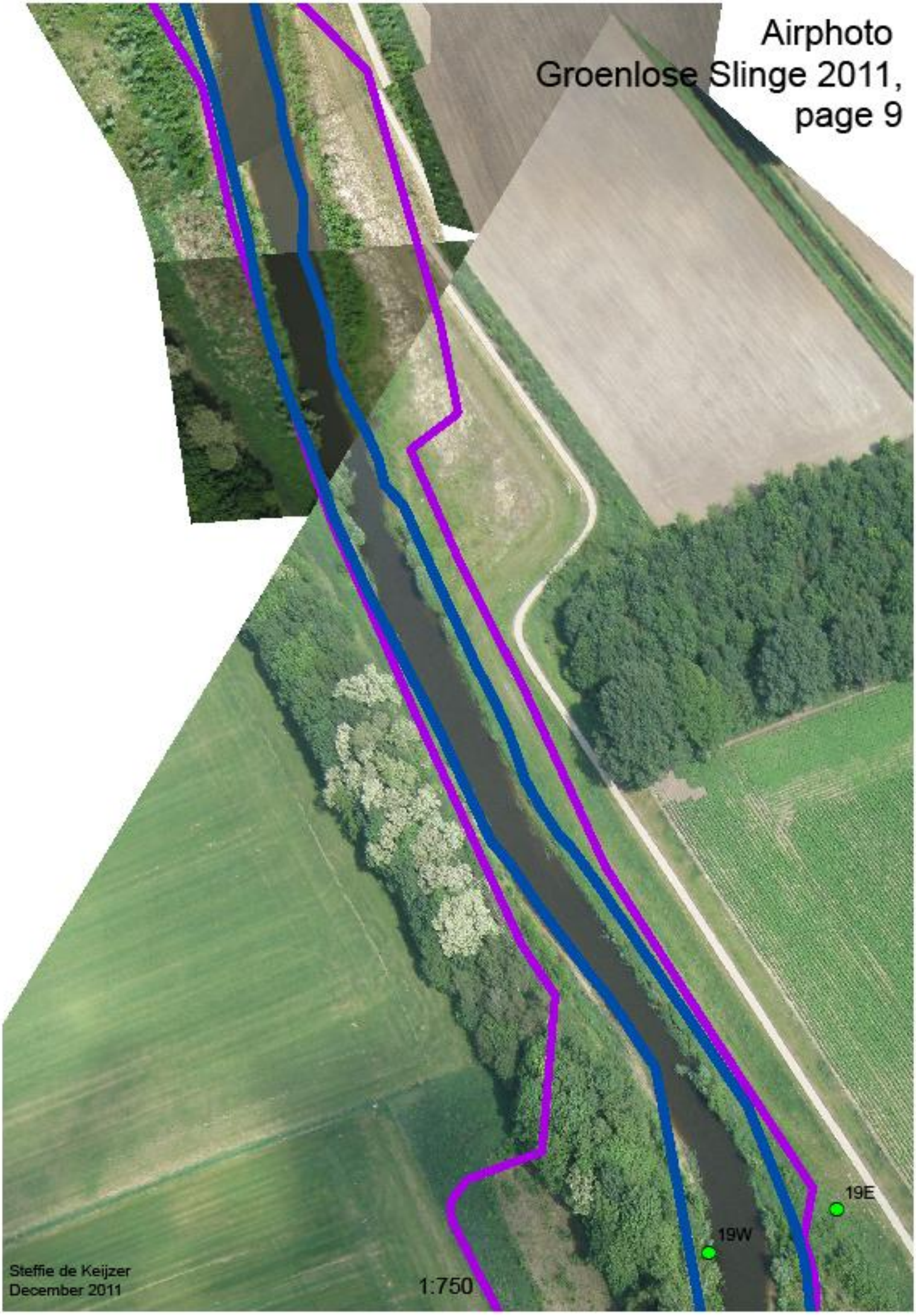
Airphoto
Groenlose Slinge 2011,
page 9
19E
19W
Steffie de Keijzer
December 2011
1:750

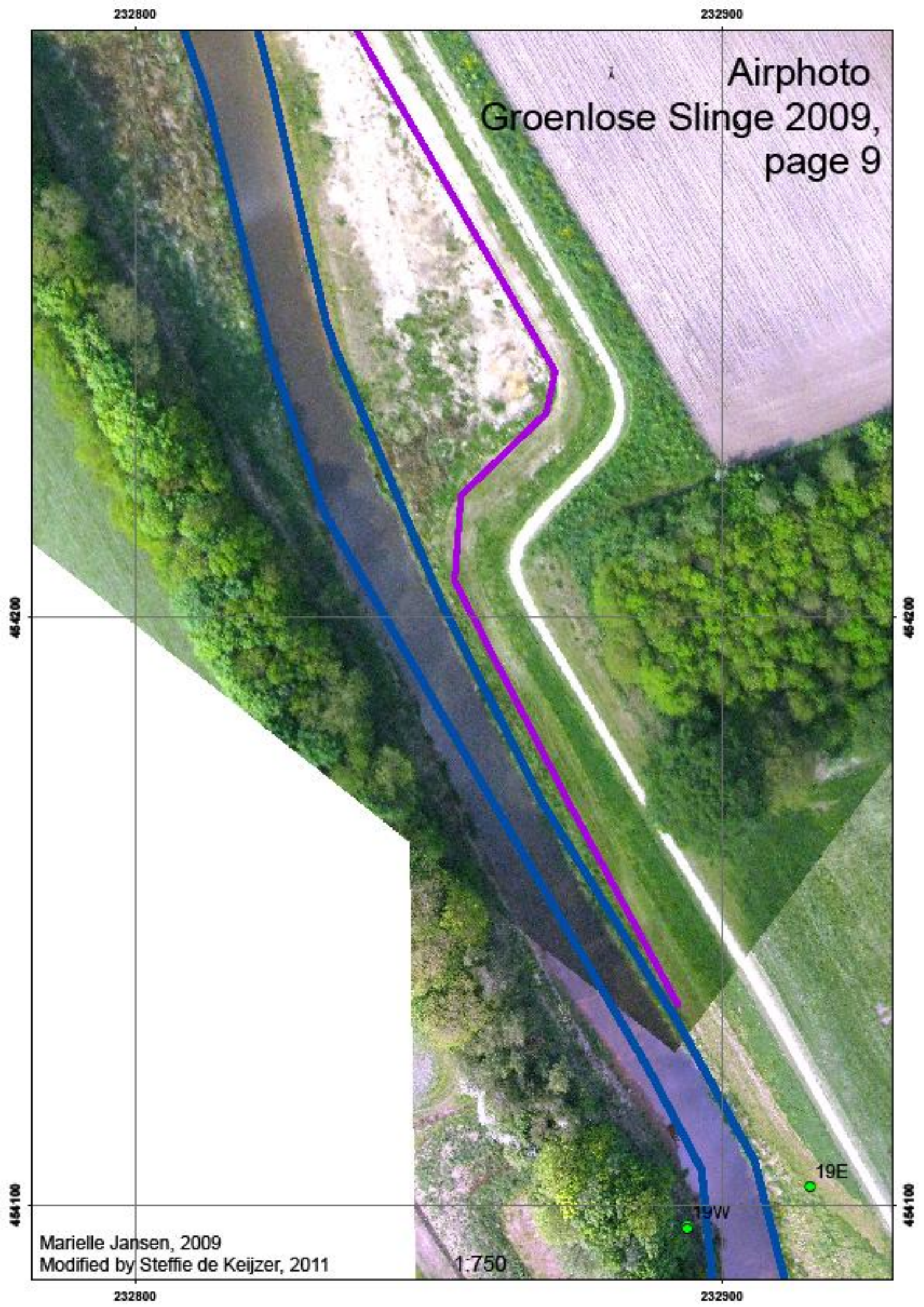
232800
232900
Airphoto
Groenlose Slinge 2009,
page 9
454200
454100
19E
19W
Marielle Jansen, 2009
Modified by Steffie de Keijzer, 2011
1:750

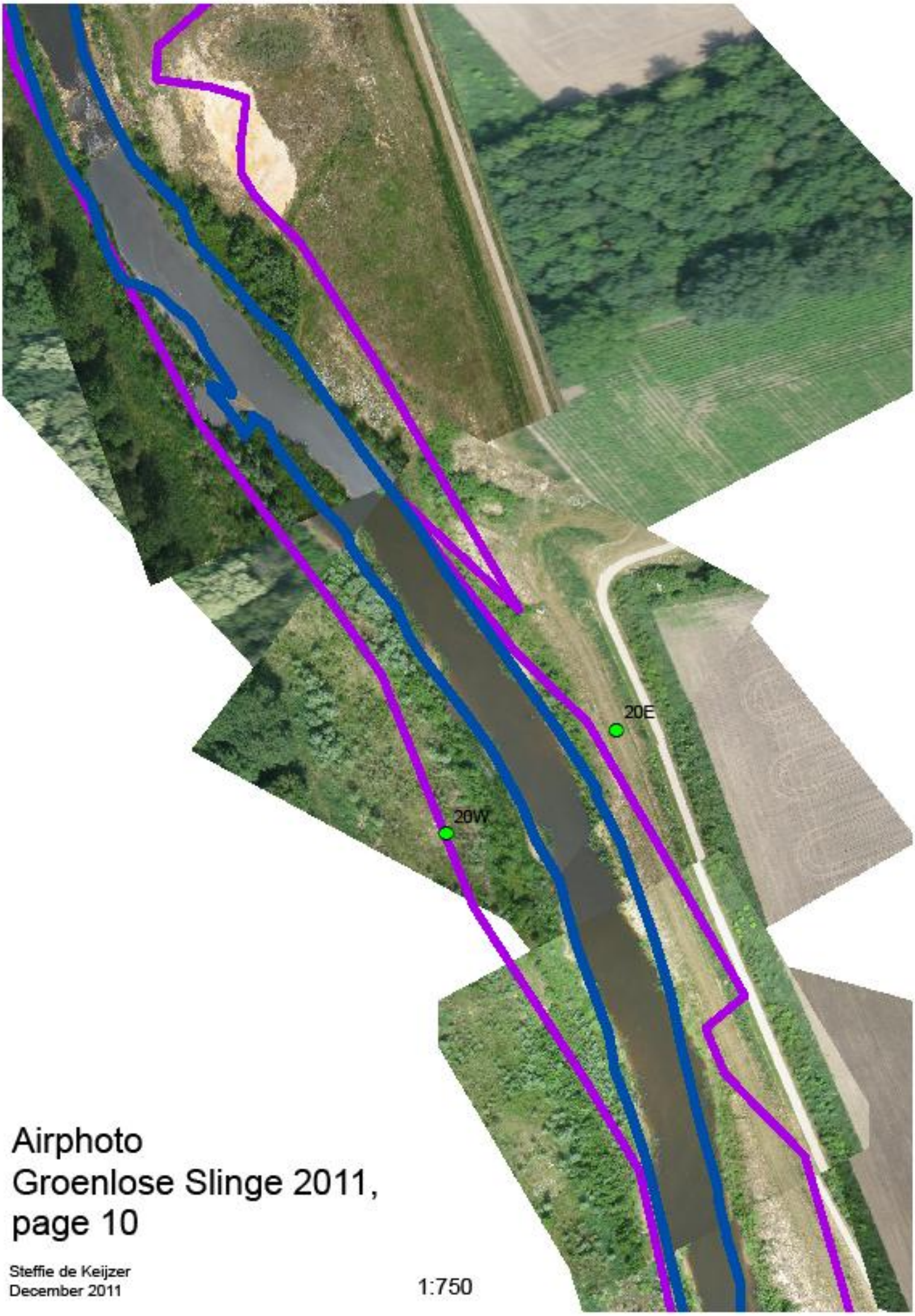

Airphoto Groenlose Slinge 2011, page 10

Steffie de Keijzer
December 2011

1:750

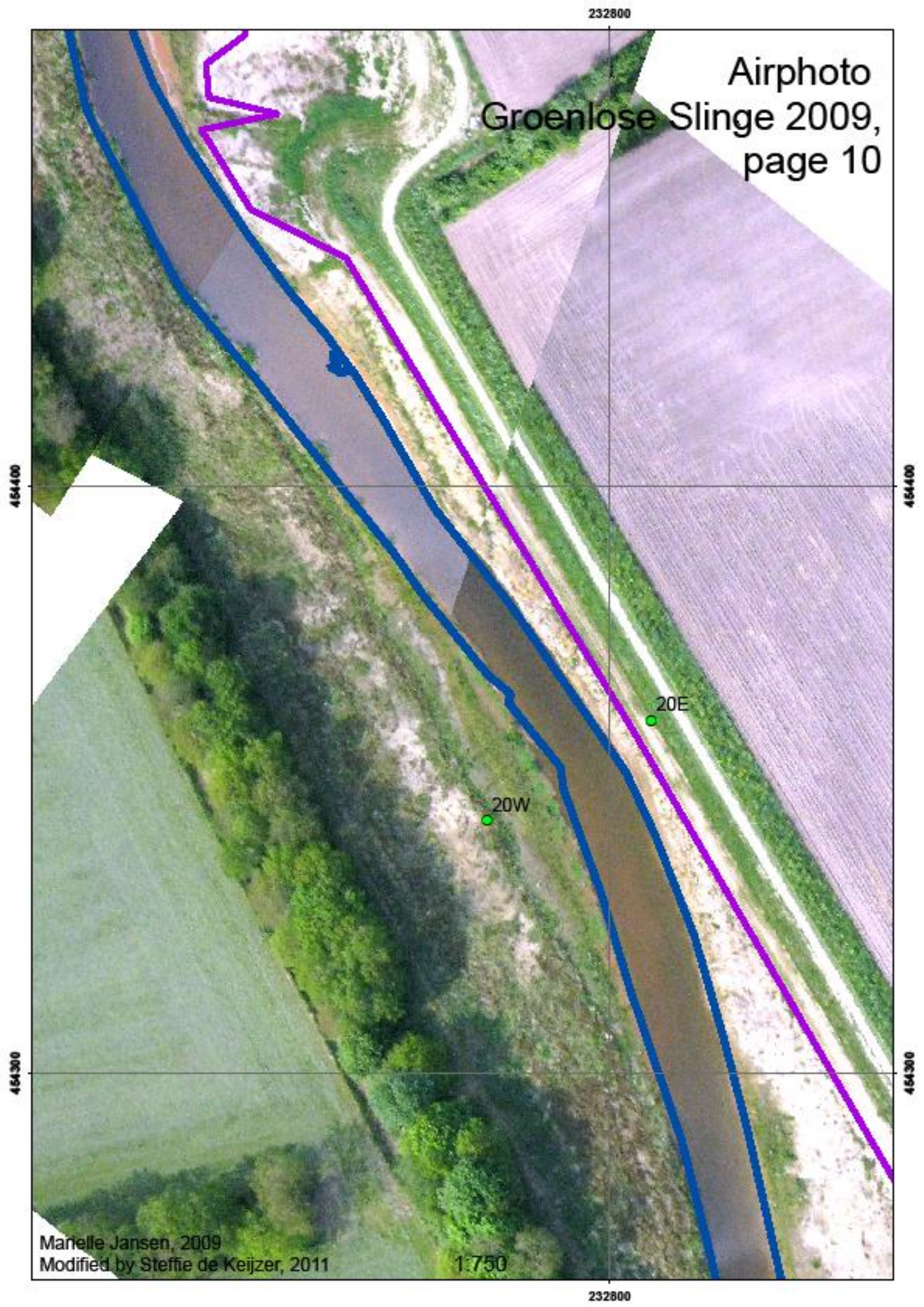
232800
Airphoto
Groenlose Slinge 2009,
page 10
454400
454300
20E
20W
Marielle Jansen, 2009
Modified by Steffie de Keijzer, 2011
1:750
232800

Appendix 9: Hydrographs of the Meibeek

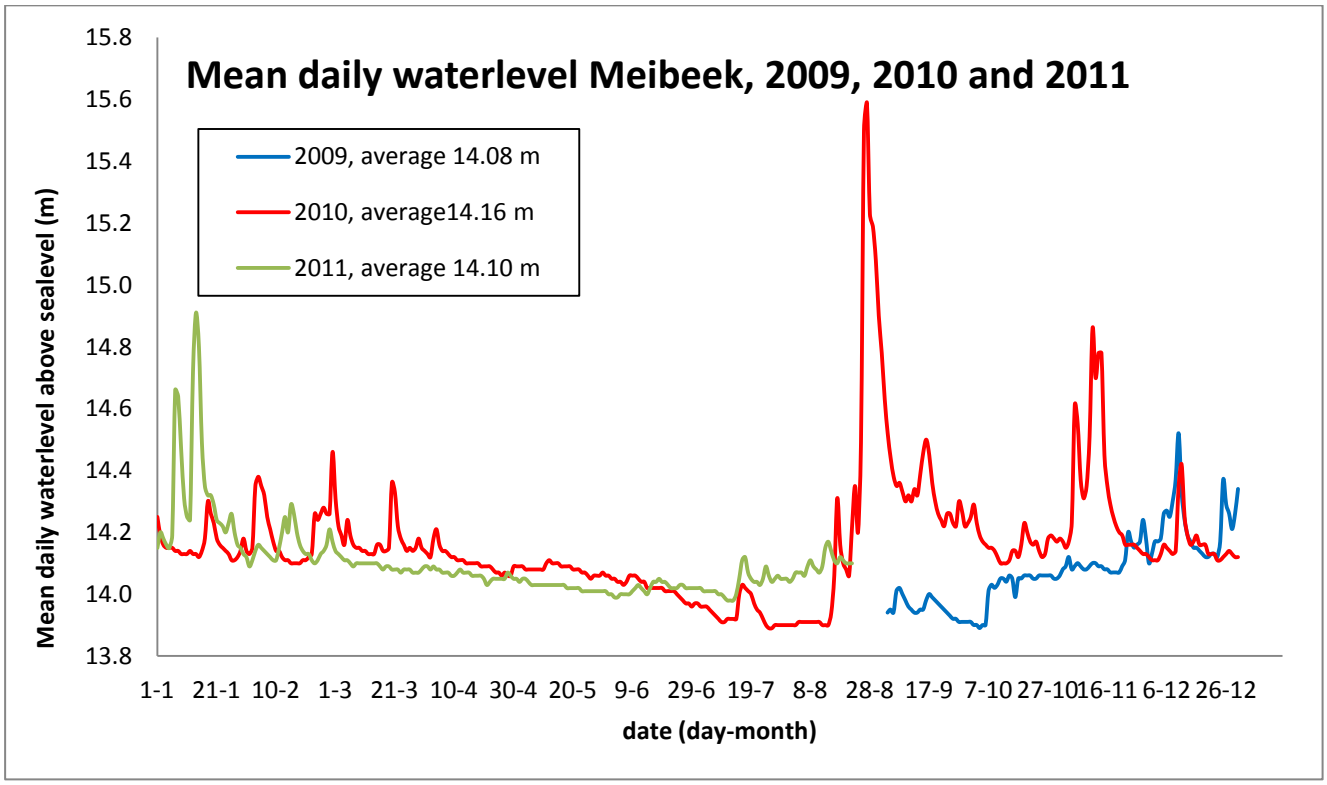

Appendix 10: List of vegetation names (Latin, English and Dutch)

Latin	English	Dutch
Alnus	alder	els
Alnus glutinosa	black alder	zwarte els
Alnus incana	grey alder	grijze els
Betula	birch	berk
Betula pubescens	downy birch	zachte berk
Caltha palustris	kingcup	gewone dotterbloem
Conyza Canadensis	Canadian horseweed	canadees raaigras
Equisetum fluviatile	horsetail	holpijp
Glyceria maxima	reed mannagrass	liesgras
Jacobaea vulgaris	ragwort	jacobskruid
Metha aquatic	water mint	watermunt
Phragmites australis	common reed	riet
Quercus	oak	eik
Rumex hydrolapthum	great water dock	paardenzuring
Salix alba	white willow	schietwilg
Salix aurita	eared willow	geoorde wilg
Sparganium erectum	branched bur-reed	grote egelskop
Tanacetum vulgare	tancy	boerenwormkruid
Typha	bulrush	lisdodde
Urtica dioica	common nettle	brandnetel

Appendix 11: Photos 2011

Airphotos and landphotos took in 2011 can be found on CD3 (Airphotos 2011) and on CD4 (Landphotos 2011)